



January 2021

Characerization, Depolymerization And Fractionation Of Alkali Lignin

Audrey Lynn Lavallie

[How does access to this work benefit you? Let us know!](#)

Follow this and additional works at: <https://commons.und.edu/theses>

Recommended Citation

Lavallie, Audrey Lynn, "Characerization, Depolymerization And Fractionation Of Alkali Lignin" (2021).
Theses and Dissertations. 4083.
<https://commons.und.edu/theses/4083>

This Dissertation is brought to you for free and open access by the Theses, Dissertations, and Senior Projects at UND Scholarly Commons. It has been accepted for inclusion in Theses and Dissertations by an authorized administrator of UND Scholarly Commons. For more information, please contact und.common@library.und.edu.

CHARACERIZATION, DEPOLYMERIZATION AND FRACTIONATION OF
ALKALI LIGNIN

by

Audrey L. LaVallie
B.S. Science Education, University of Michigan, 1980
M.S. Soils, Texas A&M University, 1996

A Dissertation
Submitted to the Graduate Faculty

of the

University of North Dakota

in partial fulfillment of the requirements

for the degree of
Doctor of Philosophy

Grand Forks, North Dakota

August
2021

Copyright 2021 Audrey L. LaVallie

This dissertation, submitted by Audrey L. LaVallie in partial fulfillment of the requirements for the Degree of Doctor of Philosophy from the University of North Dakota, has been read by the Faculty Advisory Committee under whom the work has been done and is hereby approved.

Dr. Alena Kubátová, Chair

Dr. Irina Smoliakova, Co-chair

Dr. David Pierce

Dr. Qianli Chu

Dr. Yun Ji

This dissertation is being submitted by the appointed advisory committee as having met all of the requirements of the School of Graduate Studies at the University of North Dakota and is hereby approved.

Dr. Chris Nelson (Dean of the Graduate School)

Date

PERMISSION

Title: Characterization, Depolymerization, and Fractionation of Alkali Lignin

Department: Chemistry

Degree: Doctor of Philosophy

In presenting this dissertation in partial fulfillment of the requirement for a graduate degree from the University of North Dakota, I agree that the library of this University shall make it freely available for inspection. I further agree that permission for extensive copying for scholarly purposes may be granted by the professor who supervised my dissertation work or, in her absence, by the chairperson of the department or the dean of the graduate school. It is understood that any copying or publication or other use of this dissertation or part thereof for financial gain shall not be allowed without my written permission. It is also understood that due recognition shall be given to me and the University of North Dakota in any scholarly use which may be made of any material in my dissertation.

Audrey L. LaVallie

TABLE OF CONTENTS

ABBREVIATIONS.....	ix
LIST OF FIGURES.....	xii
LIST OF TABLES.....	xix
LIST OF EQUATIONS AND FORMULAS.....	xxiii
ACKNOWLEDGMENTS.....	xxiv
ABSTRACT.....	xxvi
CHAPTER I. INTRODUCTION.....	1
I.1. Significance of Lignin and Lignin Derivatives.....	1
I.2. Sources of Technical Lignins.....	2
I.3. Chemical Structure of Lignin.....	7
I.4. Molecular Weight Determination of Lignin.....	16
I.4.1. Overview of Methods Used to Determine Molecular Weight.....	16
I.4.1.1. Non SEC-Based Methods.....	16
I.4.1.2. SEC Methodology and Advantages/Disadvantages.....	19
I.4.2 Sample Preparation and Lignin Solubilization for GPC Analysis.....	35
I.5. Folin-Ciocalteu Method of Quantification of Phenolic Hydroxyls in Lignin	
Samples.....	43
I.6. Methods for the Processing of Technical Lignin.....	48
I.6.1. Fractionation of Alkali Lignin.....	49
I.6.1.1. Fractionation by Membrane.....	49
I.6.1.2. Fractionation by Acid Precipitation.....	54
I.6.1.3. Fractionation by Solvents.....	59
I.6.1.4. Fractionation by Preparatory SEC.....	65
I.6.2. Oxidation of Lignin by Hydrogen Peroxide with and without Alcohol	
Solvents.....	68
I.6.2.1. Alkaline Hydrogen Peroxide Treatment.....	69
I.6.2.2. Acidic Hydrogen Peroxide Treatment.....	71
I.6.3. Subcritical Water Treatment of Alkali Lignin.....	82
I.7. Statement of Purpose.....	90

CHAPTER II. Characterization of Lignin.....	95
II.1. GPC Method Development.....	95
II.1.1. Description of Whole Lignins.....	95
II.1.2. Experimental.....	98
II.1.2.1. Materials.....	98
II.1.2.2. Calibration Standards and Preparation.....	101
II.1.2.3. Lignin Samples and Preparation.....	101
II.1.2.4. Instrumentation.....	104
II.1.2.5. Data Analysis.....	105
II.1.3. Results.....	105
II.1.3.1 Evaluation of GPC Parameters.....	105
II.1.3.1.1. Calibration.....	106
II.1.3.1.2. Selection of Wavelength.....	106
II.1.3.1.3. Selection of Suitable Calibration Standards.....	108
II.1.3.1.4. Evaluation of Blank Contribution.....	115
II.1.3.2. Whole Lignin Sample Preparation and Evaluation.....	120
II.1.3.3. Preparation and Evaluation of Samples from a Lignin-Solvent Study.....	132
II.2. Folin-Ciocalteu Method of Quantification of Phenolic Hydroxyl Groups in Lignin.....	144
II.2.1. Experimental.....	144
II.2.1.1. Materials.....	144
II.2.1.2. Folin Oxidation Method Development.....	145
II.2.1.3. Folin Oxidation Method.....	150
II.2.2. Results of Folin Analysis of Lignin Model Compounds and Lignin-Solvent Samples.....	152
II.2.3. Optimization of Method using Design of Experiment.....	157
II.2.3.1. Statistical Method.....	157
II.2.3.2. Results of Statistical Method.....	158
II.2.3.3. Conclusions of Statistical Approach.....	167

CHAPTER III. Processing of Technical Lignins.....	172
III.1. Fractionation of Alkali Lignin.....	172
III.1.1. Experimental.....	172
III.1.1.1. Materials and Methods.....	172
III.1.1.2. Lignin Fractionation via Preparative SEC.....	173
III.1.1.3. Analysis of Lignin MW Fractions.....	174
III.1.1.3.1. Analytical SEC of Lignin MW Fractions.....	174
III.1.1.3.2. Thermal Carbon Analysis of the Fractions.....	174
III.1.1.3.3. ESI HRMS (Electrospray High Resolution Mass Spectrometry) Analysis.....	175
III.1.1.3.4. TD-Py-GC-MS Analysis.....	176
III.1.1.3.5. ³¹ P NMR Analysis.....	177
III.1.2. Results and Discussion.....	178
III.1.2.1. Mass Distribution after SEC Fractionation.....	178
III.1.2.2. Mass distribution within Separate Fractions.....	180
III.1.2.3. Mean Molecular Weights of the Fractions Obtained.....	182
III.1.2.4. Thermal Carbon Analysis of Fractions.....	186
III.1.2.5. Identification of Species in Fractionated Lignin.....	191
III.1.2.6. Hydroxyl Group Quantitation by ³¹ P NMR Spectroscopy.....	193
III.1.3. Conclusions.....	198
III.2. Oxidation of Lignin by Hydrogen Peroxide with and without Alcohol Solvents.....	199
III.2.1. Experimental.....	199
III.2.1.1. Materials.....	199
III.2.1.2. Lignin Degradation Procedure.....	199
III.2.1.3. Chemical Characterization of Peroxide-Treated Lignin Samples.....	203

III.2.2.	
Results.....	205
III.2.2.1. Lignin Buffering Capacity.....	205
III.2.2.2. Depolymerization and Mass Balance.....	210
III.2.2.3. Carbon Mass Balance Closure.....	213
III.2.2.4. Solvent Effect.....	215
III.2.2.5. Size Exclusion Chromatography.....	217
III.2.3. Conclusions.....	220
III.3. Subcritical Water Treatment of Alkali Lignin.....	221
III.3.1. Experimental.....	221
III.3.1.1. Materials and methods.....	221
III.3.1.2. Subcritical Water Treatment.....	222
III.3.1.3. Analysis of Subcritical Water Reaction Products.....	223
III.3.1.4. Thermal Carbon Analysis.....	223
III.3.1.5. Gel Permeation Chromatography.....	224
III.3.1.6. Gas Chromatography-Mass Spectrometry Analysis.....	224
III.3.1.7. Thermal Desorption-Pyrolysis-Gas Chromatography-Mass Spectrometry Analysis.....	225
III.3.1.8. Elemental Analyses	226
III.3.2. Data Processing.....	226
III.3.3. Results and Discussion.....	228
III.3.3.1. Mass Balance Closure of Subcritical Water-Treated Lignin Products.....	228
III.3.3.2. Molecular Weight Distribution of Subcritical Water Reaction Products.....	230
III.3.3.3. Contribution of Low Molecular Weight (TD) Products.....	232
III.3.3.4. Comprehensive Characterization of SW Lignin Degradation Products Obtained at 300 °C.....	235
III.3.3.5. Gas Phase and Unresolved Pyrolytic Analysis Markers.....	235
III.3.3.6. Comparison of Oligomer/Polymer Distribution.....	241

III.3.3.7. C/H and C/O Ratios.....	242
III.3.3.8. Repolymerization vs Deoxygenation: Consideration and Insights.....	245
III.3.4. Conclusions.....	246
IV. References.....	248
APPENDICES	
Appendix 1: FC Workflow.....	266
Appendix 2: TCA Workflow.....	269
Appendix 3: Thermograms.....	270
Appendix 4: Minitab Data.....	272
Appendix 5: LLE-GC-MS Workflow.....	275
Appendix 6: GPC Workflow.....	276
Appendix 7: TD-Py-GC-MS Workflow.....	277

ABBREVIATIONS

ACE	Acetone
ACN	Acetonitrile
ANOVA	Analysis Of VAriance
Conc	concentration
Da	Daltons
DAD	Diode array detector
DCM	Dichloromethane
DEE	Diethyl ether
DFT	Density functional theory
DLS	Dynamic light scattering
DMAc	dimethylacetamide
DMF	dimethylformamide
DMSO	Dimethyl sulfoxide
DPPH	2,2-diphenyl-1-picryldrazyl assay
DSL	Differential static light scattering
DTMPA	diethylenetriaminepentamethylene-pentaphosphoric acid
DTPA	diethylenetriaminepentaacetic acid
EA	Ethyl acetate
EIC	Extracted ion current
ELSD	Evaporative light scattering detector
ESI	Electrospray ionization
EtOH	Ethyl alcohol
FC or F-C	Folin-Ciocalteu reagent
FID	Flame ionization detector
FTIR	Fourier transform infrared spectroscopy
G	Guaiacol
GAE	Gallic acid equivalents
GC	Gas chromatography
GDVB	Glucose rings divinylbenzene
GFC	Gel filtration chromatography
GPC	Gel permeation chromatography
HP SEC	High performance size exclusion chromatography
HPLC	High performance liquid chromatography
HR	Hydrodynamic radius
HSQC-NMR	Heteronuclear single quantum coherence nuclear magnetic resonance

LALS	Low-angle light scattering
LALLS	Low-angle laser light scattering
LC	Liquid chromatography
LLE	Liquid-liquid extraction
MALS	Multi-angle light scattering
mAU	Milli absorbance units
MeOH	Methyl alcohol
<i>m/z</i>	Mass-to-charge ratio
min	minutes
M_n	Number-average molecular weight
M_w	Weight-average molecular weight
M_p	Peak maximum molecular weight
M_z	Z-average molecular weight
MS	Mass spectrometry
mTHF	methyltetrahydrofuran
MW	Molecular weight
P2	Pinoresinol
PDI or PI	Polydispersity index
PEG	Polyethylene glycol
PMMA	Poly(methyl methacrylate)
PS	Polystyrene
PSDVB	Polystyrene/divinylbenzene
Py-GC	Pyrolysis - gas chromatography
RALS	Right-angle light scattering
R _g	Radius of gyration
RI	Refractive index
S	Syringol
S _b	Standard deviation of slope
SEC	Size exclusion chromatography
SP	pooled standard deviations
SLS	Static light scattering
S _y	Standard error of y
SW	Subcritical water
<i>t</i> *	Critical <i>t</i> value
TCA	Thermal carbon analysis
TD-Py-GC-MS	Thermal desorption-Pyrolysis-Gas chromatography-Mass Spectrometry
THF	Tetrahydrofuran

TIC	Total ion current
TMDP	2-Chloro-4,4,5,5-tetramethyldioxaphospholane
t_0	statistical t value
t_r	Retention time
VPO	Vapor pressure osmometry
VWD	Variable wavelength detector

LIST OF FIGURES

Figure 1. Major linkage groups in lignin with outlines of the exact linkages. Figures based on the data by Doherty et al. ¹	9
Figure 2. A section of lignin with two aromatic rings, showing the β -O-4' ether bond with ring numbering and carbon designations.....	10
Figure 3. (a) Lignin (general), ² (b) European Beech (hardwood) lignin. ³	12
Figure 4. Proposed structures of kraft lignin by Rak et al. ⁴ (a) and Zakzeski et al. ⁵ (b).....	14
Figure 5. Placement of M_p , M_n , M_w , M_z and M_{z+1} on a symmetrically distributed, one-mode molecular weight profile as molecular fraction vs molecular weight. ⁶	23
Figure 6. (a) Solubility percentage of original lignin by percentage of acetone in acetone- water in acetone-water solvent mixes, (b) MW by percentage of acetone in acetone-water solvent mixes; taken from Sadeghafir et al. ⁷	37
Figure 7. A phase map showing complete dissolution of lignin (black squares) and incomplete dissolution (white squares) as a function of kraft lignin wt% originally present and wt% of NaOH in solutio	40
Figure 8. Phosphomolybdic acid, $H_3PMo_{12}O_{40}$. ⁹ Phosphotungstic acid is identical, with the exception of having instead a tungsten center ($H_3PW_{12}O_{40}$).....	44
Figure 9. Oxidation of 4-hydroxyphenol to semiquinone, followed by another oxidation step to benzoquinone. ⁹	45
Fig. 10. Proposed breakdown of lignin in alkaline solution by hydrogen peroxide via photocatalysis. ¹⁰	71
Figure 11. Proposed mechanism for oxidation of α -hydroxyl groups in lignin under acidic conditions. In this instance, acetaldehyde (ethanal) is produced as a side product during cleavage of the bond at the α -O-4' location. ¹¹	72
Figure 12. (a) Proposed ring-opening mechanism by Ahmad et al., ¹² (based on Gierer et al. ¹³) by the OH^+ ion under acidic conditions, (b) proposed depolymerization of lignin via the β -O-4' linkage through the action of the OH^+ ion after a dehydration process in acidic media.	74

Figure 13. Depolymerization schemes under acidic conditions, accomplished by direct H₂O₂ action, via (a) creation of a carbocation after rearrangement of the α -carbon bond to the aromatic ring, (b) cleavage of the C α – C β bond and creation of a carboxylic group at the α -carbon, (c) ring opening reaction through the removal of ring substituents, (d) oxidation of an α -carbon hydroxyl group, producing an aliphatic ketone. Panel (e) shows a proposed condensation reaction through acidic action.¹⁴75

Figure 14. (a) Polystyrene monomer unit, and (b) poly (methyl methacrylate) monomer unit. (Images from Sigma-Aldrich).....106

Figure 15. (a) UV-Vis absorbance curve for polystyrene.....
250 nm (gray) and at 220 nm (black). (Peaks at 10 and 10.7 minutes are additives).
The peak retention times are approximately 6.7, 7.7, 8.4 and 9.2 min.107

Figure 17. Calibration curves including least-square linear equations for (a) seven PS standards (from 580 to 271800 M_p) and (b) Seven PMMA standards (from 50 to 56600 M_p).....109

Figure 18. Standards curves for several combinations of PS and PMMA standards, where PS mixes 1,2 encompass 580, 1480, 5030, 8450, 38100, 70950 and 271800 M_p; (a) PS mixes 1,2 and PMMA 960, 56600 M_p, with 0.00874 S_b and 0.0294 S_y; (b) PS mixes 1,2 and PMMA 960, 2880, 17810 M_p, with 0.01019 S_b and 0.03508 S_y; (c) PS mixes 1,2 and PMMA 960, 4640 M_p, with 0.01112 S_b and 0.03613 S_y; (d) PS mixes 1,2 and PMMA 960, 17810 M_p, with 0.01163 S_b and 0.03766 S_y.....113

Figure 19. (a) Unstabilized THF blank with solvent peak and injection pressure pulse (negative peak) for a 30- μ L injection volume and a flow rate of 0.3 mL/min (Agilent Plgel Mini-Mix D column); (b) BHT elution in relation to THF for a 30- μ L injection volume and a flow rate of 0.3 mL/min (Agilent Plgel Mini-Mix D column).....116

Figure 20. Chromatograms of blanks with mixed solvents, each injected as 30 μ L for a 15-minute program with mobile phase (unstabilized THF) flow rate of 0.3 mL/min, for (a) THF:water (1:1), two consecutive injections initially in the overall sequence, (b) acetone:water (1:1), two consecutive injections after THF:water injections, (c) THF:water (95:5), three consecutive injections after two initial blanks in another sequence, (d) alkaline lignin dissolved in 100% THF (1 mg/mL) and first injections of THF:water (1:1), Acetone water (1:1) and THF:water (95:5), (e) alkaline lignin dissolved in 100% THF (1 mg/mL)... and 2nd injections of THF:water (1:1), acetone:water (1:1) and the third injection of THF:water (95:1).....117

Figure 21. Comparison of M_p, M_n, and M_w (peak-, number-, and weight-average

molecular weight, respectively) values for (a) lignins with M_w values below 10,000 Da; (b) lignins with M_w values over 10,000 Da.....	124
Figure 22. Comparison of M_p , M_n , and M_w (peak-, number-, and mass-molecular weight, respectively) values for kraft lignin dissolved in various solvents and combinations of solvents.....	136
Figure 23. Overlay of chromatograms of all lignin-solvent samples shown as (a) peaks with full response, and as (b) a close-up of the peak bases.....	138
Figure 24. Average % recovery of original lignin in the liquid fraction of each solvent or solvent system.....	140
Figure 25. Left: A solution of gallic acid (100 μ g/mL) reacted with 50 μ L FC reagent and 0.4 M Na_2CO_3 after two hours, with the liquid solution poured off after the reaction. Right: The same reaction after three hours.	147
Figure 26. Absorbance of a solution of gallic acid (100 μ g/mL) with 50 μ L FC reagent and 0.4 M Na_2CO_3 over 24 hours.....	148
Figure 27: Microplate setup for oxidation of lignin by Folin reagent. Purple represents lignin as 200 μ g/mL sample in column 12 halved down to column 3 with acetonitrile:water (1:1) solution; blue is control as guaiacol (about 70 μ g/mL) and blanks are acetone:water (1:1). Final solutions will contain Folin reagent (50 μ L in each well) and Na_2CO_3 (150 μ L of 0.4 M solution) in each well, as well.....	151
Figure 28. (a) Microplate results for gallic acid reacted with 50 μ L FC and 0.4 M Na_2CO_3 after two hours of incubation, (b) results for the same protocol with guaiacol.....	153
Figure 29: (a) Slopes for lignin model compounds (as absorbance vs nmol carbon per well in a range of 14 – 770 nmol carbon based on FC assay with an initial 200 μ g/mL diluted through 10; (b) slopes for lignin/solvent samples (in a range of 6 – 427 nmol carbon) also at an initial concentration of 200 μ g/mL in microplate wells; (c) slopes for the same lignin/solvent samples (in a range of 2 – 427 nmol carbon) but on an equal volume basis.....	154
Figure 30. Minitab design summary and analysis of variance for 2^4 full factorial evaluation of FC phenol reactions, with four replicates ($\alpha = 0.05$).....	159
Figure 31. The normal plot of the standardized effects for 2^4 full factorial evaluation of FC phenol reactions, with four replicates ($\alpha = 0.05$).....	160

Figure 32. Main effects and interaction plots for 2^4 full factorial evaluation of FC phenol reactions, with four replicates ($\alpha = 0.05$).....160

Figure 33 Normal probability plot and residuals vs. fits plot for 2^4 full factorial evaluation of FC phenol reactions, with four replicates ($\alpha = 0.05$).....161

Figure 34. Design and analysis of variance for 2^{4-1} fractional factorial evaluation of FC phenol reactions, with four replicates ($\alpha = 0.05$).....162

Figure 35. The normal plot of the standardized effects for 2^4 full factorial evaluation of FC phenol reactions, with one replicate and the factorial interaction plot ($\alpha = 0.05$).....162

Figure 36. Comparison of p-values for full (2^4) and fractional (2^{4-1}) factorial model evaluation of FC phenol reactions, with four replicates and $\alpha = 0.05$163

Figure 37. Normal probability plot and residuals vs. fits plot for 2^{4-1} fractional factorial evaluation of FC phenol reactions, with four replicates ($\alpha = 0.05$).....163

Figure 38. Minitab design summary and analysis of variance for 2^4 full factorial evaluation of FC phenol reactions, with one replicate ($\alpha = 0.05$).....164

Figure 39. The normal plot of the standardized effects for 2^4 full factorial evaluation of FC phenol reactions, with one replicate and the factorial interaction plot ($\alpha = 0.05$).....165

Figure 40. Normal probability plot and residuals vs. fits plot for 2^4 full factorial evaluation of FC phenol reactions, with one replicate ($\alpha = 0.05$). The residuals vs. fits plot showed better variance than the four-replicate model.....165

Figure 41. Design and analysis of variance for 2^{4-1} fractional factorial evaluation of FC phenol reactions, with one replicate ($\alpha = 0.05$).....166

Figure 42. Normal plot of the standardized effects and interaction plots for 2^{4-1} fractional factorial evaluation of FC phenol reactions, with one replicate ($\alpha = 0.05$).....166

Figure 43. Normal probability plot and residuals vs. fits plot for 2^{4-1} fractional factorial evaluation of FC phenol reactions, with one replicate ($\alpha = 0.05$).....167

Figure 44. Comparisons of p-values for all factorial models of the FC phenol study.....	168
Figure 45. Individual contour plots for the four-replicate full factorial model with four factors, each paired with each other without hold values for factors outside the pair.....	170
Figure 46. Individual contour plots for the one-replicate full factorial model with four factors, each paired with each other without hold values for factors outside the pair.....	171
Figure 47. (a) Chromatogram of alkali lignin separation by preparative SEC, at concentration 10,000 ppm in a mobile phase of THF:water (9:1) and total injection volume 500 mL (through an extended loop capillary). Five fraction sections are superimposed for retention times 14-16, 16-18, 18-20, 20-22 and 22-24 min. b) Subsequent analytical-scale SEC of the collected fractions. Detection was conducted using a diode array detector within the 212-750 nm working range.....	179
Figure 48. (a) ESI-TOFMS spectra of molecular counts vs m/z based on deconvoluted data for lignin fractions 1 – 5. Spectra are scaled to a maximum of 10,000 m/z, with the exception of fraction 5 which has a maximum of 9000 m/z. (b) Comparison of SEC vs ESI-TOFMS number-average and weight-average molecular weights for all lignin fractions.....	184
Figure 49. (a) Carbon mass distribution by TCA temperature fraction for each lignin fraction as stacked columns, (b) Normalized carbon mass distribution for each individual lignin fraction (and unfractionated lignin) by TCA temperature fraction, (c) Carbon mass sums for all SEC fractions at each temperature step of TCA compared to alkali lignin carbon masses (normalized) generated at the same temperature fractions.....	186
Figure 50. Organic groups by temperature fraction normalized for each sample as SEC Fractions 1 – 5.....	190
Figure 51. (a) TD-Py-GC-MS analysis of evolution of species by temperature fraction by area (mass) for lignin fractions 1 – 5. (b) % mass (by area) evolved for fractions 1-5 normalized to lignin area.....	191
Figure 52. ³¹ P NMR spectra of SEC weight fractionated lignin samples. The top spectrum belongs to the lowest molecular weight fraction, 3NA-81-6, while the second spectrum from the bottom is for the highest molecular weight fraction, 3-NA-2. The bottom spectrum is a pre-eluate fraction comprised mostly of impurities of carbohydrate origins.....	196

Figure 53. (a) The initial pH values for basic and acidic solutions at pH 11 and 3 respectively, and change of pH of the solutions after addition of lignin, and the subsequent change in pH after autoclaving of the lignin solution (0% H₂O₂, 0% MeOH); (b) a second set of “neutral” aqueous samples, monitored for actual initial pH and subsequent pH values after treatment with H₂O₂/MeOH and autoclaving; (c) comparison of samples that had initial pH values of 3, 7 and 11; (d) the same pH 3, 7, 11 results compared to an expanded pH range (0.5 and 13) to assess extreme pH impact, and monitored for actual initial pH and subsequent pH values after treatment with H₂O₂/MeOH and autoclaving.....205

Figure 54. Percent of original lignin mass present in the liquid fractions of autoclaved samples which had been treated (H₂O₂ and MeOH) or left untreated; mass was determined by gravimetry. Initial pH values were 3, 7 and 11.....211

Figure 55. Comprehensive total carbon analysis of neutral (pH 7) liquid fractions for varying H₂O₂/MeOH treatments and autoclaving, and then subjected to vacuum- and syringe-filtered (20 and 0.2 um, respectively) filtration, compared to wt% carbon by gravimetry (and vacuum filtration).....213

Figure 56. Distribution of carbon by the TCA temperature fraction for the liquid fraction of neutral pH samples subjected to varying H₂O₂/MeOH treatment and autoclaving, followed by vacuum filtration.....214

Figure 57. Comparison of wt% carbon in liquid fractions of lignin, post autoclaving, in aqueous solutions with methanol, ethanol and isopropanol (a) at 0 and 25% v/v (no hydrogen peroxide), and (b) at 0 and 25% v/v in 10% H₂O₂ solutions.....216

Figure 58. Gel permeation chromatograms showing (a) the calibration standards curve (PS and PMMA) for an untreated lignin profile (b) decrease in average molecular weight with increased H₂O₂ addition.....218

Figure 59. LLE-GC-MS characterization (a) compared of yields to TCA analyses of TD fractions (200 and 300 °C) of SW treated lignin samples; (b) distribution of classes of organic compounds in LLE extracts in untreated lignin, 200 °C SW treated lignin and 300 °C SW treated lignin. Data are presented are mean values and one standard deviation for three replicates.....228

Figure 60. GPC analysis of thermally untreated lignin and SW treated (300 °C) lignin (filtered and unfiltered liquid fractions and solids residue) including PMMA and PS calibration on logarithmic scale.....231

Figure 61. TCA characterization of liquid product SW treated lignin samples and comparison to untreated lignin: (a) wt.% C of initial lignin C. The insert shows

gravimetric yield for solid and liquid fractions; (b) normalized to total carbon content.233

Figure 62. Comparison of TD-Py-GC-MS and TCA analyses of organic products from 300 °C SW treated lignin as (a) liquid filtered fraction without gas determination, (b) liquid filtered fraction including gases, nonintegrated area, and unresolved area (c) solid residue including including gases, nonintegrated area, and unresolved area.236

Figure 63. TD-Py-GC-MS semiquantitative gases (a-c) & organics (d-f) profiles for (a, d) SW treated (300 °C) liquid fraction, (b, e) SW treated (300 °C) solid fraction and (c, f) thermally untreated lignin samples. For SW treated liquid fraction the pyroprobe program was started at 110 °C to eliminate impact of water on consecutive fractions. Thus, a total of 110 and 200 °C should be compared to 200 °C for untreated lignin.239

LIST OF TABLES

Table 1. General delignification process descriptions and M_n , M_w values for four types of technical lignins.	4
Table 2. Softwood, hardwood and herbaceous plant composition as percentages of cellulose, hemicellulose and lignin, ¹⁵ as well as H, G, S unit percentages. ¹⁶	8
Table 3. Lignin linkage occurrence by percentage in softwoods, hardwoods and plants, ¹⁷ 'nd' denotes 'not determined.'	10
Table 4. Number of linkages and monolignol units per 100 aromatic rings for several technical lignins. ¹⁸	11
Table 5. Bond dissociation energies (kcal/mol) for common lignin linkages. *The β -1' linkage reported here for the Parthasarathi et al. study was based on their $C\alpha$ - 1' bond dissociation energy. ¹⁹	11
Table 6. Semiquantitative estimation of relative content of interunit linkages in lignin during soda processing, using 2D HSQC-NMR spectra. ²⁰	15
Table 7. Molecular weight and polydispersity comparison by lignin source and GPC method, for indulin AT, indulin C, lignosulfonate, soda pulping and kraft alkaline lignins. (The abbreviation r.t. is used for room temperature).....	32
Table 8. Method parameters and molecular weight findings for several filtration membrane fractionation studies.....	52
Table 9. Method parameters and molecular weight findings for several acid precipitation fractionation studies.....	57
Table 10. Method parameters and molecular weight findings for several solvent precipitation fractionation studies.....	61
Table 11. Method parameters and molecular weight findings for a preparatory SEC fractionation study.....	67
Table 12. Method parameters and findings for several lignin oxidation studies with hydrogen peroxide as the primary catalyst.....	79
Table 13. Comprehensive list of lignin subcritical water treatment studies without additives conducted with a suite of analytical protocols, including experimental conditions, analytical methods and main findings.....	84

Table 14. Lignin study sample sources, composition, pH, method of MW evaluation, production process, and references.....	99
Table 15. Available commercial polystyrene and poly(methyl methacrylate) standards listed by peak molecular weight (M_p), retention times and retention volumes obtained on PLgel Minimix-D column with THF as a mobile phase (3 μ L injection volume and 0.3 mL/min flow rate).....	109
Table 16. Standard deviation of the slope (S_b) and standard error of predicted y values (S_y) for various combinations of PS and PMMA standards. All PS standards were evaluated at 250 nm, while PMMA standards were evaluated at 250 and 220 nm. PS 1 (mix one) consisted of 580, 5030, 38100 and 271800 M_p . PS 2 (mix 2) was 1480, 8450, and 70950 M_p . PMMA 1 was 550, 2880, 10280 and 56600 M_p , while PMMA 2 was 960, 4640 and 17810 M_p	110
Table 17. T-test results for comparisons of PS mixes 1,2 (1 mg/mL) standards curve (with 580, 1480, 5030, 8450, 38100, 70950 and 271800 M_p) to calibration curves composed of PMMA and combined PS/PMMA standards. Results include t-test statistical values t_o , critical t values t^* , and degrees of freedom for a two-sided pooled t-test at 95% and 99% confidence levels.....	114
Table 18. Lignin samples, descriptions, chromatograms and molecular weights as peak-, number-, mass- and z-averages (M_p , M_n , M_w , M_z). All samples were run in duplicate; only one chromatogram is shown and molecular weights are averages of two values for samples which were 2.5 mg/mL in concentration, with 2.5% water before injection.....	121
Table 19. Molecular weight and polydispersity comparison by lignin type and researcher/methodology for indulin AT, indulin C, lignosulfonate, soda pulping and kraft alkaline lignins.	126
Table 20. Molecular weight ranges for lignosulfonate and kraft lignin as compiled by several reference studies.....	129
Table 21. Lignin samples, descriptions, chromatograms and molecular weights as peak-, number-, mass- and z-averages (M_p , M_n , M_w , M_z). All samples were run in triplicate; only one chromatogram is shown and molecular weights are averages of three values for samples which were approximately 0.5 mg/mL in concentration. Red lines show integration area.....	131

Table 22. Lignin-solvent study samples' descriptions, chromatograms and molecular weights as peak-, number-, mass- and z-averages (M_p , M_n , M_w , M_z). All samples were run in triplicate; only one representative chromatogram is shown and molecular weights are averages of three values for samples which were 1.0 mg/mL in concentration.....	133
Table 23. Average original lignin mass, solvent volume, concentration of lignin in the liquid fraction and average % recovery of original lignin for each solvent (system).....	139
Table 24. Lignin samples, descriptions, chromatograms and molecular weights as peak-, number-, mass- and z-averages (M_p , M_n , M_w , M_z). All samples were run in duplicate; only one chromatogram is shown and molecular weights are averages values for both samples. Red lines show integration areas.....	142
Table 25. Comparison of MW values for lignin samples solubilized in acetone:water (50% acetone) solvent systems. Preparation for GPC differed- one sample was solubilized in THF:water (less than 10% water) and the other in THF:water (1:1). Concentrations were 1 mg/mL and 0.45 mg/mL respectively.....	143
Table 26. Recommended parameters of Folin reagent oxidation of bio-oils (Rover), shaded in gray, in comparison to parameters investigated in this study. (Parameters used in the method are bolded).....	149
..	
Table 27. Factorial ANOVA (analysis of variance) statistical parameters of a 2^4 design, with four factors and two levels designated.....	150
Table 28 Solubilization levels and initial concentrations of lignin solutions in various solvent systems and the final concentration for analysis after dilution for comparison by the same volume.....	152
Table 29. Distribution of lignin sample across fractions as measured via TCA and diode array detector (DAD) in preparative SEC. ¹	178
Table 30. Actual and expected MW range (by calibration curve) MW ranges, and % molecules in each fraction of higher or lower MW than expected for each fraction.....	181
Table 31. ESI-TOFMS and SEC calibration number-average (M_n) and weight-average (M_w) values for five fractions of lignin and unfractionated lignin.....	185

Table 32. Comparison of the number of mmoles of hydroxyl groups present per g of alkali lignin found by Meadwest Vaco vs the results obtained in the present study using ³¹ P NMR spectroscopy.....	194
Table 33. Number of mmoles determined in NMR samples in the SEC weight fractions per g of alkali lignin.....	195
Table 34. Experimental set-up for lignin oxidation by H ₂ O ₂ ; percentages of hydrogen peroxide, methanol and water were on a (v/v) basis; pH was ensured by using appropriate HCl and NaOH concentration prior to lignin, peroxide and methanol addition.....	201
Table 35. Experimental set-up for lignin oxidation by H ₂ O ₂ ; percentages of hydrogen peroxide, methanol and water were on a (v/v) basis, out of a total solution volume of 25 mL.....	202
Table 36. Molecular weight as number-average <i>M_n</i> , weight-average <i>M_w</i> and z-average <i>M_z</i> of liquid fractions of treated lignin by various combinations of hydrogen peroxide and methanol (% v/v).	220
Table 37. Experimental steps and methods of this study.....	223
Table 38. MW values calculated for liquid and solid fractions of alkali lignin degradation products (300 °C SW treated) and untreated alkali lignin, determined by GPC.....	231
Table 39. Elemental analysis and C/H and C/O ratios calculated for SW treated samples (filtered liquid and residue solids) and for untreated lignin samples. The ratios are based on C, H, and O content of identified species present in samples from TD-Py-GC-MS analysis. Ratios were calculated without noncondensable gases generated during analysis, and also with the gases (CO ₂ , CO and CH ₄).....	243

LIST OF EQUATIONS

[1]	$M_n = \frac{\sum N_i M_i}{\sum N_i}$	23
[2]	$M_w = \frac{\sum N_i M_i^2}{\sum N_i M_i}$	23
[3]	$M_z = \frac{\sum N_i M_i^3}{\sum N_i M_i^2}$	23
[4]	$H_2O_2 + H^+ \leftrightarrow HO^+ + H_2O$	72
[5]	$t_o = \frac{\bar{u}_1 - \bar{u}_2}{sp \sqrt{\frac{1}{n_1} + \frac{1}{n_2}}}$	105
[6]	$sp = \frac{(n_1 - 1)s_1^2 + (n_2 - 1)s_2^2}{n_1 + n_2 - 2}$	105

ACKNOWLEDGMENTS

I would like to thank Dr. Alena Kubátová especially for her acceptance of me into graduate school despite the fact that I was an older-than-traditional student and had completed an M.S. more than 20 years in the past. I actually met Alena while I was working at Turtle Mountain Community College and participating in the IREC Grant, which Alena oversaw from UND. She was, and still is, the most proficient and amazing analytical chemist and chromatographer I have ever met. I would also like to thank Dr. Evguenii Kozliak for his great humor and going the extra mile to make my journal papers into works of art. I would also like to thank Irina Smoliakova, as my co-advisor, who is an amazing instructor and mentor. Additionally, I have to thank the other dedicated instructors I have come to know and greatly admire: Dr. David Pierce, Dr. Yun Ji, Dr. Rick Chu, Dr. Guodong Du, Dr. Julia Zhou, Dr. Jerome Delhommelle, and Dr. Tao Yu, (a brilliant man who left us way too early). We all appreciate the help, humor, and hard work of Michael Whitney, Kim Myrum, Shane Johnson, Dave Knittel and Shaina Mattingly every day as well.

I have a special place in my heart for my graduate buddies, who accepted me wholeheartedly and made me feel like I was 25 again: Sarah Reagen, Jessica Emond, Hannah Han, Solene Bechelli, Wen Sun, Nafisa Bala, Honza Bilek, Rahul Shahni, Di Sun, Muneer Shaik, Honza Chalupa, Nastya Andrianova, Klara Kukowski, Jana Rostova, Ivana Brzoňová, Brett Nesor, Josh Hatton, and Rich Cochran. There are also quite a few people at NDSU whom I met while working on the EPSCoR grant that I will miss as well. A special thanks goes to our post-doc, Dr. Bin Yao, for being such a great guy and a big help.

I would like to thank the University of North Dakota, UND Chemistry Department, and UND Graduate School for accepting me into the program and providing financial

support. I also appreciate the support from the following funding agencies: The North Dakota EPSCoR Programs (Dakota BioCon tracks I and II), CSMS, UND Graduate School, Dr. Ernest & Jennie Coon teaching award.

Finally, I would like to thank my husband and daughter for providing the love and support that I rely on, and for sacrificing so much to put me through graduate school. Larry, my husband, passed away a month before my defense, but I carry him here in my heart and he is with me in all I do. My daughter, Nicole, is a blessing, and I'm sure she knows that I cannot thank her enough for her unconditional love and help in all matters.

To my family

ABSTRACT

Lignin may serve as a potential source of renewable chemicals and as a possible wealth of materials for replacement of petroleum-based fuel and petrochemicals. Lignin is a plant component that constitutes the second most common natural polymer on earth, behind only cellulose, and is the most common natural polymer with an aromatic network. Technical lignins (isolated from chemical processing of raw lignin) are produced as waste in the papermaking and biorefinery industries; an estimation of U.S. waste lignin is about 24 million tons yearly, more than the estimated 10.5 million tons of plastics discarded annually.

The exact structures of natural lignin and technical lignins are still not known, thus research continues on characterization of the many forms of technical lignins, which can differ substantially.

In this work, we have developed a gel permeation chromatography (GPC) method by HPLC with a variable wavelength UV-Vis detector; this was applied to raw lignin and technical lignins in order to establish a feasible method of determining molecular weights for a polymer which is insoluble in a pure aqueous or a pure organic solvent.

Characterization of lignin was continued with a modified Folin-Ciocalteu method for quantification of phenolic hydroxyl groups in lignin model compounds and technical lignins. Additionally, analysis of four factors of the experiment were statistically evaluated using a 2⁴ full factorial (ANOVA) design of experiment, giving information on main influences and interactions of the method.

Fractionation of lignins was carried out by preparative size exclusion chromatography. Further analysis of molecular weight distribution in the individual fractions was performed by electrospray ionization high resolution time-of-flight mass spectrometry

(ESI HR TOF-MS), thermal carbon analysis (TCA) and thermal desorption-pyrolysis-gas chromatography-mass spectrometry (TD-Py-GC-MS). Additional information about phenolic and aliphatic hydroxyl groups was supplied through phosphitylized standards and lignin samples evaluated via ^{31}P NMR analysis.

Oxidative depolymerization of alkali lignin was accomplished through addition of hydrogen peroxide to a water matrix at various percentages (v/v), also with variation of added methanol as a co-solvent. Lignin samples with initial pH values of 3, 7 and 11 were evaluated for wt% of solubilized (depolymerized) material under two sets of filtration, and analyzed for pH change as well.

Depolymerization was also done through subcritical water (SW) treatment of alkali lignin. TCA and TD-Py-GC-MS analyses of 300 °C SW samples were performed as described above, while the mass range for MS analysis was 10 – 550 m/z . This range had a lower limit which allowed monitoring of noncondensable gases (H_2O , N_2 , O_2 , CO_2). In addition, a novel method of mass balance was implemented through normalization of TCA and TD-Py-GC-MS data. SW treated samples were compared to untreated lignin profiles to determine the predominant species yielded at each temperature fraction. The process of condensation with concomitant gas formation through the temperature fractions was monitored through elemental analysis as C/H and C/O ratios.

A summary of results finds that GPC method development allowed a determination of THF:water ratios which in turn led to complete solubilization in extraction solvents. FC method development resulted in quantitative phenolic OH count per nmol carbon in whole technical lignins and solubilized alkali lignin samples.

Fractionation methodology was found to effectively limit MW ranges within individual fractions, although not to the extent expected. Both hi-MW and low-MW compounds outside expected ranges were found in every fraction.

Oxidation of lignin by hydrogen peroxide did show depolymerization of samples, but this may have been due primarily to thermal effects. Peroxide reactions resulted in excessive ring-opening which in turn allowed a large amount of condensation and an actual increase in MW and a loss of solubilized material due to filtration of condensed material. Additionally, the lignin in basic and acidic solutions showed a very noticeable buffering effect.

Subcritical water treatment of lignin samples resulted in a good mass balance for depolymerized materials in the liquid fraction; the extent of degradation was found to be more extensive than thought when looking at the GPC profiles.

CHAPTER I. Introduction

I.1. Significance of Lignin and Lignin Derivatives

Lignin, a plant component that constitutes the most common natural polymer containing an aromatic network, has been of interest in terms of chemical properties since the mid nineteenth century; early work centered on its structure and reactions.¹ Although many functional groups and linkages are known, the exact structures of natural lignin and technical lignins (byproducts of lignocellulosic refineries) are still not known, and research continues on lignin characterization.²

With the advent of papermaking mills, interest in lignin as a waste material that could be industrially utilized in the early twentieth century resulted in simple applications, with lignin used as a dispersive, tanning agent, adhesive and as a source of vanillin. By 1970, interest had turned to possible higher level uses for lignin.¹ Lignin was perceived as a compound which could be transformed into biodegradable products, as well as depolymerized into phenols for the chemical industry if separation into monomer species, e.g. containing one aromatic ring, from a complex crosslinked matrix could be accomplished.³

Lignin production is plentiful enough to serve as an industrial feedstock, and sources estimate that production could be increased.⁴ Worldwide production of lignin was estimated at 60 million tons a year in 2006.⁵ U.S. production of pulp at 40% of world total (in 2012)⁶ allows an estimation of U.S. lignin at about 24 million tons at about the same time.⁷ Thus lignin production in the U.S. is greater than the estimated 3.4 million tons of electronic waste⁸ and 10.5 million tons of plastics⁹ produced in the U.S., out of a total of 260 million tons of municipal waste dumped per year.¹⁰

I.2. Sources of Technical Lignins

The main source of lignin as waste is from the papermaking industry, although some lignin waste also emanates from liquid-fuel biorefineries. The majority of papermaking operations in the U.S. use the kraft delignification process or “sulfate process,” which relies on the use of sodium hydroxide and sodium sulfide.¹¹ A less common delignification process in the U.S. produces lignosulfonates as a side product of papermaking; the reaction combines sulfur dioxide and hydrogen sulfite with wood in the “sulfite process.” Both processes produce sulfur-containing lignin, although sulfur content in kraft lignin is less than 3%, while lignosulfonates contain up to 8% sulfur.⁶ Currently, low-grade applications and combustion constitute the major uses for the sulfur lignins.¹²

Most papermaking and biofuel operations combust lignin byproducts for energy¹³ and the amounts of lignin consumed are not well documented. Kraft lignin, with a higher energy content by weight than carbohydrates, is usually used on site at paper mills to fuel the mill itself. After wood residues are pulped by a chemical mix called white liquor and heated, cellulose and hemicellulose are separated as the main products for paper making, while lignin remains in a waste solution called black liquor. After a partial evaporation process, the liquor consists of 80% solids, but is conventionally burned in this liquid form in a kraft recovery boiler, which provides steam energy to the mill and also allows recovery of several pulping chemicals.¹⁴

Low-grade applications other than combustion are almost exclusively limited to lignosulfonates and include its continued utilization in low-grade applications, but it is also found more recently as a component in ceramics, dyes, drywall, and pesticides, usually as

an emulsifier.¹⁵ Lignosulfonates have also been successfully used as dust reducers on unpaved roads and as a binder in particle board.¹⁶

Interesting uses for lignosulfonates have also been found in the agriculture field as binders in animal feed pellets, and there has been some success in using lignin as an outside protective layer for slow-release fertilizers,¹⁷ especially if combined with calcium-containing compounds.¹⁸ Lignosulfonates have been used as matrices for chelating micronutrients,¹⁹ and some of these materials are sold commercially, although there are few published studies on the testing of the lignosulfonate-micronutrient complexes. N-Carrying fertilizers composed mainly of lignosulfonates, through the processes of ammonization and ammoniation of lignin, have been found to be beneficial to plants in at least one study.²⁰

Non-sulfur lignins are also extant: (1) soda lignin is produced from biomaterial treated with NaOH alone, (2) Klason lignin results from processing wood with sulfuric acid to solubilize the cellulose, (3) while cellulolytic enzyme lignin is obtained from wood treatment with carbohydrate-digesting enzymes. Milled wood lignin is produced by mechanical grinding by ball mill followed by extraction with a dioxane/water solvent.²¹ Organosolv lignin is produced through wood treatment with an aqueous organic solvent at 140 °C to 220 °C, and has the advantage of recovery of the solvent through distillation.⁶

Isolation processes for lignin (from lignocellulosic biomass) are summarized in Table 1, which also lists basic effects on lignin introduced by these treatments. Molecular weight (MW) as number-average molecular weight (M_n) and weight-average molecular weight (M_w) are also included, as well as the polydispersity index (PI), defined as M_w/M_n , an indication of how wide the distribution in molecular sizes exists within that type of lignin, post processing.

Table 1. General delignification process descriptions and M_n , M_w values for four types of technical lignins.

Technical Lignin Production/References	Kraft lignin	Sulfonate lignin	Soda alkaline lignin	Organosolv lignin
Process name	Sulfate	Sulfite	Soda (alkaline hydrolysis)	Organosolv
Process agents	NaOH, Na ₂ S	metal sulfite, SO ₂ ,	NaOH	Organics: methanol, ethanol, acetic acid, formic acid (acid catalyst)
Process description ^{15, 22,23}	High pH (basic), 150-170 °C, ether bonds cleaved, some condensation, lignin precipitated at pH 5 - 7.5	Hydroxyl groups sulfonated, lignin is solubilized; 140 - 160 °C, pH 1.5–2.0; ether bonds cleaved, benzyl carbocations formed.	Primarily non-wood biomass used; placed in pressurized reactor at 140–70 °C with about 15 wt% alkali base (usually NaOH)	Cleavage of ether bonds resulting in small MW species enables solubilization; 90 - 220 °C depending on source, ethanol (if used) 25 - 75% (v/v)
Chemical characterization ^{15,24}	Sulfur content 1- 2 wt% as thiols; hydrophobic; C=C bonds, fewer ether bonds, fewer methoxy groups	Highly crosslinked product (carbocation- π electrons attraction), 5 wt% sulfur as sulfonate groups (SO ₃ ⁻), preserving solubility	High carboxylic acid content, very dispersed, must be heated to coagulate. No sulfur, very pure (no hemicellulose)	Smaller MW, higher purity, hydrophobic, no sulfur
M_n (g mol⁻¹) ¹⁵	Softwood 3000	Not available	Wheat straw 1700	Hardwood 800
M_w (g mol⁻¹) ²²	1000–3000	20,000–50,000	800–3000	500–4000
Polydispersity Index (PI) (g mol⁻¹) ²² (M_w/M_n)	2.5–3.5	6–8	2.5–3.5	1.3–4.0

Additional details of technical lignin processing were necessary for GPC method development (Section I.C.) and interpretation of results of molecular weight (MW) distribution. Parameters of processing are often supplied by manufacturers, with more or less detail.

The kraft process, as indicated in Table 1, utilizes NaOH and Na₂S in a heated solution. This method dissolves lignin in a highly alkaline solution; if kraft lignin is not further treated and is dried, it has a pH of 8-10 if redissolved.^{25,26}

Alkaline or soda lignin, as indicated, involves use of NaOH or another strong base, and produces a sulfur-free lignin. Protobind 1000™ (GreenValue, Granit, Switzerland) is a mixed wheat straw/Sarkanda grass lignin processed by NaOH, which guarantees a product with a minimum of 90% lignin, so that cellulose and hemicellulose are still present (< 4%), although there is no sulfur present.^{27,28}

Occasionally a product marketed as “alkali or alkaline lignin” contains sulfur or is listed as “kraft lignin.” “Alkaline lignin” sold by TCI America (Portland, OR) has a stated pH of 8- 10, but also contains 20-29% sulfonate in the anhydrous form.²⁹ Sigma Aldrich, (St. Louis, MO) sells a “low sulfonate alkali (kraft) lignin” (product # 471003) with sulfur level specified as < 3.6% (at 3% water content) and a pH of 10 – 11. Sigma Aldrich also markets an “alkali (kraft) lignin” (product # 370959) with a pH of 5.5 – 7.5 and an unspecified sulfur content (at 10% water content).³⁰ The pH value of 5.5 – 7.5 reflects that fact that alkali lignin is typically retrieved from black liquor, the original alkaline solution, through acidification and precipitation.

Indulin AT lignin, distributed until recently by Meadvestvaco, Inc., and now supplied by Ingevity, Inc. (Charleston, NC), is an acidified kraft pine lignin produced as a byproduct of the paper industry.³¹ The acid hydrolysis process removes sodium and hemicellulose, although sulfur remains intact.³² The pH of indulin AT lignin (5–7) is slightly lower than that of alkali kraft lignin. Indulin C, also marketed by Ingevity, Inc., is an unsulfonated kraft lignin, advertised by the company as highly purified and highly functionalized in carboxylic acids as well as aliphatic and aromatic hydroxyl groups, with an alkaline pH of 9–10.

Lignosulfonate lignin is produced during delignification processes in which primarily α -O-4' ether bonds are cleaved by sulfurous acid (formed from SO₂ addition to the aqueous solution used in the sulfite process), where proton combines with a hydroxyl group removed from lignin to form water, and the remaining bisulfite group bonds to the lignin at the residual carbocation site to produce a sulfonate. The process may also use a sulfite salt of Ca, Mg, Na, Al or NH₄ along with, or in place of, sulfurous acid. The sulfite pulping reaction results in a higher percentage of sulfur, 3.5–8%, compared to alkali lignin, which is typically listed as 1–3%. The presence of sulfonate groups makes this type of lignin water-soluble.³³

A lignosulfonate lignin used in this study is produced by Borregaard Lignotech (Sarpsborg, Norway). Aro et al. stated that the typical pH of a sulfite process (and the lignin produced therein) as 1–5, although a neutralizing process entails a pH of 4–7. A commercial site listed its dark brown lignosulfonate product which contains sulfur as a “grade three” lignosulfonate, with a pH of 4–7;³⁴ however, additional lignosulfonate products had a variety of pH levels dependent upon the processing parameters enlisted. An additional product by Lignotech, marketed as Lignotech D-2495 (CAS 8061-53-8 for ammonium version and 8061-51-6 for the sodium version) is lighter in color than the dark brown lignosulfonate product, and has a pH listed in a Lignotech company missive as being between 4–6.5. The sulfur content is 6.8% and it is listed as an “ammonium/sodium lignosulfonate powder for use as a general dispersant or binder.”

Dealkaline lignin is produced through dealkalization of black liquor, a solution of solubilized lignin produced during the papermaking process. TCI America (Portland, OR) describes dealkaline lignin marketed by their company as starting out as sodium

lignosulfonate (TCI product # L0098) which is subjected to desulfonation (partial), oxidation, hydrolysis and demethylation. The result is a lignin which still retains sulfate (10 – 20% based on anhydrous mass) and has a pH of 3 – 4. The TCI dealkaline lignin (TCI product # L0045) is then used as a base to produce TCI alkaline lignin (TCI product # L0082) by adjusting pH up to 8 – 10.


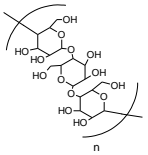
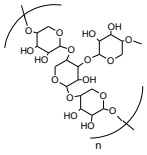
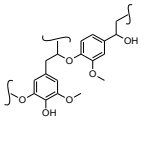
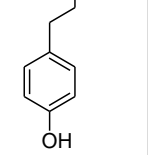
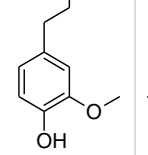
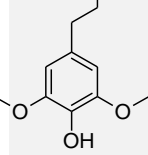
I.3. Chemical Structure of Lignin

The exact structure of native lignin and technical lignins (industrial derivatives of lignin) has been elusive, although several early studies have provided evidence as to many of the functional groups and linkages within the crosslinked mass of lignin; researchers included Klason (1898, lignosulfonates),³⁵ Erdtman (1933, phenol and coniferyl alcohol reactivity),³⁶ Lange (1944, spruce lignin),³⁷ and Freudenberg (1965, spruce lignin),³⁸ as well as Adler (1977, numerous wood types).³⁹ More advanced instrumental techniques have been utilized since the 1990s; researchers who pioneered instrumental analysis of lignin from the 1950s to 1990s include Goldschmid (UV-Vis),⁴⁰ Hergert (FTIR),⁴¹ Lundquist (NMR),⁴² and Gellerstedt (SEC).⁴³ Simulation programs are now validated with HSQC-NMR spectra of compounds with specific functional groups and linkages.⁴⁴ It is best to recall, however, that lignin structure, particularly of technical lignins, can vary widely, depending on the source of lignin (feedstock), the isolation process used to obtain the lignin, and the preparation for analytical studies.

Lignin consists of three basic phenylpropanoid (monolignol) units of *p*-coumaryl alcohol, coniferyl alcohol, and sinapyl alcohol. Once linked together by several different linkages, the monolignols become *p*-hydroxyphenyl (H), guaiacyl (G) and syringyl (S)

units, respectively (see Table 2 for structures).⁴⁵ The lignin network forms randomly within the plant cell wall and serves as support and as a barrier to outside attack. Percentages of compositional lignin (as opposed to cellulose and hemicellulose) and percentages of H, G and S units for hardwoods, softwoods and herbaceous plants are shown in Table 2.

Table 2. Softwood, hardwood and herbaceous plant composition as percentages of cellulose, hemicellulose and lignin,⁴⁶ as well as H, G, S unit percentages.⁴⁷

<p>48</p> 						
Biomass	Cellulose (%)	Hemicellulose (%)	Lignin (%)	Hydroxyphenyl (H)	Guaiacyl (G)	Syringyl (S)
Softwoods	33 - 42	22 - 40	27 - 32	< 5	>95	0
Hardwoods	38 - 51	17 - 38	21 - 31	0 - 8	25 -50	46 -75
Herbaceous plants	0 - 40	20 - 50	25 -95	5 - 33	33 - 80	20 - 54

Eight main linkage groups are illustrated in Figure 1. Other linkages also occur, but are found in low percentages. Among the eight types listed, the β -O-4' linkage is by far the most important, constituting 43 – 84% of the linkages in trees and plants. This is followed by the β -5' bond which ranges from 3 – 12%, and is quite a bit less abundant. The other linkages are less abundant than the β -5' bond.

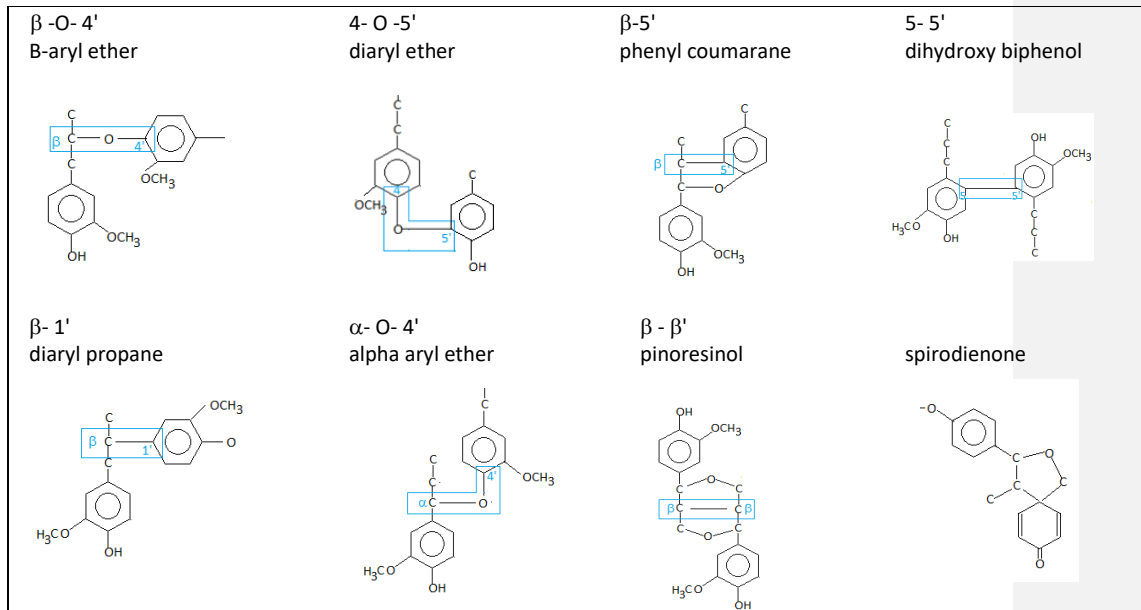


Figure 1. Major linkage groups in lignin with outlines of the exact linkages. Figures based on the data by Doherty et al.¹⁵

An illustration of the β -O-4' ether bond is shown in Figure 2, with α , β , and γ carbon positions in relation to the aromatic ring and numbering for both rings in relation to the bond.

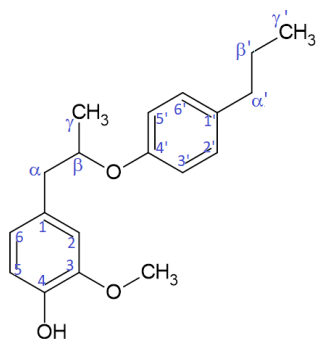


Figure 2. A section of lignin with two aromatic rings, showing the β -O-4' ether bond with ring numbering and carbon designations.

The percentages of each linkage in hardwoods, softwoods and plants differ according to the source. Table 3 shows linkage percentages presented in a study by Rinaldi et al.⁴⁹

Table 3. Lignin linkage occurrence by percentage in softwoods, hardwoods and plants,¹⁵ 'nd' denotes 'not determined.'

Biomass	% β -O-4'	% 5-5'	% β -5'	% 4-O-5'	% β -1'	% α -O-4'	% β - β '
Softwoods	43 - 50	5 - 7	9 - 12	4	1 - 9	5 - 7	2 - 6
Hardwoods	50 - 65	< 1	3 - 11	6 - 7	1 - 7	< 1	3 - 12
Herbaceous plants	74 - 84	nd	5 - 11	nd	nd	nd	1 - 7

A study by Constant et al. determined the β -linkages and H, G, S content in technical lignins by combined FTIR, pyrolysis-GC-MS and 2D HSQC-NMR analyses, as shown in Table 4;⁵⁰ note that the occurrence of linkages and monolignol groups are reported as number per 100 aromatic groups. This gives a good insight into relative linkage and monolignol content for several technical lignins.

Table 4. Number of linkages and monolignol units per 100 aromatic rings for several technical lignins.⁵⁰

Technical lignin	β -O-4'	β -5'	β - β '	H	G	S
Indulin kraft	6.1	0.3	1	3	97	0
Soda	3.4	0	0.7	11	39	50
Organosolv Alcell	5.3	0.8	2.8	0	37	63

The linkage most often cleaved is the β -O-4' bond, which constitutes 43 - 84% of lignin linkages in trees and plants, but breakdown does not necessarily produce monomers as products. However, the low bond dissociation energy of the β -O-4' bond makes it a primary target, followed by other ether bonds. Carbon-carbon bond energies are higher and require typically high temperatures or catalysts in order for bond disruption to take place. Bond dissociation energies of several lignin linkages are listed in Table 5; Parthasarathi calculated bond energies using DFT theory -based M06-2X hybrid exchange-correlation functional and the 6-311++G(d,p) Gaussian basis set.⁵¹ Values supplied by Huang et al. were theoretically calculated through computational simulation by using the density functional theory basis set B3P86/6-31G(d,p).⁵²

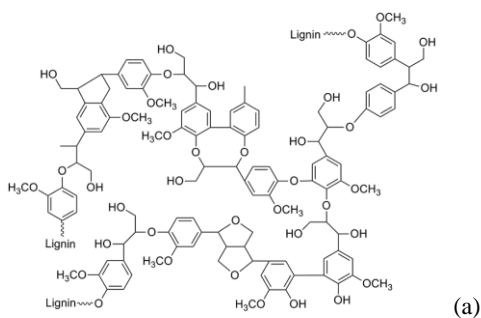
Table 5. Bond dissociation energies (kcal/mol) for common lignin linkages. *The β -1' linkage reported here for the Parthasarathi et al. study was based on their $C\alpha$ - 1' bond dissociation energy.⁵¹

Bond dissociation energies (kcal/mole)	β -O-4'	5-5'	β -5'	4-O-5'	β -1'	α -O-4'
Bond in linkage	(C_β - O)	(5 - 5')		(4 - O)	(C_β - 1')	(C_α - O)
Parthasarathi et al. (2010) ⁵¹	65	115	130	81	70*	53
Huang et al. (2015) ⁵²	50	116		68	83	44

It is of note that the values provided by the computer simulations were based on the actual chemical bond, not the linkage group. Beta and alpha carbon linkages to oxygen in

the ether links had lower dissociation energies than the connecting oxygen bond to a carbon on benzene, the other half of the ether linkages. This established where the cleavage occurs in the ether linkage groups. Parthasarathi et al. determined average bond energies for a variety of compounds.⁵¹ The Huang et al. study averaged the values for 63 lignin model compounds and the average values are reported here in Table 5.⁵² Simulations for a number of compounds showed that methoxy groups had little influence on the bond energy if they occurred on the ring connected to the aliphatic carbon in the ether bonds, but did have influence if they occurred on the ring connected to the oxygen in the ether bond. Additionally, substituents located on aliphatic carbons influenced the ether bonds, particularly carbonyl groups which lowered the energy of the bond, while substituents on the aromatic rings had little influence.⁵²

There are a number of proposed structures for lignin, although the overall structure may differ somewhat depending on the wood or plant source for the lignin. Two examples are shown in Figure 3, where 3a represents lignin with bond angles that are most likely, while 3b shows a version where linkages are emphasized.



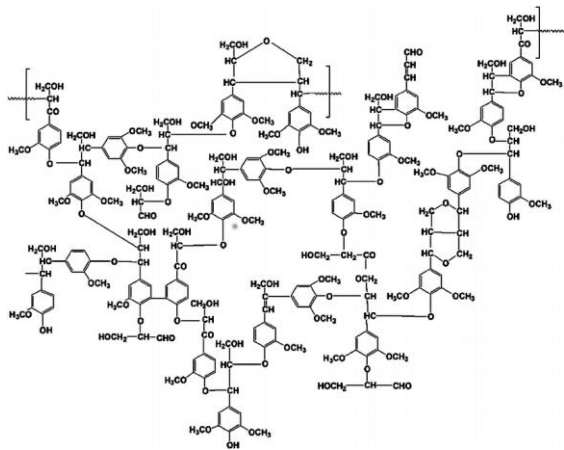


Figure 3. (a) Lignin (general),⁵³ (b) European Beech (hardwood) lignin.⁵⁴

Kraft lignin, the primary lignin investigated in this study, has been studied extensively for structure, linkages and reactions; it has been characterized fairly well by researchers such as Marton (1971, softwood kraft lignin),⁵⁵ Gierer (1985; kraft, soda and sulfite lignins),⁵⁶ and Sjostrom (1993, many applications),⁵⁷ and others. Several researchers have proposed possible structures for kraft lignin (Figure 4).

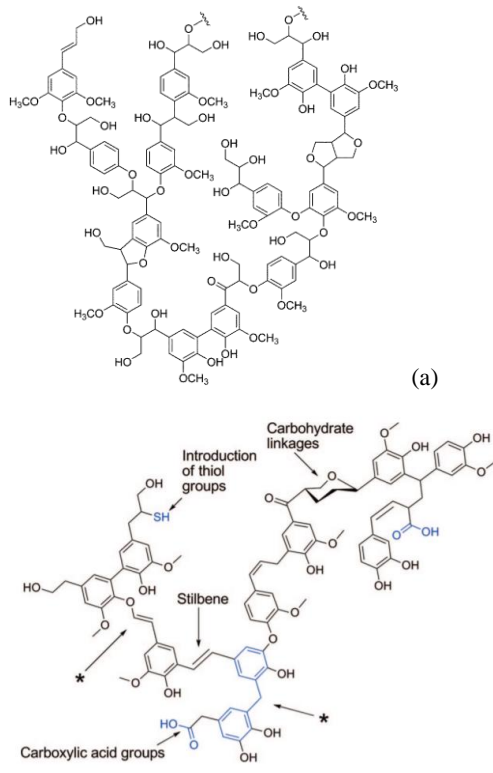


Figure 4. Proposed structures of kraft lignin by (a) Rak et al.⁵⁸ and (b) Zakzeski et al.⁵⁹

The main differences between unadulterated lignin and kraft technical lignin are: (1) a reduction in β -O-4' bonds, (2) an increase in free phenolic OH groups, (3) fewer methoxy groups, (4) increased number of C = C bonds and (5) added sulfur bonded to aliphatic carbon (1-3%).²⁴ A study by Xue et al. monitored the incidence of eucalyptus (hardwood) lignin after one hour and five hours of soda (alkaline) processing, closely related to kraft processing (alkaline NaOH used as depolymerization agent, without Na₂S) with results shown in Table 6. The beta linkages clearly decline during the soda process and demethoxylation is indicated by the decreasing S/G ratio.⁶⁰

Table 6. Semiquantitative estimation of relative content of interunit linkages in lignin during soda processing, using 2D HSQC-NMR spectra.⁶⁰

Kraft processing	% β-O-4'	% β-5'	% β-β'	S/G ratio
1 hour processing	23.3	1.0	10.4	1.8
5 hours processing	16.4	0.4	7.1	1.6

Major chemical reactions of the kraft process have been outlined by a number of researchers.^{61, 62} Functional groups can be added to the structure of lignin through attack by the OH- and/or HS- ions. These include carbon-carbon double bonds between the alpha and beta carbons (or beta and gamma carbons) to the phenol ring as well as sulfur addition to the alpha carbon.⁵⁹

Changes produced in technical lignins by isolation processes are significant for strategies to further depolymerize the lignin and for its reactivity and use in industrial applications. Increase in OH groups can affect viability as a possible fuel source or reactivity in composites, while increased C=C groups also affect reactivity. Demethoxylation during the process leads to increased bonding sites, although it may eliminate certain monomers from being available upon depolymerization. The content of sulfur in kraft and liginosulfonate lignins limits the uses of either, and the deleterious effect of sulfur on catalysts may limit certain forms of depolymerization. molecular weight is a particularly crucial aspect of lignin, especially if the polydispersity index is large. For industrial applications, a limited range of molecular weight is generally required, while in laboratory applications it is an indication of the effectiveness of a depolymerization method.

I.4. Molecular Weight Determination of Lignin

I.4.1. Overview of Methods Used to Determine Molecular Weight

I.4.1.1 Non-SEC based methods

Several methods are currently used for the determination of molecular weight of lignin samples; the most common include evaluation by osmometry, viscometry, end-group analysis, light scattering and size-exclusion chromatography (SEC), which includes gel permeation chromatography (GPC) and gel filtration chromatography (GFC).^{62, 63} Methods can be absolute or secondary; the former does not require calibration, while the latter method requires calibration with standards. Osmometry, viscometry and light scattering are absolute methods, which yield an average molecular weight for a sample. If molecular weight distribution is needed, these methods have to be combined with SEC, typically as gel permeation chromatography (GPC), which is a secondary, or inferred method. Light scattering is absolute only if SEC is not used in conjunction with it.^{62, 63}

Of the main methods of MW determination, end-group analysis is possible only if end-groups are able to be chemically analyzed, and the method also loses accuracy with the presence of long chain lengths in the sample.⁶² Vapor-pressure osmometry (VPO), dependent upon colligative properties (concentration) of the solution,⁶⁴ is considered to be effective for molecules with weights less than 25,000 g/mol.⁶³ Cryoscopy, a more unusual method of MW determination, is also a method dependent on colligative properties (concentration) of the solution; both osmometry and cryoscopic methods are detrimentally influenced by lignin-solvent associations.⁶⁴ However, osmometry, by use of osmotic

pressure calculations, can give important information on whether molecules are aggregated or homogeneous in solution.⁶²

Viscometric methods for determining MW are used widely in industry.⁶² Capillary viscometry works on the assumption that longer chains are proportional to viscosity; the flow time of the solution is compared to the flow time of the solvent alone. As long as solution concentration is low and similar to solvent density, the flow time ratio is assumed to be equal to the viscosity ratio. Intrinsic viscosity (the inverse of molecular density) and the Mark-Houwink equation are used to determine MW of the sample.

Static light scattering (SLS) with a viscometer allows calculation of intrinsic viscosity which relates molecular size to MW, although the relationship is not always in constant proportion.⁷² Some software packages are capable of backcalculating MW when using differential viscometry; elution volume and intrinsic viscosity are measured directly and hydration response is established with standards.⁶⁵

Molecular size is not to be confused with molecular weight; however, the measurements of particles referred to as hydrodynamic radius and radius of gyration are associated in some cases with molecular weight measurements. Common methods for particle size analysis include differential static light scattering (DSLS), multi-angle light-scattering (MALS) and SLS/intrinsic viscosity, which are all light-scattering methods. SLS molecular size is based on the radius of gyration (R_g), also called root-mean-square radius. Hydrodynamic radius (HR) is based on the comparison of a sphere that diffuses at the same rate as the sample molecule and is calculated from intrinsic viscosity or DLS. DLS calculates diffusion velocities from scattered light intensity, gathered in real time (typically

for batch modes). The diffusion velocities, when entered into the Stokes-Einstein equation, yield particles sizes.⁶³

Light scattering is an absolute method of M_w determination (average MW); however, SEC is needed if a MW distribution is desired. If calibration is required, the method is no longer an absolute method. A light source, typically a laser source, is shone on the sample, resulting in absorption and re-emission as scattered light (emitted in many directions and not as a coherent beam). Scattered light intensity is detected and measured against the incident light intensity. The incident light can be shone from several angles, which is reflected in the method name: low-angle light scattering (LALS), right-angle light scattering (RALS) and multi-angle light scattering. The latter method is the most used among these methods.⁶²

Light scattering is also categorized by how light intensity is processed; static light-scattering measures average intensity over a defined time period, while dynamic light scattering (DLS) measures intensity fluctuation over very short time intervals. SLS is the only one of the two methods that is usually used with SEC because the acquisition time is manageable. Light scattering can also be combined with a viscometer.⁶³

RALS works on the assumption that intensity from scattered light is equal from all directions, which is not well suited to anisotropic scatterers (substances which produce varied intensities in different directions). LALS attempts to correct for anisotropic scattering but does not detect well for smaller molecules; RALS/LALS in combination are often used. MALS is efficient for all molecules but does not work well for very small particles.⁶³

1.4.1.2. SEC methodology and advantages/disadvantages

Gel permeation chromatography (GPC) and gel filtration chromatography (GFC) are types of size exclusion chromatography (SEC), although some studies refer to GPC and SEC as being interchangeable terms.^{62,66} Gel filtration chromatography (GFC) is a type of chromatography done via liquid chromatography (LC) with low pressure aqueous mobile phases and is used often for analysis of biological compounds,⁶⁷ while synthetic polymers and plastics require an organic mobile phase and GPC customarily is used for these applications, also via LC.⁶⁸ An advantage of SEC is the short analysis time, where flow rate can be set to enhance resolution and the amount of solvent used is minimal. However, the rapidity of the method also leads to a loss of resolution, particularly for similar sized compounds. Resolution can be improved, however, with a larger volume column or several columns linked together.⁶⁹

GPC methodology employs a size exclusion principle to separate analyte particles principally on the basis of steric interaction with a microporous gel layer. Dissolution of the sample into an appropriate solvent (the mobile phase) is a preparative step for injection into a mobile phase; for GPC the solvent is organic and can include alcohols, ketones and esters, as well as solvents known to work well with lignin: moderately polar tetrahydrofuran (THF) and polar aprotic solvents dimethylformamide (DMF), dimethylacetamide (DMAc) and dimethyl sulfoxide (DMSO). Solvents sometimes used include hexane, diethyl ether, dioxane, dichloromethane and other related compounds, but these are discouraged due to safety and environmental concerns.⁷⁰

Subsequent elution (via LC pump pressure) of the mobile phase through a column lined with an adsorbent bed consisting of a gel material of varying pore sizes (stationary phase), prompts the size exclusion effect. This effect allows larger molecules (larger hydrodynamic radius) to elute first by bypassing small, more tortuous pathways which are traversed by smaller molecules. Column stationary phases consist of porous gel beads which are semipermeable; the gel can consist of polystyrene-divinylbenzene (PS-DVB), silica and other specialized phases. The range of pore sizes is well defined and the material must be stable, inert, and have a uniform particle and pore size for better resolution.⁶⁹ Columns can be analytical, primarily used for determination of molecular weight distribution, and preparatory, whereby separation of compounds is accomplished for separate collection. Ideally, separation is based solely on particle size and not on chemical interactions between molecules themselves or with the stationary phase.

The elution is based on the retention of the particle within the pore pathways, but may also depend on “absorption” to the gel material coating the passageways; the attraction of the solute to the gel will produce a non-ideal situation where travel is slowed and/or material is retained. This is more likely to occur when solvents like DMF, which are at least somewhat hydrophilic, interact with PS-DVB gels.⁶⁹ Equally undesirable are “association” effects where separate particles of the sample become bound together and give a falsely large particle weight. Lignin contains hydroxyl, carboxyl and ether groups, and can be susceptible to hydrogen bonding, stereoregular association (van der Waals attraction along well-ordered chains), and possibly charge transfer (electrostatic attraction); these can be difficult to manage in aqueous solutions.⁷¹ However, organic solvents/mixtures, particularly

THF/water, can be effective solubilization agents, minimizing interactions with biopolymers (and self-interaction).⁷²

In concentration detectors (RI, UV), signals are based on the fact that the analytes have been effectively separated on the column, tend to form a coil conformation, and produce a signal which has an intensity proportional to the concentration of particles of various sizes. The signal is temporally related to a “retention” time (or more appropriately, retention volume) of the particles.^{63, 67}

UV/Vis, refractive index (RI), viscosity and light scattering are common detectors, and can be used in combination for more accurate results. The most effective detection of molecular weight combines a concentration detector (UV/Vis, RI) with a molar mass detector (viscometer, light scattering) in order to compare molecular weights determined in different ways, or at least to combine two concentration detectors.^{64, 73}

Solvents used with SEC can be categorized primarily as either aqueous (typically with buffers), for GFC analysis, or organic; the latter are varied and range from polar solvents such as DMF and DMSO to nonpolar organic solvents such as THF, chloroform or toluene. Ovens on some LC models can heat columns and detectors to impose thermal conditioning, which decreases thermal fluctuation, which in turn may improve retention time and detector response consistency. Heating also decreases the viscosity of solvents and thus backpressure, particularly the very viscous such as trichlorobenzene. Solubility of samples can be problematic, especially for samples with organic and polar components which vary with pH, such as lignin.

GPC columns are manufactured by several companies and typical stationary phases include polystyrene, poly(styrene-co-divinylbenzene), silica, or cross-linked poly(methyl methacrylate), with a vast array of pore sizes and column diameters. The poly(styrene-co-divinylbenzene) column is the most common as the absorptive properties towards commercial polymers is low.⁷⁴ The specific arrangement is proprietary to the company, as are additional groups which act as deactivators or perform some other function related to a specific solute.

Polymethacrylate-based stationary phases are usually used for aqueous mobile phases alone, while silica and polyimide-based columns are used for aqueous, nonpolar and polar organics, depending upon modifications.

GPC does not evaluate molecular weight in an absolute sense and analysis of data requires that a calibration curve be constructed for the samples in a sequence run through the instrument. The choice of calibration standards tends to be based on narrow-distribution molecular weight standards which comprise a discrete range of molecular weights which are predicted to be represented in the sample. Many standards chosen for calibration are commercially available and are designated by the M_p (molecular weight of the peak of a narrow distribution curve) of the standard.

Once samples are analyzed within a sequence containing the standards, a calibration curve is made which relates $\log(M_p)$ vs retention volume in a linear equation, and unknown sample retention times yield a molecular weight by comparison to the curve. The molecular weight resulting from the curve can be used to calculate several different types of molecular weights which depend on the mathematical operation performed; these include

M_n (number average), M_w (weight-average) and M_z (z or centrifuge-average) molecular weights as the most commonly calculated forms:⁷⁵

$$M_n = \frac{\sum N_i M_i}{\sum N_i} \quad [1]$$

$$M_w = \frac{\sum N_i M_i^2}{\sum N_i M_i} \quad [2]$$

$$M_z = \frac{\sum N_i M_i^3}{\sum N_i M_i^2} \quad [3]$$

M_n , M_w and M_z appear on a symmetrically distributed, one-mode molecular weight profile in Figure 5.

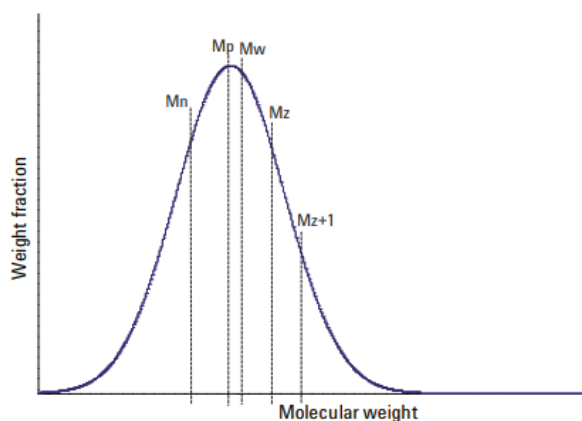


Figure 5. Placement of M_p , M_n , M_w , M_z and M_{z+1} on a symmetrically distributed, one-mode molecular weight profile as molecular fraction vs molecular weight.⁷⁵

Although GPC is considered to be a powerful method of molecular weight determination, with a number of advantages, there are drawbacks, as pointed out in many studies, as well as gray areas in terms of standardization of the method.

Advantages of GPC have also been enumerated by numerous researcher, these include having a large range of solvents and columns available for many types of analytes, and a relative ease of use for many forms of the method. Others have pointed out that the signal depends on hydrodynamic size, which is dependent on the solvent and on the solute relationship to the standards, and is also dependent on interaction with the stationary phase, as well as on the solute conformation.⁶² Lange et al. described SEC as an effective method but believed that it had a number of problems stemming from solubility, standards selection and detector sensitivities.⁶⁴ Industrial evaluators extolled GPC as a powerful technique for measuring MW distribution but recommended that light scattering and/or viscometry should be used in conjunction with it.⁶³

The need for derivatization of lignin is not a universally accepted idea,^{62,64} although several studies,^{65,76-78} did perform some type of derivatization of lignin, particularly acetylation. Derivatization in this case is comprised of replacing active hydrogens (in OH groups) with an acetyl group, although silyl, alkyl, and acyl units, as well as others, could also be used. Derivatization can be used to protect functional groups, make the solute visible to detectors, improve solubility or prevent bonding to a solvent or stationary phase. The most cited reason for acetylation of lignin, if mentioned, was to improve solubility in an organic solvent like THF.^{74, 83} However, validation of the method by determining MW by a different approach was not done by any of the studies.^{65,76-78} Asikkala et al. compared molar masses of the pure softwood kraft lignin to the same samples with acetic acid added to a solution, and found little difference in molar mass, but this experiment was not performed with acetylated lignins.⁷⁸

Compared to results from a number of studies with acetylated kraft lignins, a study by Delado et al., also with acetylated softwood alkali kraft lignin, showed a M_w value of 15375 g/mol,⁷⁷ which was quite high in comparison to the more modest range of about 4500 to 6500 g/mol for other studies,^{76,78} while a study by Chen and Li, which did not mention any derivatization at all, had a M_w of 19650 g/mol for kraft lignin (hardwood).⁷⁹ Due to the use of different feedstocks as well as lack of comparison to other methods, it is not clear whether acetylation produces any advantage in MW determination.

Oberlechner et al. believed that there was some evidence that acetylation causes a loss of low MW particles and degradation of high MW molecules,⁶² while another researcher objected to the practice of derivatization because it led to structural changes in lignin.⁶⁴ A study by Schmidl showed that non-derivatized lignin yielded results via GPC analysis similar to results yielded in studies which used acetylation; this was achieved by using the appropriate column and mobile phase.⁸⁰

Another facet of the derivatization debate was addressed by Asikkala et al., who suggested that acetylation protocols for GPC methods with styrene-DVB stationary phases and THF mobile phases are problematic in a number of studies because complete acetylation was difficult to achieve, thus leading the author to propose some sort of standardization.⁸¹

On the other hand, Asikkala et al. found that derivatization could lead to better control of association and absorption effects. Polar associations were minimized in aqueous solutions by acetylating with acetic anhydride in pyridine, although the method required long reaction times. Asikkala et al. also investigated a method whereby acetyl bromide in glacial acetic acid was used as a derivatization agent in a THF mobile phase to minimize

association effects. One of the advantages of this method was the short reaction time at room temperature. The authors contended that if association effects did not cause extensive distortion, analysis without derivatization could take place with the correct column and conditions.⁷⁸ This aligned with findings in a study by Andrianova et al.⁸¹

Although there is substantial evidence that acetylation can be avoided by developing a method with a suitable column and stationary phase, a number of studies employed this technique despite concerns that it may produce structural changes as well as association and absorption effects when used. Derivatization can involve several different agents, and acetylation methods themselves can vary considerably as well, making the process non uniform.

Another area of debate is whether aqueous (GFC) or organic (GPC) mobile phases are best for MW analysis. It is clear that aqueous phases have far more problems with association and absorption problems; Chen and Li found that pH had to be kept at 7 or above for aqueous phases. If pH was lower, absorption effect was enhanced, as was made clear by comparing peak areas at different pH values (when the solute is absorbed on the column, less of it elutes). They believed that hydrogen bonding was responsible for the absorption between lignin and the stationary phase, which was polar. However, solubility at around pH 7 was fine for lignosulfonates, but kraft lignins had to be dissolved in an aqueous phase of pH 12, which proved to be deleterious to the column.⁷⁹

Hydrogen bonding was also thought to be the reason for association (linking of solute molecules) between lignin solute particles by Glasser et al., although this was not directly linked to aqueous mobile phases.⁶⁵ Asikkala contended that association effects occur with organic solvents as well as aqueous solvents, including DMF, DMSO, and

THF,⁷⁸ although Schmidl found association problems common in polar solvents only.⁸⁰ A study by Andrianova et al. found that glucose-divinylbenzene (GDVB) stationary phases in GPC columns created retention problems for PMMA standards and lignin in comparison to polystyrene divinylbenzene (PSDVB) stationary phases, probably due to hydroxyl group interaction between analyte and mobile phase.⁸¹

Glasser et al. found that a low hydrodynamic volume for lignin, which was more compact and spherical, was optimized in THF; low hydrodynamic volume is nearer to true volume of the solute and is more likely to represent true molecular weight. This study used RI and differential viscometer detectors, and utilized Viscotec Unical 2.71 software to calculate hydrodynamic volumes from a hydrodynamic response established through standards used with the viscometer; the response was represented as a linear relationship between elution volume and hydrodynamic volume.⁶⁵

Additional dilemmas are due to the use of an aqueous mobile phase include ion exclusion (some components of the solute absorb to the mobile phase while others do not), ion exchange, and increased hydrodynamic volume- effects that tend to be minimal with organic mobile phases. The latter problems are related to the polarity of the mobile and stationary phase and their attraction to polar components in lignin. Chen and Li found that these secondary effects were minimized through control of ionic strength as relatively high ionic strengths (but not too high) helped to minimize the hydrodynamic volume and reduce absorption.⁷⁹ Although the authors tried several ionic strength values in solution, these had varying effects, creating the impression that ionic strength would have to be carefully tested for each set of method parameters being used, making it difficult to standardize an aqueous approach.

Schmidl tested an aqueous mobile phase as well and was forced to institute a very high pH (13) when evaluating kraft and organosolv lignin in order to make them soluble. He found that a significant damage occurred to quartz cells, quartz windows and column fittings.^{80,82} Many columns do not tolerate high pH or even sudden changes in pH.⁸² Overall, the resolution for average MW and retention times between lignin types was lacking and molecular weight values were well below low-angle laser light scattering (LALLS) measurements. The study noted an increased spherical shape with increased ionic strength, leading to increased retention times, seemingly due to charge repulsion with the mobile phase.⁸⁰

Although GPC may avoid common pitfalls of GFC (absorption of analyte to polar stationary phase, association between analyte molecules, high pH and use of buffers), this version of molecular weight analysis is not without problems. Some researchers find derivatization time-consuming and also find that the eluents are very expensive.⁷⁹

Although he did not find aqueous mobile phases effective, Schmidl believed that solubility of lignin in THF was inconsistent, but also contended that varying amounts of water as a contaminant affected the results; he preferred VPO and LALLS detectors.⁸⁰ Andrianova et al., however, found that solubility was consistent for a THF:water 1:1 ratio, after which THF was added until water was < 10%, and that detection via DAD and ELSD yielded similar results.⁸¹

Schmidl also used DMSO as an eluent, with LiBr present, on a Jordi Gel GBR (glucose-divinylbenzene stationary phase) column and found that absorption was not a problem due to the deactivated column, and that lignin association with DMSO was broken

up by the use of LiBr. However, different levels of LiBr produced a wide variation in results and LALLS values still differed from the DMSO molecular weights.⁸⁰

The question of which detector is most suitable is also of important consideration in GPC methodology. As stated earlier, M_v (viscosity molecular weight) is not equal to M_w (weight-average molecular weight), although viscometry is commonly used in industry. Because of the preference for more exactitude in research, it is used primarily as a detector in line with other types of detectors. Although viscometry and light-scattering detectors are considered to be more sensitive to MW than UV and RI detectors,⁷³ viscometric detectors are also known to be more sensitive to high MW, while RI detectors are concentration dependent.⁷⁴

Last, but certainly not least, of the contentious issues associated with GPC is the question of appropriate calibration standards. For organic mobile phases these are typically polystyrene (PS) commercial standards, and for aqueous systems these are often some form of methacrylate. There is a concern that standards that do not have the same structure and conformity as lignin, including hydrodynamic volume, and thus will not behave similarly in the porous media of the column and may also be subject to interactions with the GPC environment that lignin does not experience. Properties such as branching and viscosity may also affect retention. Lange et al. stated that PS standards produced error in MW calculations because of this, although the same study also considered the difference in estimated MW to not be substantial.⁶⁴ A number of studies looked at MW determined through the use of low molecular weight lignins and commercial standards and found that results were nearly the same or differed very little.^{62,66} Thus, the widespread use of commercial standards is continued (and even promoted) in the interests of ease, availability

and standardization.⁶⁴ Andrianova et al. showed that polymethyl methacrylate (PMMA) standards (with polar sites) and polystyrene (PS) together formed linear calibration curves when column, mobile phase and other method parameters were chosen carefully.⁸¹

However, several studies have instituted unusual standards or methods of calibration that have achieved reliable results. Sameni et al. conducted an SEC investigation of indulin and kraft lignin by utilizing a column with a sulfonated styrene-DVB copolymer stationary phase, which tolerated pH levels of 7–13, and an alkaline mobile phase (0.1 M NaOH).⁹⁰ Sodium polystyrene sulfonates were used as standards; M_n and M_w values were somewhat lower than for other studies investigating kraft lignin, but values varied widely for the reviewed kraft studies.⁸³

The choice of detector is less obvious, but practicality may dictate the continued popular use of UV/Vis and RI detectors, although there is some indication that light-scattering will become commonplace, especially in combination with UV or RI, within the near future. LALLs and viscometric results for MW values are sometimes substantially higher than more conventional methods for one type of lignin but are similar to other light scattering methods for similar types of lignin.^{65,84} RDI methods, although not considered to be particularly sensitive, produced values which were very high for some types of lignins in one study.⁷⁹ In inspecting a fair number of studies, a great deal of variability seems to exist for most detectors, although this may be due to interaction with other method parameters.

Although the choice of detector is important, it appears that UV in conjunction with light scattering would seem to be quite powerful; however, UV detectors alone are often used in lignin studies as lignin absorbs well between 250 – 280 nm (Table 7). Perhaps of greater priority is the question of column and mobile phase choice. Although aqueous

methods seem to be effective, fine-tuning is clearly necessary and results could vary with a change in column or detector. Methods with organic mobile phases seem more robust and less dependent on changes in other method parameters, and clearly have very little trouble with stationary phase interactions or association, particularly with mobile phases with little or no polarity.

The main trouble with organic solvents is the question of solubility and a possible inconsistency in the types of particles that achieve dissolution. Avoidance of derivatization is applaudable since there exists a shared opinion amongst many that structural changes in lignin do occur, but practically speaking it may be of more benefit to acetylate and possibly include higher MW particles that might not otherwise be included.

GPC has been said to be best for determining relative molecular weights, although it appears that absolute methods of molecular weight evaluation also may be linked to and defined by the surrounding parameters of the method used. A number of studies utilizing GPC or GFC to investigate technical lignins are outlined in terms of methodologies and results for molecular weights in Table 7.

Table 7. Molecular weight and polydispersity comparison by lignin source and GPC method, for indulin AT, indulin C, lignosulfonate, soda pulping and kraft alkaline lignins. (The abbreviation r.t. is used for room temperature).

Lignin type	M _n	M _w	PI	Lignin Source (and if acetylated)	Lignin Concentration	Column (GPC)	Mobile phase	Flow rate	Volume injected	Temp.	Detector	Standards	References
Kraft alkaline	866	2565	12.34	Kraft black liquor, acidified to pH 2		PSS MCX column- (sulfonated styrene-divinylbenzene copolymer)	0.1 M NaOH solution		25 µL	r.t.	UV, 280 nm.	sodium polystyrene sulfonates	Sameni et al. (2016) ⁸³
	1598	15375	9.62	Pine alkali kraft, precip. at pH 3, acetylated	0.2% (wt/v) (2 mg/mL)	Ultrastyrigel (100, 500, 1000 Å) in series	THF	1 mL/min	100 µL		Photodiode array (PDA)	PS	Delgado et al. (2019) ⁷⁷
	1000	4500	4.50	Filtered and precip. black liquor from kraft process; acetylated		Styrigel HR2, HR1, Ultrastyrigel 104 Å in series	THF	0.8 mL/min			410 RI	PS	Brodin et al. (2009) ⁷⁶
	1000	3300	3.30	Hardwood kraft-derivatized with acetic anhydride in pyridine	1 mg/mL	Styrigel HR-5E and Styrigel HR-1, in series	THF	0.5 mL/min			UV, 280 nm., RI	PS	Asikkala et al. (2012) ⁷⁸
	1000	3900	3.90	Hardwood kraft-derivatized with acetyl bromide in acetic acid	1 mg/mL	Styrigel HR-5E and Styrigel HR-1, in series	THF	0.5 mL/min			UV, 280 nm., RI	PS	Asikkala et al. (2012) ⁷⁸
	7523	19650	2.70	Kraft Birch-from Tianjin Institute	3 mg/mL; filt 0.45 µm.	Ultrahydrogel 250 and 1000 columns	0.01 M NaOH/aqueous, pH 10-12	0.6 mL/min	100 µL		Differential refractometer	Pullulan, PEG	Chen and Li (2000) ⁷⁹
	1510	2330	1.54	Alkaline-extracted lignin from ball-milled Poplar.	2 mg/mL	Plgel mixed-B, 7.5 mm ID (styrene-DVB copolymer and derivatives)	THF	1 mL/min		r.t.	Unspecified	Mono-disperse PS	Yuan et al. (2013) ⁸⁵
	GPC: 1900 Indulin AT; 1630 Alkali kraft	GPC: 3060 Indulin AT; 2740 Alkali kraft	1.6 Indulin AT; 1.68 Alkali kraft	Indulin AT, alkali kraft lignin (Meadwestvaco, Inc., Sigma); some samples acetylated for comparison	1 - 10 mg/mL (0.1 - 1%)	Jordi Gel GBR, PLgel 1000 or 500 Å	THF, unstabilized	1.0 mL/min	100 µL	r.t.	UV, DAD detector 220 – 750 nm.	PS, PMMA	Andrianova et al. (2018) ⁸¹
	313	597	1.91	TCI kraft alkaline	2.5 mg/mL	Plgel Minimix-D	THF	0.3 mL/min	30 µL	r.t.	UV, 250 nm	PS, PMMA	This study-TCI alkaline

	897	6624	7.39	Sigma kraft alkali	2.5 mg/mL	Plgel Minimix-D	THF	0.3 mL/min	30 µL	r.t.	UV, 250 nm	PS, PMMA	This study-Sigma alkali
	1062	4542	4.28		2.5 mg/mL	Plgel Minimix-D	THF	0.3 mL/min	30 µL	r.t.	UV, 250 nm	PS, PMMA	This study-Denmark kraft
Indulin AT	2200	19800	9.00	Commercial lignin, Meadwestvaco, Inc.; acetylated.	3- 6 mg/mL	Three Ultrastyrigel columns in series (styrene-divinylbenzene copolymer)	THF	1 mL/min			Differential Viscometer in series with RI	PS	Glasser et al. (1993) ⁶⁵
	1191	6096	5.12	Commercial, Meadwestvaco, Inc.		PSS MCX column-(sulfonated styrene-divinylbenzene copolymer)	0.1 M NaOH solution		25 µL	r.t.	UV, 280 nm.	sodium polystyrene sulfonates	Sameni et al. (2016) ⁸³
	1700	8000	4.70	Softwood kraft-derivatized with acetyl bromide in acetic acid	1 mg/mL	Styrigel HR-5E and Styrigel HR-1, columns in series	THF	0.5 mL/min			UV, 280 nm., RI	PS	Asikkala et al. (2012) ⁷⁸
	1600	6500	4.10	Softwood kraft-derivatized with acetic anhydride in pyridine	1 mg/mL	Styrigel HR-5E and Styrigel HR-1, columns in series	THF	0.5 mL/min			UV, 280 nm., RI	PS	Asikkala et al. (2012) ⁷⁸
	897	6568	7.39	Commercial lignin, Meadwestvaco, Inc.	2.5 mg/mL	Plgel Minimix-D (styrene-DVB copolymer and derivatives)	THF	0.3 mL/min	30 µL	r.t.	UV, 250 nm	PS, PMMA	This study
Indulin	1300	3700	2.90	Commercial lignin, Meadwestvaco, Inc.; acetylated.	3- 6 mg/mL	Three Ultrastyrigel columns in series	THF	1 mL/min			Viscotek Differential Viscometer in series with RI	PS	Glasser et al. (1993) ⁶⁵
	587	3137	5.35	Commercial lignin, Meadwestvaco, Inc.	2.5 mg/mL	Plgel Minimix-D	THF	0.3 mL/min	30 µL	r.t.	UV, 250 nm	PS, PMMA	This study-ndulin C
Soda pulping		8000	4.80	Lignin ext'd from straw by NaOH; precip'd at pH 1.6.	1 mg/mL	Two PolarGel-M columns (styrene-DVB and derivatives)	DMSO with 0.1% (w/w) LiBr	1 mL/min	100 µL	60 °C	UV; RI; viscosimetric detector; two-angle LSD	polyethylene-glycol, polyethylene oxide, glucose	Wormeyer et al. (2011) ⁸⁶

	1084	5008	4.62	Commercial non-wood soda lignin, GreenValue		PSS MCX column-(sulfonated styrene-divinylbenzene copolymer)	0.1 M NaOH solution		25 µL	r.t.	UV, 280 nm.	sodium polystyrene sulfonates	Sameni et al. (2016) ⁸³ (Protobind)
	825	2563	3.11	Protobind 1000; GreenValue	2.5 mg/mL	Plgel Minimix-D	THF	0.3 mL/min	30 µL	r.t.	UV, 250 nm	PS, PMMA	This study-Comm. non-wood soda lignin
Lignosulfonates	7200	64000	8.80	Borregaard Lignotech-Na sulfonate spruce	2 - 5 mg/mL; filt 0.45 µm.	Jordi (glucose-DVB), 10000 Å, 500 x 10 mm	9% DMSO/aqueous (+ SDS) PH adj. to 10.5.	1 mL/min	200 µL	60 °C	Dawn-F MALLS (fluor. filter); RI.	PSS and polysaccharide	Fredheim et al. (2002) ⁸⁴
	3441	7082	2.05	Commercial (China) Na lignosulfonate	3 mg/mL; filt 0.45 µm.	Ultrahydrogel 250 and 1000 columns (hydroxylated polymethacrylate)	0.1 M NaNO ₃ /aqueous, pH 7	0.6 mL/min	100 µL		Differential refractometer.	Pullulan, PEG	Chen and Li (2000) ⁷⁹
	241	1952	8.11	Ginn Mineral Tech.	2.5 mg/mL	Plgel Minimix-D	THF	0.3 mL/min	30 µL	r.t.	UV, 250 nm	PS, PMMA	This study-Lignotex Lignosulfonate
	336	3002	8.95	Borregaard Lignotech	2.5 mg/mL	Plgel Minimix-D	THF	0.3 mL/min	30 µL	r.t.	UV, 250 nm	PS, PMMA	This study-Lignotech D
	780	3660	4.70	TCI Ligno-sulfonates	2.5 mg/mL	Plgel Minimix-D	THF	0.3 mL/min	30 µL	rm. Temp.	UV, 250 nm	PS, PMMA	This study- TCI Lignosulfonate
	1062	4542	4.28	This study- Denmark kraft alkali lignin	2.5 mg/mL	Plgel Minimix-D	THF	0.3 mL/min	30 µL	r.t.	UV, 250 nm	PS, PMMA	This study-Denmark kraft

1.4.2. Sample Preparation and Lignin Solubilization for GPC Analysis

Sameni et al. showed that diverse types of lignin displayed very different solubilities in a variety of solvents.⁸³ For many studies, the choice of solvent is dependent only upon what works best in solubilizing the type of lignin being considered, and, if GPC is used for analysis, it follows that the same solvent system is used as the mobile phase. This choice, in turn, may dictate the type of column used for analysis.

However, solubility studies of lignin and its extracts may present a dilemma for many researchers. A number of extraction solvents are not column-friendly, and if the researcher uses several solvents there is always the problem of which is compatible with the mobile phase. Most of the information concerning solubility of lignin in a wide variety of solvents is part of the body of work done by researchers performing fractionation of lignin by strategically selected solvent(s), which is often done for the purpose of finding fractional MWs or of correlating hydroxyl groups or other functional groups with a particular solvent. A number of fractionation studies present lignin solubilities in various solvents as a characterization property.

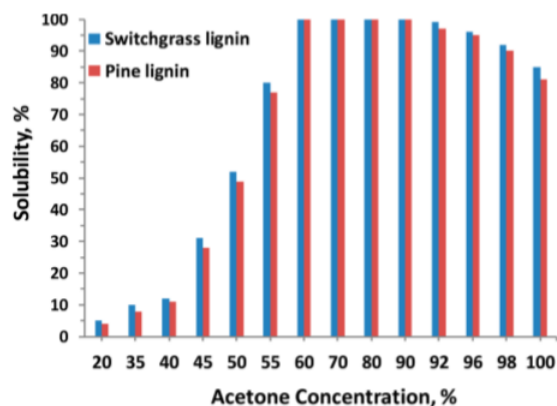
Analyzing lignin samples for MW by GPC is a process that is not standardized within the chemical research community,⁶⁴ and particularly pressing problems are associated with solubilization of lignin, which is not totally soluble in pure aqueous or organic mobile phases; combinations of solvents is often limited by the type of column being used. A significant problem for some researchers is to choose a mobile phase for GPC analysis which is compatible with an entirely different solvent used to solubilize or extract lignin fractions.

Three basic approaches to resolve solvent incompatibility between extraction solvent and mobile phase solvent were implemented by the majority of studies reviewed:

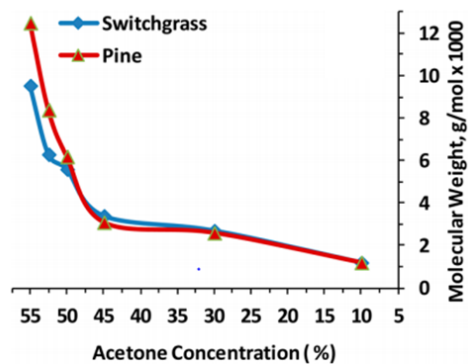
- (1) The use of derivatization, primarily acetylation, applied to lignin samples. The advantages of this method included the relative ease of the process and the fact that lignin was found to be completely soluble in THF. The primary disadvantages were the altered hydrodynamic volume, molecular weight and column interactions caused by the presence of derivatization agent functional groups. The extraction solvent had to be removed and the samples dried before being transferred to the organic mobile phase solvent.
- (2) Dissolution of lignin samples, without derivatization, into the solvent used as the mobile phase for GPC analysis or a solvent compatible with the mobile phase. Mobile phase solvents which offer universal solubility for lignin samples in general, as long as lignin and base concentrations are favorable, are alkaline aqueous solutions with a pH of 11 or higher. Advantages of the latter solutions include the ability to dissolve many types of lignin completely, but disadvantages are numerous for aqueous solvents and include lignin association, ion exclusion and uncertain effects of buffering agents,⁷⁹ as well as column incompatibility due to the caustic nature of the solution.⁸⁰
- (3) Use of an organic mobile phase which is identical to or soluble with the choice of lignin extractant. This situation can be easily addressed by having or purchasing a column conducive to the solvent needed for extracting the lignin; however, this could readily become an expensive situation if several solvents must be accommodated by way of several columns. However, dissolution in

solvent systems (usually two solvents) that can serve as the mobile phase within the limits of common columns is a more realistic objective.

A study by Sadeghifar et al. demonstrated the use of derivatization to purportedly solve the problem of incompatibility between extraction and mobile phase solvents. Kraft switchgrass and pine organosolv lignin samples were fractionated/precipitated in different ratios of acetone and water, dried, acetylated, then solubilized in THF for GPC evaluation with tetrahydrofuran as the mobile phase. Solubilities of lignin, determined gravimetrically, are presented in Figure 6a, and can be compared to Figure 6b, the molecular weights determined for each solubility level.⁸⁷



(a)



(b)

Figure 6. (a) Solubility percentage of original lignin in acetone-water solvent mixes, (b) MW by percentage of acetone in acetone-water solvent mixes; taken from Sadeghafir et al.⁸⁷

Not unexpectedly, MW decreased as solubility declined as, apparently, large molecules were the first to be excluded as solubility decreased; however, the determination of MW was accomplished for each fraction, as this study was intended as a method of determination of characteristics of solvent-fractionated lignin.⁸⁷

Allegretti et al. used a slightly different approach to derivatization by noting the solubility of Protobind® lignin in several organic solvents and then performing Soxhlet extraction of lignin by the most effective solvent (ranked by solubility, low toxicity, low viscosity and easy evaporation), which was methyl ethyl ketone (MEK). The liquid extract was fractionated via ultrafiltration, dried and then derivatized (acetylated) before being evaluated by GPC with a THF mobile phase. The M_n and M_w values, as expected, decreased as fractionation cut-off ranges decreased.⁸⁸

Derivatization of lignin was used in the above studies,^{87,88} although there was no attempt to compare the results to analyses which did not employ derivatization.

The second approach as outlined above was not based on derivatization but on solubilizing lignin samples in a mobile phase which was identical or compatible with the solvent used to process the samples. A study by Ang et al. demonstrated this idea by subjecting alkali lignin to base-catalyzed depolymerization in a batch reactor, followed by sequential fractionation with 1-propanol, ethanol and methanol. The dissolved lignins were dried and analyzed by GPC with a water:acetonitrile, pH 11 mobile phase (with sodium nitrate buffer), and completely dissolved without derivatization.⁸⁹

High-pH aqueous solutions alone are often sufficient to dissolve lignin of most types, but are dependent on concentrations of lignin and base/buffer added to the solution. However, high pH is damaging to the column unless it specifically is rated for high pH. A study by Melro et al. demonstrated that 40% solubility of lignin occurred at pH 10, with efficiency increasing rapidly such that lignin was completely dissolved at pH 11. A phase map from the same study showed dissolution as a function of wt% lignin vs wt% NaOH in Figure 7.⁹⁰

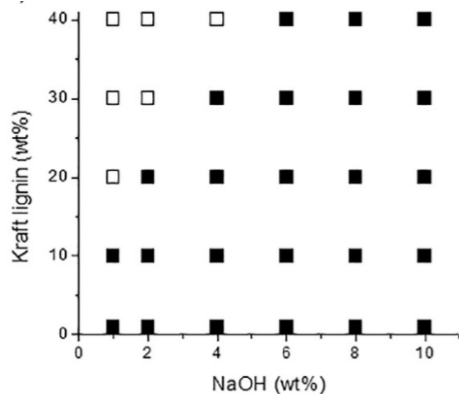


Figure 7. A phase map showing complete dissolution of lignin (black squares) and incomplete dissolution (white squares) as a function of kraft lignin wt% originally present and wt% of NaOH in solution.⁹⁰

Thus high-pH alkaline solutions are attractive as universal solvents, but the properties of the solution may have negative impacts on equipment and the solution must also meet criteria for repeatability and should not be subject to association and ion exclusion effects. Aqueous systems can be problematic for interactions between lignin molecules (association) and for interaction with column components (ion exclusion).^{79,80}

A study by Liu et al. was similar to the Ang investigation in that lignin was extracted with a glycerol-ethanol solvent, dried, dissolved in tris-acetate buffer solution and placed into an aqueous solvent system (with tris-acetate buffer) in which it was soluble.⁹¹ However, problems associated with buffer addition to control pH or ionic strength were clearly delineated in a study by Chen and Li; small adjustments in electrolyte or buffer strength resulted in lignin solubility which varied widely.⁷⁹

Klett et al. demonstrated the use of a nonaqueous GPC mobile phase, without derivatization, as an example of the third solubilization strategy outlined above. Kraft lignin

in an acetic acid-water solution was fractionated with CO₂ gas expansion antisolvent methodology in a reactor, filtered, dried and mixed with 0.05 M LiBr in N,N-dimethylformamide (DMF), which also served as the mobile phase for GPC analysis. The researchers in this case were able to ascertain complete solubility (or an acceptable level) of the lignin in the solvent system of choice for use in the GPC protocol.⁹²

As final commentary, an interesting study by Lange et al. offered a critique of GPC practices in general, but also offered an in-depth look into the solubility issues surrounding GPC use. The overall message of the study was that, although there was a lack of cohesiveness and standardization in GPC protocols used currently, there were also possible solutions to creating a more favorable environment for mutual comparison of GPC results. The authors suggested a method of correcting for derivatization by applying a correction factor, which would account for changes in molecular weight, changes in hydrodynamic volume and interactions with column stationary phases.⁶⁴

Solubility issues explored by Lange et al. centered around the basic premise of sending a “plug” of lignin (in its own solvent system) through a “THF-based” GPC system as being possible, but beset with problems if the lignin solvent mixture was not soluble in THF, as precipitation of lignin was inevitable. Lange et al. also conceded that additions of solvents to the sample and the mobile phase which would ensure mutual solubility might also be practicable, although secondary solvents would have to be allowable on the column(s) of choice.⁶⁴

This viewpoint would seem to be the most astute, as various inherent problems are associated with the use of derivatization and with aqueous mobile phases. Although the reviewed studies produced molecular weight distributions that were reasonable, validation

was lacking in the form of molecular weight yields for the same lignins by different means as comparison.^{87-89,91}

For this study, derivatization appeared to be unnecessary for GPC analysis of technical lignins, and the choice was made to select solvents for extraction and for the mobile phase which would be compatible. Most GPC columns in present use have a limited number of secondary solvents which can be used as mobile phases, and often the amount of secondary solvent is only allowed at a restricted percentage.

I.5. Folin-Ciocalteu Method of Quantification of Phenolic Hydroxyls in Lignin Samples

Various methods are used for determination of lignin hydroxylation, some of which can differentiate between hydroxyl locations on the molecule, i.e., aliphatic or phenolic in the case of lignin. Fairly common is NMR analysis following phosphorylation of the hydroxyl group.⁹³ However, this method requires careful sample preparation and complex data interpretation and therefore there is an ongoing effort to find a high-throughput method. The Folin-Ciocalteu (F-C) reagent consists of a phosphotungstic/phosphomolybdic complex, which is reduced by phenols or by other compounds capable of reduction. F-C reagent has maximum absorption at 765 nm radiation, although other wavelengths are used often in literature (725, 750 and 765 nm),⁹⁴ wherein absorption intensity is presumably proportional to the concentration of the phenolic compounds in the solution.

The Folin-Denis reagent, as it was initially called when created in the early part of the 20th century, was for the purpose of detecting proteins. The improved version, the F-C reagent, was developed in 1927, but a drawback of this chemical was its rapid decomposition in alkaline solution, which made it necessary to use an excess of reagent to obtain a complete reaction. Unfortunately, this F-C excess resulted in precipitates and high turbidity, making spectrometric analysis difficult. Li salts were added to the reagent, which cleared the turbidity.⁹⁵ Improvements on the method were developed by Swain and Hills and also Singleton and Rossi for determination of phenolic compounds in food and wine, respectively.⁹⁶

The developers of the reagent and reaction methodology, Folin and Denis, described the reaction as taking place in the acidic conditions present when the sample was combined with the F-C reagent.⁹⁷ An alkali solution added as Na_2CO_3 was a necessary part of the overall reaction which produced molybdate (or tungstate) and the characteristic blue color of the test, which was colorimetrically determined, with intensity being proportional to phenol concentration. Phenol groups are oxidized by phosphomolybic acid (Figure 8) or phosphotungstic acid, while the reduced metal oxides react with F-C reagent colorimetrically.⁹⁸

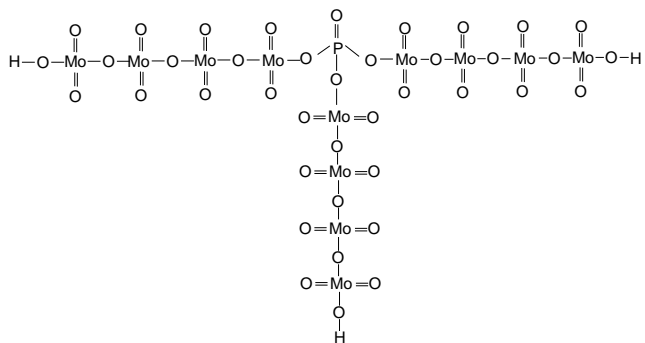


Figure 8. Phosphomolybdic acid, $\text{H}_3\text{PMo}_{12}\text{O}_{40}$.⁹⁹ Phosphotungstic acid is identical, with the exception of having instead a tungsten center ($\text{H}_3\text{PW}_{12}\text{O}_{40}$).

The F-C reagent is thought to be a mix of octahedrally complexed phosphotungstates and phosphomolybdates arranged around a central phosphate, in an acid solution.¹⁰⁰ The phosphotungstates are colorless in the +6 state of the Mo atom, while the phosphomolybdates give the reagent its characteristic yellow color. Rover et al. describe

reduction of MoO_4^{4-} units to MoO_3^{3+} species, with a final product of $(\text{PMoW}_{11}\text{O}_{40})$.¹⁰⁰ However, Bancuta et al. describe final reduction products as W_8O_{23} and Mo_8O_{23} ,⁹⁴ and most researchers refer to reduction of MoO_4^{4-} units to MoO_5^{+5} units.^{94,96,98} Molybdates are considered to be more easily reduced, thus F-C reactions are probably limited to the molybdate component of the reagent.⁹⁸

In its simplest form, phenol acts as a reducing chemical, becoming oxidized in the process (thus the antioxidant reputation) and it is converted to semiquinone,⁹⁶ or other quinones during the reaction with units of MoO_4^{4-} in the Folin-Ciocalteu reagent, producing MoO_5^{+5} units. The mechanism is not fully understood, although reactions which convert phenols to quinones are well known. Less understood is exactly which phenol reaction occurs, as well as the exact phosphotungstic or phosphomolybdic reduction mechanism. Rangel et al. described the reduction as occurring as a reversible one- or two-electron addition,⁹⁸ while Everette et al. considered the reaction to probably involve a single electron which resulted in semiquinone formation (Figure 9).⁹⁶ Rover et al. described the reaction as an electron passing to a nonbonding orbital in the phosphotungstic or phosphomolybdate complex.¹⁰⁰

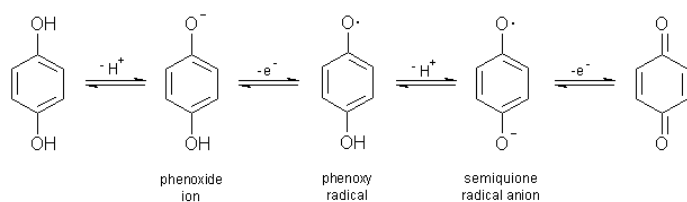


Figure 9. Oxidation of 4-hydroxyphenol to semiquinone, followed by another oxidation step to benzoquinone.⁹⁹

The Folin-Ciocalteu reagent assay for phenolics (or proteins) has numerous versions as determined by various researchers, and these are typically designed for UV spectrophotometric analysis in a cuvette as the sample holder. The challenge in this study was to devise a method in which microplates could be used, which would reduce reagent use across the board and allow multiple sample absorbance determinations per instrument reading.

Rover et al. designed a micro-scale method for bio-oil by dissolving a 20- μ L bio-oil sample in ethanol, followed by filtration with a 0.45 μ m syringe filter. The sample was diluted with 1.58 mL of deionized water. Then 100 μ L of FC reagent was added to the samples, which was mixed and allowed to incubate for 1 to 8 min. After this, 300 μ L of 2 M sodium carbonate solution was added to each sample, and the samples were allowed to incubate for two hours. At the end of this time, light absorbance at 765 nm was determined in 1-cm cuvettes.¹⁰⁰

Gallic acid at different concentrations is typically used as the calibration standard for FC assays; gallic acid has three hydroxyl groups attached to the benzene ring and theoretically gives an optimal response. However, a study by Stratil et al., which evaluated a number of phenolic compounds with a variety of hydroxyl groups and substituent types by FC and several other phenolic-detecting assays, found that absorbance was not strictly proportional to hydroxyl presence on the ring. Gallic acid was found to have a response at about the same level as catechol response (with two hydroxyl groups on the ring), ostensibly due to substituent and bonding influence on hydroxyl reactivity.¹⁰¹

Allegretti et al. utilized Folin-Ciocalteu assay as a metric for the extent of monomeric production in separate lignin fractions subjected to Soxhlet extraction followed

by a two-membrane cascade filtration. The group hypothesized that the blue chromophore was unstable in strong bases, so that DMSO was used as a solvent to ensure total solubility under pH neutral conditions. The results were reported as gallic acid equivalents (μg gallic acid per mL of working solution). The study found that with the FC method, only two phenolic groups of gallic acid were reactive, so one GAE was considered to be two phenolic group equivalents.⁸⁸

A study by Kang evaluated degradation of alkaline lignin in a batch reactor (5 g lignin in 60 mL water) at temperatures from 260 to 360 °C with residence times from 0 to 60 min. The liquid product fraction was evaluated by Folin-Ciocalteu assay; the liquid product included dichloroethylene-extracted bio-oil from the liquid phase and bio-oil from the solid phase (also extracted by dichloroethylene). Results were expressed as total mg gallic acid per g of lignin per sample with UV/Vis absorbance measured at 760 nm. Total phenol content was measured for the varied temperatures and residence times, thus the analysis was used primarily as a measure of degradation extent during depolymerization by thermal treatment. The study found that maximum production of phenol, ostensibly due to thermal degradation of the lignin, occurred between 280 and 320 °C.¹⁰²

Application of Folin reagent as a metric for oxidation capacity of lignin was not commonly encountered in the literature, although antioxidant potentials of proteins and other substances are often measured with this assay or another like it (DPPH, etc.). Devising a microplate method of Folin-Ciocalteu reaction with phenolic groups in lignin would be a timely undertaking, and would involve assessing phenolic content of individual lignin models and comparing these to whole lignins to estimate the overall phenolic content.

I.6. Methods for the Processing of Technical Lignin

Technical lignins have been the target of intensive research aiming to develop methods of depolymerization in the past several decades with the idea that valorization of residuals would offset costs in the paper and biorefinery industries, as well as contribute to chemical feedstocks containing aromatics that are normally provided through petroleum sources. Attempts to break the recalcitrant lignin into monomers or small oligomers have met with mixed success.

Various methods to depolymerize lignin exist. A number of prominent ones include ball milling, sonication, catalysis, microwave assisted, electrochemical, ionic liquids, pyrolysis, steam explosion, and subcritical/supercritical water treatment. Many methods make use of an oxidant, which can include some acids, peroxides and O₂, while pyrolysis is an anoxic method). Higher temperatures usually assist in facilitation of the oxidation process and radical mediation of the breakdown reactions are often cited, as in a sonication study,¹⁰³ a microwave-assisted study,¹⁰⁴ an electrochemical study,¹⁰⁵ a catalysis study utilizing a metal oxide of perovskite type,¹⁰⁶ and a pyrolysis study,¹⁰⁷ although high temperature was not always involved. For these same studies, conversion percentages (depolymerization of original lignin to monomers or low MW oligomers) ranged from 3 to 60%.^{104,106}

While most depolymerization methods look for a way to chemically, thermally or physically disconnect linkages in lignin, another strategy is to separate different sizes of molecules through fractionation, wherein functional groups may be separated as well. A number of fractionation strategies exist, typically as ultrafiltration (physical limitation of size by permeation through pores), acid or solvent precipitation (typically by size, although

functional groups may also differ) and by SEC (physical interaction of hydrodynamic size with porous media).

1.6.1. Fractionation of Alkali Lignin

The fractionation approaches typically aim for fractions with narrower molecular size and weight distributions that would be more homogeneous, and thus more useful, for renewable applications,¹⁰⁸ and which could also result in streamlining of characterization processes.

Currently, there are three main methods that have been used for lignin fractionation, i.e., selective solvent fractionation, differential precipitation, and membrane ultra- or nanofiltration; several of these methods have occasionally been combined.

1.6.1.1. Fractionation by membrane

Fractionation by membrane is a well-established method of purifying or separating many types of industrial materials, including petrochemicals, brines, metals, mining tailings, and emergency water supplies.¹⁰⁹ The use of a fractionation apparatus has the added advantages of controlled heat as well as controlled transmembrane pressure. Several materials, including polyethersulfone, cellulose acetate, polyacrylonitrile, aluminum oxide, polyaryl ether ketone, and ceramics (ZrO_2 , TiO_2 , etc.) are used to construct membranes intended for lignin fractionation, and may be flat or tubular in shape.¹¹⁰

Fractionation of black liquor, the liquid component of the kraft pulping process which contains the lignin fraction, has been shown to be effective especially in purifying lignin from saccharide and inorganic contaminants.¹¹¹ A study by Humpert et al. found that

the lignin concentration maximum by membrane filtration (with improved processing due to combinations of filter pore size, pressure, temperature, rotating disc application and cross-flow set up), was as much as 285 g/L, purities up to 78%, and an ash content reduction from 4.7% to 2.7% with diafiltration.¹¹¹

The main advantage of filtration by a membrane is that inclusive MW limits can be determined, depending on how closely the pore sizes are set for the membranes. In reference to the studies listed in Table 8, Polydispersity index (PI) values for a number of lignin sources were relatively low (<4) for 15 kDa fractions, and PI values steadily decreased for smaller-pore membranes, often to values < 2.0.¹¹²⁻¹¹⁵

The downside of lignin filtration is the amount of fouling and subsequent reduction of membrane flux^{111,116}, although cleaning with alkaline solutions is easily accomplished.¹¹⁷ Sophisticated fractionation methods have been developed for other industrial interests and have also been scaled up effectively, but the economic value of lignin may or may not warrant the costs associated with industrial scaling. Guo cited problems of the filtration process as being membrane tendencies to foul as well as the fact that the process is not readily scalable to satisfy industrial needs.¹¹⁸

Not unexpectedly, based on Table 8 (membrane fractionation studies), PI values decreased with decreasing membrane pore size, and reached small values around 2.0. M_n and M_w values decreased in this direction as well. With membrane fractionation, there is also a question of whether depolymerization through physical means occurs during the process. Toledano et al. found that fractionation by membrane increased lignin depolymerization when comparing structures of lignins obtained through membrane fractionation vs acid precipitation.¹¹⁹

Several studies also analyzed functional groups, particularly phenolic hydroxyls, aliphatic hydroxyls and carboxyl groups, in order to compare homogeneity between fractions. Phenolic hydroxyls and carboxyl groups increased with decreasing membrane pore size, while aliphatic hydroxyls decreased with decreasing pore size in studies by Zinoyev et al. (room temperature) and Sevastynova et al (40 - 65 °C).^{113,115} As reported by Zinoyev et al., lower MW material was considered to be more degraded and modified, thus increased phenolic hydroxyls were due to hydrolysis of β -O-4' bonds, and the decrease in aliphatic hydroxyls occurred with increased formation of condensed carbon framework.¹¹⁵

Norgren et al. (room temperature) also found phenolic hydroxyls to increase with decreasing membrane pore size.¹¹⁴ Helander et al. showed that sulfur accumulated at lower MW fractions.¹²⁰ Studies reviewed for ultrafiltration methodologies are presented in Table 8.

Table 8. Method parameters and molecular weight findings for several filtration membrane fractionation studies.

Membrane Filtration							
Lignin type	Filtration method	Analysis	Results:	Mn	Mw	PI	Reference
Black liquor of alkaline pulping of <i>Miscanthus sinensis</i> (Chinese silver grass)	Ceramics material (TiO ₂) membranes (tubular and multichannel) with serial cut-offs of 5, 10 and 15 kDa.	GPC with 3 Styragel columns, RI detector, acetylated samples, PS standards	Liquor >15 kDa 15 kDa 10 kDa 5 kDa	1879 2032 1891 946 940	5654 6300 3544 2022 1806	3.01 3.10 1.87 2.14 1.92	Toledano (2010) ¹¹²
Weak black liquor of kraft pulping of softwoods	Ceramics material (TiO ₂ and ZrO ₂) membranes with cut-off of 1 kDa (4.6 bar)-samples evaporated and acid precip'd to various pH	Three Ultrastyrigel columns, mobile phase THF, UV detector. PS standards. Samples acetylated.	Acetylated: Liquor pH 9 1 kDa pH 9 1 kDa pH 6.5 1 kDa pH 4	847 508 503 467	3525 1096 1074 973	4.2 2.2 2.1 2.1	Helander (2013) ¹²⁰
Two industrial black liquors and 3 isolated lignins, including indulin AT	Ultrafiltration cell (press 2.5- 3 bar, room temp) with regenerated cellulose membranes. Isolated lignins in alkaline soln. Cascade from 100 kDa, to 30, 10, 5, 3 and 1 kDa.	SEC: Three PolarGel M columns with DMSO (0.5% w/v LiBr) as mobile phase, flow rate 0.5 mL/min, temp 40 C, UV and RI detectors; PS sulfonate standards.	Indulin AT: 100 kDa 100-30 30-10 10-5 5-3 3-1 < 1	1028 1432 695 438 220 66 70	10008 3892 1454 919 525 148 140	9.74 2.72 2.09 2.10 2.39 2.24 2.00	Zinovyev (2016) ¹¹³
Industrial black liquors from kraft pulping of softwood (and hardwood and Eucalyptus).	Serial fractionation with 15 kDa and 5 kDa ceramic membranes at 120 °C. Permeate and retentate acidified at 60-65 °C to pH 9	3 Styragel columns in series with THF mobile phase, flow rate 0.8 mL/min and RI detector. All samples were acetylated. PS standards.	Softwood lignin Permeate 15 Permeate 5	1000 580 490	4470 2280 1700	4.5 3.9 3.5	Brodin (2009) ¹²¹

Kraft softwood biomass leached with 0.1 M NaOH. Filtrate adjusted to pH 2; precip'd lignin centrifuged, washed.	Stirred cell ultrafiltration with polyethersulfone membranes with serial cut-off 30, 10, 8, 5 kDa. Pressure 275 kPa. Sample dissolved in 0.1 M NaOH prior to fract. The fractions precip'd with 1 M HCl.	Samples acetylated, THF mobile phase, system with undesignated type of columns, but with cut-offs of 10000, 500 and 100 Å. Differential refractometer detector. PS standards. Five permeate fractions.	>30 kDa	2190	41400	19	Norgren (2000) ¹¹⁴
			10-30 kDa	3750	14900	3.9	
			8-10 kDa	1480	4060	2.7	
			5-8 kDa	1480	2850	1.9	
			<5 kDa	950	1910	2.0	
Lignin: Industrial weak black liquor prior to evaporation step.	Ultrafiltration by ceramic TiO ₂ and ZrO ₂ membranes and cellulose (10 kDa) Temp 40-65 °C, press 3.5 bar, first 5 then 1 kDa for permeate. Retentate from 5 kDa to 10 kDa at room temp and 0.35 MPa). All precipitated by acidification to pH 9.	Acetobrominated samples, 25 uL injected into THF mobile phase, with PLgel 5 um, 500 Å and 5 um 1000 Å, with DAD. 0.5 mL/min flow, PS standards.	>10	9500	33500	3.5	Sevastyanova (2014) ¹¹⁵
			5-10 kDa	2300	4900	2.2	
			1-5 kDa	2000	4700	2.3	
			0-1 kDa	1200	2700	2.1	

1.6.1.2. Fractionation by acid precipitation

Similar to membrane fractionation studies, most acid precipitation studies were implemented directly with black liquor, thus investigation sometimes included measurement of lignin purity and solubility/recovery.¹²²⁻¹²⁴ Zeta potential was explored in several studies since this was an indication of the charge on the lignin colloid and was thus an indicator of the tendency for the colloid to precipitate. Zeta potential was found to be affected by pH, decreasing with a decrease in pH.^{122,125}

While the majority of reviewed studies (shown in Table 9) used black liquor from soda-pulping only,^{122,123,126,127} an exception was a study by Laurencon et al. in which acid precipitation was carried out with black liquor from kraft alkaline treated softwood and hardwood.¹²⁴

Precipitation by acid was performed in sequential steps with one sample^{124,125,127} or as a one-step process whereby individual samples were treated with a specific amount of acid.^{122,123} Acid precipitation of one sample by sequential pH decrease was considered more feasible as a purification and fractionation method, as stated in a study by Laurencon et al. Notably, molecular weight results for both hardwood and softwood liquors treated sequentially showed a fairly wide variety of M_n and M_w , as well as a wide variation in polydispersity index.¹²⁴ One-step processes which produced samples with varying pH, but which later brought all samples to one final pH value,^{122,123,127} showed little variation in M_n , M_w and polydispersity values, and the values in a study by Surina et al. were far lower than values in the study by Laurencon et al.^{122,124}

Molecular weight distribution was analyzed via SEC in the majority of acid precipitation studies as GPC^{122,123,127} and GFC.¹²⁵ M_n and M_w values decreased as pH decreased in general (see Table 9). As observed by Laurencon et al., high molecular mass particles with lower solubility and weaker acidity precipitated first, with molecular mass being of primary importance since high mass particles were able to precipitate with partial protonated status.¹²⁴ The tendency for higher M_n and M_w in higher pH samples would thus seem reasonable, which was typical for acid precipitation studies which were reviewed in Table 9. However, there seems to be a tendency possibly for massive precipitation, which would make acid fractionation a poor choice for fractionation unless handled very carefully (attention to pre-treatments or choice of lignin source). The study by Laurencon et al. showed that 85.4% of hardwood lignin and 87.1% of softwood lignin precipitated in the pH range of 9 – 7.¹²⁴

A study by Surina et al. showed fewer phenolic hydroxyl groups with increased acid (lower pH), which were detected by UV analysis.¹²² A study by Li et al. which involved successive acid precipitation of one sample also found that phenolic hydroxyls (by ³¹P NMR) declined with decreasing pH.¹²⁷ This would seem to indicate the polar or H-bond aspects of acids attracted phenolic groups over non-phenolics, which could be an advantage of acid precipitation if separation of functional groups is a goal.¹²²

A number of studies combined fractionation types for comparison purposes; results were varied. A comparison study of acid precipitation vs membrane fractionation of black liquor (Silver Grass) by Toledano et al. revealed small variation in PI values and lower M_w values for acidified samples in comparison to membrane fractionation.¹¹⁹ However, a study by Wang et al. (soda-pulped cornstalk black liquor) also compared membrane filtration to

acid fractionation with the result that acid precipitated fractions had higher PI and M_w values than membrane filtered fractions. Although comparison of method effectiveness was inconclusive, Wang et al. described acid precipitation as superior to solvent extraction and ultrafiltration on a cost basis (high cost of solvents and equipment/operation respectively).¹²⁵ High costs of solvent and membrane fractionation were also cited by Li et al.¹²⁷ Results for acid precipitation methodologies by several investigators are presented in Table 9.

Table 9. Method parameters and molecular weight findings for several acid precipitation fractionation studies.

Acid Precipitation								
Lignin Source	Acid Fractionation Method	Analyses	SEC Conditions	SEC Samples	M _n	M _w	PI	Reference
Steam-exploded corn stalk black liquor by soda pulping	Ultrafiltration of 6, 10, 20, >20 kDa, and multi fractionation of one sample to pH 5.3, 4.0, 2.0	Zeta potential, particle size distribution, FTIR, SEC	Hydrophilic column, alkaline/tri-acetate buffer mobile phase, UV detector, flow rate 0.5 mL/min, nonacetylated samples, PS standards	Retenate >20 kDa Permeate 20 kDa Permeate 10 kDa Permeate 5 kDa pH 5.3 pH 4.0 pH 2.0	5065 4526 2592 1582 4265 3377 3628	15867 7332 4575 2882 15099 13745 7963	3.13 1.62 1.76 1.82 3.54 4.07 2.19	Wang et al. (2013) ¹²⁵
Hemp and flax black liquor by soda pulping containing anthraquinone	Single step method acid addition to achieve specified concentration levels of 5, 25, 50 and 72 wt%; final pH adjusted to 5	Zeta potential, elemental analysis, nitrobenzene oxidation, UV/Vis, GPC	GPC: Separon Hema s-300 column, RI and diode array detector (280 nm), LiBr (0.005 M) in DMF mobile phase at 1 mL/min flow rate, lignin filtered by 0.45 µm and concentration 5 mg/mL, PS standards	5 wt% acid solution 25 wt% 50 wt% 72wt%	478 455 458 480	9823 9440 9367 9593	20.56 20.76 20.46 20.01	Surina et al. (2015) ¹²²
Pine softwood and Eucalyptus hardwood black liquor by kraft pulping	Sequential acidification of a sample to pH 9, 7, 5, 3	Elemental analysis, FTIR, H-1 NMR, GPC	GPC: Two Supelco TSK-HXL columns, RI and UV (254 nm) detectors, mobile phase THF at 0.8 mL/min, lignin concentration 5 mg/mL, PS standards	Hardwood pH 9 Hardwood pH 7 Hardwood pH 5 Hardwood pH 3 Hardwood pH 1 Softwood pH 9 Softwood pH 7 Softwood pH 5 Softwood pH 3 Softwood pH 1	621 413 442 276 433 2543 2444 2106 1874 210	5316 4794 4352 3890 3630 13895 12443 12643 10301 3464	8.56 11.6 9.84 14.08 8.39 5.46 5.09 6.00 5.50 16.48	Laurencon et al. (2015) ¹²⁴

Chinese fir black liquor by soda pulping	Sequential acidification of a sample to pH 8, 5, 2; final pH of all adjusted to 2	Elemental analysis, TGA, FTIR, P-31 NMR, Py-GC-MS, GPC	THF mobile phase, RI detector, lignin 1 mg/mL concentration, acetylated samples, PS standards	ph 8 pH 5 ph 2	8780 7679 5934	16115 14218 11001	1.84 1.85 1.85	Li et al. (2014) ¹²⁷
Oil palm trunk fiber black liquor by soda pulping	Initial pH 10.9, acidified samples to pH 7, 5.5, 5, 3.5, 2; precipitation with ethanol to remove polysaccharides, then all samples acidified to final pH 2	HPLC for phenolic acids and aldehydes for nitrobenzene oxidation, UV, FTIR, NMR, TGA, DSC, GPC	GPC: PL-gel mixed D column, THF mobile phase at 1 mL/min, samples at 0.2% concentration, injected volume 200 μ L, PS standards	ph 7 pH 5.5 pH 5.0 pH 3.5 pH 2.0	1420 1450 1430 1470 1480	2020 2120 2020 2060 2100	1.42 1.46 1.41 1.40 1.42	Sun et al. (2001) ¹²³

1.6.1.3. Fractionation by solvents

A third commonly investigated method of fractionation was that of solvent or anti-solvent precipitation, the latter being a method used when the lignin has been extracted with another solvent first. The combinations of solvents possible as well as the sequence of administration, make the number of studies quite large. A strategy of a number of investigators was to sequence solvents on the basis of solubility parameters- by increasing Hildebrand solubility parameters,¹²⁸ increasing hydrogen-bonding capacity,¹²⁹ increasing Hildebrand and Hansen parameters,¹³⁰ or by decreasing solubility parameters most amenable to lignin.¹³¹ The Hildebrand solubility parameter for lignin was indicated as about 11, while Hansen parameters representing high polarity were considered best.¹²⁸

A number of lignin sources with various solvent combinations seem to have successfully produced lignin fractions with low PI which are generally associated with low M_n and M_w values, with the exception of Li et al., which showed a variety of both high and low M_n and M_w fractions (Table 10).¹³⁰ No one particular suite of solvents seems to stand out as most effective in terms of low PI values, although a few seem to be relatively ineffective: applying acetone/water in varying compositions on a wide variety of lignin types,¹²⁹ or increasing amounts of hexane added to acetone soluble lignin from wheat straw pulped by the Organosolv process.¹³²

Other solvent fractionation strategies included the addition of nonpolar solvent in increasing amounts to a polar solution,^{132,133} or by addition of “green” solvents,¹³⁴ or by pretreatment with ionic liquid. Preferable effective strategies would rely on environmentally-friendly solvents, as in the case of Duval et al., where softwood kraft

lignin (with Lignoboost processing) was fractionated with ethyl acetate, ethanol, methanol and acetone.¹³⁴

Several studies showed an increase in M_n and M_w with successive solvent application-^{128,130,134-136} an example was the study by Li et al. in which solvents with increasing solubility for lignin were used. PI also increased during this process, so that the entire sequence may not be needed- the first step of fractionation might be the only one necessary. Li also reported a decrease in methoxy and phenolic/aliphatic hydroxyl groups, signifying that not only the lowest M_n and M_w particles were in the first precipitation, but the most degraded as well.¹³⁰ Of note, Jiang et al. precipitated kraft lignin successively with solvents which increased in solubility factors close to that of lignin and found that M_n , M_w and PI decreased sequentially.¹³¹

In perusing Table 10, it can be seen that several solvent systems/sequences were successful, if low PI and M_n , M_w values are the metric. However, the expense of solvents and environmental soundness must also be considered. A major advantage of this method is the application of relatively inexpensive instrumentation and a moderately easy process scale up. On the other hand, MW is one of the solubility-determining parameters but not the only one.¹³⁷ Diverse lignin functional groups may significantly affect the composition of the fraction extracted into a certain solvent,¹³⁸ since polymer solubility is known to be affected by their chemical structure and stereochemistry,¹³⁷ thus MW of each fraction would be difficult to control.¹¹⁹ Furthermore, a non-desired additional chemical alteration of lignin may take place.¹³⁹ Several studies reviewed for results of solvent precipitation fractionation of lignin are presented in Table 10.

Table 10. Method parameters and molecular weight findings for several solvent precipitation fractionation studies.

Solvent Precipitation								
Lignin Source	Solvent Fractionation Method	Analyses	SEC Conditions	SEC Samples	M _n	M _w	PI	Reference
Steam-exploded corn stalk residue from bioethanol production	Sample mixed with benzyl alcohol, dioxane, or ethanol in stirred vessel, then heated to extract lignin; solvent:water added as 3:1, 5:1, and 7:1 (mass:mass)	FTIR, H-1 NMR, XRD, GPC	GPC: Two 79911GP columns, UV detector 254 nm, THF mobile phase at 1 mL/min and samples acetylated, PS standards	Raw sample Benzyl alcohol lignin Dioxane lignin Acid precipitated (for comparison)	2598 2739 2439 2158	6160 5433 4847 4244	2.37 1.98 1.99 1.97	Guo et al. (2013) ¹¹⁸
Bamboo subjected to formic acid-based Organosolv process; filtered then lignin extracted with pentane	Crude lignin sequentially fractionated with ether, ethyl acetate, methanol, acetone, dioxane:water (9:1 v/v)	H1-NMR, HSQC, DPPH assay, TGA, DSC, GPC	GPC: Acetylated lignin samples, filtered, concentration of 1 mg/m, mobile phase THF, PS standards	Unfractionated lignin Ethyl acetate lignin Methanol lignin Acetone lignin Dioxane:water lignin	4360 2930 4120 7950 6800	8280 3870 5760 13160 11820	1.90 1.32 1.40 1.66 1.74	Li et al. (2012) ¹³⁰
<i>Caragana sinica</i> (Chinese pea shrub) dewaxed with toluene/ethanol, lignin extracted with water at 80 °C for 2 h	Lignin solution extracted successively with 70% ethanol, 70% ethanol/1% NaOH, 1 M KOH, 1 M NaOH, 3 M KOH, 3 M NaOH at 75 °C for 3 h; liquid/solid ratio 25:1 g/mL; lignins precipitated at pH 1.5 – 2.0	Nitrobenzene oxidation, GPC and 2-D NMR	GPC: RI detector, PL-gel 10 µm mixed-B 7.5 mm ID column, THF mobile phase at 1.0 mL/min, sample at concentration 2 mg/mL, 20 µL injected, PS standards	70% Ethanol 70% Ethanol/1% NaOH 1M KOH 1M NaOH 3M KOH 3M NaOH	760 480 730 580 330 320	1630 1560 1340 1140 930 910	2.15 3.28 1.84 1.98 2.83 2.89	Xiao et al. (2011) ¹⁴⁰

industrial softwood (southern pine and Norwegian spruce) kraft lignins	Dry lignin (500 g) added to 2.5 L of first solvent; filtrates collected, then undissolved material extracted by next solvent; solvents were dichloromethane, n-propanol, methanol, DCM/MeOH	Elemental analysis, TGA, DSC, total sulfur analysis, C-13, P-31 NMR, GPC	GPC: Samples acetylated and filtered (0.45 µm pore size), four Styragel columns in series, UV detector, THF mobile phase at 1 mL/min, injection volume 20 µL, PS standards	Southern pine lignin SP DCM SP Propanol SP MeOH SP DCM/MeOH Norwegian pine lignin NP DCM NP Propanol NP MeOH NP DCM/MeOH	1500 380 650 740 1150 960 420 720 460 1490	6900 611 1620 2070 5960 3830 882 2390 1890 6240	4.6 1.6 2.5 2.8 5.2 4.0 2.1 3.3 4.1 4.2	Dodd et al. (2014) ¹²⁸
Steam-exploded corn stalk subjected to soda pulping, lignin precipitated by acid addition to pH 2.0	Dried lignin (1 g) dissolved in 50 mL 95% ethanol-water (v/v); insoluble material dissolved in 80% ethanol-water solution; final Insolubles from this extraction also collected	UV (190-400 nm), FTIR, H-1 NMR, TGA, functional group analysis, GPC	TSK G3000PWx1 column; sample concentration of 20 mmol/L in mobile phase of alkaline tris-acetate buffer at 0.5 mL/min flow rate, 20 µL injection volume, polyethylene-glycol standards	Unextracted lignin 95% ETOH/water lignin 80% ETOH/water lignin ETOH/water insoluble lignin	3878 2611 4067 8523	12234 6743 8894 24736	3.15 2.58 2.18 2.90	Wang et al. (2013) ¹⁴¹
Softwood kraft lignin post LignoBoost process (purification)	Lignin in concentration of 100 g/L in ethyl acetate, stirred and filtered, then insoluble fraction extracted sequentially by ethanol, methanol, acetone	SEC, GPC, Klason lignin analysis	Columns PL-gel mixed-D 5 µm (1-40K and 500-20K), UV detector (280 nm), samples derivatized with acetyl bromide, filtered (0.45 µm), mobile phase THF at 0.5 mL/min, PS standards	Unextracted lignin Ethyl acetate lignin Ethanol lignin Methanol lignin Acetone lignin	1010 350 1010 2110 2990	6500 750 2060 3740 5150	6.44 2.14 2.04 1.77 1.72	Duval et al. (2016) ¹³⁴
Eucalyptus dewaxed wood powder, pretreated with ionic liquid AmimCl and ethanol in molar ratio 1:5 with 4 wt% water added, heated to 160 °C for 12 h, then filtered	Ionic liquid treated lignin was fractionated by heating separately with several antisolvents (water, MeOH, DCM, isopropanol), then each centrifuged	FTIR, GPC	PL-gel 5 µm 500 Å column, multi-angle light scattering detector, samples acetylated, filtered, THF mobile phase at 1.0 mL/min, PS standards	Untreated lignin Unfractionated IL-lignin Isopropanol IL-lignin Water IL-lignin DCM IL-lignin MeOH IL-lignin	NR 873 860 831 814 780	6700 960 960 941 910 873	NR 1.10 1.12 1.13 1.12 1.12	Liang et al. (2016) ¹³⁵

BioChoice lignin/pine kraft lignin subjected to Lignoboost process (purification)	Lignin dissolved in methanol, and soluble sample sequentially precipitated with solvents with decreasing solubility parameters (ethyl acetate, ethyl acetate/petroleum ether, petroleum ether)	Elemental and functional group analysis, P-31 NMR, TGA, DSC	Two Styragel columns with UV detector (280 nm), THF mobile phase at 0.7 mL/min at 35 °C, samples acetylated and at concentration of 1 mg/mL, 50 µL injection volume, PS standards	Unfractionated lignin MeOH/acetone lignin Ethyl acetate lignin EA/pet. ether lignin Petrol. ether lignin	1562 3395 1647 626 364	5202 10244 2468 770 407	3.33 3.02 1.50 1.23 1.12	Jiang et al. (2017) ¹³¹
Wheat straw Organosolv lignin	Lignin dissolved in acetone, filtered, then soluble fraction precipitated in three fractions based on increasing amounts of n-hexane; Soxhlet extraction of lignin in acetone and n-hexane also done.	Optical microscopy, elemental analysis, DPPH assay, FTIR, P-31 NMR, HSQC, TGA, DSC, XPS, GPC	Two/three PL-gel 5 µm columns, diode array detector, THF as mobile phase at 0.75 mL/min with acetobrominated samples, PS standards	Unfractionated lignin Acetone lignin 4:1 ACE:HEX lignin 1:1 ACE:HEX lignin 1:4 ACE:HEX lignin Soxhlet acetone lignin Soxhlet hexane lignin	920 1100 1800 1100 610 610 610	4600 23600 7700 3900 3500 10800 5000	5.0 21 4.3 3.5 5.7 18 7.7	Lange et al. (2016) ¹³²
Industrial softwood kraft lignin	Lignin dissolved in acetone, filtered, then soluble fraction precipitated in three fractions based on increasing amounts of n-hexane	P-31 NMR, GPC	Three Styragel columns (HR 1, 5E, 6) with UV detector (254 nm), THF mobile phase at 1.0 mL/min, samples acetobrominated, 50 µL injection volume, PS standards	Unfractionated lignin Acetone insoluble 4:1 ACE:HEX kraft lignin 1:1 ACE:HEX kraft lignin 1:4 ACE:HEX kraft lignin (data for one of three kraft lignin samples)	2400 3000 2300 1600 1100	14500 34000 3400 2000 1200	6.1 11 1.8 1.3 1.1	Cui et al. (2014) ¹³³
Soda wheat straw (25%) and Sarkanda grass (75%) lignin; maple, birch, poplar Organosolv lignin; kraft pine Indulin AT; wheat straw lignin from a mild alkaline process; soda wheat straw	Each lignin suspended in acetone/water of differing concentrations, stirred; insoluble and soluble lignin collected	FTIR, P-31 NMR, SEC	SEC: TSK gel Toyopearl HW-55F column, UV detector (280 nm), 0.5 M NaOH as mobile phase, Na-polystyrene sulfonate standards	For 70% Acetone:H ₂ O: Organosolv lignin Wheat str/grass lignin Wheat straw lignin Alk. wheat straw lignin Kraft pine lignin	70% ACE: H ₂ O ND 1750 1439 2481 1074	70% ACE: H ₂ O ND 16979 10795 15632 6338	70% ACE: H ₂ O ND 9.7 7.5 6.3 5.9	Boeriu et al. (2014) ¹²⁹

Softwood and hardwood kraft lignin; birch and spruce Organosolv lignin (acetic acid)	Each lignin sample suspended in diethyl ether, stirred, filtered, then soluble residue was precipitated sequentially by diethyl ether/acetone (4:1 v/v) and then acetone	P-31 NMR, Py-GC-MS, SEC, DSC	SEC: PSS CX 100 and 100000 columns, UV detector (280 nm), 0.1 M NaOH mobile phase, polystyrene sulfonate standards	Kraft softwood lignin Kraft hardwood lignin Organosolv birch lignin Organosolv spruce lignin	1050 1140 1880 1510	1730 1760 2600 2290	1.65 1.55 1.39 1.51	Roppnen et al. (2011) ¹⁴²
Kraft lignin from <i>Eucalyptus pellita</i>	Lignin pH 2.0; sequential precipitation by Soxhlet successively of soluble portion by ethyl ether, methane chloride, n-propanol, ethanol, methanol, dioxane	UV (260- 400 nm), nitrobenzene oxidation, GPC, FTIR, H-1 and C-13 NMR, TGA	GPC: P-gel 10 mm Mixed-B 7.5 mm ID column, THF mobile phase at 1.0 m/min, samples at 2 mg/mL concentration and 20 µL injection volume, PS standards	Ethyl ether lignin Methene chloride lignin Propanol lignin Ethanol lignin Methanol lignin Dioxane lignin	640 1000 1730 1900 2640 4950	650 1140 2550 2900 4200 7800	1.0 1.1 1.5 1.6 1.6	Yuan et al. (2009) ¹³⁶
Dry softwood kraft lignin	Lignin combined with aqueous ethanol (80%), or acetone (60%) and/or PGME (60%) solution; water added in stages to precipitate lignin	P-31 NMR, SEC, elemental analysis, UV (280 nm)	SEC: PSS MCX 1000 and 100000 A columns and DAD detector (280 nm), 0.1 M NaOH eluent (pH 13) at 0.5 mL/min), polystyrene sulfonate standards.	Unfractionated lignin 80% ETOH lignin 50% ETOH lignin 60% Acetone lignin 30% acetone lignin 60% PGME lignin 30% PGME lignin	2100 3000 2400 3400 1800 1900 2000	4100 7600 3300 18900 2700 4300 2800	1.98 2.54 1.38 5.62 1.46 2.24 1.45	Jaaskaleinen et al. (2017) ¹⁰⁸

1.6.1.4. Fractionation by preparatory SEC

Kirk et al. as early as 1969 considered preparative fractionation of lignin by GPC as an effective approach for collecting lignin fractions solely based on the molecular size.¹³⁹ An apparent advantage of this method is that the molecular size cut-offs are easy to control by varying the retention time windows for collection post GPC processing. Furthermore, as a type of SEC, GPC is known to be a scalable technique.^{143,144}

A study by Botaro et al. looked at fractionation as a function of size exclusion chromatography; the SEC process can be configured to separation of large amounts of material depending upon the scale of the process. Moreover, because analytes are separated by retention time, an almost infinite number of timed “cuts” can be engineered for very precise intervals. Acetosolv sugarcane lignin which had been precipitated by water addition was used as the feedstock and the preparatory SEC method fractionated the original lignin into nineteen fractions using a mobile phase of dioxane:water (9:1); Botaro et al. reported the number-average MW as ranging from 340 to 1250 Da. Ostensibly, high MW material should elute first, followed by mid-range size and ending in the lowest MW sizes. This pattern, however, was not adhered to with the successive samples in the study.¹⁴⁵

The use of a preparatory column with a Sephadex stationary phase in the study by Botaro et al. may have been problematic, as illustrated in a study by Andrianova et al., in which two columns (with THF mobile phase) were tested for linearity and cohesiveness of calibration curves using PS, PMMA and lignin standards; fractionation performed with hydroxypropylated cross-linked dextran stationary phase produced a separation that was not based exclusively on MW due to amplification of undesired non-SEC interactions. However, a highly cross-linked porous polystyrene/divinylbenzene matrix-based (PSDVB) stationary

phase allowed for lignin separation based solely on its MW. The suggested SEC analysis conditions were deemed to be relevant for the translation of an analytical method to a preparative scale SEC.⁸¹ Non-SEC interactions between lignin and the stationary phase in SEC, purportedly arising from the heteropolymeric nature of lignin and the variety of its functional groups, have been considered as possible sources of error by other researchers as well.¹⁴⁶⁻¹⁴⁸

Utilization of a method as reported by Andrianova et al., was the inspiration for conducting our own fractionation study utilizing preparative size exclusion chromatography. There is also a distinct lack of studies in this particular field and this, also, was a reason to address fractionation via the preparative SEC methodology. Results for preparative SEC fractionation of lignin are shown in Table 11.

Table 11. Method parameters and molecular weight findings for a preparatory SEC fractionation study.

Preparatory SEC								
Lignin Source	Solvent Fractionation Method	Analyses	SEC Conditions	SEC Samples	M _n	M _w	PI	Reference
Acetosolv sugarcane lignin, precipitated by water addition	Lignin dissolved in dioxane/water (9:1 v/v), also used as mobile phase at 1 mL/min on Pharmacia preparatory column XK 50/100 (20 C), Sephadex stationary phase; 19 fractions of 60 mL collected; repeated with methanol-soluble Acetosolv lignin (eight fractions)	Vapor pressure osmometry, FTIR, GPC	GPC: individual fractions with PL-gel 500, 10 ³ , 10 ⁴ Å in series, UV detector (254 nm), THF mobile phase at 1.0 mL/min, sample concentration 1.25 mg/mL, 10 – 20 µL volume injection, PS standards	Unfractionated Lignin Fraction 2 Fraction 5 Fraction 8 Fraction 11 Fraction 14 Fraction 17 (Selected fractions from preparatory SEC)	1250 1360 1160 490 470 330 270	14320 28970 8000 920 950 570 14260	11.4 21.3 6.9 1.9 2.0 1.7 51.9	Botaro et al. (2009) ¹⁴⁵

1.6.2. Oxidation of Lignin by Hydrogen Peroxide with and without Alcohol Solvents

Oxidation of lignin, with various forms of oxidants, has been utilized in a number of studies involving lignin depolymerization. Lignin is susceptible to a variety of chemical reagents that are able to break oligomeric strands into monomers or dimers, particularly at linkages with low bond dissociation energies. Chlorine dioxide, ozone, dimethyldioxirane and hydrogen peroxide have been employed as oxidants in the depolymerization of lignin.¹⁴⁹ Although H₂O₂ was not as effective as the other agents in depolymerization ability, it is nevertheless far more environmentally sound and, in some cases, cheaper than other reagents. Furthermore, H₂O₂ may often be combined with metallic catalysts to improve degradation or selectivity.^{150,151}

Hydrogen peroxide has been applied as both a delignifying agent in biomass, but also as a direct depolymerization agent of technical lignins in a large number of studies. Aqueous solutions are often basic or acidic (neutral pH is less common) in peroxide-mediated depolymerization studies; a variety of catalysts are also utilized, commonly combined with metal oxides and alcohols.

Interestingly, a mix of heated methanol and water acting on lignin may be called liquefaction, although the presence of water is considered to have a negative effect on the ability to liquefy lignin (render it into smaller molecules).¹⁵² Moreover, water as a matrix for H₂O₂ alone is considered to be less than desirable because of the exothermic nature of the mixture and the fact that the solution does not follow Raoult's law. The same study found that H₂O₂ was not effective at lignin breakdown without the presence of a mineral or organic acid.¹⁵³

Suggested mechanisms for H₂O₂ oxidation differed for alkaline (pH >10) and acidic conditions (pH < 4)- for alkaline H₂O₂ oxidation the perhydroxyl anion (HOO⁻) was considered to be the active oxidation species by a number of researchers,^{150,153-157} while the OH⁺ ion was most commonly named as the active agent in acidic H₂O₂ oxidation.^{153,157,158} Radical mediation was proposed by Asha for H₂O₂ solutions exposed to light energy,¹⁵⁹ and also suggested by Agnemo et al.¹⁴⁹ Alkaline oxidation was generally seen to be more productive in terms of lignin conversion,¹⁵⁷ although improvements in oxidative strategy such as the use of a H₂O₂ stabilizer, diethylenetriaminepentamethylene-pentaphosphoric acid (DTMPA)¹⁵⁶ and the implementation of higher temperatures (> 90 °C)^{156,157} made acidic conditions productive as well.

1.6.2.1. Alkaline hydrogen peroxide treatment

The alkaline hydrogen peroxide depolymerization of lignin is performed when NaOH or another base has been added to raise pH usually in an aqueous solution. In alkaline conditions H₂O₂ produces O₂ and a number of radical and anionic species, which are capable of degrading lignin through various routes; reactive species include hydroxyl anion (HO⁻), hydroxyl radical (•OH), perhydroxyl radical (HOO•), perhydroxyl anion (HOO⁻), and superoxide radical (O₂•⁻). The perhydroxyl anion is considered to be the major mediator of lignin breakdown in alkaline solution,^{155,157} capable of cleaving linkages,¹⁵⁰ although the presence of radicals results in nonselective attacks on the lignin structure and on H₂O₂.¹⁵⁶ Overoxidation of lignin may produce gases (CO₂ and CO) rather than monomers.¹⁵³ The number of carboxyl, carbonyl, and hydroxyl groups were found to increase, and MW of treated lignin was noted as decreasing.¹⁵⁵ Aromatic cleavage, or ring-

opening, was observed by He et al.,¹⁵⁴ although Junghans et al. did not observe this.¹⁵⁵ Additionally, an increase in carboxyl groups after treatment with alkaline hydrogen peroxide was also noted by He et al.¹⁵⁴

A general mechanism, as proposed by Asha et al. for alkaline H₂O₂ attack may start with hydroxyl radical withdrawal of a hydrogen from an aliphatic carbon on the phenylpropanoid structure, then creation of a C=C bond followed by transformation of an oxygen in an ether bond to a carbonyl oxygen, effectively breaking the β-O-4' bond. Subsequent action by the superoxide radical might lead to ring-opening and degradation of lignin to CO₂ and low MW products.¹⁵⁹

A mechanism proposed by Xiang et al. includes the perhydroxyl anion, HOO⁻, as the main oxidative species, also leading to aryl ether breakage and ring-opening of chromophores. The same study found that carboxylic acids which were formed constituted up to 56 wt% of the original lignin weight at 120 °C, the product of 98% conversion of initial lignin.¹⁵⁷ A study by Gierer et al. showed that cleavage of the β-O-4 bond occurred at temperatures as low as 30 °C when carbonyls were present at aliphatic alpha positions of the phenylpropanoid unit.¹⁶⁰

A proposed mechanism of the radical reaction, mediated through perhydroxyl anion and hydroxyl radical reaction, as envisioned by Asha et al. is presented in Figure 10.¹⁵⁹

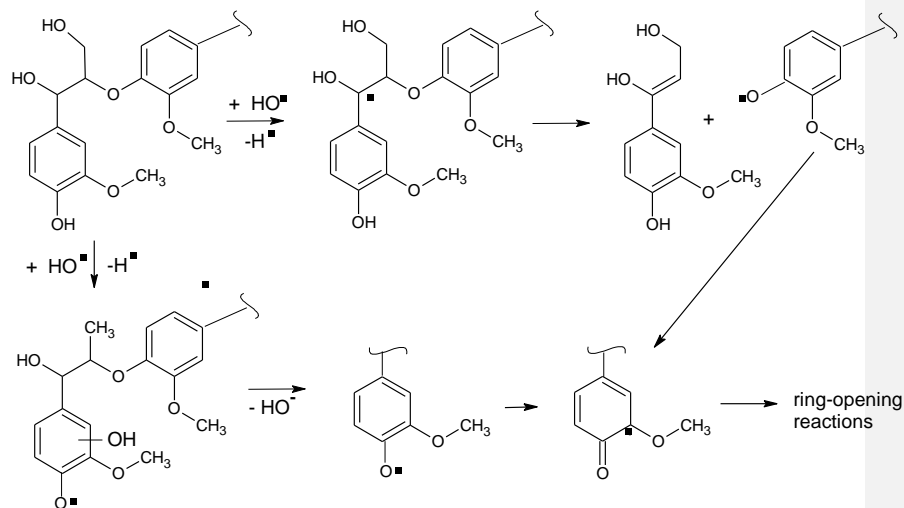
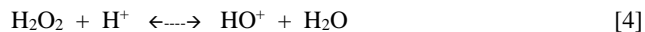


Figure 10. Proposed breakdown of lignin in alkaline solution by hydrogen peroxide via photocatalysis.¹⁵⁹

The mechanism proposed by Asha et al. for the reaction in alkaline solution delineated not only depolymerization of lignin, but concurrent production of quinones which ultimately led to ring-opening through additional oxidation by the superoxide radical, $O_2^{\bullet-}$.¹⁵⁹

1.6.2.2. Acidic hydrogen peroxide treatment

Although depolymerization of lignin under alkaline conditions is a more common form of peroxide depolymerization, since radical activity occurs, there are several studies which addressed H_2O_2 effectiveness under acidic conditions.^{153,158,161,162} A mechanism proposed by Ahmad et al. suggested that HO^+ (hydroxyl cation) species produced oxidative cleavage of β-aryl ether bonds and ring opening, through the reaction:¹⁵³



A study by Kishimoto gave some insight into H_2O_2 oxidation under acidic conditions for lignin model compounds. In the experiments lignin models were exposed to 3X the molar amount of H_2O_2 , with diethylenetriaminepentaacetic acid (DTPA) present in an acidified solution; the final solutions were heated to 70 °C and samples were withdrawn at various times. Results showed that nonphenolic aromatic models had no reactivity, while phenolic models with a methyl benzylic group showed limited reactivity (15%). However, nonphenolic and phenolic models with α -hydroxyl groups were almost completely reacted within 1 hour as long as a hydroxyl or methoxy substituent was present in the para position to the benzylic alcohol, as shown in Figure 11.¹⁶¹

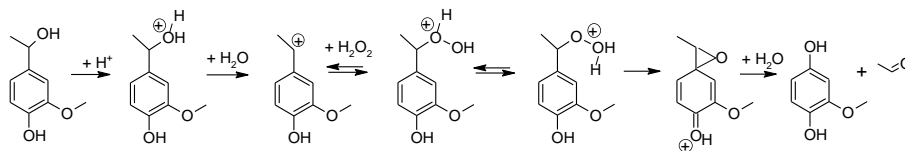
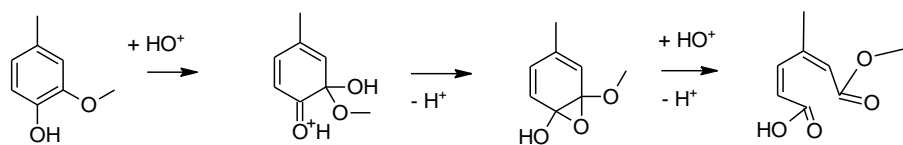


Figure 11. Proposed mechanism for oxidation of α -hydroxyl groups in lignin under acidic conditions. In this instance, acetaldehyde (ethanal) is produced as a side product during cleavage of the bond at the α -O-4' location.¹⁶¹

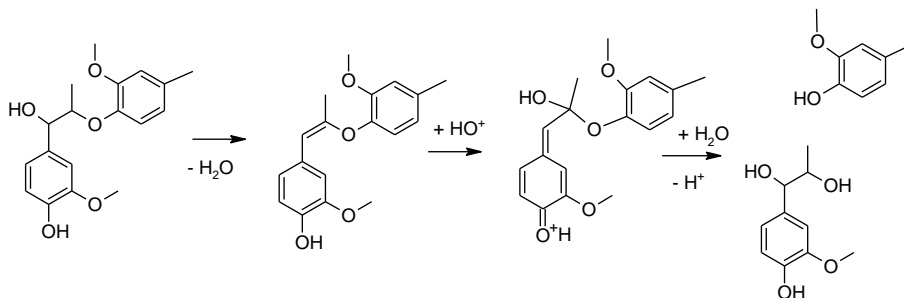
The mechanism proposed by the group outlined carbocation production at the benzylic carbon (initiated by acid attack), which allowed H_2O_2 addition at the site, followed by rearrangement to an epoxide group (as in the Dakin reaction). The intermediate product was then hydrolyzed, producing a phenol and an aldehyde. Aldehydes constituted 25% of the products in this set of reactions. It was found that the reactions provided the greatest yield of products at a pH of 1.3, whereas production decreased substantially at higher pH, essentially stopping at a pH of 3.0.¹⁶¹

A study by Kadla et al. showed that stabilization of H₂O₂ through the addition of DTMPA inhibited radical production and increased H₂O₂ oxidative ability, resulting in 80.2% conversion of lignin at 110 °C.¹⁵⁶ The study also found that carboxylic acid groups increased significantly, methoxy groups decreased and phenolic OH declined in favor of an increase in aliphatic OH, in comparison to untreated lignin. Of note, the same study found that average MW (by GPC) of the oxidized lignins increased with respect to untreated lignin. This was attributed to possible condensation reactions or rapid depolymerization which resulted in repolymerization of the released oligomers.¹⁵⁶ A study by Mancera showed that MW was also increased during lignin oxidation by H₂O₂ under acidic conditions.¹⁶²

The results of Ahmad et al. were in agreement with proposed mechanisms for ring-opening and depolymerization by way of the β-O-4' linkage, mediated by HO⁺ ion, as presented by Gierer et al.¹⁶⁰ The schemes are shown in Figure 12a and 12b, respectively.¹⁵³



(a)

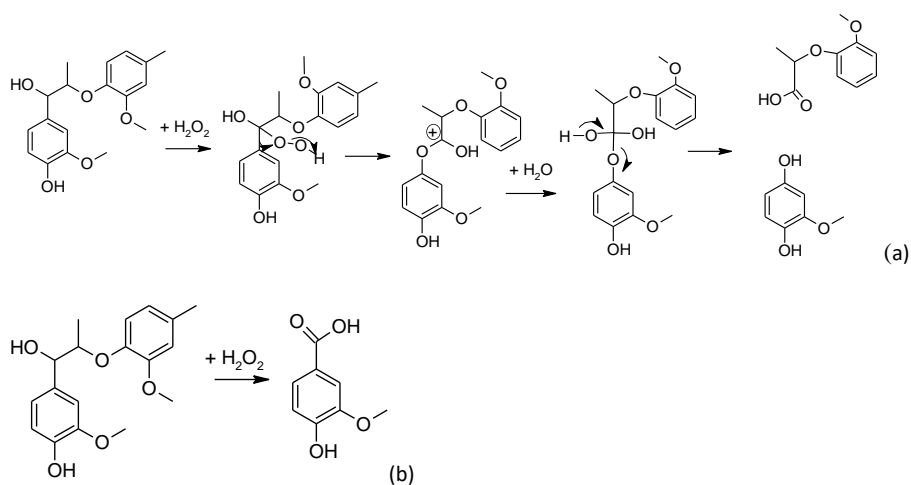


(b)

Figure 12. (a) Proposed ring-opening mechanism by Ahmad et al.,¹⁵³ (based on Gierer et al.¹⁶⁰) by the OH⁺ ion under acidic conditions, (b) proposed depolymerization of lignin via the β-O-4' linkage through the action of the OH⁺ ion after a dehydration process in acidic media.

Depolymerization of lignin under acidic conditions was also addressed by Evstigneev, who concluded that H₂O₂ decomposition of lignin occurred optimally at about 80 °C with acid (1.2 M H₂SO₄) and H₂O₂ (3.2 M) present, with lignin at a concentration of about 3.2 M. The reaction took place over 150 min and resulted in 94.5% solubility of the lignin. The same study found that Fe catalysts actually caused decomposition of H₂O₂ to the extent that degradation of lignin was compromised. It was also determined that high temperatures decomposed H₂O₂ as well, unless acid was present.¹⁵⁸ Several conditions were necessary to ensure the effectiveness of H₂O₂ breakdown in an acidic solution. Lignin had to be initially in an alkaline form, then underwent treatment with H₂O₂ in an acidic solution and was then solubilized in an alkaline solution. Solubilization extent was the metric for lignin conversion, although this was not necessarily contingent on breakdown of larger oligomers to smaller ones. This study suggested that H₂O₂ under these conditions resulted in ring-opening of aromatics, which further produced a substantial increase in carboxyl groups (0.8 to 8.9 wt% of original lignin mass) at the phenolic hydroxyl and methoxy sites, and also may have produced aliphatic carbonyl groups.¹⁵⁸

Mancera et al. undertook a study of soda lignin depolymerization via oxidation by H_2O_2 in an acidic environment and proposed a mechanism in which a carbocation was created in a bond rearrangement after hydrogen peroxide attached to an α -carbon with a hydroxyl group.¹⁶² The study also proposed several other possible scenarios for depolymerization. The study believed that a carbocation occurrence at the benzylic position could also result in addition of H_2O_2 and a subsequent Dakin-like replacement of a ring substituent which became attached to nearby lignin groups in a type of repolymerization. Mancera et al. also noted that M_n and M_w values of the oxidized lignin were somewhat higher than the values for the original soda lignin. The depolymerization schemes and the Dakin-like reaction which was thought to be responsible for condensation of lignin compounds are presented in Figure 13.¹⁶²



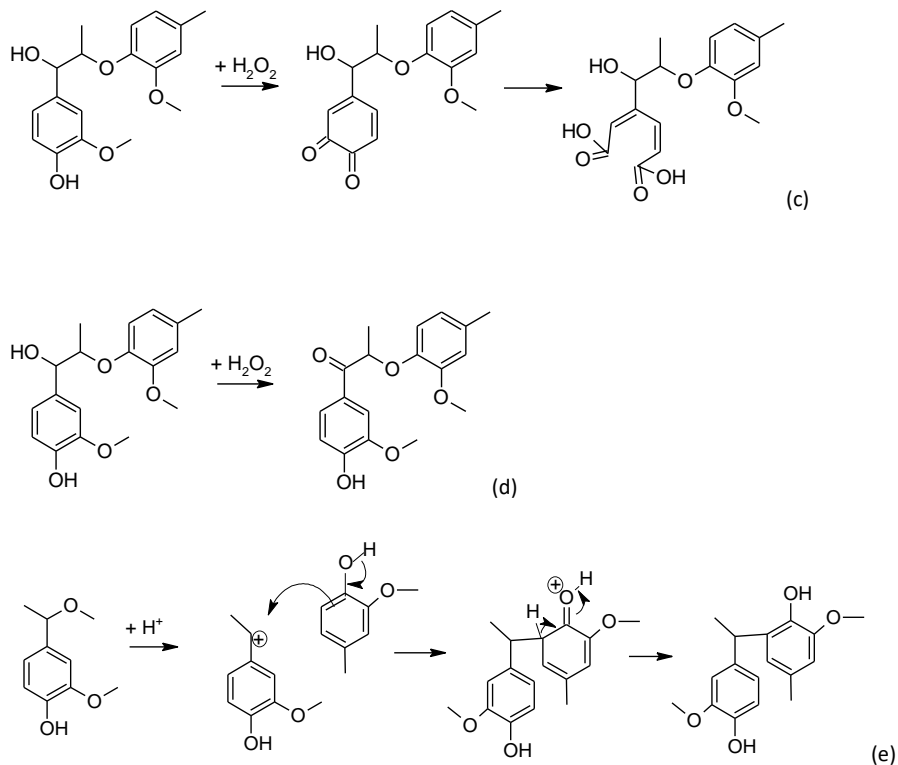


Figure 13. Depolymerization schemes under acidic conditions, accomplished by direct H_2O_2 action, via (a) creation of a carbocation after rearrangement of the α -carbon bond to the aromatic ring, (b) cleavage of the $\text{C}\alpha - \text{C}\beta$ bond and creation of a carboxylic group at the α -carbon, (c) ring opening reaction through the removal of ring substituents, (d) oxidation of an α -carbon hydroxyl group, producing an aliphatic ketone. Panel (e) shows a proposed condensation reaction through acidic action.¹⁶²

Of interest, Xiang et al. proposed that H_2O_2 oxidation of lignin was a heterogeneous reaction because of the insolubility of lignin in an acid environment, maintaining that disruption of aryl ether bonds would be difficult. A temperature of $160\text{ }^\circ\text{C}$ was found to be necessary to produce a 97 wt% conversion (compared to initial lignin weight) and carboxylic acid content was 34 wt% at this temperature. The main acid present was formic

acid as opposed to oxalic acid in alkaline oxidation, prompting the group to believe that breakdown of the lignin resulted in simple low MW species and production of CO₂ gas at temperatures > 140 °C due to severity rather than H₂O₂ oxidation. Products were believed to come from electrophilic attack of the OH⁺ ion on the aromatic ring, which degraded rapidly to simple carboxylic acids.¹⁵⁷

Studies on H₂O₂ oxidation of lignin in neutral pH solution were rare; the Evstigneev study compared their outcomes to a study by Izumrudova et al., in which H₂O₂ oxidation of lignin in a neutral solution (pH 7) took place at higher temperatures (90 °C) and longer times (6 h) to reach a solubility of only about 50 wt% of the original lignin mass.¹⁶³

In summary, the target of many of the researchers was varied; studies were undertaken to make lignin soluble (ostensibly to produce lower MW products),^{157,158} improve lignin as a dispersant,¹⁵⁴ depolymerize it by modified or varied methodology,^{150,152,156} evaluate method parameters,¹⁴⁹ produce carboxyls,¹⁵⁵ and obtain bio-oil.¹⁶⁴ A number of studies proposed mechanisms.^{149,150,154,155,159}

All studies reviewed found that carboxylic acids were a high percentage of conversion products. However, many of the studies declined to look at MW; a number found that MW increased upon lignin oxidation with H₂O₂,^{156,162} although this outcome could not be considered to be an improvement in lignin depolymerization. Several studies did find that MWs decreased after the oxidative reactions.^{152,155}

The majority of the studies reviewed showed that both acid and alkaline solvent approaches to hydrogen peroxide oxidation were successful at lignin depolymerization, although by very different (proposed) mechanisms; conversions of over 90% of the original

lignin were listed for both types of solvent systems (Table 12). Solubility problems, particularly for acid-treated samples¹⁵⁷ and even neutral-pH samples,¹⁶³ were addressed by increased temperatures and treatment times.

It was our contention to investigate lignin depolymerization (with H₂O₂ catalyst) in solvent systems which were acidic, alkaline and neutral, but identical in conditions other than pH, in order to directly compare the results. This had not been done in previously published studies. We also proposed to monitor pH before and after oxidation reactions to assess lignin buffering capacity, which had not been addressed by other investigators. Of concern was the large number of studies reporting ring-opening and production of acids; this would also be directly addressed in our study by monitoring of pH. Several studies had also reported increased condensation. Thermal carbon analysis of products vs untreated lignin would allow us to test this hypothesis as well.

Table 12. Method parameters and findings for several lignin oxidation studies with hydrogen peroxide as the primary catalyst.

Lignin type	H ₂ O ₂ Method	Analyses	Results	Reference
Hydrolytic sugar cane lignin, red spruce kraft lignin	H ₂ O ₂ (concentration NR), with/without heterogeneous methylrhenum trioxide catalysts in acetic acid at 25 °C, for 24 h; products filtered, washed with H ₂ O.	³¹ P, ¹³ C, ¹ H NMR- solids fraction	Decrease in aliphatic OH groups, increased COOH content with use of H ₂ O ₂ /catalyst.	Crestini et al. (2006) ¹⁵¹
Softwood and hardwood kraft lignins separated from black liquor through LignoForce™ process; MW 6041, 2718 g/mol respectively	H ₂ O ₂ at 25, 35 °C, for 80, 120 h respectively; 1:1, 1:0.75, 1:0.5 with lignin (mass), approximately 0.6 g/mL (18 M) concentration of liquid; reaction on dry basis (lignin)	Gravimetry GPC-UV of non-gas residue FTIR of non-gas residue ³¹ P NMR of non-gas residue Py-GC-MS of non-gas residue	Conversion: about 38% non gas residue GPC: MW at 1:1 1420, 1415 for softwood/hardwood FTIR: increase in C=O, ring-opening, decrease in methoxy groups NMR: increased COOH, decreased aliphatic OH, decrease phenolic OH for hardwood Py: 10-13 compounds by % area softwood/ hardwood	Ahmad et al. (2020) ¹⁵³
Alkaline lignin (TCI Co., Japan)	Photocatalytic reactor (batch flow) at 27 °C for 1 hour, Hg vapor lamps at 200-400 nm and 410-650 nm; lignin at 100 or 200 mg/L;) H ₂ O ₂ at 0.4, 0.8, 1.2, 1.6, 2.0 M.	UV absorbance at 276 nm for degradation of lignin	Conversion: 98% (100 mg/L) and 90% (200 mg/L)	Asha et al. (2020) ¹⁵⁹
Alkaline lignin isolated from poplar wood soda pulp	Lignin pretreated with 0.5, 1, 2% (30%) H ₂ O ₂ (0.05, 0.1, 0.2 M) adjusted to pH 11.5 with NaOH, at 60 or 80 °C in pressure tube reactor, then liquefied with MeOH or MeOH/H ₂ O in autoclave (200 and 260 °C respectively) for 30 min; contents washed with MeOH, solid/liquid filtered	Gravimetry GPC of liquid fraction GC-MS of liquid fraction FTIR: lignin, liquid, solid fractions 1H NMR of lignin, liquid fractions	Conversion: MeOH-water: 84 wt% , with 0.5% H ₂ O ₂ : 93.5% at 80 °C GPC: Mw from 1692 to 1354 with H ₂ O ₂ GC-MS: nine compounds by area FTIR: Phenols converted to quinone or aliphatic chains in some cases. NMR: Findings similar to FTIR; side chains removed	Cheng et al. (2016) ¹⁵²
Hydrolysis lignin (softwood), fraction 0.2 0.4 mm collected, extracted with ethanol	Temperature-controlled cell with 2, 4, 6, 8M H ₂ O ₂ and 0.4, 0.8, 1.2M H ₂ SO ₄ , at 20, 40, 60, 80, 100 °C, for 40, 60, 100, 120, 180 min, p NR; products washed with H ₂ O and solubility determined in 0.4 M NaOH solution	Solubility of treated lignin COOH of solubilized fraction by titration of lignin solution with HCl Phenolic OH in solubilized fraction by aminolysis of acetylated lignin then differential spectroscopy at 250 nm	Optimal solubility: About 78 wt% of original lignin at 0.1 M H ₂ SO ₄ , 2.6 M H ₂ O ₂ , 150 min at 80 °C COOH: Increased from 34 per 100 phenylpropanoid units to 68 when oxidized and 82 with addition of NaOH Phenolic OH: remained about the same (ring-opening may be in nonphenolic rings)	Evstigneev et al. (2012) ¹⁵⁸

Lignin model α-methyl syringyl alcohol	Alkaline solution bath with bubbled N ₂ ; H ₂ O ₂ (0.4 mol/L vs 0.005 mol/L of lignin model) added with MnSO ₄ , FeSO ₄ , CuSO ₄ catalysts at 25, 30, 40 °C; pH at 10, 10.5, 11, 11.5, 12, 12.5; lignin model reacted and inspected at 50, 100, 150 min, then extracted with ethyl acetate	GC-MS of solution	Conversion: GC-MS monitoring of α -methylsyringyl alcohol with time-kinetic degradation rates reported only; higher pH increased rate; Mn catalyst increased rate more than Cu, Fe	Agnemo et al. (1979) ¹⁴⁹
Organosolv beechwood lignin (hardwood); M_n 1170 and 1732 M_w	Microwave vessel 200 W for 5-30 min at 5 min increments, p NR, alkaline solution with La-modified SBA-15 catalyst and 0.47 mol/L H ₂ O ₂ oxidant; with 0.52 mol/L lignin; SPE of products	Gravimetry GC-MS of SPE products HPLC-UV of SPE products	Conversion: Max vanillin 9.9 mol%, syringaldehyde 15.66 mol% (0.38 and 0.52 mol% without catalyst or oxidant) GC-MS: Six compounds identified HPLC: Six compounds quantified	Gu et al. (2012) ¹⁵⁰
Softwood kraft lignin by LignoForce™ process; 13859 M_n and 16770 M_w	Flask with alkaline solution and H ₂ O ₂ at 60 – 100 °C for 1-3 h; H ₂ O ₂ : lignin molar ratios 0.57, 1.14, 1.71, 2.28, 2.85; products adjusted to pH 7 and dialyzed to 1000 g/mol cut-off	Gravimetry Potentiometric titration for carboxylate and phenolate GPC-UV, RI, light scattering of dialysate FTIR of dialysate	Conversion: Max carboxylate 1.53 meq/g at 80 °C, 0.77 molar ratio of NaOH/H ₂ O ₂ and 2.85 molar ratio of H ₂ O ₂ /lignin Titration: carboxylate groups increased, phenolate decreased in dialysate GPC: 11273 M_n and 14825 M_w FTIR: increased carboxyl	He et al. (2017) ¹⁵⁴
Pine wood kraft lignin from LignoBoost process; 1177 M_n and 6920 M_w g/mol	Reflux glass reactor, alkaline aqueous solution (0.5, 1, 2 mol/L) with H ₂ O ₂ (40, 80, 120 g/L) or (1.2, 2.4, 3.0 mol/L) for 1, 2, 4 hours at 29, 45, 60, 80 °C; lignin at 10, 20, 40, 60 g/L, all products acidified, solids washed and removed; solid wash and aqueous filtrate combined and oil extracted with methyl isobutyl ketone	Gravimetry GC-FID of oil GC-MS of oil ATR-IR of solids GPC of oil and solids	Conversion: Max 95 wt% at max conditions (see GPC) GC-FID: Max 18 wt% of oil GC-MS: Vanillin and apocynin identified IR: Formation of COOH, aliphatic OH, decrease in phenolic OH, no ring-opening GPC: M_w 1245 oil lowest for 80 g/L stabilized H ₂ O ₂ , 2 mol/L NaOH, 40 g/L lignin and 1 h at 45 °C	Junghans et al. (2020) ¹⁵⁵
Lignin model compounds: apocynol, α-methyl-veratryl alcohol, vanillyl alcohol, 3,4-dimethoxy alcohol, vanillin and veratraldehyde	Sealed vials in oil bath, with H ₂ O ₂ at 0.045 mole/g lignin, DTMPA, pH 11.2 K ₂ CO ₃ , reacted at 90 or 50 °C for 3 h, p NR; during and after reaction products removed at timed intervals; products were acidified to pH 2 and extracted with methylene chloride or diethyl ether.	GC-MS of liquid extract ¹ H-NMR of lignin and liquid extracts	GC-MS, NMR: conversion: phenolic models converted and H ₂ O ₂ consumed nearly completely by 90 min, pH 10-12; acetaldehyde amounts increased, non phenolic models 50- 100wt% left after 180 min	Kadla et al. (1997) ¹⁵⁶

Lignin model compounds: methyl guaiacol, 4-methyl veratrol, acetovanillone, 4-(1-hydroxyethyl)-2-methoxyphenol, 1-(3,4-dimethoxyphenyl)-ethanol, 1-(4-methoxyphenyl)-ethanol, 1-(3-methoxyphenyl)-ethanol	Sealed vials in oil bath, with 0.0225 M H ₂ O ₂ , 0.02 M lignin, DTMPA, in acidic aqueous solution w or w/o dioxane, reacted at 70 °C, p NR; during and after reaction products removed at 0-360 min (20 min intervals); products were washed with Na ₂ S ₂ O ₃ solution, acidified to pH 2 and extracted with ethyl acetate	GC-MS of liquid extract ¹ H-NMR of liquid extract	GC-MS, NMR: conversion: Two a-hydroxy models converted nearly completely by 60 min, (one after 360 min) at pH 1.3, 70 °C; Nonphenolic α-hydroxy with para H did not react simple phenolic models 75- 100wt% left after 360 min at pH 1.3, phenolic α-ketone unreactive; Reactivity slowed with increasing pH; Dimers identified as products; Decreasing pH increased condensation	Kishimoto et al. (2003) ¹⁶¹
Protobind™ lignin, pH 3-3.5	Autoclave reactor, water-ethanol solvent (10 g 1:1), 1 g lignin with 0.2, 0.4, 0.7, 1, 2, 3 mol/L H ₂ O ₂ , added, at 100, 120, 140, 160, 180 °C for 30 min, p NR; post reaction solvent was evaporated, products filtered with ethanol, liquid fraction designated as bio-oil and solid fraction as char-residue	Gravimetry TOC of lignin and char FTIR of lignin and bio-oil ¹ H-NMR of bio-oil GC-MS of bio-oil	Conversion: Max bio-oil 80 wt% at 120 C, 30 min, 1 mL H ₂ O ₂ , with char 6.6 wt%, gas 13.4 wt% TOC: 5.9% char for 1 mL H ₂ O ₂ FTIR: aromatic esters, aliphatic compounds NMR: aliphatics attached to alkenes and carbonyls GC-MS: 44 compounds as % areas	Kumar et al. (2020) ¹⁶⁴
Soda lignin from sugar cane bagasse	Reflux flask with acidic aqueous solution, with lignin and 0.89 M H ₂ O ₂ for 10- 120 min, liquid products removed at 10 min intervals; solid fraction filtered and washed (oxidized lignin)	FTIR of lignin, oxidized lignin GPC of oxidized lignin CP-MAS ¹³ C-NMR of oxidized lignin Elemental analysis of oxidized lignin	FTIR: increase in carbonyls, carboxyls, quinones; demethylation and repolymerization indicated GPC: Soda lignin <i>M_w</i> 18926, oxidized lignin 20493 NMR: indication of carbonyl increase, decrease in ether linkages, increase in self-condensation Elemental analysis: C, H reduced, O increased	Mancera et al. (2010) ¹⁶²
Precipitated poplar hardwood lignin from acid hydrolysis of biomass	Bomb reactor with alkaline, acid or neutral solution, with H ₂ O ₂ (1.5 mol/L) with 0.3 g lignin; 5, 10 min basic; 5, 10, 20, 30 min acidic; reaction products acidified to pH 2, filtered, solids washed and dried. Liquid products divided into diethyl ether soluble and insoluble. Gases collected	Gravimetry HPLC of liquid products GC-MS of ether soluble and insoluble fractions, gases	Conversion: 98 wt% solubilization for alkaline at 120 °C; 97 wt% for acid at 160 °C HPLC: Acids quantified as 51 wt% for alkaline and 34 wt% for acid method GC-MS: Main gas CO ₂	Xiang et al. (2000) ¹⁵⁷

1.6.3. Subcritical water treatment of alkali lignin

It was also noted that many studies combined hot pressurized water as a solvent with a number of depolymerization approaches, including catalysis, microwave, electrochemical, ionic liquids, and others, often attributing conversion rates to the effect of catalysts, oxidants or equipment.

One of the frequent decomposition methods employs water as the main process medium. Water in sub/near supercritical conditions dramatically changes its properties, decreasing in polarity while still being in the liquid phase (under sufficient pressure) thus enhancing solubilization and breakdown of the matrix.¹⁶⁵ Furthermore, the use of water is favored as an attractive option due to its low cost and public perception as a green and plentiful solvent. Nonetheless, achieving supercritical conditions is less economical because of high temperatures and pressures and thus the majority of studies focuses on subcritical water (SW) conditions, i.e., 100 to 370 °C at 1 to 22 MPa.

Combined with SW treatment, lignin degradation is frequently facilitated by catalysts, oxidative/reductive species or occasionally ionic liquids. Understanding the impact of SW alone in such treatments seems to be essential as a reference (i.e., baseline) when comparing the effectiveness of various catalysts. A number of studies investigated SW treatment of lignin without additives yet differing in feedstocks, temperatures, pressures and reaction times. Furthermore, the focus of these studies varied: Some authors used the SW system as a baseline for comparison to systems with additives or supercritical temperatures,¹⁶⁶⁻¹⁷⁴ as a kinetic study,¹⁷⁴⁻¹⁷⁶ or as a basis for evaluation of degradative mechanisms.^{173,174,177} Several studies focused on optimization of bio-oil production, i.e., low molecular weight (MW) solvent extractable species, with some chemical

characterization to this fraction,¹⁷⁸⁻¹⁸⁰ whereas others focused on the characterization of solid residue that is a means of producing hydrochar.^{177,181} Table 13 summarizes the results of such studies that employed comprehensive analytical protocols determining (often combined with gravimetry and occasionally total organic carbon (TOC) analysis)^{170,171,174,178} the product distribution between the liquid and solid fractions, plus solvent extractable bio-oil. In these studies, repolymerization of phenolic intermediates was viewed, either explicitly or implicitly, as the main competing path to depolymerization, thus limiting the yield of valuable phenolic monomers or contributing to hydrochar formation.

Table 13. Comprehensive list of lignin subcritical water treatment studies without additives conducted with a suite of analytical protocols, including experimental conditions, analytical methods and main findings (for abbreviations seen footnote).

Feedstock(s)	SW Treatment Conditions	Selected Analytical Methods	Findings	References
Bamboo kraft lignin; MW 2,720 g/mol	Batch reactor, 130, 180, 230 °C, 15 or 60 min, pressure NR	Gravimetry GC-MS of diethyl ether and ethyl acetate extracts of water-soluble fraction (bio-oils) GPC of water-insoluble products FTIR of water-insoluble products	Conversion to bio-oil & gas up to 21% (230 °C); bio-oil 5.4–10.6% GC-MS: 17 products quantified GPC: M _w 620-1670 g/mol (230 and 130 °C, respectively) FTIR: Increase of phenolic groups, loss of β-O-4 bonds	Zhou et al. (2014) ¹⁸²
Cellulolytic enzyme lignin from Poplar; M _n 2,750, M _w 6,000 g/mol	Flow reactor, 20 mL/min, 140 °C at 0.28 MPag, 180 °C at 1.10 MPag; 12 or 192 min Batch reactor, 140 and 180 °C, outside pressure NR, 12 or 192 min	Gravimetry GC-MS of filtered water-soluble products GPC of water-insoluble products HSQC NMR of water-insoluble products	Conversion to water-soluble products up to 42 wt% by flowthrough and 25 wt% by batch GC-MS: 18 products quantified GPC: M _n 3,000-5,000; M _w 3,000-14,000 g/mol HSQC NMR: Loss of β-O-4 bonds and methoxy groups with temperature increase	Trajano et al. (2013) ¹⁸³
Switchgrass organosolv lignin; MW~800 g/mol	Autoclave reactor, 160, 200, 220, 250 °C, for 2 h, p NR; 180 °C for 2, 4, 8 h, pressure NR	Gravimetry GC-FID of DCM extract of water soluble fraction GC-MS of DCM extract of water soluble fraction GPC, ¹ H-NMR of THF extract of water-insoluble fraction Elem. analysis, TG, FTIR, SEM of THF extract and char (residue left after THF extraction)	Conversion to water-solubles up to 40 wt% GC-FID: 23 volatiles quantified at 9.3 wt% at 250 °C GC-MS: 23 products reported as normalized GPC: At temperatures > 180 °C, decrease in product yield and M _w Elem analysis: Residue deoxygenated TG: THF-solubles same as raw lignin, char produced more coke (non-volatiles) than lignin even at 900 °C	Long et al. (2014) ¹⁸⁴
lKali lignin (Sigma-Aldrich); MW NR	Batch reactor, 200, 250, 300, 350 °C, 0, 20, 40, 60 min, pressure NR	Gravimetry GC-MS of ethyl acetate (EA) extract from filtered water-soluble fraction (light oil) GC-MS of acetone extract of filtered water-insoluble fraction (heavy oil)	Conversion to heavy oil 34 to 31 wt% and to light oil 6 to 14 wt% for 300 and 350 °C, respectively GC-MS: 20 monomer products quantified	Islam et al. (2018) ¹⁷⁹
Alkali lignin (Sigma-Aldrich); MW NR	Batch reactor, 280, 370 °C, 0-240 min; pressure NR	Gravimetry GC-MS of methanol-extract of water-soluble and -insoluble fractions HPLC of methanol-extract of water-soluble and -insoluble fractions FTIR and NMR of water-insoluble/methanol-insoluble residue	Conversion to methanol-soluble products up to 11 to 21 wt% (280 and 370 °C, respectively) GC-MS: 33 products reported as normalized HPLC: 5 major products quantified FTIR: Increased phenolic content with temperature increase	Pinkowska et al. (2012) ¹⁶⁹

Low sulfonate alkali lignin from Norway spruce, (Sigma Japan); MW 10,000 g/mol	Batch reactor, 300, 350, 370 °C, 0.5-10 s, 25 MPa	Gravimetry, TOC of aqueous liquid fraction GC-TCD/FID of gas products LC-MS, HPLC of water-soluble products FTIR, elem. analysis of lignin and char (water-insoluble products)	Conversion to water-soluble products up to 50 wt% (300 °C) Gases up to 15 wt% (370 °C) LC-MS, HPLC: 18 products, qualitative and quantified, respectively FTIR: OH group decrease in char compared to lignin.	Yong and Matsumura, (2013) ¹⁷⁴
Lignin isolated from Poplar sulfate black liquor; MW NR	Batch reactor, 220, 250, 280, 310, 340 °C at 30 min; 0.9, 1.9, 3.9, 7.0, 13.8 MPa, respectively. Also 0, 15, 30, 45, 60 min at 310 °C	Gravimetry GC-FID, GC-MS, of water-soluble fraction and ethyl acetate (EA) extract of water-soluble and water-insoluble fractions FTIR of water-insoluble/EA-insoluble residue	Conversion to water-soluble products up to 96% (340 °C) GC-FID: 12 products quantified GC-MS: 34 products, reported as normalized FTIR: Decrease in OH groups with temperature increase (OH groups negligible by 340 °C)	Jiang et al. (2014) ¹⁷²
Enzymatic/Mild Acidolysis lignin from China fi; M _n 12,372 and M _w 20,123 g/mol	Autoclave reactor, 250, 275, 300, 325, 350 °C, with pressures 3.9, 6.0, 8.6, 12.2, 16.5 MPa, respectively	Gravimetry GC-MS of ethyl acetate (EA) extract of water-soluble and -insoluble fractions GC-TCD of gas products GC-FID of EA extract LC-ESI-MS (MW distribution) of EA extract FTIR, TG of water-insoluble/EA-insoluble residue	Conversion up to 40 wt% EA-soluble products (325 °C); gases 5-10 wt% (all temperatures) GC-MS: 26 products, reported as normalized GC-TCD: Four products quantified GC-FID: Six products quantified LC-ESI-MS: Reduction of high-MW compounds at higher temperatures TG: Thermal stability of solids > lignin stability	Zhao et al. (2016) ¹⁸⁵
Alkaline lignin from Japan (Tokyo Kasei Kogyo Co.); MW NR	Batch reactor, 350 °C for subcritical section, pressure 25, 30, 40 MPa, for 5, 15, 30, 60, 90, 120, 180 and 250 min	Gravimetry GC-MS, HPLC, MALDI-TOF of methanol extract of water-soluble and -insoluble fractions FTIR of water-insoluble/methanol-insoluble residue	Conversion up to about 40 wt% methanol-soluble products GC-MS: 28 products, reported as normalized, four compounds quantified by HPLC FTIR: Loss of OH groups with temperature increase	Wahyudiono et al. (2008) ¹⁶⁸
Beech wood organosolv lignin; M _n 606, M _w 3,428 g/mol	Batch reactor, 270, 290, 310, 350 °C and 10, 20, 30, 60, 120 min residence time, pressure NR	Gravimetry, TOC of water-soluble fraction GC-MS of ethyl acetate (EA) extract from water-soluble fraction (bio-oil) GPC of lignin and EA extract	Conversion to water-solubles up to 25 wt%, bio-oil up to 13 wt% (350 °C) GC-MS: Bio-oil 14 monomers reported as normalized – eight monomers quantified GPC: Bio-oil M _n 201-218, M _w 242-291 g/mol (for 350 and 270 °C, respectively)	Hashmi et al. (2017) ¹⁷⁸
Dealkaline lignin (TCI); MW NR	Autoclave reactor, 225, 245, 265 °C; pressure NR	Gravimetry TG of water-insoluble fraction (hydrochar) FTIR of water-insoluble fraction (hydrochar) Elem. analysis of water-insoluble fraction (hydrochar)	Conversion to hydrochar up to 60% (225 °C) TG: Thermal stability of solids > stability of lignin FTIR: O-H, C-H, C-O groups fewer than in lignin Elem. analysis: C/O and C/H ratios increased from 225 to 265 °C	Kang et al. (2012) ¹⁸⁶

Hardwood-derived Organosolv lignin (Sigma); MW NR	Batch reactor, 365 °C at 500 psi for 30 min	Gravimetry GC-FID-TCD of gases GC-MS: DCM extract of water-soluble and -insoluble fractions Solid-state C-NMR of water-insoluble/DCM-insoluble residue	Conversion to DCM-soluble products 40 wt% GC-MS: 10 products reported as normalized C-NMR: Aromatics 76%, aliphatics 24% for reacted lignin (no gases added) compared to 64% and 36%, respectively, for unreacted lignin	Bembenic and Clifford (2012) ¹⁶³
Crop waste alkali Protobind® 1,000; MW NR	Batch reactor, 370 and 390 °C, 25 MPa for 5, 10, 20, 40 min	Gravimetry, TOC of aqueous liquid fraction, GC analysis GC-TCD of gases. GC-FID of water-soluble fraction ¹³ C NMR of water-insoluble fraction after 0.7 µm paper filtration Elem. analysis of water-insoluble fraction	Conversion to water-soluble products up to 33 wt% (370 °C), 40 min GC-TCD: Gases 1-5 wt% GC-FID: 13 water-soluble products, quantified ¹³ C NMR: Decrease in C-O/C-C ratio with reaction time	Barbier et al. (2012) ¹⁶⁷
Lignin-rich stream from lignocellulosic ethanol distillation, using Poplar hardwood; MW NR (lignin 53 wt% of sample)	Batch reactor, 300, 350, 370 °C for 5, 10 min; 3-8 MPa	Gravimetry, TOC of aqueous liquid fraction, GC-MS, HPLC GC-MS of diethyl ether extract (DEE) of water-soluble and -insoluble fractions (light biocrude) HPLC of filtered water-soluble products FTIR of acetone extract of water-insoluble/DEE-insoluble residue (heavy biocrude) GPC of light and heavy biocrude after 0.45 µm syringe filtration NMR of light and heavy biocrude	Conversion to light biocrude up to 17 wt% and to water-solubles up to 12 wt% (300 °C) GC-MS: 15 light biocrude compounds, quantified HPLC: Seven water solubles, quantified FTIR: Heavy biocrude similar to lignin feedstock GPC: Heavy biocrude vs light, 1300 vs 400 g/mol (at 300 °C) and 1125 vs 450 (at 350 °C) NMR: Loss of OH groups in light biocrude, preserved aromatic ring and β-double bonds in heavy biocrude	Dell'Orco et al. (2020) ¹⁷⁰
Kraft lignin with low sulfide content, 4% sulfur (Sigma); MW NR	Batch reactor, 300, 370, 400 °C; reaction times 100- 5,000 ms by 100/1000 ms increments; pressure NR	Gravimetry GC-MS of ethyl acetate-extract (EA) of water-soluble fraction (light oil) Elem. analysis of lignin samples taken during reaction at various times FTIR, TGA of EA-extract of water-insoluble fraction (heavy oil)	Conversion to light oil up to 32 wt% at 370 °C GC-MS: Seven compounds, quantified Elemental Analysis: H/C ratios decrease rapidly in reaction, implying dehydration steps	Abad-Fernandez et al. (2019) ¹⁶⁶
Alkaline lignin (TCI America); MW NR	Microwave, 270 °C for 20 min vs autoclave reactor with same conditions; pressure NR	Gravimetry GC-MS, calorimetry of DCM extract of water-insoluble fraction (biocrude).	Conversion to biocrude 2.7 wt%, 5 wt% gas GC-MS: Seven compound groups, reported as normalized	Yang et al. (2020) ¹⁸⁷

Lignin isolated from black liquor; MW NR	Autoclave reactor, 280, 310, 330, 350, 365 °C for 2 h, initial N ₂ at 3 MPa	Gravimetry, GC-FID-TCD (gases) GC-FID-TCD of gases. SEM, pore size, XRD, FTIR, TG of water-insoluble fraction (char)	Conversion to water-soluble products NR; gas products reported as negligible; solid products up to 28 wt% at 280 °C FTIR: Carbonyl, methyl, methylene, methoxyl groups decreased with temperature, except increased OH groups. XRD: Side chains in lignin decreased and repolymerization of aromatics with increased temperature	Hu et al. (2014) ¹⁷⁷
Lignin-rich residue from ethanol production (SEKAB); MW NR	Batch reactor, 320, 340, 360, 380 °C; 15, 30, 45, 60, 90, 120, 240, 480 min, pressure NR	Gravimetry GC-FID-TCD of gases GC-MS, GC-FID of ethyl acetate (EA) extract of water-soluble fraction	Conversion to EA-soluble products up to 3.7 wt% (360 °C), gases up to 24 wt% (380 °C) GC-FID-TCD: CO ₂ , CH ₄ , CO, quantified GC-MS: Phenol, methoxyphenol, catechol groups, reported as normalized; GC-FID: groups quantified.	Forchheim et al. (2014) ¹⁷⁶
Kraft indulin AT (MeadWestvaco) and kraft pine lignin (Sigma-Aldrich); MW NR	Batch reactor at 300 °C (p NR) and 374 °C (22 MPa), 10 min	Gravimetry GC-TCD for gases GC-MS of water-soluble fraction combined with acetone extract of water-insoluble fraction	Conversion to water- and acetone-soluble products 34 wt% indulin) and 59 wt% (kraft pine) and gases 4.6 and 6.2 wt% (indulin, kraft pine) at 374 °C GC-FID-TCD: Five gases, quantified GC-MS: 24 products reported as normalized	Zhang et al. (2008) ¹⁷⁵
Alkaline lignin (TCI); MW NR	Batch reactor, 260, 280, 300, 340, 360 °C for 0, 10, 20, 30, 40, 50, 60 min; pressure NR	FC, DPPH assays GC-MS of DCM extract of water-soluble and -insoluble fractions. Thermal oxidation stability of DCM extract	Conversion to phenols up to 28 wt% at 320 °C, reported as mg gallic acid by FC assay FC and DPPH: Phenol content highest at 320 °C GC-MS: identified 14 compounds	Kang et al. (2015) ¹⁸¹
Corncob lignin (Shandong Long Li Biological Technology Co.); M _w 1970, M _n 863 g/mol	Autoclave reactor, 210, 230, 250, 270 and 290 °C at 0 min retention time. 270 °C at 0, 10, 20, 30 and 40 min; pressure NR	Gravimetry GC-MS of volatiles evaporated from water-soluble fraction, water-soluble products post volatiles evaporation (light oil), acetone extract of water-insoluble fraction (heavy oil) 2D-HSQC, P-31 NMR of light and heavy oil GPC of light and heavy oils Elemental analysis of raw lignin and water-insoluble/ acetone-insoluble residue	Conversion to heavy oil up to 48 wt% (230 °C), water-soluble oil 9.5 wt% (210 °C), volatiles 8 wt% (290 °C) GC-MS: 50 products reported as normalized HSQC: Not all ether bonds broken at low temperature P-31 NMR: Aliphatic OH decrease, but phenyl OH increase with temperature increase GPC: Light oil M _w 386, 372 g/mol, heavy oil M _w 814, 833 g/mol, 210 and 230 °C, respectively Elemental analysis: Increased carbon in solid residue compared to lignin	Yang et al. (2015) ¹⁸⁰

Kraft lignin from eucalyptus; M _w 3031 g/mol	Microreactor, 130, 180, 230 °C for 15 or 60 min; pressure NR	Gravimetry GC-MS of diethyl ether (DEE) extract (oil 1) and ethyl acetate (EA) extract (oil 2) from water-soluble fraction GPC of DEE and EA extracts FTIR of water-insoluble residue	Conversion to total oil up to 10 wt.% at 130 °C and 15 min GC-MS: 10 oil compounds, reported as normalized GPC: Oil 1 M _w 407, 534 g/mol and oil 2 M _w 416, 310 g/mol (230, 130 °C, respectively) FTIR: Phenolic OH increased with temperature while CO, β-O-4 links and aromatic rings decreased	Tang and Zhou (2015) ¹⁸⁸
Biomass with 54% lignin (w/w), obtained from ethanol plant with Poplar source; MW NR	Microreactor, 300, 350, 370 °C at 5, 10, 5, 20 min, with biomass to water ratio (B:W) of 10-20%(w/w), initial pressure at 3 MPa argon gas, change in pressure NR	Gravimetry (mass conversion); TOC (of water-soluble fraction) and elemental analysis (carbon conversion) GC-MS of diethyl ether (DEE) extract of water-soluble fraction (light biocrude) HPLC of filtered water soluble products GPC of DEE extract of filtered water-soluble fraction and dimethyl ketone extract of water-insoluble fraction (heavy oil) FTIR of light biocrude and heavy oil (bio-oil)	Conversion to bio-oil and water-solubles up to 71 wt% at 300 °C, 10 min, 20% water to biomass ratio GC-MS: 9 bio-oil compounds, quantified HPLC: 11 water-soluble compounds, quantified GPC: Bio-oil M _w of 550 to 1150 g/mol (370 and 300 °C, respectively) FTIR: Bio-oil showed fewer β-O-4 linkages than lignin	Miliotti et al. (2019) ¹⁷¹

Abbreviations: ; NR – not reported; MW – molecular weight; M_n – number-average molecular weight; M_w – weight-average molecular weight; FC- Folin-Ciocalteu assay; DPPH- 2,2-diphenyl-1-picryl-hydrazyl-hydrate assay.

The central theme to improvement of conversion percentages within subcritical methodology is the depolymerization/repolymerization trends with increased temperature of treatment. Zhao et al. conducted a study on repolymerization as a result of SW treatment at temperatures ranging from 200 to 350 °C and provided arguments (based on gravimetry and production of low MW species) that 350 °C is a threshold for extensive char formation.¹⁸⁵ A similar trend was observed by Hashmi et al.¹⁷⁸

Based on these studies, facile repolymerization of lignin fragments appears to be a significant barrier hindering lignin processing. It is considered to be one of the main reasons for low efficiency of lignin depolymerization by SW in the absence of catalysts.¹⁸⁹ Echoing this conclusion, Trajano et al. interpreted HSQC data and increases in MW as evidence that repolymerization can only be reduced, but not stopped, by several parameter changes such as lower residence time and increased solid-liquid interface.¹⁸³

The GPC results on MW distribution also varied (see Table 13),^{170,171,178,180,182-184,188} depending on feedstock and, potentially, by the applied GPC protocol with and without acetylation and whether the analysis was based only on polystyrene standard calibration. Yet, these studies consistently agreed on repolymerization being significant at temperatures above 200 °C. An excellent GPC application was demonstrated by Hashmi et al. showing the occurrence of dimers and trimers in bio-oils from beech wood organosolv lignin.¹⁷⁸ Yong and Matsumura attributed the observed increase in products' MW as char formation.^{174,177} The occurrence of repolymerization, especially at higher temperatures, was assumed in these studies based on either quantification of low MW compounds (via GC-MS or LC-MS) or methods precluding speciation, such as thermal gravimetric analysis TGA, TOC and gel permeation

chromatography, with only a few studies attempting to align the quantitation results obtained by different methods.

As a result, the conclusions on repolymerization are yet to be verified by thorough quantitative analysis. SW studies of lignin decomposition may benefit from conducting an accurate mass balance closure among fractions, comparison of treatment product and feedstock analyses, and providing decisive evidence of repolymerization, which would corroborate the perception that this is the main factor limiting the process efficiency. To address this knowledge gap, our study presents a novel approach of semi-quantification of SW treatment products (subjected to thermal analysis at several temperatures, i.e., providing their fractionation). The technical novelty of our study is the application of a new tool kit, which is designed to account for high MW products in addition to GC-elutable low-MW products of lignin degradation. Previous studies provided only indirect insights into these products, based on gravimetric measurements and qualitative mass-spectrometric analysis. Quantification and assessment of depolymerization/repolymerization of higher MW compounds as well as repolymerization of lower-MW components in the liquid and solid fractions of the products of SW treatment are essential for understanding the decomposition pathways of lignin.

I.7. Statement of Purpose

Lignin shows promise as a potential source of renewable chemicals and as a possible replacement for petroleum-based fuel and petrochemicals.¹⁹⁰⁻¹⁹² Characterizing lignin is a first step in utilizing what is essentially a massive waste item, an effort which should culminate in effective depolymerization and usage of lignin as a part of the overarching theme of reducing dependence on petroleum and developing sustainable products. A suite of novel lignomics

protocols was developed previously and these have been modified to meet new challenges in the characterization of lignin.^{81,193,194}

MW characterization by SEC was an important goal of this study, with investigation into mixed mobile phases, differences in MW of a variety of technical (whole) lignins, and enabling GPC analysis of solubilized lignin in several solvents. A number of technical lignins were used for evaluation in this study; these included dealkaline, alkali, lignosulfonate, soda and indulin lignins; several were the same type of lignin but from different manufacturers.

The first part of size exclusion chromatography method development was to derive an analysis protocol for technical lignins. Technical lignins have been processed by chemical means, typically during separation of cellulosic materials from lignin in raw biomass. Standards and samples were evaluated for optimal injection volume, optimal wavelength in a variable wavelength detector (VWD) and filtering treatment prior to analysis.

A second part of the GPC method development centered around the analysis of kraft lignin dissolved in a series of different solvents and solvent mixes. Solubility differed greatly for each solvent system, so that the main challenge was to preserve the solubilized material when shifting to a different solvent and then to select column and mobile phase parameters which would optimize the method chosen.

To evaluate the oxidation level of lignins, a Folin-Ciocalteu (F-C) method was optimized for estimation of phenolic hydroxyl groups in lignins. The optimization was performed using 2⁴ factorial statistical design of experiment. Once F-C reagent amount, analyte concentration range, acetone:water solvent ratio and volume as well as development time were established, a large number of lignin model compounds were evaluated for phenolic hydroxyl concentration ranges by UV-Vis spectrophotometry and the resulting slopes served as calibration standards for

evaluation of whole lignin samples. Although model compound response varied with ring substituents, an estimation of lignin hydroxyl content was determined.

Lignin processing projects included fractionation via preparatory SEC, depolymerization by peroxide oxidation and depolymerization by subcritical water treatment.

In our first processing project, preparative SEC was used to separate kraft alkali lignin into more restricted categories ostensibly based on MW. However, one of the purposes of the separation was to gauge the effectiveness of the process as well as to determine if functional groups of various types also changed in abundance with molecular weight. To investigate the chemical nature of these fractions, including mass balance and evaluation of structural features, a number of analyses were employed, including high performance SEC, direct infusion high resolution mass spectrometry, gas chromatography-mass spectrometry (GC-MS), thermal desorption/pyrolysis-GC-MS, ³¹P NMR spectroscopy, thermal carbon analysis and transmission electron microscopy. Preparative SEC was compared to more commonly used fractionation methods of precipitation, solvent extraction, and ultrafiltration for ease of use, successful differentiation based on MW, ease of downstream analysis for functional groups, and the possibility of being scalable to industrial standards.

The second processing project of this study was to determine conversion rates of high-MW lignin to smaller molecules for peroxide/methanol oxidation of alkali lignin heated in an autoclave. Analysis was accomplished via thermal carbon analysis, a novel method of analysis for carbon content which allows monitoring of carbon (as CO₂) evolved at different temperatures. As monomers and small oligomers were the only species to be solubilized, carbon content allowed a quantitative measure of breakdown afforded by the oxidation process, and also an estimate of oligomer sizes since higher temperatures would be required for higher MW

molecules. Also, pH was monitored before and after treatment in order to pinpoint acid or base release during the process.

The third of our processing projects involved investigation of subcritical water treatment of alkali lignin in order to determine actual conversion rates attributable to that process, as well as to attempt a mass balance strategy and to determine the degree of depolymerization (and repolymerization) of final liquid and solid products.

To enable this approach, we utilized thermal carbon analysis (TCA), enabling comprehensive quantification of carbonaceous species, which allowed for carbon mass balance. This method is based on determination of the amount of carbon in all temperature fractions of TCA, which yields the carbon content of low- and high-MW lignin oligomers, including the carbon in char, which is quantitatively combusted with oxygen following the pyrolytic sequence.¹⁹¹⁻¹⁹³ The TCA results were aligned with detailed speciation profiles obtained with thermal desorption-pyrolysis gas chromatography-mass spectrometry (TD-Py-GC-MS). The thermal fractionation of alkali lignin and its degradation products was accomplished through a sequential TD program (ambient temperature, 200, 300 °C), which was compared to the amounts obtained by liquid-liquid extraction and GC-MS analysis.¹⁹⁴ The pyrolytic fractionation was achieved through a similar approach, a sequential Py program matching the TCA temperature ramp (400, 500, and 890 °C), thus enabling their direct comparison.

This study was intended to investigate carbon mass balance closure and speciation of lignin following the SW treatment by employing this newly developed suite of methods. Thus not only low MW products were delineated with liquid-liquid extraction (LLE) GC-MS, but both low and high MW species were systematically characterized through TCA, TD-Py-GC-MS, LLE GC-MS and previously validated GPC analysis.⁸¹ From the results of analyses of SW treated

lignin and untreated lignin, the extent of depolymerization was estimated and organic classes of products in the monomer-small oligomer range were determined as well several high-MW species. C/H and C/O ratios, as well as elemental analyses of treated and untreated lignin also offered quantitative evidence for repolymerization vs condensation.

CHAPTER II. Characterization of Lignin

II.1. GPC Method Development

II.1.1 Description of Whole Lignins

The first part of GPC method development was to derive an analysis protocol for whole lignins, which are also “technical lignins.” Technical lignins have been processed by chemical means, typically during separation of cellulosic materials from lignin in raw biomass. The cellulose, in pulp form, is used for paper or fuel production while lignin usually remains in solution and constitutes a waste product in the industrial sector, with limited commercial use. Lignin can be used as low-grade fuel for combustion, a dispersant for oil and as a partial substitution for phenols in various resins, among other uses.¹⁹⁵ Whole lignins are not to be confused with lignin model compounds which are simple monomers, dimers or oligomers which are considered to be products of lignin depolymerization. They are also not native lignins, which carry the original structure and properties of lignin in the plant source they are derived from.

A second part of the GPC method development centered around the analysis of kraft lignin dissolved in a series of different solvents and solvent mixtures. Solubility differed greatly for each solvent system, so that the main challenge was to insure solubility and then to select column and mobile phase parameters which would optimize the method chosen.

Several types of technical lignins were used for evaluation in this study and these include sulfur-containing lignins known as kraft and lignosulfonate lignins. The kraft process is the most common processing method used today by the paper industry. Typically, wood chips are mixed with hot water, NaOH and Na₂S and is heated to 160 – 180 °C. This method dissolves lignin in a

highly alkaline solution; if kraft lignin is not further treated and is dried it has a pH of 8-10 if redissolved.^{25,26}

Alkaline lignin is solubilized and broken down by NaOH or another strong base, without sulfur-containing reagents. “Soda lignin” is alkaline lignin treated and solubilized by NaOH alone. Protobind 1000™ (GreenValue, Granit, Switzerland) is a mixed wheat straw/Sarkanda grass lignin processed by NaOH, which guarantees a product with a minimum of 90% lignin, so that cellulose and hemicellulose are still present (< 4%), although there is no sulfur present.²⁸

Occasionally a product marketed as “alkali or alkaline lignin” contains sulfur or is listed as “kraft lignin.” “Alkaline lignin” sold by TCI America (Portland, OR) has a stated pH of 8-10, but also contains 20-29% sulfonate in the anhydrous form.²⁹ Sigma Aldrich, (St. Louis, MO) sells a “low sulfonate alkali (kraft) lignin” (product # 471003) with sulfur level specified as < 3.6% (at 3% water content) and a pH of 10 – 11. Sigma Aldrich also markets an “alkali (kraft) lignin” (product # 370959) with a pH of 5.5 – 7.5 and an unspecified sulfur content (at 10% water content.³⁰ The pH value of 5.5 – 7.5 reflects that fact that alkali lignin is typically retrieved from black liquor, the original alkaline solution, through acidification and precipitation.

Indulin AT lignin, sold until recently by Meadvestvaco, Inc., and now sold by Ingevity, Inc. (Charleston, NC), is an acidified kraft pine lignin produced as a byproduct of the paper industry.³¹ The acid hydrolysis process removes sodium and hemicellulose, although sulfur remains intact. The pH (5.0 – 7.0) is slightly lower than that of alkali kraft lignin. Indulin C, also marketed by Ingevity, Inc., is an unsulfonated kraft lignin, advertised by the company as highly purified and highly functionalized in carboxylic acids as well as aliphatic and aromatic hydroxyl groups, with alkaline pH 9 – 10.

Lignosulfonate lignin is produced during delignification processes in which primarily β -O-4' ether bonds are cleaved by sulfurous acid (formed from CO₂ addition to an aqueous solution), where proton combines with a hydroxyl group removed from lignin to form water, and the remaining bisulfite group bonds to the lignin at the residual carbocation site to produce a sulfonate. The process may also use a sulfite salt of Ca, Mg, Na, Al or NH₄ along with, or in place of, the sulfurous acid. The sulfite pulping reaction results in a higher percentage of sulfur, 3.5 – 8%, compared to alkali lignin, which is typically listed as 1– 3%. The presence of sulfonate groups makes this type of lignin water-soluble.³³ A lignosulfonate lignin used in this study is produced by Borregaard Lignotech (Sarpsborg, Norway). Aro et al. stated that the typical pH of a sulfite process (and the lignin produced therein) as 1 – 5, although a neutral process entails a pH of 4 – 7. A commercial site listed its dark brown lignosulfonate product which contains sulfur as a “grade three” lignosulfonate, with a pH of 4 – 7;³⁴ however, additional lignosulfonate products had a variety of pH levels dependent upon the processing parameters enlisted.

Dealkaline lignin is produced through dealkalization of black liquor, a solution of solubilized lignin produced during the papermaking process. TCI America (Portland, OR) describes dealkaline lignin marketed by their company as starting out as sodium lignosulfonate (TCI product # L0098) which is subjected to desulfonation (partial), oxidation, hydrolysis and demethylation to result in a lignin which still retains sulfate (10 – 20% based on anhydrous mass) and has a pH of 3 – 4. The TCI dealkaline lignin (TCI product # L0045) is then used as a base to produce TCI alkaline lignin (TCI product # L0082) by adjusting pH up to 8 – 10.

II.1.2. Experimental

Development of GPC methodology was carried out for lignin and lignin derivatives through variation of sample preparation, calibration standards preparation, flow rate, injection volume, wavelength and solvent systems. Whole lignins consisted of 12 lignin types from different manufacturers, while solubilized lignins were samples derived from ten solvent systems. All calibration standards and samples were analyzed by the 1220 Infinity II HPLC (Agilent, Santa Clara, CA), with Agilent OpenLab CDS software/GPC module, Variable wavelength detector (VWD) and Agilent Plgel Minimix-D reversed phase column (5 μm pore size, 250 mm length, 4.6 mm ID). Molecular weight lower and upper limits are 200 and 400,000 Da respectively.

II.1.2.1. Materials

GPC analysis of lignin and lignin derivatives was carried out on the 1220 Infinity II HPLC (Agilent, Santa Clara, CA), using solvents which included unstabilized tetrahydrofuran (THF), ethyl benzene, and acetone (VWR, Radnor, PA) which were HPLC grade. Deionized water was obtained from a Direct-Q 3 UV system purifier (Millipore, Billerica, MA, USA) with the total organic carbon content below 5 ppb (manufacturer specification).

Syringe filters consisted of 0.45 μm (pore size), 13-mm hydrophobic PTFE syringe filters (Tisch Scientific, North Bend, OH) and 0.2 μm (pore size), 13-mm hydrophobic PTFE syringe filters (VWR, Radnor, PA).

Table 14. Lignin study sample sources, composition, pH, method of MW evaluation, production process, and references.

Lignin sample	Source	Elemental analysis				pH	MW Method	Production Process	References
		C	H	N	S				
Dealkaline	TCI Chemicals, Ltd.	51.25	4.78	0.16	4.43	3 - 4	GPC; Plgel Minimix-D column, THF eluent, UV detec. 250 nm.	TCI ligninsulfonate is partially desulfonated, subjected to oxidation hydrolysis and demethylation; retains 10-20% sulfate (anhyd.)	TCI ²⁹ dealkaline
Alkaline	TCI Chemicals, Ltd.					8 - 10	"	TCI dealkaline lignin adjusted to high pH: 20 - 29% sulfonate (anhyd.)	TCI ²⁹ alkaline
Na ligno-sulfonate	TCI Chemicals, Ltd.	40.73	4.54	0	5.49	3.5	"	Sulfite salt (Ca, Mg, Na, NH ₄)and/or sulfuric acid treated. (3 - 8% sulfur)	TCI ²⁹ ligno-sulfonates
Lignotech™	Lignotech USA, Inc. (Borregaard)	61.4	5.81	0	2.31	Typical sulfite process pH 1 – 5	"	Sulfite salt (Ca, Mg, Na, NH ₄)and/or sulfuric acid treated. (3 - 8% sulfur)	Aro ³³ , Borregaard ³⁴
Indulin AT	Meadwestva co, Inc.	63	5.1	0.7	1.6	5 - 7	"	Acidified, purified kraft pine, retains sulfur, but is unsulfonated. High OH (aliphatic and aromatic) and carboxyl content.	Constant ⁵⁰ , Ingevity indulin AT
Indulin C	Meadwestva co, Inc.					9 - 10	"	Purified kraft pine, retains sulfur, but is unsulfonated. High OH (aliphatic and aromatic) and carboxyl content.	Ingevity indulin C
Kraft, alkali	Sigma Aldrich Corp.	61	6		1	5.5 - 7.5 (25 °C, 5% aqueous solution)	"	NaOH, Na ₂ S added, heated to 160 - 180 °C; acidified to precip. (1 -3% sulfur)	Deepa ¹⁹⁶ , Sigma ³⁰
Kraft - Denmark		59.22	6.29	0	1.57		"	NaOH, Na ₂ S added, heated to 160 - 180 °C; acidified to precip. (1 -3% sulfur)	

Soda alkali-Protobind-1000TM	GreenValue Co.	62.46	5.93	0.6	0.64	3.5	"	Wheat straw, Sarkanda grass treated by NaOH; no/low sulfur	Ariton ¹⁹⁷ ; Agrobiobase ²⁸
Lignotech DTM	Lignotech USA, Inc. (Borregaard)					Typical sulfite process pH 1 - 5	"	Sulfite salt (Ca, Mg, Na, NH ₄)and/or sulfuric acid treated. (3 - 8% sulfur)	Borregaard ³⁴ Aro ³³
acetoacetylated- 50% (kraft)	NDSU experimental						"	Kraft lignin 50% aceto-acetylated	
methacrylated- 30% (kraft)	NDSU experimental						"	Kraft lignin 30% methacrylated	

II.1.2.2. Calibration standards and preparation

GPC calibration standards included poly(methyl methacrylate) (PMMA) narrow standards with peak molecular weights (M_p) of 550-56600 Da, purchased from Agilent Technologies (Santa Clara, CA, USA), and polystyrene (PS) narrow standards with M_p of 580-271800 Da purchased from Varian (Amherst, MA, USA).

The standards were prepared as mixtures, PS mix 1 (580, 5030, 38100, 271800 M_p 1 mg/mL each), PS mix 2 (1480, 8450, 70950 M_p), and PMMA mix (960, 17810 M_p), where PS mixes were evaluated at 250 nm and the PMMA mix at 220 nm for a 30- μ L injection volume and flow rate of 0.3 mL/min.

Solvent blanks were prepared in several ways in order to evaluate column tolerance for varied solvent mixes, as samples from the lignin/solvent study were solubilized in a variety of solvent mixes. The whole lignin samples were in HPLC grade, unstabilized THF with a small percentage (< 5%) of water, so that solvent blanks were prepared with pure unstabilized THF and with unstabilized THF which contained 5% water for comparison. Several other types of solvent blanks were also evaluated to test column tolerance for water and acetone for lignin/solvent study samples: THF: water (1:1) and acetone:water (1:1). Unstabilized THF with 300 μ g/mL 4-Methyl-2,6-bis(2-methyl-2-propanyl)phenol, also known as butylhydroxytoluene (BHT), was evaluated to determine if stabilization of blanks and samples (with the ultimate aim of stabilizing waste solutions) would interfere with data analysis. All ratios (percentages) of solvents were on a (v/v) basis. All blanks were injected as 30 μ L at a flow rate of 0.3 mL/min.

II.1.2.3. Lignin samples and preparation

This study investigated alkaline lignin purchased from Sigma Aldrich (St. Louis, MO, USA), indulin lignin (Meadvestvaco, Richmond, VA), alkaline and dealkaline lignin (TCI Corp., Portland, OR), lignosulfonate lignin (Borregaard Lignotech; Sarpsborg, Norway), and commercial wheat straw/Sarkanda grass soda lignin (Protobind™ 1000, GreenValue S.A., Granit, Switzerland). Additional samples of acetoacetylated and methacrylated lignin were obtained from Dr. Dean Webster, Polymers and Coatings Dept., North Dakota State University.

Samples of kraft lignin (Sigma, St. Louis, MO) dissolved in various solvent systems were also evaluated in this study. Solvent systems with solubilized kraft lignin included: acetone:water (1:1), acetone:water (3:1), 100% acetonitrile, acetonitrile:water (1:1), 100% THF, THF:water (1:1), THF:MeOH (1:1), mTHF:MeOH (1:1), acetone:2-propanol (1:1), 100% methyl acetate.

The alkali (kraft) lignin (Sigma product # 370959) was the same alkali lignin used as a whole lignin sample, listed as having a pH of 5.5 – 7.5 and an unspecified sulfur content (at 10% water content).

Whole lignin samples were solubilized in THF:water (1:1) as 50 mg/mL stock solutions initially; this was followed by removal of 50 µL of stock diluted by HPLC grade, unstabilized THF to 1 mL for a concentration of 2.5 mg/mL. The 2.5 mg/mL samples were filtered with 0.45 µm (pore size), PTFE syringe filters. The latter samples were evaluated by the Agilent 1220 Infinity II HPLC at ambient room temperature, with a 30-µL injection volume and 0.3 mL/min flow rate, with unstabilized THF as the mobile phase. Two replicates of each lignin were evaluated. The final water content in the 2.5 mg/mL samples was calculated as 2.5%.

The same instrumental parameters were set for a later run of whole lignin samples with a different concentration and solvent composition. Each whole lignin was prepared from 5 mg of the solid, which was diluted to 5.0 mL by a solution of (1:1) THF:water (unstabilized, HPLC-grade THF), for a final concentration of 1 mg/mL. These samples were filtered with 0.2 μm (pore size) PTFE syringe filters. BHT was added to each sample for a final concentration of (300 $\mu\text{g}/\text{mL}$). The final water content in the 1.0 mg/mL samples was 50%; after injection (30 μL) into the THF mobile phase with a flow rate of 03 mL/min, water content in the HPLC column was calculated as 0.3%.

A second set of samples, other than the whole lignin samples, were also prepared from lignins in solvent systems. The latter study entailed dissolution of 3.0 g of alkali (kraft) lignin (Sigma, St. Louis, MO) in 30.0 mL each of various solvents and solvent mixes in order to evaluate solubility parameters and MW. The solutions were stirred by 2-cm magnets at 125 rpm on a stirring plate for 24 hours with occasional shaking, and then centrifuged at 3000 rpm for 20 min in 40-ml glass vessels. The liquid fraction was carefully decanted and filtered by low negative pressure through Whatman No. 1 filters to divide solid residue from liquid fractions. Filtered solids were added to centrifuged solids and dried under N_2 . Solubility of the lignin in the liquid samples was determined gravimetrically and also by thermal carbon analysis (TCA). Solvents and solvent mixes included: 50% acetone:50% water, 75% acetone:25% water, 100% acetonitrile, 50% acetonitrile:50% water, 100% THF, 50% THF:50% water, 50% THF:50% MeOH, 50% methyltetrahydrofuran (mTHF):50% MeOH, 50% acetone:50% propanol, 100% methyl acetate. Samples were done in triplicate.

Solubility levels of each sample varied from 1% to 100%, or concentrations of approximately 0.1 to 115 mg/mL. For the first analysis of the lignin samples, they were diluted

to 10 mg/mL by the solvent or solvent mix originally used. Then 0.5 mL of each solution was diluted by 5 mL of unstabilized THF to a final concentration of 1 mg/mL, with each original solvent constituting about 10% by volume of the final samples. Filtration with 0.2 μm (pore size) hydrophobic PTFE syringe filters had to be repeated several times to remove lignin material which aggregated upon dilution with THF, due to decreased solubility. BHT (300 $\mu\text{g/mL}$) was added to each sample prepared for HPLC analysis.

Each sample was analyzed by the Agilent 1220 Infinity II HPLC at ambient temperature, 30 μL injection volume and 0.3 mL/min flow rate with unstabilized THF as the mobile phase. Samples were analyzed in duplicate.

II.1.2.4. Instrumentation

All calibration standards and samples were analyzed by the 1220 Infinity II HPLC (Agilent, Santa Clara, CA), with Agilent OpenLab CDS software/GPC module, Variable wavelength detector (VWD) and Agilent Plgel Minimix-D reversed phase column (5 μm particle size, 250 mm length, 4.6 mm ID). Molecular weight lower and upper limits are 200 and 400,000 Da respectively. All sample and calibration injection volumes were 30 μL and flow rate was 0.3 mL/min, with unstabilized, HPLC grade THF as the mobile phase. The duration of the program was set for 15 min. An instrumental flow diagram is in Appendix A.

II.1.2.5. Data analysis

Agilent OpenLab CDS software 2.2 with a GPC/SEC add-on module was used for acquisition and analysis (calibrations and calculations) of all data acquired via the Agilent 1220 Infinity II HPLC. Additional analysis and calculations were done with Microsoft Office Excel software.

Various combinations of PS and PMMA standards were analyzed as least-squares linear curves via LINEST function for standard deviation of the slope (S_b) and standard error of y values (S_y), as well as y-intercept and R^2 values.

The pooled t-test equation was used for comparison of a seven-point PS standards curve to combined PS-PMMA standards curves:

$$t_o = \frac{\bar{u}_1 - \bar{u}_2}{sp \sqrt{\frac{1}{n_1} + \frac{1}{n_2}}} \quad [5]$$

and

$$sp = \frac{(n_1 - 1)s_1^2 + (n_2 - 1)s_2^2}{n_1 + n_2 - 2} \quad [6]$$

where t_o is the statistical t value, \bar{u} is average mean (slope) of a set of data points, sp is pooled standard deviations of both data sets, and n is number of data points.¹⁹⁸

II.1.3. Results

II.1.3.1. Evaluation of GPC parameters

II.1.3.1.1. Calibration

A previous study conducted by Andrianova et al. validated the use of combined PS and PMMA standards which spanned the range from 550 Da to 271,800 Da.⁸¹ PS standards are organic/hydrophobic in nature due to the repeated benzene ring in the polymer, while the PMMA standards tend to be more hydrophilic and polar (Fig. 14). The aim in this study was to construct a standards curve composed mainly of PS standards (as a widely used organic standard), but to incorporate several hydrophilic PMMA standards for a relatively universal calibration mix for any application.

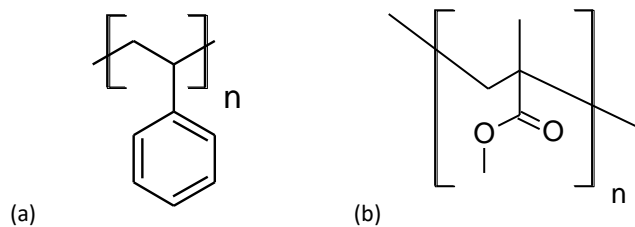


Figure 14. (a) Polystyrene, and (b) poly (methyl methacrylate). (Images from Sigma-Aldrich).

II.1.3.1.2. Selection of wavelength

Wavelength settings became important due to the variable wavelength detector of the 1220 Infinity II HPLC instrument, which measures in one wavelength exclusively. For PS standards, 250 nm was established as optimal due to the strong absorbance of the benzene ring in that area, while for PMMA 250 nm was not selective, but 220 nm was near-optimal due to absorbance of the carbonyl group below 250 nm (Figure 15).

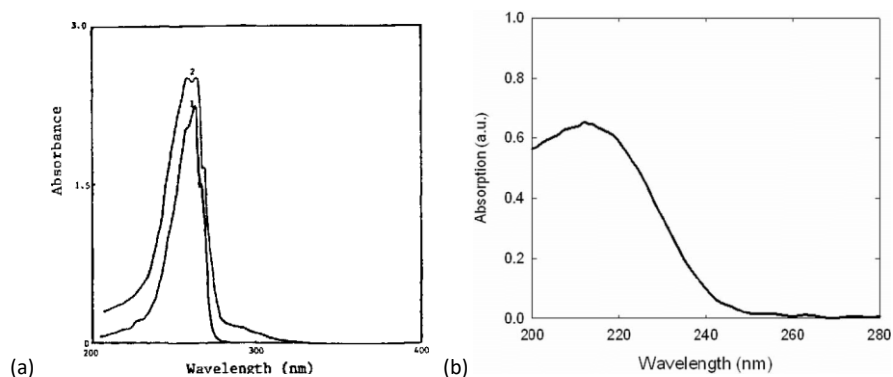


Figure 15. (a) UV-Vis absorbance curve for polystyrene (peak 2) in chloroform, from Li,T., Zhou, C., Jiang, M. UV absorption spectrum of polystyrene. *Poly. Bul.* **1991**, *25*, 211-216; (b) UV-Vis absorbance curve for PMMA film (in toluene), from Chung,H., Shin, H., Boyd, R. Implementation of sub-Rayleigh-resolution lithography using an N-photon absorber. *J Mod. Opt.* **2006**, *53*, 16-17.

PMMA standards of 550, 2880, 10280 and 56600 M_p (1 mg/mL) were evaluated at 250 and 220 nm, and results were overlaid in Figure 16. The response to PMMA standards was far better at 220 nm than at 250 nm, as evidenced by the peaks at 250 nm which are practically indistinguishable from the baseline in comparison to the same standards at 220 nm. This was expected, as Figure 15b shows good absorption for PMMA at 220 nm. Although absorbance for PMMA would be somewhat higher at 190 nm, a wavelength setting could not be chosen below 220 nm. The cutoff wavelength for THF is 220 nm¹⁹⁹ below which THF absorption increases. The increase in absorbance would add to the total signal, which would not be exclusively due to standards' absorbance. Several other sources list THF cutoff wavelength as 212 nm.

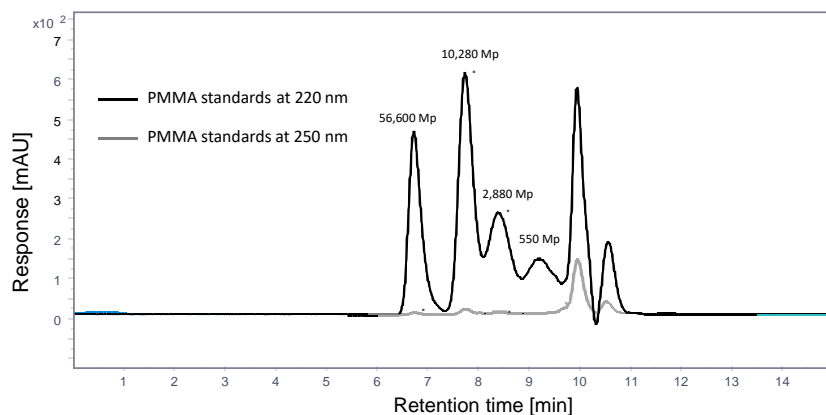


Figure 16. GPC overlaid chromatograms of four PMMA standards (1 mg/mL) evaluated at 250 nm (gray) and at 220 nm (black). (Peaks at 10 and 10.7 minutes are additives). The peak retention times are approximately 6.7, 7.7, 8.4 and 9.2 min.

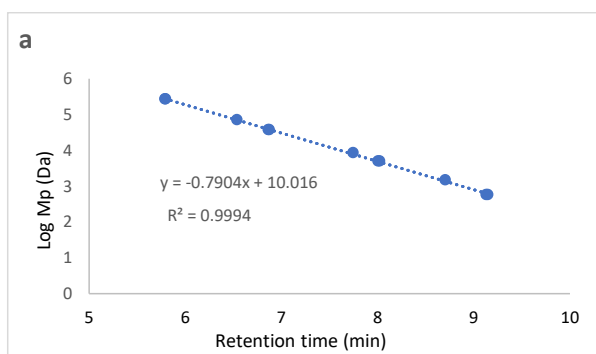
II.1.3.1.3. Selection of suitable calibration standards

The PS standards were available in the range 580 to 271800 M_p , while PMMA standards were available from 550 to 56,600 M_p . The PS standards that covered this range well, without overlap, were 580, 1480, 5030, 8450, 38100, 70950, and 271800 M_p . PMMA standards which covered the PMMA range as well were 550, 960, 2880, 4640, 10280, 17810 and 56600 M_p . The PS and PMMA values above are presented with their peak molecular weights and general retention times and volumes in Table 15. Retention times are routinely measured in thousandths of a minute, but vary somewhat with individual sequences, thus the retention times listed in Table 15 are only listed to the tenths of a minute. Retention volumes are listed to the tenths of a mL. Retention volumes are sometimes the same for different retention times, but times and volumes are intended to be general.

Table 15. Available commercial polystyrene and poly(methyl methacrylate) standards listed by peak molecular weight (M_p), retention times and retention volumes obtained on PLgel Minimix-D column with THF as a mobile phase (3 μ L injection volume and 0.3 mL/min flow rate).

PS standards (M_p)	580	1480	2340	5030	8450	19760	38100	70950	132900	271800
Retention time (min)	9.2	8.8	8.4	8.0	7.7	7.2	6.9	6.5	6.2	6.0
Retention volume (mL)	2.8	2.6	2.5	2.4	2.3	2.2	2.1	2.0	1.9	1.80
PMMA standards (M_p)	550	960	1780	2880	4640	6850	10280	17810	26080	56600
Retention time (min)	9.4	9.3	8.7	8.4	8.1	7.9	7.7	7.4	7.2	6.7
Retention volume (mL)	2.8	2.8	2.6	2.5	2.4	2.4	2.3	2.2	2.2	2.0

PS and PMMA standards from one sequence were plotted separately (as $\log M_w$ vs retention time) in Figure 17. The PS curve maintained a better R^2 value than the PMMA curve, but more precise methods were needed to determine comparative linear fit for a large number of calculated slopes for a variety of standards combinations.



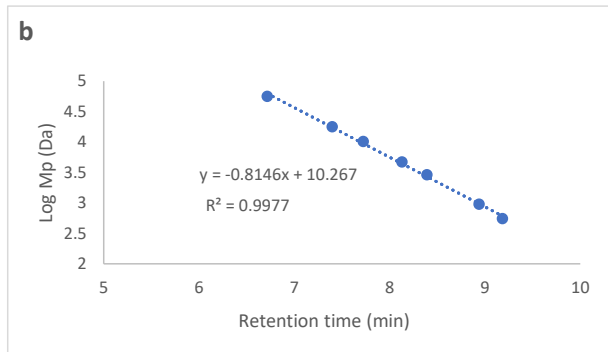


Figure 17. Calibration curves including least-square linear equations for (a) seven PS standards (from 580 to 271800 M_p) and (b) Seven PMMA standards (from 50 to 56600 M_p).

Standard deviation of the slope (S_b) and standard error of predicted y values (S_y) were determined for a number of PS and PS-PMMA combined standards curves and are shown in Table 16. Ostensibly, the lower the S_b and S_y values, the more linear the calibration curve, and the more accurate the sample evaluation.

Table 16. Standard deviation of the slope (S_b) and standard error of predicted y values (S_y) for various combinations of PS and PMMA standards. All PS standards were evaluated at 250 nm, while PMMA standards were evaluated at 250 and 220 nm. PS 1 (mix one) consisted of 580, 5030, 38100 and 271800 M_p . PS 2 (mix 2) was 1480, 8450, and 70950 M_p . PMMA 1 was 550, 2880, 10280 and 56600 M_p , while PMMA 2 was 960, 4640 and 17810 M_p .

Standards Selected	Slope	S_b	S_y	Intercept	R^2	Data Pts. n
PS mix 1,2 (5 mg/mL)	- 0.83080	0.0458	0.1272	10.4270	0.98501	7
PS mix 1,2 (1 mg/mL)	- 0.78841	0.0097 9	0.02885	10.0000	0.99929	7
PS mix 1,2 (1 mg/mL) w/o 271800	- 0.79275	0.0138 7	0.03133	10.0385	0.99877	6
PS mix 1,2 (1 mg/mL) w/o 580 M_p	- 0.77392	0.0053 2	0.01273	9.90472	0.99981	6
PS mix 1,2 (1 mg/mL) w/o 271800 and 70950 M_p	- 0.79631	0.0203 0	0.03571	10.0687	0.99805	4
PS mix 1,2 (1 mg/mL) w/o 580 and 1480 M_p	- 0.77387	0.0081 3	0.01470	9.90439	0.99966	4

PS 1,2(1, 5 mg/mL), PMMA 1,2 (1,5 mg/mL) 220	- 0.80816	0.0143 8	0.07470	10.2105	0.99182	28
PS 1,2 (1 mg/mL); PMMA 1,2 (5 mg/mL) 220	- 0.79121	0.0129 3	0.04864	10.0546	0.99680	14
PS 1,2 (1 mg/mL); PMMA 1 (5 mg/mL) 220	- 0.79141	0.0138 5	0.04890	10.0464	0.99725	11
PS 1,2 (1 mg/mL); PMMA 2 (5 mg/mL) 220	- 0.78501	0.0132 8	0.04344	9.99573	0.99771	10
PS 1,2 (1 mg/mL); PMMA 1,2 (5 mg/mL) 250	-0.78327	0.0169 1	0.05514	10.0006	0.99489	13
PS 1,2 (1 mg/mL); PMMA 1 (5 mg/mL) 250	-0.78429	0.0168 2	0.05348	9.99920	0.99633	10
PS 1,2 (1 mg/mL); PMMA 2 (5 mg/mL) 250	-0.78485	0.0167 8	0.05098	9.99621	0.99635	10
PS 1,2 (1 mg/mL); PMMA 1,2 (1 mg/mL) 220	- 0.78978	0.0118 4	0.04461	10.0398	0.99730	14
PS 1,2 (1 mg/mL); PMMA 1 (1 mg/mL) 220	- 0.79009	0.0124 9	0.04422	10.0329	0.99775	11
PS 1,2 (1 mg/mL); PMMA 2 (1 mg/mL) 220	- 0.78517	0.0126 2	0.04122	9.99571	0.99793	10
PS 1,2 (1 mg/mL); PMMA 1,2 (1 mg/mL) 250	- 0.81060	0.0203 5	0.04484	10.2489	0.99685	13
PS 1,2 (1 mg/mL); PMMA 1 (1 mg/mL) 250	-0.78345	0.0149 0	0.04744	9.98838	0.99711	10
PS 1,2 (1 mg/mL); PMMA 2 (1 mg/mL) 250	-0.78325	0.0139 5	0.04568	9.98435	0.99746	10
PMMA 1,2 (1 mg/mL) 250	-0.79097	0.0170 9	0.03004	10.0973	0.99813	6
PMMA 1,2 (1 mg/mL) 220	-0.81459	0.0174 3	0.03701	10.2668	0.99771	7
PMMA 1 (1 mg/mL) 250, 220	-0.80056	0.0201	0.04484	10.1582	0.99685	7
PMMA 2 (1 mg/mL) 250, 220	-0.82346	0.0114 7	0.01771	10.3546	0.99922	6
PMMA 1,2 (5 mg/mL) 250	-0.78982	0.0344 9	0.04621	10.0943	0.99243	6
PMMA 1,2 (5 mg/mL) 220	-0.82341	0.0169 0	0.03553	10.3456	0.99789	7
PMMA 1 (5 mg/mL) 250, 220	-0.81060	0.0203 5	0.04484	10.2489	0.99685	7
PMMA 2 (5 mg/mL) 250, 220	-0.83023	0.0307 6	0.03907	10.3969	0.99453	6
PS 1,2; PMMA 550, 2880, 10280 (220) both 1 mg/mL	-0.78787	0.0136 1	0.04602	10.0132	0.99762	10

PS 1,2; PMMA 2880, 10280, 56600 (220) both 1 mg/mL	-0.78431	0.0139 9	0.04450	0.99746	9.99286	10
PS 1,2; PMMA 960, 4640, 17810 (220) both 1 mg/mL	-0.78517	0.0126 2	0.04122	9.99572	0.99794	10
PS 1,2; PMMA 960, 2880,56600 (220) both 1 mg/mL	-0.78485	0.0101 9	0.03508	9.98937	0.99865	10
PS 1; PMMA 960, 2880, 17810 (220) both 1 mg/mL	-0.78401	0.0122 7	0.04061	9.98636	0.99804	10
PS 1,2; PMMA 960, 4640 (220) both 1 mg/mL	-0.78302	0.0111 2	0.03613	9.97201	0.99859	9
PS 1,2; PMMA 2880, 4640 (220) both 1 mg/mL	-0.77957	0.0135 0	0.04169	9.95134	0.99790	9
PS 1,2; PMMA 550, 10280 (220) both 1 mg/mL	-0.79132	0.0129 6	0.04310	10.0334	0.99812	9
PS 1,2; PMMA 4640, 17810 (220) both 1 mg/mL	-0.78549	0.0146 6	0.04406	9.99791	0.99757	9
PS 1,2; PMMA 960, 17810 (220) both 1 mg/mL	-0.78762	0.0116 3	0.03766	10.0082	0.99848	9
PS 1,2; PMMA 960, 56600 (220) both 1 mg/mL	-0.78885	0.0087 4	0.02937	10.0134	0.99914	9

The curve consisting of PS standards alone (1 mg/mL) had S_b and S_y values of 0.00979 and 0.02885 respectively, showing better fit than PMMA standards for 1 mg/mL at 220 nm (the best PMMA results at 0.01743 S_b and 0.03701 S_y), although these were not the lowest S_b and S_y values in table 16. The lowest values occurred for the PS mixes 1,2 (1 mg/mL) without standard 580 M_p (0.00532 S_b and 0.01232 S_y), but it was not desirable to leave out low MW standards for samples which were expected to have low MW values.

The next lowest S_b and S_y values (0.00874 S_b and 0.02937 S_y) occurred for the combination of the PS mix 1,2 (1 mg/mL) with PMMA values of 960 and 56600 M_p (1 mg/mL) evaluated at 220 nm wavelength. Interestingly, the S_b and S_y values were actually lower than those for PS mixes 1,2 alone. The curves with the four lowest S_b and S_y values, other than the PS mixes 1,2 (1 mg/mL) curve, were compared graphically in Figure 18.

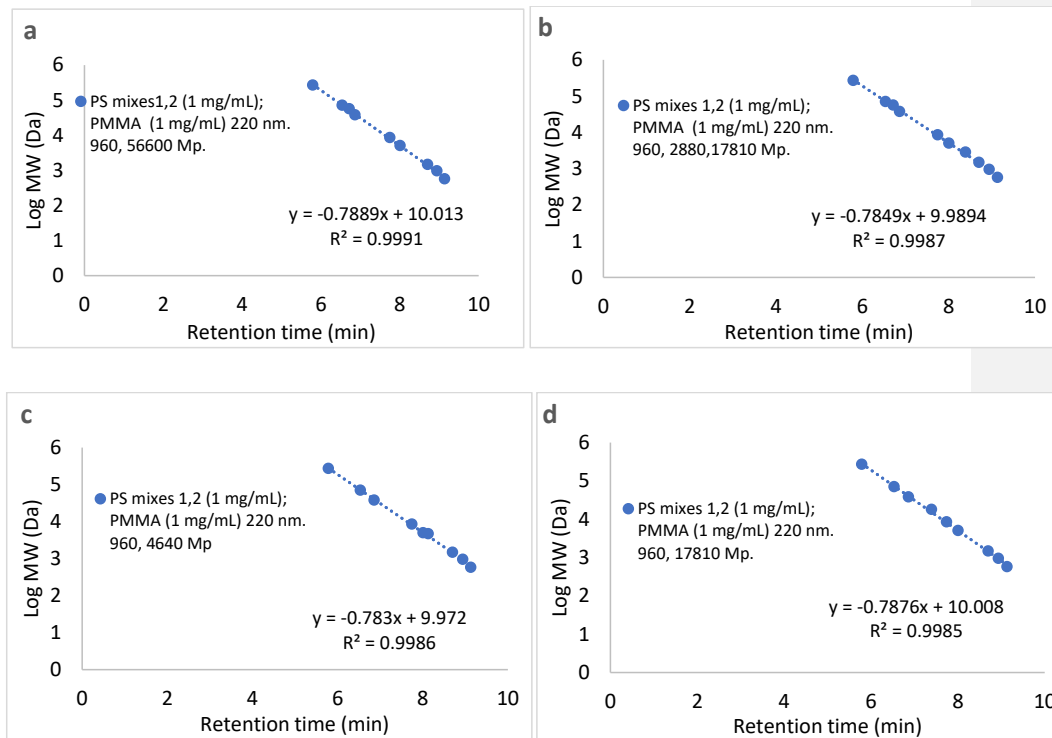


Figure 18. Standards curves for several combinations of PS and PMMA standards, where PS mixes 1,2 encompass 580, 1480, 5030, 8450, 38100, 70950 and 271800 M_p ; (a) PS mixes 1,2 and PMMA 960, 56600 M_p , with 0.00874 S_b and 0.0294 S_y ; (b) PS mixes 1,2 and PMMA 960, 2880, 17810 M_p , with 0.01019 S_b and 0.03508 S_y ; (c) PS mixes 1,2 and PMMA 960, 4640 M_p , with 0.01112 S_b and 0.03613 S_y ; (d) PS mixes 1,2 and PMMA 960, 17810 M_p , with 0.01163 S_b and 0.03766 S_y ;

In reviewing standards curves with the lowest S_b and S_y values in Figure 18, the optimal standards curve was based not only on S_b and S_y values, but also on evenly spaced data points. Thus curve (d) PS mixes 1,2 and PMMA 960, 17810 M_p , with 0.01163 S_b and 0.03766 S_y , was considered to be the best selection for sample evaluation due to well-spaced data points and low S_b/S_y values, although some combinations of PS/PMMA had curves with lower S_b/S_y .

To compare the PS mixes 1,2 (1 mg/mL) to various PS-PMMA curves, two-sided pooled t-tests were conducted to determine if each PS-PMMA curve was statistically the same as the PS curve.

T-test values for several comparisons are shown in Table 17, where critical t values (t^*) are taken from standard two-sided t-test tables and calculated for 95% and 99% confidence levels. The null hypothesis was that the slopes were statistically the same, and any rejection of the null hypothesis meant that the difference between slopes was significant and therefore the slopes were not statistically the same.

Table 17. T-test results for comparisons of PS mixes 1,2 (1 mg/mL) standards curve (with 580, 1480, 5030, 8450, 38100, 70950 and 271800 M_p) to calibration curves composed of PMMA and combined PS/PMMA standards. Results include t-test statistical values t_o , critical t values t^* , and degrees of freedom for a two-sided pooled t-test at 95% and 99% confidence levels. F

Standard sets (in comparison)	Statistical t value (t_o)	Degrees of freedom	Critical value (t^*) for 95%	Significance at 95% confidence	Critical value (t^*) for 99%	Significance at 99% confidence
PS mixes 1,2 (1 mg/mL) vs PMMA mixes 1,2 (1 mg/mL) at 220 nm.	3.309	12	2.18	significant	3.06	significant
PS mixes 1,2 (5 mg/mL) vs PMMA mixes 1,2 (5 mg/mL) at 220 nm	2.649	12	2.18,	significant	3.06	not signif.
PS mixes 1,2 (1 mg/mL) vs PMMA mixes 1,2 (5 mg/mL) at 220 nm	4.744	12	2.18	significant	3.06	significant
PS mixes 1,2 (1 mg/mL) vs PS mixes 1,2 (1 mg/mL) and PMMA 960, 17810 M_p (5 mg/mL) at 220 nm	0.3149	14	2.15	not signif.	2.98	not signif.
PS mixes 1,2 (1 mg/mL) vs PS mixes 1,2 (1 mg/mL) and PMMA 960,17810 M_p (1 mg/mL) at 220 nm	0.1324	14	2.15	not signif.	2.98	not. signif.
PS mixes 1,2 (1 mg/mL) vs PS mixes 1,2 (1 mg/mL) and PMMA 1,2 (1 mg/mL) 4640, 17810 at nm.	0.4481	14	2.15	not signif.	2.98	not signif.
PS mixes 1,2 (1 mg/mL) vs PS mixes 1,2 (1 mg/mL) and PMMA 1,2 mixes (1 mg/mL) 220	0.2691	19	2.09	not signif.	2.86	not signif.

It was clear that PMMA mixes 1,2, in concentrations of 1 or 5 mg/mL, had a statistically different slope value in comparison to the PS mixes 1,2 (1 mg/mL) standards slope at a 95% confidence level, although PMMA mixes 1,2 (1 mg/mL at 220 nm), when added to the PS mixes 1,2 (1 mg/mL) and then compared to the PS mixes 1,2 (1 mg/mL) did not produce a statistically different curve.

The final nine-point calibration curve chosen for sample evaluation consisted of PS standards of 580, 1480, 5030, 8450, 38100, 70950, and 271800 M_p , augmented by two PMMA standards of 960 and 17810 M_p also showed no significant difference to the PS mixes 1,2 (1 mg/mL) curve.

II.1.3.1.4. Evaluation of blank contribution

Controls (blanks) of THF:water (1:1), acetone:water (1:1) and THF:water (95:5) were evaluated, as were unstabilized THF samples with 300 $\mu\text{g/mL}$ of BHT, in order to assess the feasibility of using mixed solvents which were similar to the solvents used for the lignin/solvents study.

Unstabilized THF blanks had a height of 45 – 65 mAU, while BHT height was also in the range of 45 – 65 mAU. A blank with the THF solvent peak which was typical of all project blanks of unstabilized THF and a blank with THF/BHT are shown as Figure 19a and 19b respectively. It was found that the solvent peak, which was ostensibly due to contaminants in the THF itself, occurred at about 11.4- 11.7 minutes retention time and was located shortly after a negative peak. Negative peaks are observed when solute has lower absorbance than the mobile phase but may also represent a pressure “pulse” when low-molecular weight solvent in the

injected sample creates a pressure disturbance in the baseline. When blanks were evaluated for molecular weight (as samples) of this peak, M_w values varied from 7 to 14 Da, thus the peak represented very small particles.

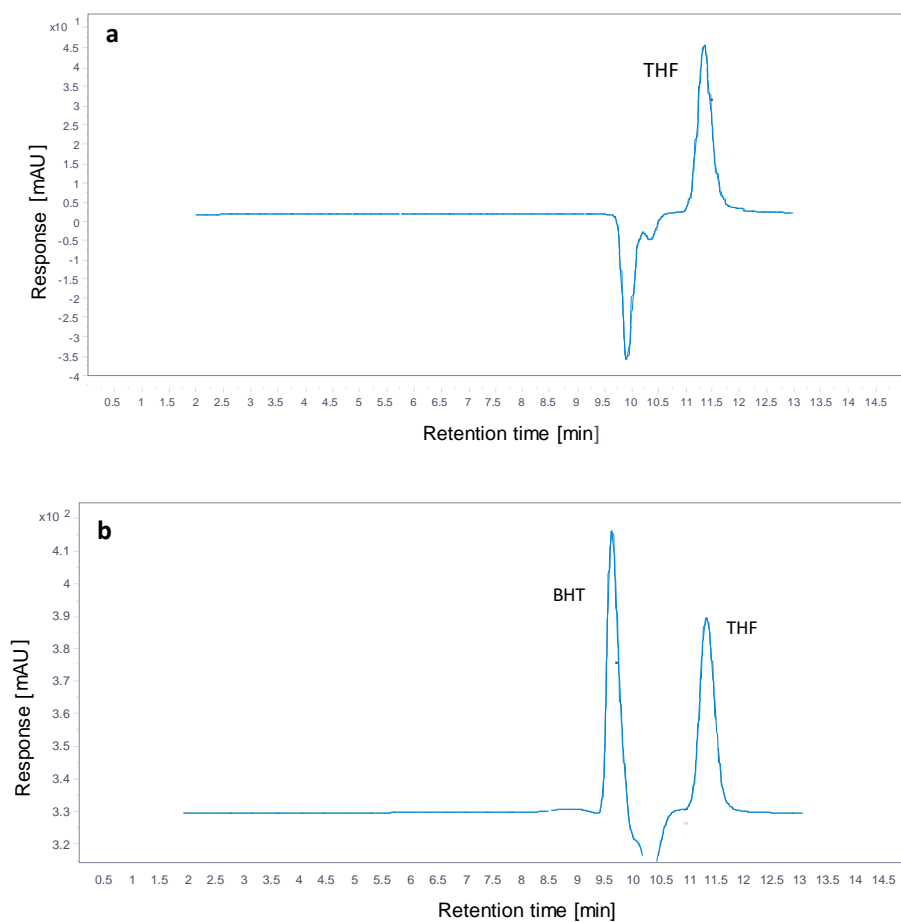
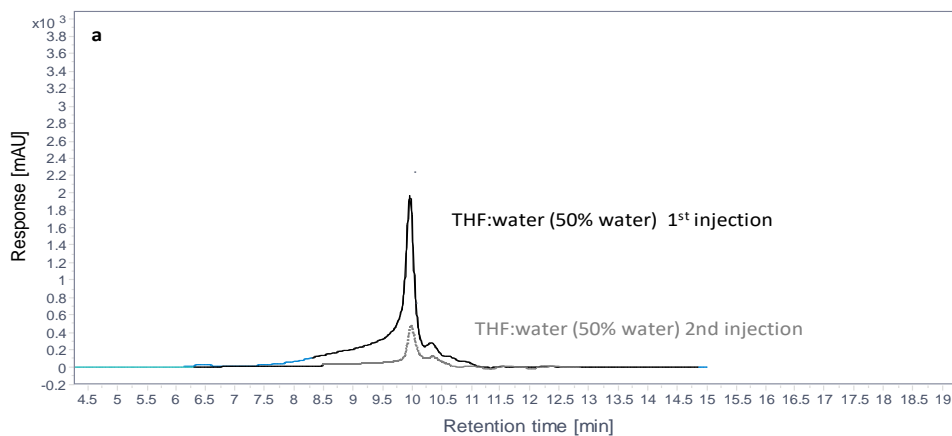
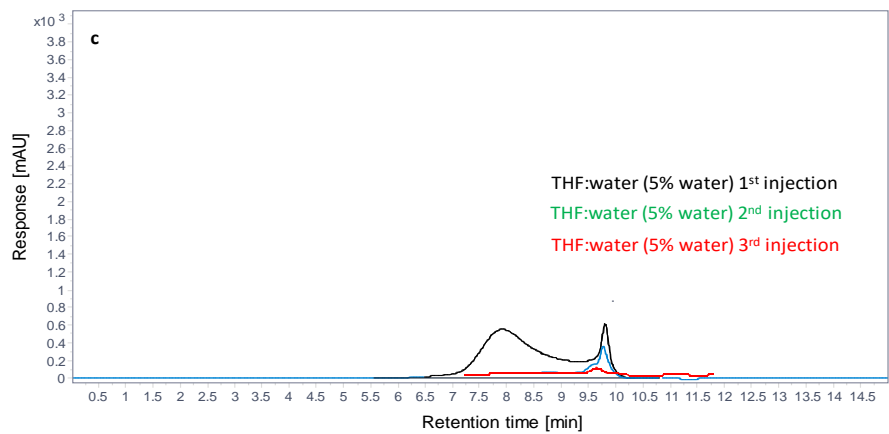
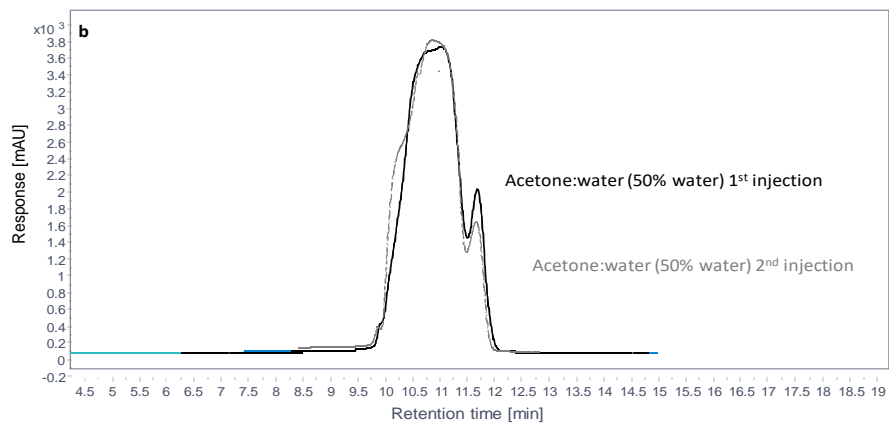


Figure 19. (a) Unstabilized THF blank with solvent peak and injection pressure pulse (negative peak) for a 30- μ L injection volume and a flow rate of 0.3 mL/min (Agilent Plgel Mini-Mix D column); (b) BHT

elution in relation to THF for a 30- μ L injection volume and a flow rate of 0.3 mL/min (Agilent Plgel Mini-Mix D column).

Butylhydroxytoluene is a stabilizing agent for THF; it was evaluated with THF to observe its relative retention time, which was 9.4 – 9.7 min. Injections were also made for solvent mixtures of THF:water (1:1), Acetone:water (1:1), THF:water (95:5) to gauge the effect on the column (Agilent Plgel Mini-Mix D). At least two consecutive injections were made for each water-organic solvent blank, and were compared to alkaline lignin (Sigma, Santa Clara, CA) which had been dissolved in 100% THF for a final concentration of 1 mg/mL. The chromatogram overlays for these are shown in Figure 20. Although the former two solutions were 50% water, this amount was diluted by injection into the mobile phase, so that the 15 μ L of water in the 30 μ L injection was spread throughout the 15 minute run, which at 0.3 mL/min was 4.5 mL, resulting in 0.3% of the mobile phase. The manufacturer's recommended level for water in the Plgel Mini-Mix D column was < 10%, while acetone was listed as an acceptable solvent for the column.





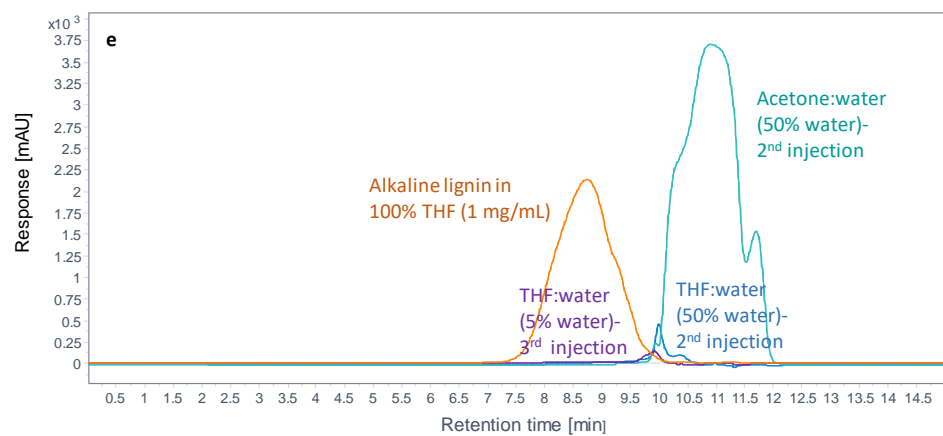
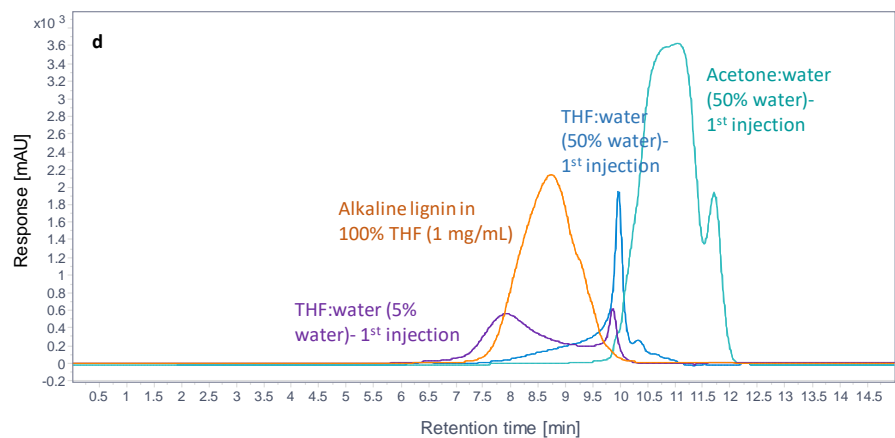


Figure 20. Chromatograms of blanks with mixed solvents, each injected as 30 μ L for a 15-minute program with mobile phase (unstabilized THF) flow rate of 0.3 mL/min, for (a) THF:water (1:1), two consecutive injections initially in the overall sequence, (b) acetone:water (1:1), two consecutive injections after THF:water injections, (c) THF:water (95:5), three consecutive injections after two initial blanks in another sequence, (d) alkaline lignin dissolved in 100% THF (1 mg/mL) and first injections of THF:water (1:1), Acetone water (1:1) and THF:water (95:5), (e) alkaline lignin dissolved in 100% THF (1 mg/mL), and 2nd injections of THF:water (1:1), acetone:water (1:1) and the third injection of THF:water (95:1).

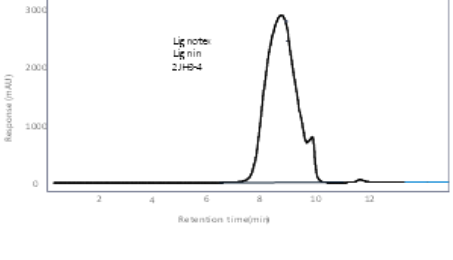
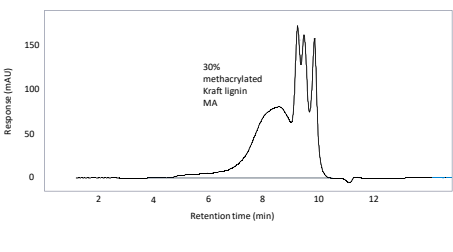
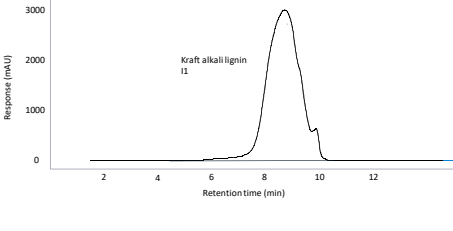
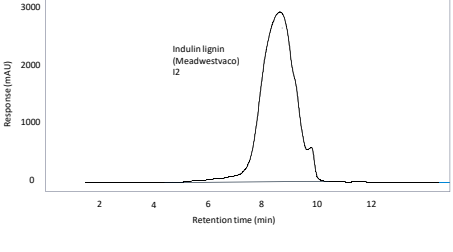
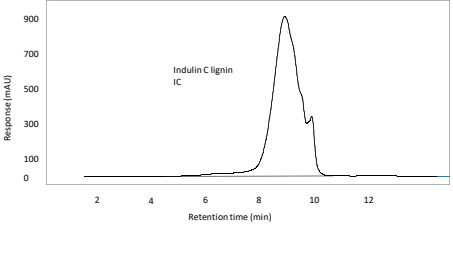
The chromatograms of the mixed solvents showed that the THF:water (1:1) mix had an increasing amount of material detected from 6.0 to 10.0 minutes. The presence of material at a retention time of six minutes corresponded to a MW of approximately 200,000 Da. This type of elution may have been indicative of removal of column lining, i.e., divinylbenzene/polystyrene. The 95% THF: 5% water sample also showed a similar pattern of elution, but the intensity (amount) of material eluting was not nearly as high. The acetone:water profile was entirely different, showing elution starting at about 10 minutes. Of interest was the tendency of high-MW material to decrease in intensity with serial injections of the same solution, either signifying that the water content had a decreasing impact on the column, or that extraneous material deposited in the column in previous runs had been cleaned out. The percentage of water in samples ready for injection were determined to be safe only for <10% of the volume of the solvent mix, as recommended by the manufacturer (Agilent).

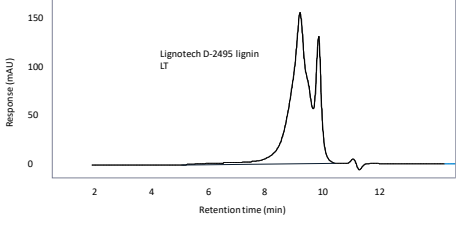
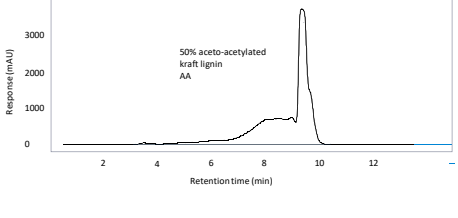
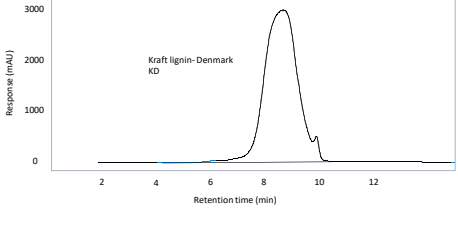
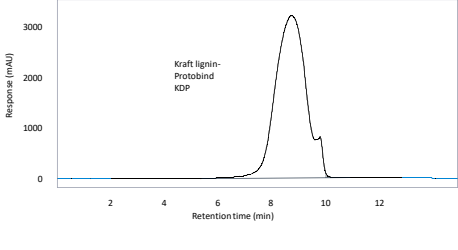
II.1.3.2. Whole lignin sample preparation and evaluation

Whole lignins, lignins processed for separation from cellulosic materials, which are also referred to as “technical lignins,” were collected from several sources (see Materials section) and evaluated for MW at a concentration of 2.5 mg/mL in THF with a water content of 2.5%. Chromatograms and MW values are shown in Table 18.

Table 18. Lignin samples, descriptions, chromatograms and molecular weights as peak-, number-, mass- and z-averages (M_p , M_n , M_w , M_z). All samples were run in duplicate; only one chromatogram is shown and molecular weights are averages of two values for samples which were 2.5 mg/mL in concentration, with 2.5% water before injection.

Lignin Sample Description and (Sample Code)	Chromatogram (Response as mAU)	M_p	M_n	M_w	M_z	Polydispersity (M_w/M_n)
Dealkaline lignin-TCl (2JH3-1)		180	335	2568	328469	7.666
Alkaline lignin-TCl (2JH3-2)		195	313	597	1276	1.909
Lignosulfonate lignin-TCl (2JH3-3)		146	241	1952	201580	8.114

Lignotex lignin-Ginn Mineral Tech. (2JH3-4)		1311	780	3660	195636	4.695
30% methacrylated kraft lignin-NDSU (MA)		465	490	32169	3174017	65.718
Kraft alkali lignin-Sigma (1)		1402	897	6624	421438	7.388
Indulin AT lignin-Meadwestvaco (12)		1427	920	6568	350437	7.143
Indulin C lignin-Meadwestvaco (1C)		1029	587	3137	192445	5.349

Lignotech D-2495 lignin-Borregaard (LT)		546	336	3002	258864	8.948
50% aceto-acetylated kraft lignin-NDSU (AA)		415	555	159883	14917035	288.337
Kraft lignin-Denmark (KD)		3285	1062	4542	64885	4.278
Kraft lignin, Protobind-GreenValue (KDP)		1257	825	2563	39510	3.108

graphical representation of GPC results for the whole lignins tested, with comparisons of respective M_p , M_n and M_w values is shown in Figure 21.

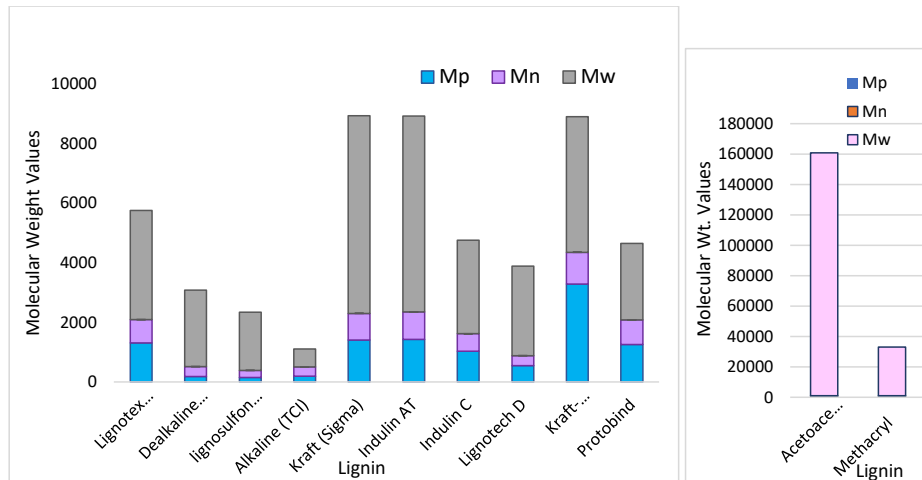


Figure 21. Comparison of M_p , M_n , and M_w (peak-, number-, and mass-molecular weight, respectively) values for (a) lignins with M_w values below 10,000 Da; (b) lignins with M_w values over 10,000 Da.

Comparisons of respective values for M_p , M_n and M_w for whole lignins in the study demonstrated that for commercial lignins with M_w values below 10,000 Da, high M_w values (> 6000 Da) occurred for principally Kraft lignin (Sigma Aldrich) and indulin AT lignin (Meadwestvaco); however low M_w values (< 3000 Da) occurred for alkaline lignin (TCI), dealkaline lignin (TCI), lignosulfonate lignin (TCI), Protobind-1000 lignin (GreenValue), indulin C (Meadwestvaco) and Lignotech (Borregaard). Kraft lignin (Denmark) showed a medium M_w value between 3000 – 6000 Da. Lignins with M_w above 10,000 Da were chemically processed lignins which had been 30% methacrylated and 50% acetoacetylated (Figure 21b) and showed very high M_w values at about 30,000 and 160,000 Da respectively, which were many times higher than M_p and M_n values for the same lignin (kraft) without modification.

TCI and Lignotech lignins seem to show a higher degree of depolymerization, possibly due to processing constraints. Kraft lignin, with the exception of the TCI alkaline lignin,

generally showed higher M_w values, possibly due to a lack of processing after precipitation from black liquor sources. GPC values from this study were compared to literature values for the same lignin categories to ascertain similarity, as shown in Table 19. Comparisons were viewed with some caution as many of the outside studies determined molecular weights through different instrumental parameters or with varying lignin sources.

Table 19. Molecular weight and polydispersity comparison by lignin type and researcher/methodology for indulin AT, indulin C, liginosulfonate, soda pulping and kraft alkaline lignins.

Lignin type	M _n	M _w	PI	Ref.	Lignin Source	Conc. Lignin	Column (GPC)	Mobile phase	Flow rate	Inj. Vol.	Temp	Detector	Standards
Indulin AT	2200	19800	9.00	Glasser	Commerical lignin, Meadwestvaco, Inc.; acetylated.	3- 6 mg/mL	Three Ultrastyrigel columns in series (styrene-divinylbenzene copolymer)	THF	1 mL/min			Differential Viscometer in series with RI	PS
	1191	6096	5.12	Sameni	Commerical, Meadwestvaco, Inc.		PSS MCX column-(sulfonated styrene-divinylbenzene copolymer)	0.1 M NaOH solution		25 µL	rm. Temp.	UV, 280 nm.	sodium polystyrene sulfonates
	1700	8000	4.70	Asikkala	softwood kraft-acetyl bromide in acetic acid	1 mg/mL	Styrigel HR-5E and Styragel HR-1, columns in series	THF	0.5 mL/min			UV, 280 nm., RI	PS
	1600	6500	4.10	Asikkala	softwood kraft-acetic anhydride in pyridine	1 mg/mL	Styrigel HR-5E and Styragel HR-1, columns in series	THF	0.5 mL/min			UV, 280 nm., RI	PS
	897	6568	7.39	This study	Commerical lignin, Meadwestvaco, Inc.	2.5 mg/mL	Plgel Minimix-D (styrene-DVB copolymer and derivatives)	THF	0.3 mL/min	30 µL	rm. Temp.	UV, 250 nm	PS, PMMA
Indulin	1300	3700	2.90	Glasser	Commerical lignin, Meadwestvaco, Inc.; acetylated.	3- 6 mg/mL	Three Ultrastyrigel columns in series	THF	1 mL/min			Viscotek Differential Viscometer in series with RI	PS
	587	3137	5.35	This study-indulin C	Commerical lignin, Meadwestvaco, Inc.	2.5 mg/mL	Plgel Minimix-D	THF	0.3 mL/min	30 µL	rm. Temp.	UV, 250 nm	PS, PMMA
Soda pulping		8000	4.80	Wormeyer	Lignin ext'd from straw by NaOH; precip'd at pH 1.6.	1 mg/mL	Two PolarGel-M columns (styrene-DVB and derivatives)	DMSO with 0.1% (w/w) LiBr	1 mL/min	100 µL	60 °C	UV; RI; viscosimetric detector; two-angle LSD	polyethylene-glycol, polyethylene oxide, glucose
	1084	5008	4.62	Sameni-Protobind	Commercial non-wood soda lignin, GreenValue		PSS MCX column-(sulfonated styrene-divinylbenzene copolymer)	0.1 M NaOH solution		25 µL	rm. Temp.	UV, 280 nm.	sodium polystyrene sulfonates

	825	2563	3.11	This study-Comm. non-wood soda lignin	Protobind 1000; GreenValue	2.5 mg/mL	Plgel Minimix-D	THF	0.3 mL/min	30 µL	rm. Temp.	UV, 250 nm	PS, PMMA
Ligno-sulfonates	7200	64000	8.80	Fredheim	Borregaard Lignotech- Na sulfonate spruce	2 - 5 mg/mL; filt 0.45 µm.	Jordi (glucose-DVB), 10000 Å, 500 x 10 mm	9% DMSO/ aqueous (+ SDS) PH adj. to 10.5.	1 mL/min	200 µL	60 °C	Dawn-F MALLS (fluor.filter); RI.	PSS and polysaccharide
	3441	7082	2.05	Chen and Li	Commercial (China) Na lignosulfonate	3 mg/mL; filt 0.45 µm.	Ultrahydrogel 250 and 1000 columns (hydroxylated polymethacrylate)	0.1 M NaNO ₃ /aqueous, pH 7	0.6 mL/min	100 µL		Differential refractometer.	Pullulan, PEG
	241	1952	8.11	This study-Lignotech h	Borregaard Lignotech	2.5 mg/mL	Plgel Minimix-D	THF	0.3 mL/min	30 µL	rm. Temp.	UV, 250 nm	PS, PMMA
	336	3002	8.95	This study-Lignotech h D	Borregaard Lignotech	2.5 mg/mL	Plgel Minimix-D	THF	0.3 mL/min	30 µL	rm. Temp.	UV, 250 nm	PS, PMMA
	780	3660	4.70	This study-Ligno-sulfonates	TCI Ligno-sulfonates	2.5 mg/mL	Plgel Minimix-D	THF	0.3 mL/min	30 µL	rm. Temp.	UV, 250 nm	PS, PMMA
Kraft alkaline	866	2565	12.34	Sameni	Kraft black liquor, acidified to pH 2		PSS MCX column- (sulfonated styrene-divinylbenzene copolymer)	0.1 M NaOH solution		25 µL	rm. Temp.	UV, 280 nm.	sodium polystyrene sulfonates
	1598	15375	9.62	Delgado	Pine alkali Kraft, precip. at pH 3, acetylated	0.2% (wt/v) (2 mg/mL)	Ultrastryragel(100, 500, 1000 Å) in series	THF	1 mL/min	100 µL		Photodiode array (PDA)	PS

	1000	4500	4.50	Brodin	Filtered and precip. black liquor from Kraft process; acetylated		Styragel HR2 ,HR1, Ultrastyrigel 104 Å in series	THF	0.8 mL/min			410 RI	PS
	1000	3300	3.30	Asikkala	hardwood kraft-acetic anhydride in pyridine	1 mg/mL	Styragel HR-5E and Styragel HR-1, in series	THF	0.5 mL/min			UV, 280 nm., RI	PS
	1000	3900	3.90	Asikkala	hardwood kraft-acetyl bromide in acetic acid	1 mg/mL	Styragel HR-5E and Styragel HR-1, in series	THF	0.5 mL/min			UV, 280 nm., RI	PS
	7523	19650	2.70	Chen and Li	Kraft Birch-from Tianjin Institute	3 mg/mL; filt 0.45 µm.	Ultrahydrogel 250 and 1000 columns	0.01 M NaOH/aqueous, pH 10-12	0.6 mL/min	100 µL		Differential refractometer	Pullulan, PEG
	1510	2330	1.54	Yuan	Alkaline-extracted lignin from ball-milled Poplar.	2 mg/mL	Plgel mixed-B, 7.5 mm ID (styrene-DVB copolymer and derivatives)	THF	1 mL/min		rm. Temp.	Unspecified	Mono-disperse PS
	313	597	1.91	This study-TCl alkaline	TCl kraft alkaline	2.5 mg/mL	Plgel Minimix-D	THF	0.3 mL/min	30 µL	rm. Temp.	UV, 250 nm	PS, PMMA
	897	6624	7.39	This study-Sigma alkali	Sigma kraft alkali	2.5 mg/mL	Plgel Minimix-D	THF	0.3 mL/min	30 µL	rm. Temp.	UV, 250 nm	PS, PMMA
	1062	4542	4.28	This study-Denmark kraft		2.5 mg/mL	Plgel Minimix-D	THF	0.3 mL/min	30 µL	rm. Temp.	UV, 250 nm	PS, PMMA

Additionally, molecular weight ranges for lignosulfonates and kraft lignin from several sources are listed in table 20. For the few sources listed in table 20, it is clear that molecular ranges for the same type of lignin vary greatly. With the exception of the Borregaard reference, which is an estimate for the Lignotech product, the other estimates are based on the results of several studies surveyed by the authors. This serves to illustrate that M_n and M_w values for individual samples would also vary substantially, as was indeed also seen in Table 19.

Table 20. Molecular weight ranges for lignosulfonate and kraft lignin as compiled by several reference studies.

Lignin Type	Molecular Weight Range (g/mol)	Reference
Lignosulfonate lignin	1000 – 100,000	Zhor and Bremner ²⁰⁰
	20,000 – 80,000	Borregaard ³⁴
	1000 – 150,000	
Kraft lignin	1500 – 25,000	Vishtal ²⁰¹
	200 – 200,000	Moerck ²⁰²

The wide range of M_n and M_w values for each type of lignin in Table 19 varied significantly with column type, mobile phase and detector, and these were inconsistent for the same type of method. Although viscometric and light-scattering techniques tend to give higher values of M_n and M_w , and a number of researchers found them very effective, GPC with UV or RI detection was also found to be the method of choice^{76-79,83}. A number of investigators either recommended or used viscometric and light scattering detectors in conjunction with SEC.^{62,63,65,83,84,86}

The use of viscometry and/or light scattering did not always lead to consistently high results compared to SEC techniques alone. Glasser et al. showed a very high M_w level for

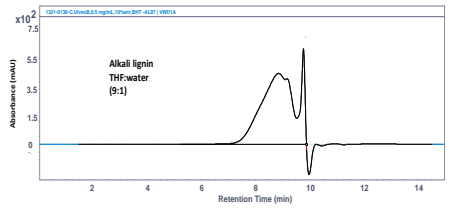
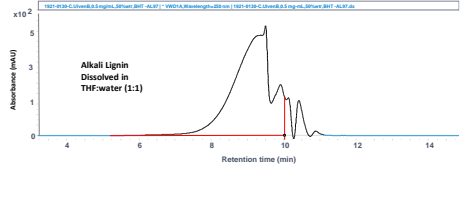
indulin AT lignin via visometric detector in series with RI, which were much higher than those of other studies using different methods, yet showed modest M_w levels for indulin C which were very similar to other studies' values.⁶⁵ Fredheim showed high M_w values with MALLS in line with an RI detector for lignosulfonates,⁸⁴ but Delgado also showed a very high M_w value for kraft lignin with a photodiode detector⁷⁷ Even if more studies that have produced M_n and M_w data were included in an overall comparison, many more replicate studies would have to be before there could be firmly established behaviors for columns, detectors and eluents that are represented here, and these would also have to be done in relation to lignin samples from standard, known sources.

The need for derivatization also presents as a complex issue with no clear answers. Number-average (M_n) molecular weight values in this study for kraft lignin (313 g/mol for TCI samples and 897 g/mol for Sigma samples), seemed low compared to other kraft lignin M_n values in studies which used derivitized lignin samples, with values of 1000 and 1000 g/mol,^{76,78} although 897 g/mol is not too far from 1000 g/mol. Delgado et al. had an M_n value of 1598 g/mol with nonderivitized kraft lignin.⁷⁷ Yuan et al. had an M_n value of 1510 g/mol, and also did not specify a derivitization method.⁸⁵ The GFC methods of Sameni et al., and Chen and Li yielded M_n values of 866 g/mol and 7523 g/mol respectively.^{79,83} It would seem that method parameters can be chosen to avoid derivitization, and there is always the concern about structural changes if it is done.

As a matter of interest in the effect of solvent systems on solubility of samples in preparation for GPC analysis, an additional method of preparation of lignin samples was undertaken, wherein a lignin sample supplied by Dr. Chad Ulven, North Dakota State University, was dissolved in THF:water at a 9:1 ratio and also a 1:1 ratio (50% water). The lignin sample

was an alkali kraft lignin sample and GPC conditions were the same as those for whole lignins as evaluated above, with the exception that concentrations of lignin were somewhat different, and, as noted, the solvent system used to prepare the samples was changed to THF:water (9:1) and (1:1). The results for these GPC analyses are shown in Table 21.

Table 21. Lignin samples, descriptions, chromatograms and molecular weights as peak-, number-, mass- and z-averages (M_p , M_n , M_w , M_z). All samples were run in triplicate; only one chromatogram is shown and molecular weights are averages of three values for samples which were approximately 0.5 mg/mL in concentration. Red lines show integration area.

Lignin Sample and Solvent Description	Chromatogram (Response as mAU)	M_p	M_n	M_w	M_z	Poly-dispersity (M_w/M_n)
Ulven Lignin 0.55 mg/mL Solvent: THF:water (9:1)		186	605	1950	11907	3.22
Ulven Lignin 0.51 mg/mL Solvent: THF:water (1:1)		355	513	2133	80613	4.16

Samples in THF:water (1:1) were problematic in that the resolution of low-MW material was not well-defined and gave a sort of wave-like appearance at retention times past 10 min. However, both THF:water (1:1) and (9:1) samples were integrated only to 10 min as this

corresponded to an extrapolated calibration standard mass of 130 g/mol- a very low MW for lignin samples.

Of interest, the samples dissolved in THF:water (1:1) showed higher-MW compounds eluting at earlier retention times in comparison to THF:water (9:1) samples; this effect is apparent on the chromatograms and also is reflected in the substantially higher M_z values. However, this effect did not greatly impact M_n or M_w values. The method was considered to be feasible but might be better implemented with a slower flow rate or with a column and set of parameters which would offer more resolution. Using the THF:water (1:1) sample preparation allowed better dissolution of higher-MW particles, but it may be questionable as to whether enough of them existed to significantly affect M_n and M_w values. The results do, however, shed light on the relative amount of high-MW compounds in a kraft lignin which has been filtered via 0.2 μm pore size syringe filters.

II.1.3.3. Preparation and evaluation of samples from a lignin-solvent study

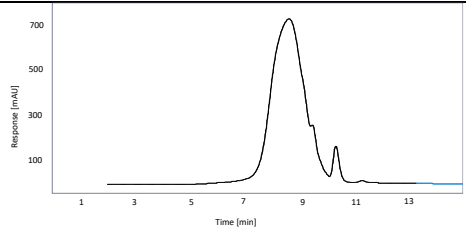
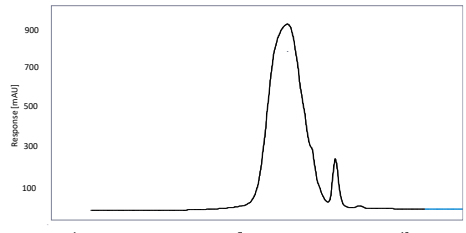
Kraft lignin (Sigma Aldrich, St. Louis, MO) was dissolved over 24 hours in several solvents and solvent combinations (see II.2.3. Lignin Samples and Preparation Section). Lignin had a wide range of solubility in the various solvents and solvent systems after preparation, ranging from 5.0 mg/mL to over 100 mg/mL.

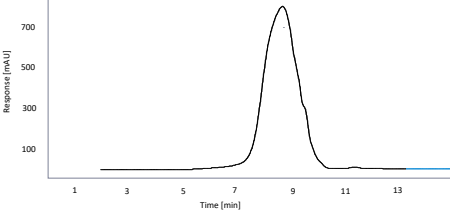
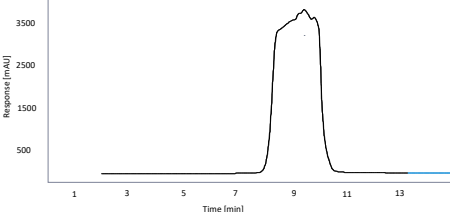
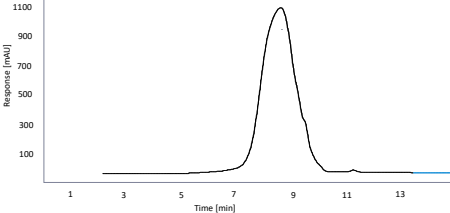
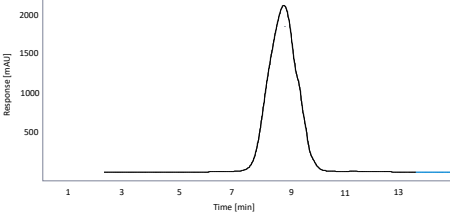
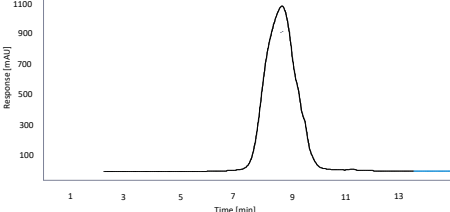
Lignin samples were diluted to 1 mg/mL, with each original solvent constituting less than 10% by volume of the final samples. The initial GPC analysis of the solubilized solutions was accomplished without derivatization in order to evaluate the effectiveness of a GPC protocol wherein the extraction solvent differed from the mobile phase (THF), and constituted less than

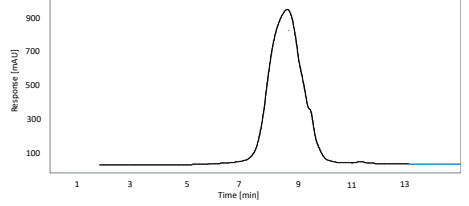
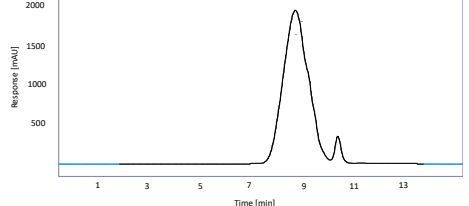
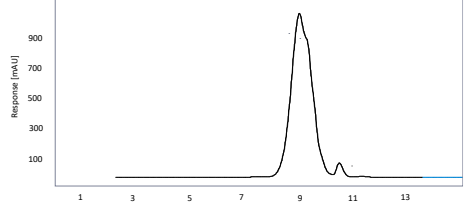
10% of the injected volume. Precipitation occurred after addition of THF to many samples, so that consequent filtering did remove higher MW molecules in some samples.

The samples were evaluated for MW as M_n , M_w and M_z ; chromatograms and MW values are shown in Table 22.

Table 22. Lignin-solvent study samples' descriptions, chromatograms and molecular weights as peak-, number-, mass- and z-averages (M_p , M_n , M_w , M_z). All samples were run in triplicate; only one representative chromatogram is shown and molecular weights are averages of three values for samples which were 1.0 mg/mL in concentration.

Lignin Sample Description and (Sample Code)	Chromatogram (Response as mAU)	M_p	M_n	M_w	M_z	Poly-dispersity (M_w/M_n)
Kraft lignin in 50% acetone-50% water (LL60)		1721	731	2637	5541	3.62
Kraft lignin in 75% acetone-25% water (JE10)		1748	694	2742	5803	3.95

Kraft lignin in 50% acetonitrile- 50% water (LL61)		1665	1081	2802	5871	2.59
Kraft lignin in 100% acetonitrile (ET27)		421	388	1036	2101	2.67
Kraft lignin in 50% THF- 50% water (JE40)		1768	1193	3074	6646	2.58
Kraft lignin in 100% THF (BY44)		1492	1041	2351	4962	2.26
Kraft lignin in 50% THF- 50% MeOH (LB55)		1630	1141	2583	4992	2.27

Kraft lignin in 50% mTHF- 50% MeOH (LB50)		1700	1042	2914	8553	2.80
Kraft lignin in 50% propanol- 50% acetone (BM93)		1334	599	1629	2885	2.72
Kraft lignin in 100% methyl acetate (LB62)		946	493	1013	10335	2.06

A graphical representation of GPC results for the lignin-solvent samples tested, with comparisons of respective M_p , M_n and M_w values is shown in Figure 22.

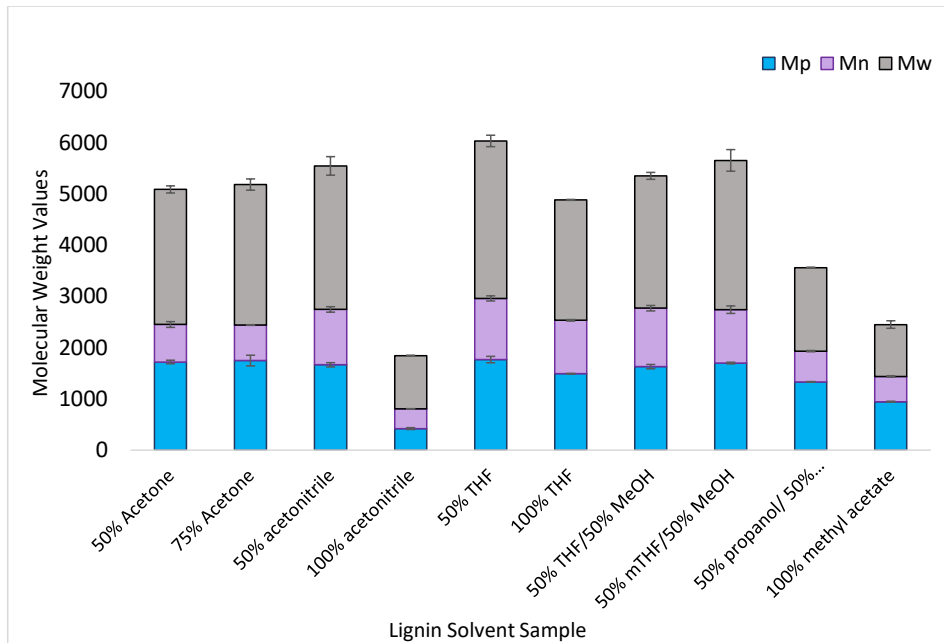


Figure 22. Comparison of M_p , M_n , and M_w (peak-, number-, and mass-molecular weight, respectively) values for kraft lignin dissolved in various solvents and combinations of solvents.

Comparisons of respective values for M_p , M_n and M_w for kraft lignin dissolved in various solvents showed very similar levels across the board, with the exception of lignin in 100% acetonitrile, 100% methyl acetate and 1:1 propanol:acetate; the latter samples showed low values for all three molecular weights. The similarity of M_p , M_n and M_z values for all the rest of the samples brought up an intriguing pair of hypotheses:

1. All solvents dissolved high MW molecules as well as low, with the only difference being that fewer molecules across the range were being dissolved in low-solubility solvents. This would mean that M_n and M_z would be similar for all solvents, but only intensity (number of

molecules dissolved) would differ. The exception of the three solvents with low M_n and M_w may be due to very low solubilities for lignin overall in those solvents.

2. Low solubility solvents were able to dissolve only low MW materials, while high solubility solvents were able to dissolve high MW molecules as well as low MW molecules. The use of THF as a diluent may have decreased solubility of the original samples to a level similar to 100% THF samples, and thus the close proximity of M_n and M_w values. Notably, M_w values lower than 3000 g/mol are present for every sample, reflecting a general lack of high MW molecules. The 100% acetonitrile, 100% methyl acetate and 1:1 propanol:acetone samples may have had very low M_n and M_w due to extremely poor lignin solubility.

An overlay of all the lignin-solvent samples showed that peaks aligned very closely, with the exception of the 100% acetonitrile sample, which indicated a lower average MW, but which also had a very high response. The concentration of lignin in the acetonitrile sample was actually quite low, so that it was very possible that samples with higher concentrations (i.e. 50% acetone with over 100 mg/mL) had lost a range of higher MW molecules due to precipitation and subsequent filtration. None of the samples show responses below 7 min which corresponded to a MW of approximately 36,000 Da (Figure 23).

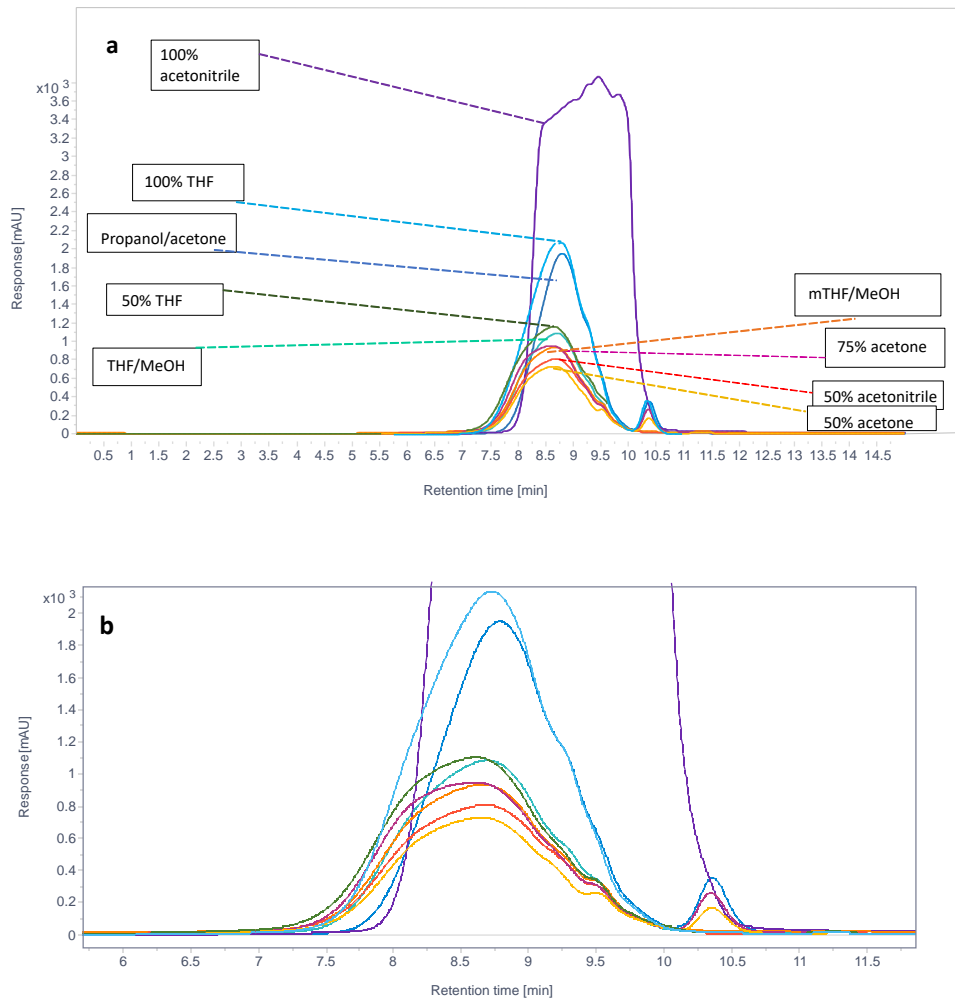


Figure 23. Overlay of chromatograms of all lignin-solvent samples shown as (a) peaks with full response, and as (b) a close-up of the peak bases.

The average amount of original lignin recovered in the solvent was calculated from thermal carbon analysis (TCA) carbon yields for 5 μ L samples of each liquid fraction in triplicate; these

values, with average original mass of lignin, original volume of solvent and percentage recovery in the liquid fraction, are presented in table 23.

Table 23. Average original lignin mass, solvent volume, concentration of lignin in the liquid fraction and average % recovery of original lignin for each solvent (system).

Solvent System	original lignin	solvent	% lignin recovery	st. deviation	concentration of
	in solution (g)	extractd (mL)	of original lignin	of % lignin recov.	liq fract.(mg/mL)
75% Acetone	2.9883	25.94	80.23	9.72	93.27
50% acetone	2.9897	28.22	74.19	13.00	78.61
50% CAN	2.9879	27.81	72.17	7.95	77.55
100% CAN	3.0006	20.41	not detectable	0.00	5.00 [†]
50% THF	2.9915	28.67	108.39	4.14	113.11
100% THF	3.0009	18.84	12.74	7.80	20.30
50% mTHF 50% MeOH	2.9895	23.08	12.74	7.80	60.40
50% THF 50% MeOH	2.9950	18.92	66.74	4.20	105.63
50% 2-propanol 50% Acetone	3.0382	23.08	31.84	4.20	41.91
Methyl Acetate	2.9966	23.74	7.40	0.33	9.34
					[†] estimated by comparison
					with diluted solutions of
					other solvents

A chart showing average percent recovery of original lignin in the liquid fraction is shown in Figure 24.

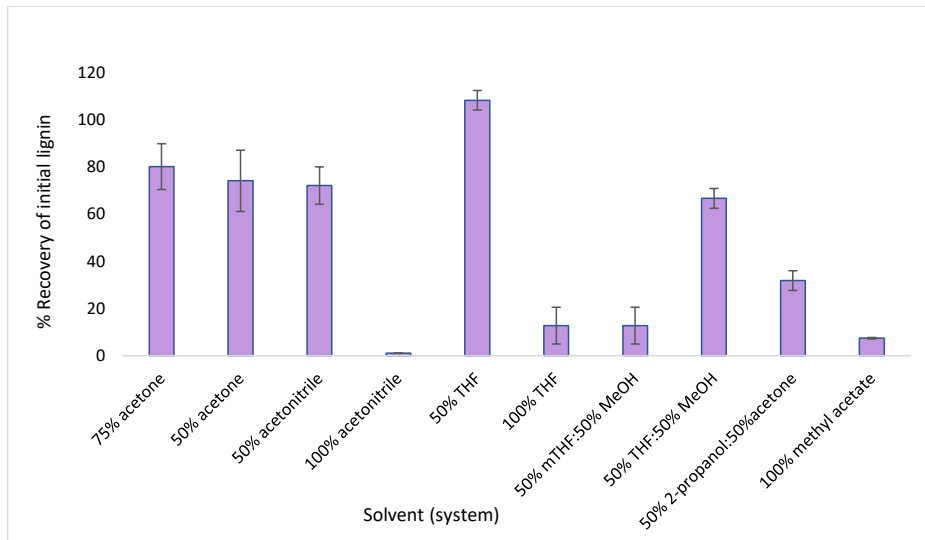


Figure 24. Average % recovery of original lignin in the liquid fraction of each solvent or solvent system.

Although pure solvents such as acetonitrile and THF show very little ability to solubilize lignin, which may be due to a net balance of repulsion over attraction, particularly of lignin polar groups to an organic solvent, 1:1 solutions of the same solvents with water show a remarkable increase in solubility of lignin. Perhaps this is due to a shift in balance of forces, favoring attractive forces of lignin polar groups to water and attractive forces of nonpolar lignin groups to an organic solvent over repulsive forces, possibly due to an advantageous spatial arrangement. The solubility of lignin in a 1:1 solution of acetone was also high, as was solubility in a 3:1 acetone:water mix. Although solubilities in this study differ somewhat from acetone-water solubilities in a study by Sadeghafir et al., the latter study also shows progressively better solubility as acetone increases from 50% to 100% (Figure 6). Acetone has a polarity (relative to

water at 1.00) of 0.355, compared to acetonitrile (0.460) and THF (0.207), so that apparently polarity does not determine lignin solubility alone (Table 24).

The effect of solvent systems on solubility of samples in preparation for GPC analysis was investigated in addition to THF dilution with less than 10% water content, as above. An additional method of preparation of lignin samples was undertaken, wherein kraft alkali lignin, (Sigma, St. Louis, MO) was dissolved in THF:water at a 1:1 ratio. The lignin sample was an alkali kraft lignin sample and GPC conditions were the same as those for lignins referenced above, with the exception that several were lower in concentration than 1 mg/mL and, as noted, the dilution solvent system included a greater percentage of water.

The samples in this case had been previously solubilized in acetone:water solvent systems that included 20, 30, 40 and 50% acetone, which generally showed increasing solubility of lignin as acetone approached the 50% level. Equal volumes were removed and diluted with THF:water (1:1) such that the highest lignin concentration (50% acetone) had a final concentration of about 0.5 mg/mL, while other samples had correspondingly lower concentrations due to the comparison on an equal volume basis. Samples were evaluated in duplicate.

In a similar investigation with whole lignins, one sample type was dissolved in THF:water (9:1) and (1:1) ratios, resulting in a comparison showing more extensive dissolution of high-MW compounds for the (1:1) ratio, but which also had a low impact on Mn and Mw compared to the (9:1) ratio. In this case, for samples solubilized in varying solvent systems, only the (1:1) ratio was investigated, and it was considered that the effect was the same, i.e., high-MW compounds more readily dissolved, but did not have much impact on Mn and Mw values in comparison to preparation in THF:water (9:1); in this case, more in-depth evaluation of the effect

of a high percentage of water in the solvent used for solubilization/preparation of samples for GPC, which were already dissolved in a water/solvent system, was the goal. The most direct comparison was for the sample LL60 in Table 22 (acetone:water 1:1) to the acetone:water (1:1) sample in this sequence.

Table 24. Lignin samples, descriptions, chromatograms and molecular weights as peak-, number-, mass- and z-averages (M_p , M_n , M_w , M_z). All samples were run in duplicate; only one chromatogram is shown and molecular weights are averages values for both samples. Red lines show integration areas.

Lignin Sample and Solvent Description	Chromatogram (Response as mAU)	M_p	M_n	M_w	M_z	Poly-dispersity (M_w/M_n)
acetone:water (2:8) 0.11 mg/mL Solvent: THF:water (1:1)		303	427	1109	48376	2.60
acetone:water (3:7) 0.18 mg/mL Solvent: THF:water (1:1)		370	468	1763	75543	3.77
acetone:water (4:6) 0.30 mg/mL Solvent: THF:water (1:1)		364	506	1969	75882	3.77

acetone:water (1:1)		363	513	2455	83521	4.79
0.45 mg/mL						
Solvent: THF:water (1:1)						

Since samples solubilized/prepared for GPC with THF (less than 10% water) were evaluated for MW only for acetone:water combinations of 75 and 50% acetone, the only sample which could be compared was the LL60 sample from Table 22 to the 50% acetone sample in Table 24. However, this showed some notable results, as shown in Table 25:

Table 25. Comparison of MW values for lignin samples solubilized in acetone:water (50% acetone) solvent systems. Preparation for GPC differed- one sample was solubilized in THF:water (less than 10% water) and the other in THF:water (1:1). Concentrations were 1 mg/mL and 0.45 mg/mL respectively. Chromatogram axes are not the same).

Sample	Mp	Mn	Mw	Mz	Poly-dispersity (M _w /M _n)	
50% acetone:water sample in THF:water (<10% water)	1721	731	2637	5541	3.62	
50% acetone:water sample in THF:water (1:1)	363	513	2455	83521	4.79	

Of interest, the sample dissolved in THF:water (1:1) has a lower M_p and is centered in a lower-MW range than the other sample, and yet seems to have solubilized more high-MW compounds, as was found with the whole lignin samples. However, the number of high-MW samples does not appear to have affected MW values other than the M_z and PI values; M_n and M_w are actually somewhat lower for the (1:1) sample, although the values are still very close.

The use of a preparation solvent of THF:water(1:1) was considered superior in terms of solubilizing higher-MW compounds and possibly showed a more accurate range of MWs for the acetone:water series (20 – 50% acetone) than a simple preparation in THF with a small percentage of water would. When looking at the trends for M_n , M_w and M_z for the acetone:water series, M_p changed little, while M_n and M_w increased somewhat with increase in acetone percentage. M_z and PI showed significant increases; however, M_z values seemed to plateau after 30% acetone, implying that higher MW compounds were limited in size at around this point, or that solubilization ability was limited.

II.2. Folin-Ciocalteu Method of Quantification of Phenolic Hydroxyl Groups in Lignin

II.2.1. Experimental

II.2.1.1. Materials

Greiner 96-well polystyrene nonsterile microplates were used for the assay arrays (Greiner Bio-One, Kremsmunster, Austria), while alkali (kraft) lignin and Folin-Ciocalteu Phenolic Reagent (2N) were obtained from Sigma Aldrich (St. Louis, MO, USA).

Solvents used included acetone, acetonitrile, tetrahydrofuran, methyltetrahydrofuran, methanol, isopropanol, methyl acetate (VWR, Arlington Heights, IL, USA), which were GC and HPLC grade. Sodium carbonate (Na_2CO_3) ACS grade was also purchased from VWR.

Deionized water was obtained from a Direct-Q 3 UV system purifier (Millipore, Billerica, MA, USA) with the total organic carbon content below 5 ppb (manufacturer specification).

II.2.1.2. Folin oxidation method development

Optimization of microplate parameters were determined after a long period of experimentation and were also determined via Minitab statistical software, using factorial (resolution V) design, for comparison. The section immediately after “FC Analysis” is “*FC Phenol Reaction Method Development*,” wherein parameter determination is covered in a more in-depth manner.

Generally, lignin samples had to be solubilized in a solvent system amenable to dissolution, and the solution had to have a workable concentration for signaling in a UV-Vis detector within its range of detection. In addition, Na_2CO_3 is added to produce alkalinity, which is necessary for colorimetric change, and the concentration had to be adjusted. Also, Folin-Ciocalteu reagent (2N) could be adjusted to produce colorimetric change at a minimal amount, in order to save on reagent use.

Due to instrument change on a daily basis, a control sample of guaiacol of known concentration also had to be added with each measurement. One of the most important parameters was the time period allowed for reaction development, as a too-early interval would

not differentiate results substantially between analytes, while a too-long development period could coincide with salt deposition at the bottom of the microplate wells.

In a micro-scale Folin reagent study performed on bio-oil, Rover et al. recommended 20 μL of bio-oil be dissolved in ethanol, filtered and diluted in 1.58 mL water, with 100 μL FC reagent added. Sodium carbonate (2.4 M) was added as 300 μL and the sample was developed for 2 hours at 765 nm, the most common wavelength for Folin reagent experiments analyzed via UV-Vis. A guaiacol standard calibration was implemented for concentrations of 50, 100, 250, and 500 $\mu\text{g}/\text{mL}$. The samples were evaluated in cuvettes as opposed to microplate wells.¹⁰⁰

In modifying the method for microplate analysis, reagent amounts had to be reduced substantially; the equivalent of 2 mL of a sample had to be fit into 240 μL of volume. Testing proceeded mainly according to a one-change-at-a-time methodology, which is not considered to be the most productive; hence, the testing via Minitab factorial experimental design was accomplished shortly afterward. Concentration of the salt solution was the most pressing problem because of precipitation tendencies (Figure 25), so this parameter was investigated first; a concentration of 0.15 M (as 0.4 M in 150 μL) was an improved parameter over the recommended 0.36 M.



Figure 25. Left: A solution of gallic acid (100 $\mu\text{g}/\text{mL}$) reacted with 50 μL FC reagent and 0.4 M Na_2CO_3 after two hours, with the liquid solution poured off after the reaction. Right: The same reaction after three hours (note opaque wells near the center).

Whereas absorbance in a cuvette is determined by a horizontal light beam which transects through the middle area of solution in the cuvette, bypassing precipitation on the cuvette bottom, a microplate is not able to avoid this problem because of the orientation of the vertical light beam, which passes from top to bottom of the sample.

Two hours for development, even at this reduced salt amount, was also deemed to be optimal for incubation time. Interestingly, readings taken over 24 hours did not actually reach full development even during this time period, as signaled by continued colorimetric development (Figure 26).

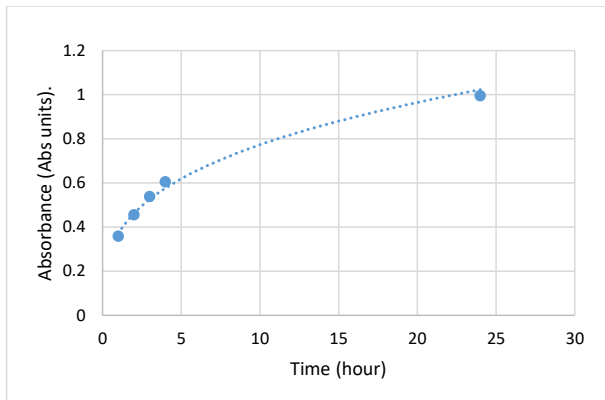


Figure 26. Absorbance of a solution of gallic acid (100 µg/mL) with 50 µL FC reagent and 0.4 M Na₂CO₃ over 24 hours.

Lignin concentration, particularly for highly reactive models such as catechol, could not exceed 200 µg/mL or saturation of the detector occurred. In addition, trials with half-volumes of 120 µL did not produce reliable results. Interestingly, Folin reagent required 50 µL for good development of the blue colorimetric response, although this constituted 21% of the total volume of the sample. Even so, per sample, this saved on the expenditure of Folin reagent in comparison to the recommended 100 µL per sample.¹⁰⁰ Table 26 shows the parameters recommended by Rover et al. in comparison to the actual parameters tested in this study.¹⁰⁰

Table 26. Recommended parameters of Folin reagent oxidation of bio-oils (Rover), shaded in gray, in comparison to parameters investigated in this study. (Parameters used in the method are bolded).

Optimization of Parameters	Recommended (Rover et al.) ¹⁰⁰	This study, Parameter 1	Parameter 2	Parameter 3	Parameter 4	Parameter 5
Volume of sample in microplate wells (250 μ L max.)	2 mL	240 μ L	120 μ L			
Lignin concentration (μ g/mL)	500	250	200	100		
Salt (Na_2CO_3) final concentration (Molar)	0.36	1.5	0.75	0.375	0.15	0.125
Folin reagent amount (μ L) and % of liquid sample	100 (5%)	100 (42%)	50 (21%)	25 (10.5%)		
Development time interval (hours)	2	1	2	3		

A statistical design of experiment approach was also accomplished, whereby a 2^4 factorial, resolution V, 4-replicate system was used; two parameter choices per level were allowed and the choices were made based on preliminary experiments. By this time, it was clear that because of salt deposition problems, a low level of Na_2CO_3 addition (0.15 M) was necessary or a possibly lower level (0.125 M) might suffice. Incubation time would have to be either 1 or 2 hours because of the same limitation, and Folin reagent could be the full 100 μ L or possibly less, per sample. In addition to this, an investigation into the delivery mode of acetonitrile was also considered; it was present as ACN:water (1:1) in the original solution added to lignin due to its ability to enhance solubility, but there was speculation as to whether it could also be effective when delivered as a reagent to lignin in an aqueous solution with Folin reagent and Na_2CO_3 . Table 27 delineates the statistical parameters of the factorial design.

Table 27. Factorial ANOVA (analysis of variance) statistical parameters of a 2⁴ design, with four factors and two levels designated.

Factorial design of experiment: two levels, 4 factors (parameters)	Incubation time (hr)	FC reagent (μL)	Na ₂ CO ₃ concentration (Molar)	Acetonitrile (ACN) delivery
Level 1	1	100	0.125	ACN added later
Level 2	2	50	0.15	ACN added immediately

The main purpose of a factorial evaluation of a variety of parameters is to compare residual differences between actual absorbance response levels vs. predicted response levels based on regression analysis. The findings of the analysis inform as to whether there are “main effects” for the factors, i.e., the Folin amount in this experiment would make a significant difference in the absorbance of the sample. A “p” value between 0 and 1, below the threshold of significance (usually 0.05) shows how likely it is that there is a main effect (we can reject the null hypothesis that there is no real effect of the factor on the outcome). The threshold of 0.05 represents the confidence interval α , which shows in this case that there is a 5% chance that we are saying the factor has an effect when it actually does not. The study can also illustrate significant associations between factors, i.e., parameters are not independent and are in fact linked. It is always best to have parameters that are not inter-related, as statistical analysis of “best choice” becomes nonapplicable if factors are not independent.

II.2.1.3. Folin oxidation method

The final protocol entailed the dilution of a 200 μg/mL sample down to 20 μg/mL within 10 wells of the microplate, having been made in a 1:1 acetone:water mixture and then diluted by one-half each step with the same solution in one row of the Greiner microplate. At least two

repeats (rows) of the same solution were plated. A control sample of guaiacol (70 $\mu\text{g}/\text{mL}$) in a 1:1 acetone was run with each plate (Figure 27). The slopes for all samples were adjusted to guaiacol standards (70 $\mu\text{g}/\text{mL}$) which were included in each microplate row. An average value for all guaiacol standards was determined and each plate average was compared to this to determine an adjustment factor to the original slope value, so that comparisons between samples were possible.

Folin-Ciocalteu reagent (2N) was added as 50 μL to each well, followed by incubation for eight minutes. This was followed by addition of 0.4 N Na_2CO_3 as 150 μL . Blanks containing the same mixture of 1:1 acetone:water mix, FC reagent and Na_2CO_3 , without lignin, were placed in the last microplate column. At this point the samples were allowed to incubate for two hours, while rotating on a Labnet (Big Flats, NY, USA) Orbit P4 shaker, set to 40 rpm.

Evaluation of absorbance at 765 nm wavelength was accomplished by a Varian Cary 50Bio UV/Vis Spectrophotometer connected to a Varian Cary 50MPR Microplate reader.

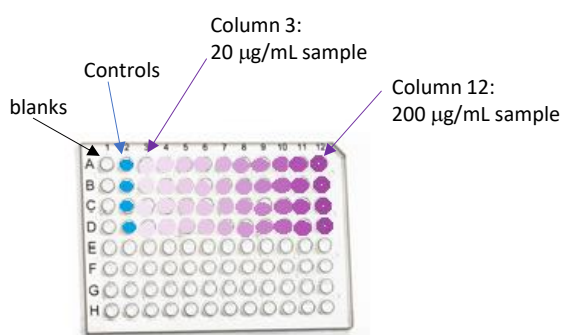


Figure 27: Microplate setup for oxidation of lignin by Folin reagent. Purple represents lignin as 200 $\mu\text{g}/\text{mL}$ sample in column 12 halved down to column 3 with acetonitrile:water (1:1) solution; blue is control as guaiacol (about 70 $\mu\text{g}/\text{mL}$) and blanks are acetone:water (1:1). Final solutions will contain Folin reagent (50 μL in each well) and Na_2CO_3 (150 μL of 0.4 M solution) in each well, as well.

Lignin model compounds and lignin-solvent samples were all diluted by their respective initial solvents to a concentration of 200 µg/mL prior to analysis by FC assay. However, lignin-solvent samples which were evaluated on a same-volume basis were diluted with a different approach. Initial concentrations of the samples differed considerably in their own solvent systems, so that the highest concentration was diluted to 200 µg/mL, which required that 0.01 mL be diluted to 5.65 mL. Thereafter, all other lignin-solvent samples were diluted in the same manner. Initial concentrations are shown in Table 28.

Table 28 Solubilization levels and initial concentrations of lignin solutions in various solvent systems and the final concentration for analysis after dilution for comparison by the same volume.

Solvent mix	wt.% C of	-	avg. orig.	avg.	avg.	Orig.	withdra	5.65
-	Initial	s.d.	lignin (g)	lignin	solvent	conc.	w	mL. (Dilute to
	Lignin C			in soln	(mL)	(mg/mL)	0.01	this)
				(g)			(mg)	final. Conc.
								(ug/mL)
75% acetone: water	80.21	9.72	2.9883	2.397	25.71	93.23	0.932	165
50% acetone: water	74.19	13	2.9897	2.218	28.22	78.6	0.786	139
50% acetonitrile: water	72.16	7.95	2.9879	2.156	27.81	77.53	0.775	137
100% acetonitrile: water	3.4	0	3	0.102	20.41	5	0.05	9
50% tetrahydrofuran	108.41	4.14	2.9915	3.243	28.67	113.11	1.131	200
100% tetrahydrofuran	12.73	7.8	3.0009	0.382	18.84	20.28	0.203	36
50% mTHF: 50% MeOH	12.74	7.8	2.9895	0.381	23.08	16.51	0.165	29
50% THF: 50% MeOH	66.74	4.2	2.995	1.999	18.92	105.66	1.057	187
50% isoprop: 50% ace	31.83	4.2	3.0382	0.967	24.3	39.79	0.398	70
100% methyl acetate	7.41	0.33	2.9966	0.222	23.74	9.35	0.094	17

II.2.2. Results of Folin Analysis of Lignin Model Compounds and Lignin-Solvent Samples

The general method of lignin model compound comparison was by determination of a slope for each compound from a diluted sequence of the compound in a microplate, starting with

200 $\mu\text{g}/\text{mL}$ and reducing by half until a value of approximately 20 $\mu\text{g}/\text{mL}$ was reached. An average slope for absorbance was determined for all repeated rows of the same sample, after subtraction of blanks. The 2nd to 7th well absorbances constituted the five points of each slope. The slope for gallic acid clearly showed a higher value than guaiacol (with three hydroxyl groups compared to one group), but not three times the slope for guaiacol (Figure 28).

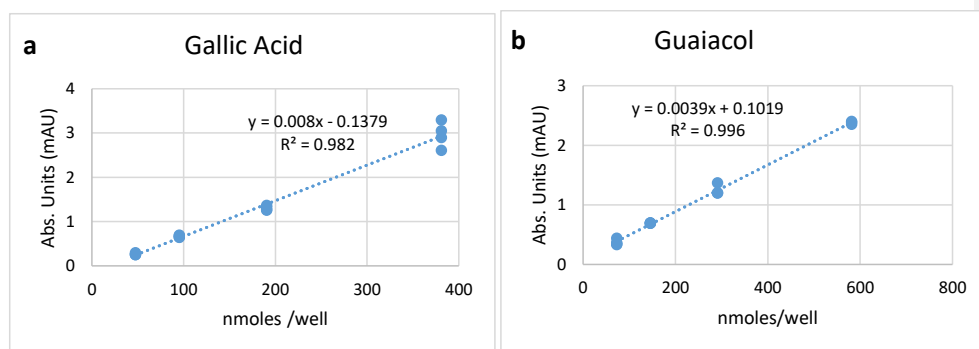
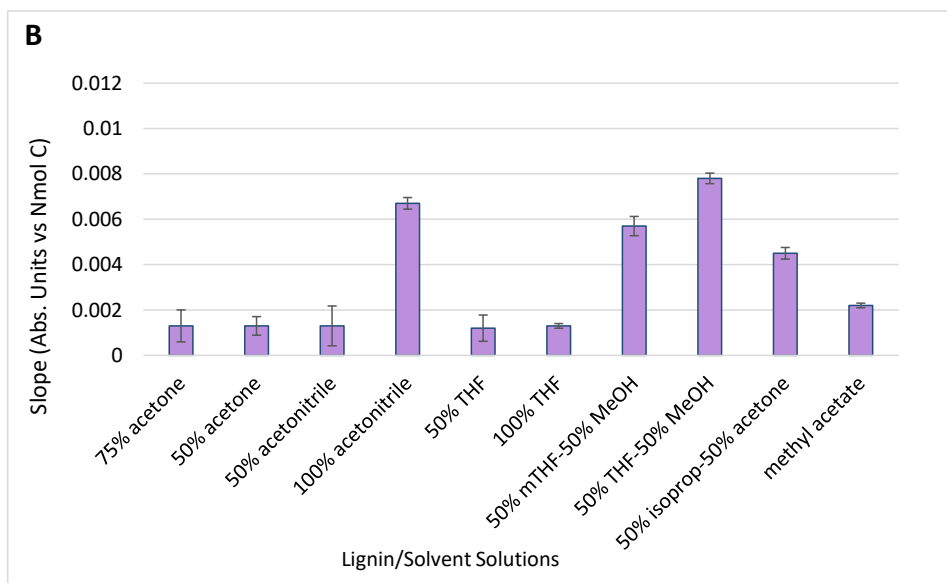
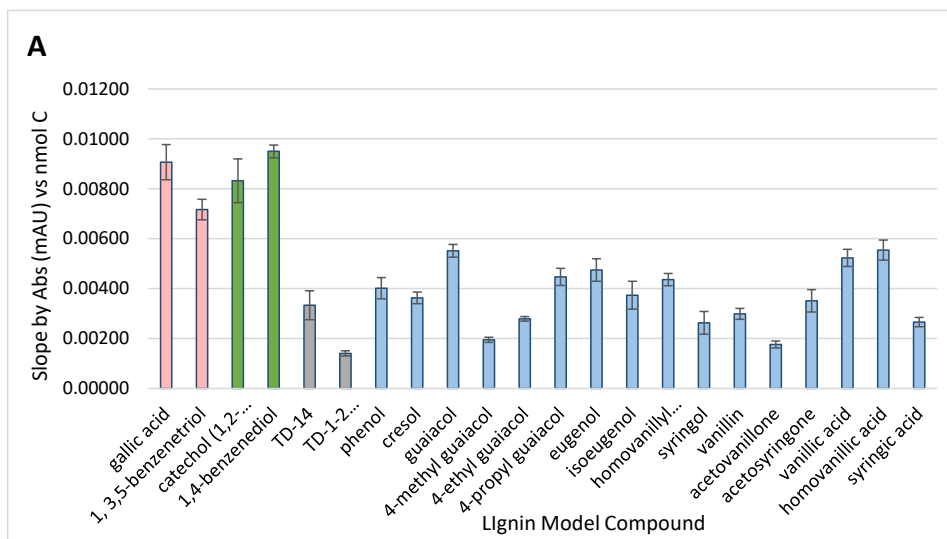


Figure 28. (a) Microplate results for gallic acid reacted with 50 μL FC and 0.4 M Na_2CO_3 after two hours of incubation, (b) results for the same protocol with guaiacol.

Slopes of lignin model compounds as milli-absorbance units (mAU) vs nmol carbon per well are shown in Fig. 29a, while those of lignin/solvent solutions (same mass) are in Figure 29b, with lignin/solvent solutions (same volume) are in Figure 29c.



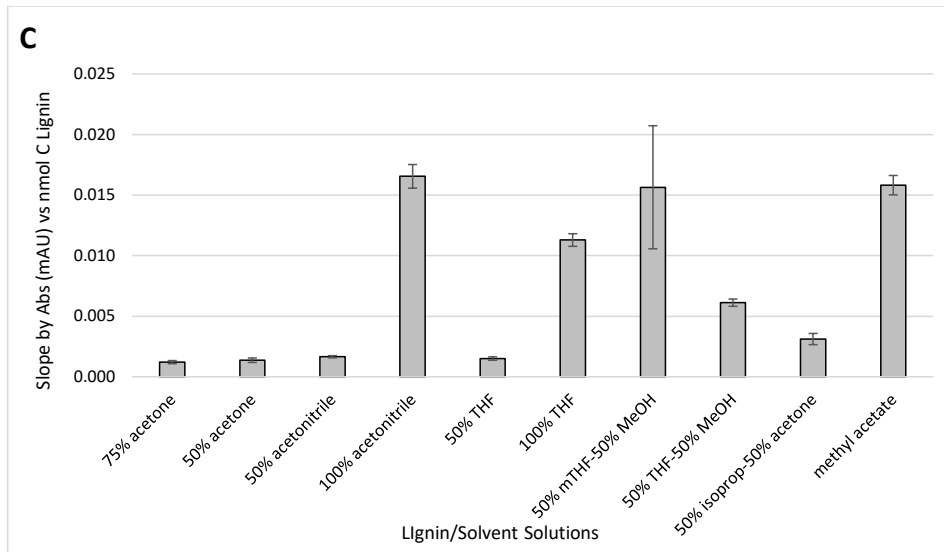


Figure 29: (a) Slopes for lignin model compounds (as absorbance vs nmol carbon per well in a range of 14 – 770 nmol carbon based on FC assay with an initial 200 $\mu\text{g/mL}$ diluted through 10; (b) slopes for lignin/solvent samples (in a range of 6 – 427 nmol carbon) also at an initial concentration of 200 $\mu\text{g/mL}$ in microplate wells; (c) slopes for the same lignin/solvent samples (in a range of 2 – 427 nmol carbon) but on an equal volume basis.

It is apparent by comparing lignin model compounds that each species has an individual response to the assay, although there is a definite distinction between polyhydroxyl compounds such as gallic acid, benzenetriol and catechol (with slopes at about 0.0080) and the monohydroxyl compounds such as alkyl-guaiacols, eugenol and cresol (with slopes centered around 0.0040). Guaiacol and homovanillic acid had the highest slopes at about 0.006. This study also found that gallic acid, despite having three hydroxyl groups, did not have a slope much different than that of catechol (with two hydroxyl groups). The dimers, TD-1,4 and dehydrovanillin, per benzene ring, had the same number of hydroxyl groups, on average, as the monohydroxyl compounds. The protocol in this study was able to effectively discriminate

between polyhydroxylated benzene rings and monohydroxylated rings, and standard deviations were modest. However, discrimination between tri-hydroxyl and di-hydroxyl groups was not possible, and it was apparent that substituents in the model compounds had an effect on the slope values when other parameters were held constant. Stratil et al. found that gallic acid had an FC reaction similar to that of a dihydroxyl compound and also found that monohydroxyls varied in reaction to FC reagent, ostensibly due to differing structures and substituents.¹⁰¹

The lignin model compounds served as a calibration set for determining hydroxyl content in the lignin/solvent samples. It was immediately apparent that solvent systems which had a high solubility level for alkali lignin (50% THF, 50% acetone, 50% acetonitrile, 75% acetone) had low slopes, indicating low hydroxyl content on benzene rings, ostensibly due to H-bonding with solvents or possibly some other type of bond which prevented an oxidation reaction from occurring. Conversely, the lower solubilities in some solvent systems, which included 100% acetonitrile, 100% THF, mTHF:MeOH (1:1), THF:MeOH (1:1), acetone:2-propanol (1:1), and 100% methyl acetate, allowed more unreacted hydroxyl groups to be oxidized by the FC reaction.

As such, the same-mass evaluation of the lignin-solvent samples did not accurately portray the solubility differences between the samples. However, the lignin/solvent samples arranged on an equal volume basis showed accurate estimations- high slope values for solvents with low solubility and lower values for those with high solubility. Because absorbance per nmol carbon was the basis of evaluation, it appeared that slopes mirrored solubility more accurately when solubility was represented as wt% carbon than as $\mu\text{g/mL}$ concentration.

Exceptions were THF:MeOH and acetone:2-propanol samples, which did not reflect the respective solubilities of 66.74 and 31.84 wt.% of original carbon. Thus dilution based on wt% C differences may have been more appropriate.

Of interest, the solvent samples with easily solubilized lignin, as in 50% and 75% acetone:water, 50% acetonitrile:water and 50% THF:water showed a reaction to FC similar to 4-methyl guaiacol or acetovanillone, which were both monohydroxyl (phenolic) compounds and which also showed low reactivity in general compared to other monohydroxyls. Somewhat soluble lignin (50% THF:MeOH and 50% isopropyl:acetone samples) showed more reactivity to FC reagent, while practically insoluble lignin (in 100% acetonitrile, 100% THF, 50% mTHF:MeOH and methyl acetate) showed a high level of reactivity either somewhat above the level of di- and tri-hydroxyls (gallic acid, etc.) or up to one and a half times as much.

The idea that the slopes for lignin-solvent samples with low lignin solubility would show values above those of di- and tri-hydroxy lignin model compounds was not unexpected, as the latter samples had been dissolved in acetone:water (1:1). This allowed solubility of the model compounds but also rendered some phenolic hydroxyls on the compounds unavailable for oxidation because of expected hydrogen bonding to the aqueous portion of the solvent mixture.

II.2.3. Optimization of Method using Design of Experiment

II.2.3.1. Statistical method

Data was taken from FC phenol reaction plates by compiling absorbance readings for the 100 µg/mL microplate wells in each guaiacol diluent series which featured either one or two hours of incubation time, 8% or 16% total ACN content per well, 50 µL or 100 µL FC reagent

and 0.2M or 0.4M Na₂CO₃ concentration per well, and all possible combinations of these factors. Four replicates were done for each series.

Although runs were randomized, the entry of data into Minitab software (Minitab LLC, PA State College, PA, USA) was entered in standard order and processed as a 2⁴ full factorial (full resolution) with four replicates, via factorial ANOVA (ANalysis Of VAriance) statistical test. Assumptions of the test are that the variable should be normally distributed, continuous and have a similar spread across groups, as well as at least five data points per group.

Tools of analysis included the analysis of variance, residuals plots, contour plots and main effects/interactions plots. The corresponding fractional 2⁴⁻¹ factorial for four replicates was also evaluated; this entailed manual entry of data into 32 design-designated slots.

A similar procedure was accomplished with one replicate selected randomly from all the data sets considered previously. This set of models entailed manual entry of only 16 runs for full 2⁴ factorial consideration, and eight runs for the ½ fractional model.

II.2.3.2. Results of statistical method

The FC phenol reagent study was evaluated as a 2-level, 4-factor (2⁴), 4-replicate factorial by Minitab software initially as a full resolution model. Results of design and analysis are shown in Figure 30. Factors, with levels:

- 1) Incubation time (1 or 2 hours).
- 2) Na₂CO₃ concentration (0.2 or 0.4 M M).
- 3) FC reagent amount (50 or 100 µL).
- 4) Acetonitrile delivery (as acetonitrile:water (1:1) initially or added with other reagents).

Full Factorial Design			
Design Summary			
Factors:	4	Base Design:	4, 16
Runs:	64	Replicates:	4
Blocks:	1	Center pts (total):	0
All terms are free from aliasing.			

Factorial Regression: absorb. versus time, Na2CO3 conc., .

Analysis of Variance					
Source	DF	Adj SS	Adj MS	F-Value	P-Value
Model	15	11.2609	0.75073	100.16	0.000
Linear	4	10.0173	2.50432	334.10	0.000
time	1	0.2780	0.27801	37.09	0.000
Na2CO3 conc.	1	0.1289	0.12895	17.20	0.000
FC amt.	1	0.0399	0.03990	5.32	0.025
ACN %	1	9.5704	9.57042	1276.80	0.000
2-Way Interactions	6	1.1538	0.19231	25.66	0.000
time*Na2CO3 conc.	1	0.0026	0.00262	0.35	0.557
time*FC amt.	1	0.0040	0.00399	0.53	0.469
time*ACN %	1	0.0998	0.09984	13.32	0.001
Na2CO3 conc.*FC amt.	1	0.0405	0.04049	5.40	0.024
Na2CO3 conc.*ACN %	1	0.1395	0.13948	18.61	0.000
FC amt.*ACN %	1	0.8674	0.86741	115.72	0.000

Figure 30. Minitab design summary and analysis of variance for 2⁴ full factorial evaluation of FC phenol reactions, with four replicates (alpha = 0.05).

The gold standard for evaluation of main effects and interactions was the full factorial, 2⁴, 64-run model, and results were intended to be compared to a 2⁴⁻¹ fractional model as well as one-replicate full factorial and 2⁴⁻¹ fractional models. Alpha values for all models was 0.05. The main effects showed that all four factors were significant with p values < 0.001, while no interactions were significant, but there was a problem in that the relationships “time*ACN%,” “Na₂CO₃* ACN%,” FC*ACN%,” showed increased absorbance for lower levels of ACN. Also, to a lesser extent, “Na₂CO₃*FC” had some interaction. A normal plot showed these results in Figure 31, while main effects and interaction plots are illustrated in Figure 32.



Figure 31. The normal plot of the standardized effects for 2⁴ full factorial evaluation of FC phenol reactions, with four replicates (alpha = 0.05).

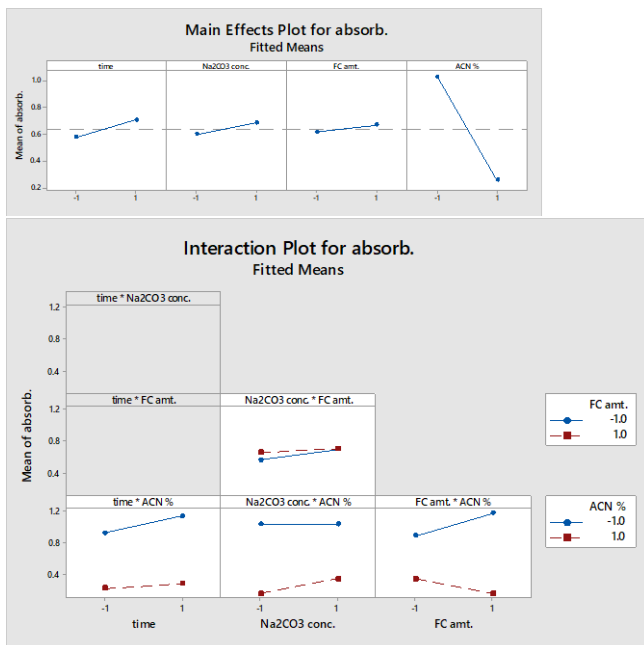


Figure 32. Main effects and interaction plots for 2⁴ full factorial evaluation of FC phenol reactions, with four replicates (alpha = 0.05).

Interestingly, the lower percentage of acetonitrile was more effective in producing a higher absorbance, probably due to dissolution problems with the analyte. This phenomenon was reflected in interaction plots with the other three factors, although the factors (time, Na_2CO_3 concentration and FC amount) are not thought to be responsible for the effect through interaction. The only other minor interaction was Na_2CO_3 with the FC reactant. When FC concentration was increased for increased concentrations of Na_2CO_3 , absorbance of the solution changed very little, possibly suggesting a slight inhibition of FC effect by the salt.

A refined model of the full factorial (with non-significant interactions removed) yielded a normal residual plot which was linear, and a residual vs. fits plot which showed fairly good variance of samples, except for lower-end fitted values (Figure 33). Transformation of data did not seem to be indicated.

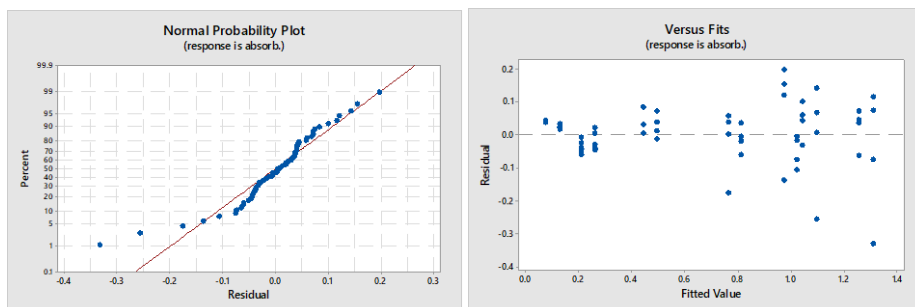


Figure 33 Normal probability plot and residuals vs. fits plot for 2^4 full factorial evaluation of FC phenol reactions, with four replicates ($\alpha = 0.05$).

A $1/2$ -fractional factorial (32 runs), with four replicates, was carried out with the same data and showed some difference in results from the full factorial model. The resolution for this model

was IV, which resulted in aliasing of 2-factor interactions with each other; AB + CD, AC + BD, AD + BC. Design and analysis of variance are shown in Figure 34.

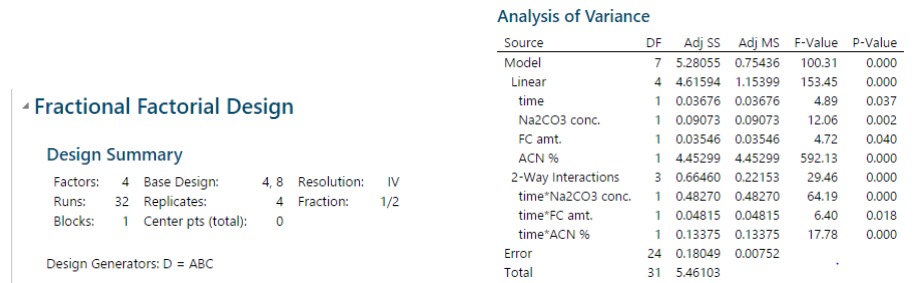


Figure 34. Design and analysis of variance for 2^{4-1} fractional factorial evaluation of FC phenol reactions, with four replicates (alpha = 0.05).

The 2^4 fractional factorial evaluation of FC phenol reactions with four replicates showed interactions of time with all other factors to be significant, but this was not surprising considering that all of these two-factor interactions had aliases (Figure 35). Information about interaction significance was not reliable; a foldover would be required, and might require as many runs as needed to make a full factorial.

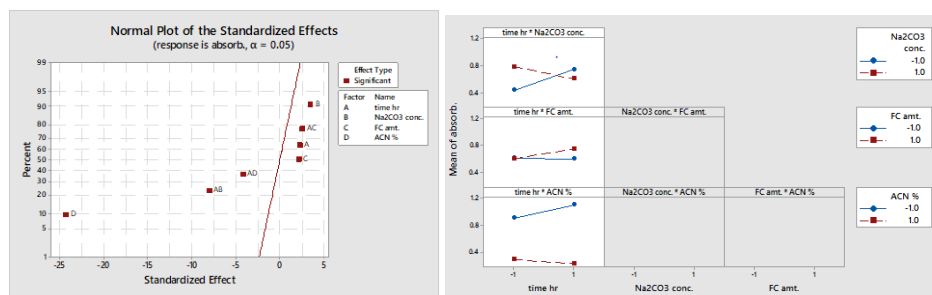


Figure 35. The normal plot of the standardized effects for 2^4 full factorial evaluation of FC phenol reactions, with one replicate and the factorial interaction plot (alpha = 0.05).

Resolution IV showed only the significance of the main effects, which agreed somewhat with full factorial results, although the factor of time was exaggerated in significance (Figure 36).

Summary of 2^4 Models p-Values (for $\alpha = 0.05$)

	4 rep: Full fact.	Refined full fact.	2^{4-1} fract. Fact.
A. Time	<0.001	<0.001	<0.037
B. Na ₂ CO ₃	<0.001	<0.001	<0.002
C. FC	0.025	<0.033	<0.040
D. ACN	<0.001	<0.001	<0.001
A*D	<0.001	<0.001	<0.001
B*C	<0.024	<0.031	(AB, AC)
C*D	<0.001	<0.001	

Figure 36. Comparison of p-values for full (2^4) and fractional (2^{4-1}) factorial model evaluation of FC phenol reactions, with four replicates and alpha = 0.05.

The normal probability plot for the fractional model showed less linearity than that of the full factorial model, and the residuals vs. fits plot was similar to the full factorial plot (Figure 37).

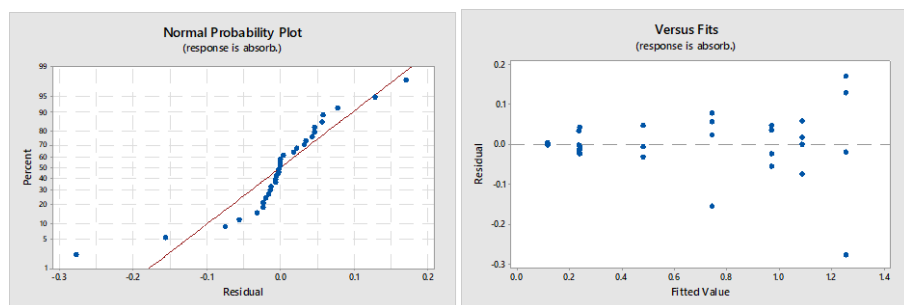


Figure 37. Normal probability plot and residuals vs. fits plot for 2^{4-1} fractional factorial evaluation of FC phenol reactions, with four replicates ($\alpha = 0.05$).

Evaluation of a four-replicate model was cumbersome as it required 64 or 32 runs respectively for full or fractional factorial models. One-replicate models were also evaluated for comparison, at full and $\frac{1}{2}$ -fraction (full and IV resolution); these required only 16 and 8 runs respectively. The factorial design and analysis of variance are shown in Figure 38 for the one-replicate model.

Full Factorial Design					
Design Summary					
Factors:	4	Base Design:	4, 16		
Runs:	16	Replicates:	1		
Blocks:	1	Center pts (total):	0		
All terms are free from aliasing.					
Analysis of Variance					
Source	DF	Adj SS	Adj MS	F-Value	P-Value
Model	10	2.66927	0.26693	146.45	0.000
Linear	4	2.28349	0.57087	313.21	0.000
time hr	1	0.05061	0.05061	27.77	0.003
Na2CO3 conc.	1	0.06781	0.06781	37.20	0.002
FC amt.	1	0.04806	0.04806	26.37	0.004
ACN %	1	2.11701	2.11701	1161.49	0.000
2-Way Interactions	6	0.38578	0.06430	35.28	0.001
time hr*Na2CO3 conc.	1	0.00007	0.00007	0.04	0.850
time hr*FC amt.	1	0.00002	0.00002	0.01	0.926
time hr*ACN %	1	0.01675	0.01675	9.19	0.029
Na2CO3 conc.*FC amt.	1	0.03114	0.03114	17.08	0.009
Na2CO3 conc.*ACN %	1	0.01042	0.01042	5.71	0.062
FC amt.*ACN %	1	0.32739	0.32739	179.62	0.000
Error	5	0.00911	0.00182		
Total	15	2.67838			

Figure 38. Minitab design summary and analysis of variance for 2^4 full factorial evaluation of FC phenol reactions, with one replicate ($\alpha = 0.05$).

The normal plot of the standardized effects and interaction plots showed the same significant factors and interactions as the four-replicate model (Figure 39).

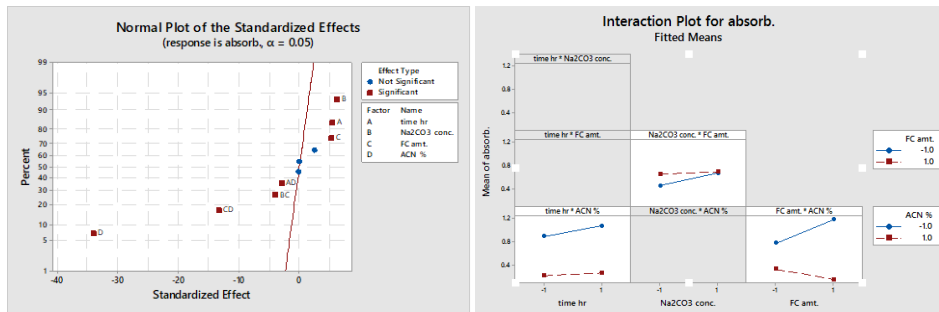


Figure 39. The normal plot of the standardized effects for 2^4 full factorial evaluation of FC phenol reactions, with one replicate and the factorial interaction plot ($\alpha = 0.05$).

For the refined model, normal probability plot and residuals plot vs. fits were similar to the four-replicate model (Figure 40).

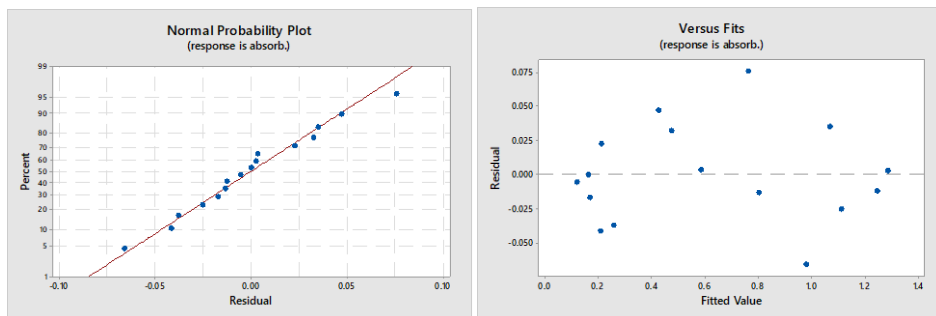


Figure 40. Normal probability plot and residuals vs. fits plot for 2^4 full factorial evaluation of FC phenol reactions, with one replicate ($\alpha = 0.05$). The residuals vs. fits plot showed better variance than the four-replicate model.

A $1/2$ -fractional factorial (8 runs), with one replicate, was also carried out; the resolution for this model was also IV, resulting in 2-factor interactions aliased with each other; $AB + CD$, $AC + BD$, $AD + BC$. F and p values were not initially forthcoming- the $AC+BD$ interaction was removed from the available terms to allow for error calculation. The results were somewhat less

reliable than the fractional version (2^{4-1}) for the four-replicate model. Design and analysis of variance are shown in Figure 41, while normal plot of the standardized effects and interaction plots are shown in Figure 42.

Fractional Factorial Design

Design Summary

Factors: 4 Base Design: 4, 8 Resolution: IV
 Runs: 8 Replicates: 1 Fraction: 1/2
 Blocks: 1 Center pts (total): 0

Design Generators: D = ABC

Analysis of Variance

Source	DF	Adj SS	Adj MS	F-Value	P-Value
Model	6	1.26317	0.210529	43.93	0.115
Linear	4	1.04782	0.261954	54.66	0.101
time hr	1	0.01416	0.014157	2.95	0.335
Na ₂ CO ₃ conc.	1	0.03799	0.037987	7.93	0.217
FC amt.	1	0.02774	0.027738	5.79	0.251
ACN %	1	0.96793	0.967934	201.96	0.045
2-Way Interactions	2	0.21536	0.107678	22.47	0.148
time hr*Na ₂ CO ₃ conc.	1	0.16858	0.168580	35.17	0.106
time hr*ACN %	1	0.04678	0.046777	9.76	0.197
Error	1	0.00479	0.004793		
Total	7	1.26797			

Figure 41. Design and analysis of variance for 2^{4-1} fractional factorial evaluation of FC phenol reactions, with one replicate (alpha = 0.05).

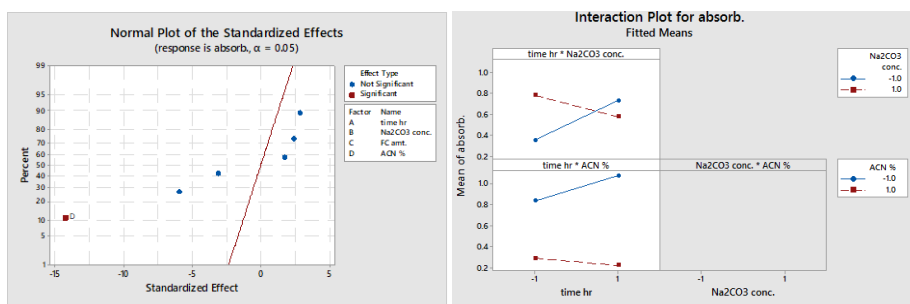


Figure 42. Normal plot of the standardized effects and interaction plots for 2^{4-1} fractional factorial evaluation of FC phenol reactions, with one replicate (alpha = 0.05).

The main effects plots and analysis of variance showed only factor “D” or ACN% to be significant, while interaction significance could not be estimated due to aliasing. A normal probability plot and residuals vs. fits plot for the 2^{4-1} fractional factorial model with one replicate showed linearity and good variance, but points were sparse (Figure 43).

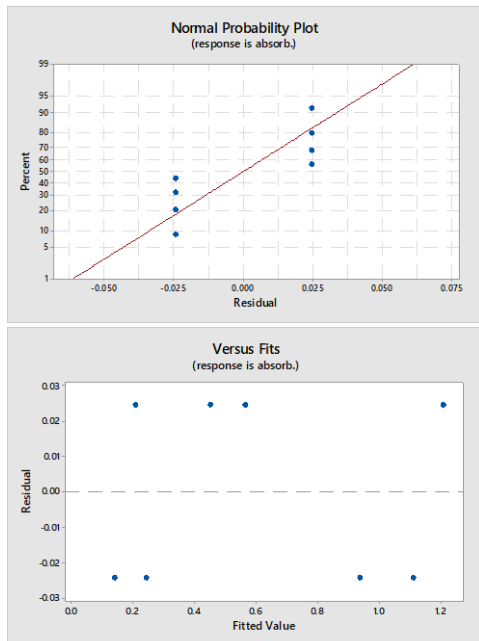


Figure 43. Normal probability plot and residuals vs. fits plot for 2^{4-1} fractional factorial evaluation of FC phenol reactions, with one replicate ($\alpha = 0.05$).

II.2.3.3. Conclusions of a statistical approach

Figure 44 shows a comparison of p-values across the board for full and fractional models of both the four-replicate and one-replicate versions of the study.

Summary of 2^4 Models p-Values (for $\alpha = 0.05$)

	4 rep: Full fact.	Refined full fact.	2^{4-1} fract. Fact.	1 rep: Full fact.	Refined full fact.	2^{4-1} fract. Fact.
A. Time	<0.001	<0.001	<0.037	<0.003	<0.002	<0.335
B. Na ₂ CO ₃	<0.001	<0.001	<0.002	<0.002	<0.001	<0.217
C. FC	0.025	<0.033	<0.040	<0.004	<0.002	<0.257
D. ACN	<0.001	<0.001	<0.001	<0.001	<0.001	<0.045
A*D	<0.001	<0.001	<0.001	<0.029	<0.031	<0.197
B*C	<0.024	<0.031	(AB, AC)	<0.009	<0.007	(AB)
C*D	<0.001	<0.001		<0.001	<0.001	

Figure 44. Comparisons of p-values for all factorial models of the FC phenol study.

Results for significant main effects and interactions agreed fairly well for the full and refined versions of both the four-replicate and one-replicate models, leading to the conclusion that one replicate would be sufficient for this study- bringing total runs from 64 to 16, which would save on time and resources. The one-replicate full factorial actually gave better information than the fractional factorial for four-replicates, and in fewer runs (16 vs 32).

Of interest is the fact that the four-replicate fractional model (2^{4-1}) did adhere to the findings of the full factorial model when it came to main effects of the factors. However, fractional studies in either case (four-replicate or one-replicate) did not give enough information about two-factor interactions, which would be important in this case as it became apparent that the supposed interaction of ACN% with all other factors was actually due to a dissolution issue. The fractional factorial for the one-replicate study was actually not even accurate for predicting significance of the factors, having found only one of them significant (ACN%).

In terms of the study factors themselves, it was clear from the results that time of incubation, Na_2CO_3 concentration, FC amount and ACN% had significant effects on results. It was readily apparent that two hours of time was superior in terms of increasing absorbance in samples, as was the higher concentration of Na_2CO_3 .

One of the important points of the study was to determine if Na_2CO_3 concentration would interact negatively with time (producing less absorbance for a longer time), but this interaction was not seen. The implication was that 0.4M Na_2CO_3 was not depositing material at the bottom of the microplate wells within the two-hour incubation time.

The amount of FC added to each plate was less significant than the other factors ($p= 0.025$), although the one-replicate study overemphasized its significance ($p= 0.004$). This was a case where it was apparent that 100 μL of FC would produce greater absorbance, but the addition of 50 μL was far more economical.

ACN% was seen as significant, not only as a main effect, but also in terms of interaction with other factors. The lower level of ACN% (8% total in solution) was more effective in producing greater absorbance, and this was thought to be due to better dissolution of the analyte initially, while an elevated final amount (16%) was initially ineffective at dissolution. The fact that several interactions with ACN% were found to be significant also pointed toward an across-the-board explanation rather than multiple negative interactions, although it could be said that addition of Na_2CO_3 and FC did have a negative effect on the higher level of ACN% by not producing the dissolution level expected.

A series of contour maps reflects these findings for the four-replicate full factorial model (Figure 45) and for the one-replicate full factorial model (Figure 46). The plots are quite similar,

and both show complexity in the ACN% interactions and the better performance of the lower value.

Optimal values for the four factors in the study were:

- 1) Two hours of incubation time is optimal for the experiment since three hours produced a wider variance of results and saturation effects for some compounds, while one hour was not enough to develop sufficient absorbance for compounds which did not react well.
- 2) Na_2CO_3 concentration at 0.4M, since this concentration produced better absorbance, and, crucially, did not show signs of deposition.
- 3) FC amount at 50 μL , although 100 μL was somewhat better for absorbance levels. The difference was not enough to overcome the cost factor.
- 4) ACN% was kept at 8% total in solution, since this meant an initial 1:1 acetonitrile:water solution for total dissolution of the compound. The introduction of total acetonitrile to the analyte compound apparently did not work towards dissolution of the compound initially or later, since absorbance did not increase with addition of water in FC and Na_2CO_3 solutions during the process,

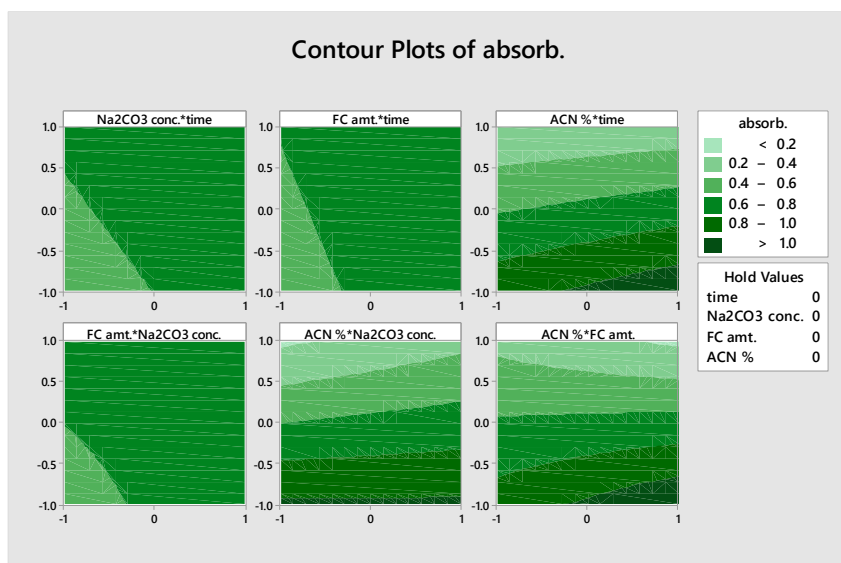


Figure 45. Individual contour plots for the four-replicate full factorial model with four factors, each paired with each other without hold values for factors outside the pair.

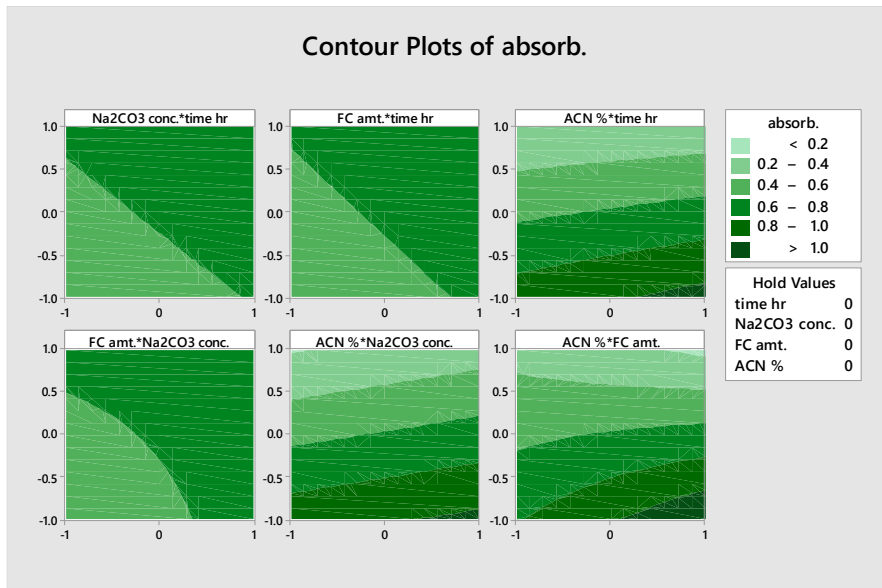


Figure 46. Individual contour plots for the one-replicate full factorial model with four factors, each paired with each other without hold values for factors outside the pair.

CHAPTER III. Processing of Technical Lignins

III.1. Fractionation of Alkali Lignin

III.1.1. Experimental

III.1.1.1. Materials and methods

Alkali lignin was purchased from Sigma-Aldrich (St. Louis, MO, USA). The alkali lignin was determined to have an elemental make up of C (64.14%), H (5.79%), S (1.39%) and N (0.46%) by Atlantic Microlab, Inc. (Norcross, GA, USA). HPLC grade unstabilized tetrahydrofuran (THF) containing no preservatives was obtained from Fisher Scientific (Fair Lawn, NJ, USA). Deionized water was obtained using a Direct-Q® 3 system, Millipore, Billerica, MA, USA.

For preparative SEC, alkali lignin was completely dissolved in a 1:1 (v/v) THF:water mixture at a concentration of 50 mg/mL and further diluted with THF to form a lignin solution with a final concentration of 10 mg/mL containing 10% of water. When the water content was decreased to 1%, no precipitation was observed.

For column calibration, two sets of narrow-range polymeric standards were used, i.e., a polystyrene (PS) standard set with MW peak maxima (M_p) of 580–19,760 Da purchased from Varian (Amherst, MA), and PMMA standards (M_p 550 – 56600 Da) from Agilent Technologies (Santa Clara, CA, USA). Pinoresinol ($\geq 95\%$ purity, Sigma Aldrich) was used as a lignin structure model compound to verify the calibration.⁸¹

For ³¹P-NMR analysis, a set of lignin model compounds, including phenol, guaiacol, methyl guaiacol, ethyl guaiacol, propyl guaiacol, vanillin, acetovanillin, syringaldehyde, vanillic acid, homovanillic acid, biceosol (all $\geq 95\%$ purity, Sigma Aldrich) were analyzed with respect to chemical shift, for identification and quantitation, while pyridine ($\geq 99.8\%$), cyclohexanol ($\geq 99\%$), 2-chloro-4,4,5,5-tetramethyldioxaphospholane (TMDP) ($\geq 95\%$), deuteriochloroform (\geq

99.8%), chromium acetylacetonate ($\geq 97\%$) (all from Sigma Aldrich) were used for sample preparation.

III.1.1.2. Lignin fractionation via preparative SEC

To confirm SEC separation is primarily controlled by size exclusion, calibration was performed with a set of standards differing in functional groups (PS, PMMA standards and pinoresinol), as was performed in a previous work.⁸¹

Preparative SEC fractionation was performed on an Agilent 1100 Series HPLC system utilizing a preparative PLgel column (300 × 25 mm, with 10 μm particle size and a 1,000 Å pore size). The system was equipped with a diode array detector (DAD). For this work, the analytical flow cell was replaced by a preparative flow cell (Agilent Technologies). Unstabilized THF was used as a mobile phase at a flow rate of 5.0 mL/min; it was essential to use unstabilized THF to obtain pure lignin fractions without butylated hydroxytoluene or other additives used for THF stabilization. An extended loop capillary was installed into the injection loop to perform a 500 μL injection of a 10 mg/mL lignin solution.

Several fractionations were performed slightly varying collection time windows yet providing comparable results (the SEC data from fractionations 1 and 2 are shown in supplementary information) while optimizing the protocol.

In the final fractionation protocol, the pre-eluate was collected first, during retention times where no increase in the DAD signal was observed. Then MW fractions 1 – 5 were obtained in the following elution time windows: 14–16, 16–18, 18–20, 20–22, and 22–24 min. The fraction collection was performed manually. The procedure was repeated 10 times resulting in a final volume of 100 mL for each of the six collected fractions. Each fraction was concentrated by

evaporation under a stream of nitrogen to a final volume of 2 mL. As a control, a 100 mL aliquot of THF was also dried to a final volume of 2 mL.

III.1.1.3. Analysis of lignin MW fractions

III.1.1.3.1. Analytical SEC of lignin MW fractions

The obtained SEC fractions, a blank sample (concentrated THF), an aliquot of pure THF and an intact lignin solution (50,000 ppm w/v) were analyzed by HP SEC on an Agilent 1100 Series HPLC system equipped with a DAD with an analytical high pressure flow cell, utilizing a PLgel analytical column (300 × 7.5 mm, with a 5 μm particle and a 1,000 Å pore sizes, 500–60,000 Da separation range) equipped with a PLgel guard column (50 × 7.5 mm). The SEC column was lined with a polystyrene divinylbenzene stationary phase, and was calibrated with PS standards. Unstabilized THF was used as a mobile phase at a flow rate of 1.0 mL/min. The injection volume for all samples was set to 20 μL. The evaporative light-scattering detector (ELSD) nebulization and evaporation temperatures were set to 40 °C, with nitrogen as a nebulizing gas set at a flow rate of 1.6 L/min.

SEC determination of MW as M_n (number-average MW) and M_w (mass-average MW) values were based on standard SEC equations.⁷⁵

III.1.1.3.2. Thermal carbon analysis of the fractions

A thermal optical analyzer from Sunset Laboratory Inc. (Portland, OR, USA) was employed to obtain quantitative thermal carbon evolution profiles enabling a comprehensive carbon fractionation and characterization.^{194,203} For TCA analysis, a sample (20 μL) was introduced on a Pall Flex 2500QAT-UP tissue quartz filter (Pall Corp, East Hills, NY, USA), dried on a hot plate

at 40 °C for 4 min and placed into an oven. The sample was desorbed/pyrolyzed at selected temperature steps for specific time durations. A detailed description of the applied TCA protocol can be found elsewhere.^{194,203} Briefly, thermal desorption temperatures were 30, 200 and 300 °C, while pyrolysis took place at 400, 500 and 890 °C in helium atmosphere. This sequence was followed by oven cooling to 550 °C and introduction of an oxidizing carrier gas mixture of He with 10% of O₂ and heating to 890 °C in order to evolve the coked carbon fraction. All the evolved species were converted to CO₂ and then to methane, thus allowing for quantification with a flame ionization detector.

III.1.1.3.3. ESI HRMS (Electrospray High Resolution Mass Spectrometry) analysis

For high resolution mass spectrometry of the mass distribution of different lignin fractions, an Agilent HR TOF-MS system G1969A with a mass resolution of >13,000 (at m/z 2,722) and mass accuracy <2 ppm (m/z 609.2807) with ESI was used.²⁰⁴ Samples were introduced via direct infusion with a syringe pump at a flow of 5.0 $\mu\text{L}\cdot\text{min}^{-1}$. The analysis was performed in the positive ion mode with electrospray ionization (i.e., the capillary potential) and collision-induced dissociation (the fragmentor potential) set to 3500 and 150 V, respectively. Nitrogen at a flow rate of 4 $\text{L}\cdot\text{min}^{-1}$ was used as a nebulizing gas. The nebulization temperature and pressure were set to 250 °C and 20 psi, respectively. The TOF-MS system was calibrated with [(CsI)_n+Cs]⁺ clusters formed by an introduction of cesium iodide [30 $\text{mmol}\cdot\text{L}^{-1}$ solution in ACN/water 1:1 (v/v)] via direct infusion at a flow rate of 5 $\mu\text{L}\cdot\text{min}^{-1}$.

Mass Hunter software package B.07.00 was used for data processing. The mass spectra of lignin were deconvoluted using a built-in tool utilizing an unbiased isotope model with a peak spacing tolerance of 0.0025 m/z . The maximal assigned charge state was not limited. Hydrogen

was considered as the charge carrier. The peaks selected for deconvolution were filtered based on their absolute height (≥ 100 counts) and the relative height of the largest peak, which was set to $\geq 0.1\%$ of the largest peak unless otherwise stated. The maximum number of peaks was not specified.

III.1.1.3.4. TD-Py-GC-MS analysis

TD-Py-GC-MS was performed on a CDS Analytical Inc. 5200 pyroprobe (Oxford, PA) connected to an Agilent GC 7890 with 5975C MS. The GC-MS was equipped with a 51 m HP 5MS column (0.25 μm film thickness and 0.25 mm inner diameter). There was no solvent delay and the GC inlet was kept at 300 °C, with the 10:1 split ratio. The quartz tube with quartz wool was cleaned outside of the probe at 1200 °C for 5 seconds. The sample was introduced at 5.0-10.0 μL volume onto the quartz wool filter before the probe was inserted and, once inserted, the probe was heated sequentially through 200, 300, 400, 500, and 890 °C. The probe was held at each temperature for 30 s except for the 890 °C step, which was held for 10 s. The transfer line and valve oven were kept at 300 and 320 °C, respectively, and the pyroprobe assembly was held at 300 °C.

Temperature steps 200, 300, 400, and 890 °C were repeated twice during the runs to ensure that all potential polymers had evaporated for analysis. The resulting GC-MS data showed that the second run for each temperature yielded no residual polymers before the next increased temperature step. Total ion current (TIC) chromatograms of the fractions and blank sample were analyzed for lignin compounds and peaks were labeled when compounds were identified with $\geq 80\%$ NIST library accuracy search results.

III.1.1.3.5. ^{31}P NMR analysis

A Bruker AVANCE 500 NMR spectrometer was used to record ^1H , $^{13}\text{C}\{^1\text{H}\}$, and $^{31}\text{P}\{^1\text{H}\}$ spectra. Samples for ^1H and $^{13}\text{C}\{^1\text{H}\}$ NMR spectra were prepared in CDCl_3 , unless specified otherwise, while samples for $^{31}\text{P}\{^1\text{H}\}$ were obtained using in a mixture of pyridine (py) and CDCl_3 (ratio of 1.6:1). For quantitative $^{31}\text{P}\{^1\text{H}\}$ NMR studies, the pulse width was optimized to give the 90° flip angle at approximately $10\ \mu\text{s}$. The optimized pulse delay was 20 s. The $^{31}\text{P}\{^1\text{H}\}$ NMR spectra of TMDP and its hydrolysis product were obtained at 256 scans, while spectra of phosphitylated lignin, lignin degradation products and other analytes were obtained using 1024 scans.

A general procedure for the phosphitylation reaction was as follows: $400\ \mu\text{L}$ of 1.6:1 (v/v) mixture of pyridine and CDCl_3 were added to a 4.0 mL vial with a magnetic stir bar. Then a compound to be phosphitylated was introduced to the vial. During quantification studies, chromium acetylacetonate (1.0 mg) and cyclohexanol ($10\ \mu\text{L}$, the internal standard for integration) were added to the vial before introducing the phosphitylation reagent. Two molar equivalents of TMDP were added dropwise to the solution. After stirring at room temperature for 5 min, the phosphitylated sample was transferred to an NMR tube. $^{31}\text{P}\{^1\text{H}\}$ NMR spectra were recorded within 1 hour after preparation of the sample. Prior to phosphitylation, samples that were dissolved in water/DCM solvent were dried using a rotary evaporator at 20 torr for 60 seconds to remove solvents from the system since the presence of hydroxyl groups in the solvents was not conducive to the phosphitylation reaction.

The $^{31}\text{P}\{^1\text{H}\}$ NMR signal of phosphitylated cyclohexanol was observed at $\delta 145.2$ ppm. A sample of hydroxylated TMDP, 2-hydroxy-4,4,5,5-tetramethyl-1,3,2-dioxaphospholane, was produced by adding two drops of water to a solution of $250\ \mu\text{L}$ py, $150\ \mu\text{L}$ CDCl_3 , and $15\ \mu\text{L}$

TMDP, which was stirred for 5 min. The $^{31}\text{P}\{^1\text{H}\}$ NMR signal of hydroxylated TMDP was observed at δ 132.2 ppm.

III.1.2. Results and Discussion

As demonstrated in our previous work,⁸¹ the application of a highly cross-linked porous PSDVB stationary phase allowed for lignin separation based primarily on MW. So, in this study, lignin was effectively separated into five main fractions via preparative SEC (Figure 47). As a result, a narrower MW distribution of species within the fractions was achieved.

III.1.2.1. Mass distribution after SEC fractionation

The distribution of lignin among the fractions was assessed using two methods, by UV-Vis absorbance intensity and also by TCA results, which were based on quantification of total carbon. Similar distribution profiles were obtained, as shown in Table 29.

Table 29. Distribution of lignin sample across fractions as measured via TCA and diode array detector (DAD) in preparative SEC.¹

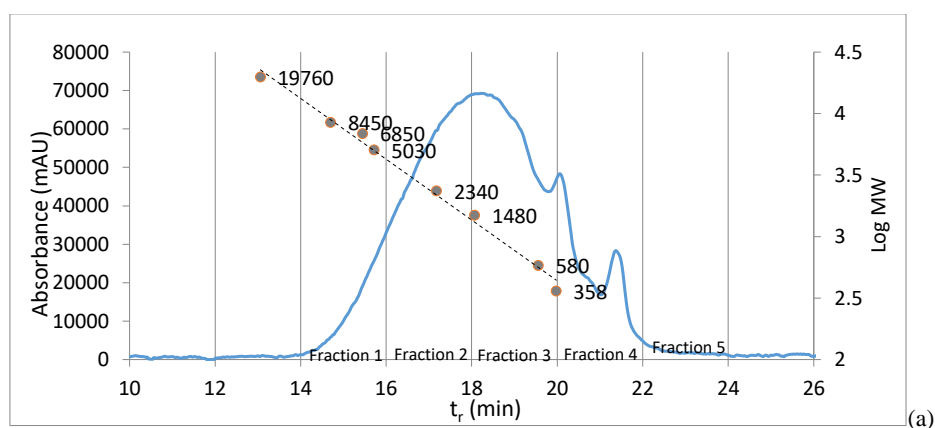
Fraction #	1	2	3	4	5
TCA % distribution of lignin across fractions	3.9	32	43	20	0.47
DAD % distribution of lignin across fractions	5.6	37	43	14	0.30

¹ TCA mass distribution is based on carbon wt.% of the sample, while SEC analysis via DAD of mass distribution is based on absorbance of particles in the UV-Vis range of 212 – 750 nm.

As expected, the determined mean values of molecular weights, represented as M_p , M_n and M_w , were found to differ significantly for each fraction, showing sequentially decreasing molecular weight ranges. For the most part, preparative SEC was represented chromatographically by a smooth bell-shaped curve, with the exception of small spikes of

absorbance near MW 580 and 225 (Figure 47a). Both anomalies may be due to small amounts of contaminants in the solvent.

After the separation, each fraction was subjected to GPC individually in order to ascertain molecular weight distribution within the fraction and also to note overlap between fractions in terms of molecular weight distribution.. The results are shown in Figure 47b. Most of the fractions yielded nearly bell shaped curves, although with some tailing and fronting. These features, respectively, were most pronounced for Fractions 1 and 5.



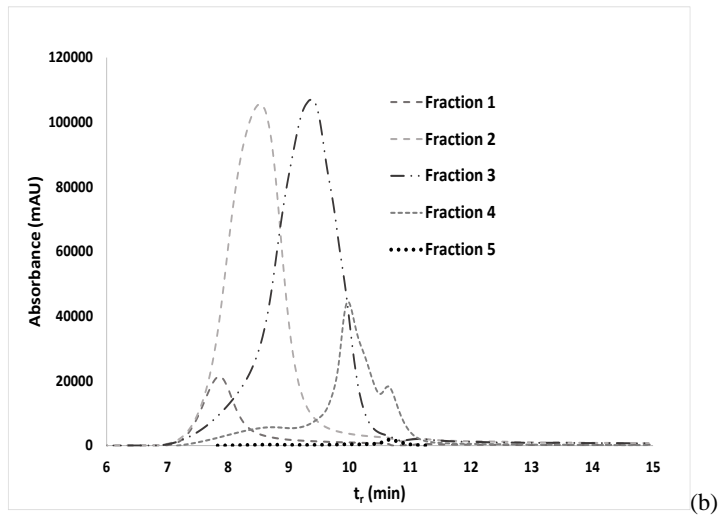


Figure 47. (a) Chromatogram of alkali lignin separation by preparative SEC, at concentration 10,000 ppm in a mobile phase of THF:water (9:1) and total injection volume 500 mL (through an extended loop capillary). Five fraction sections are superimposed for retention times 14-16, 16-18, 18-20, 20-22 and 22-24 min. b) Subsequent analytical-scale SEC of the collected fractions. Detection was conducted using a diode array detector within the 212-750 nm working range.

III.1.2.2. Mass distribution within separate fractions

Table 30 shows actual and expected molecular weights for each fraction.

Table 30. Actual and expected MW range (by calibration curve) MW ranges, and % molecules in each fraction of higher or lower MW than expected for each fraction.

Lignin Fraction	1	2	3	4	5	
Mp (most abundant MW in g/mol)	5294	2396	1964	433	191	
Expected MW range (g/mol)	4300-13300	1400- 4300	440- 1400	140-440	<140	
Actual MW range (g/mol)	180- 14500	160- 14500	160- 14500	60- 10200	90- 5600	
% molecules in expected range	58	69	61	50	5	
% molecules larger than expected	0	16	29	44	95	
% molecules smaller than expected	42	15	10	6	NA	

The expected MW ranges were calculated using the preparatory SEC calibration curve, which was aligned to the retention times of the respective fractions. Then, the actual MW ranges were determined by molecular counts above a baseline, by evaluating the percentages of molecules with specific molecular weights within the chromatographic data. The results are shown in Table 30, where it can be seen that they largely correlate with the SEC curve rise/fall actual ranges, nonetheless being broader than the expected values, thus corroborating the observed peak fronting and tailing.

Overall, the relative amounts of larger than expected particles increased with retention time whereas smaller than expected particles were in abundance at first and then decreased with retention time. These trends may be explained by interactions between the lignin components of different sizes: Apparently, some lower-MW molecules adsorbed on polymers of Fraction 1 while some higher-MW molecules adsorbed on lower-MW particles. This trend was particularly pronounced in Fraction 5, i.e., monomers and dimers. Thus, the interactions of the highest- and lowest-MW species are most significant.

This result was unexpected and different from the data obtained when the MW fractionation was conducted on a smaller, analytical scale. This difference in scales shows one limitation of SEC in application to lignin: If one has to obtain an accurate MW fractionation, multiple runs through the column may be essential. However, Fractions 1 and 5 accounted for only a small portion of lignin, whereas Fractions 2-4 showed neither significant fronting nor tailing.

Thus, Fractions 1-5 were subjected to detailed chemical characterization without their further purification, as described in the subsequent sections. However, prior to this step, the average MW values obtained by SEC calibration were verified by an alternative, independent method.

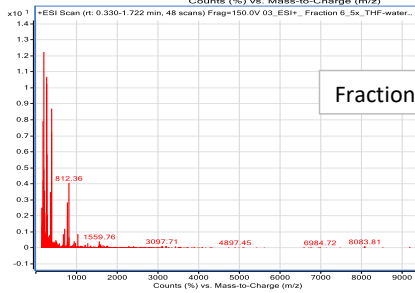
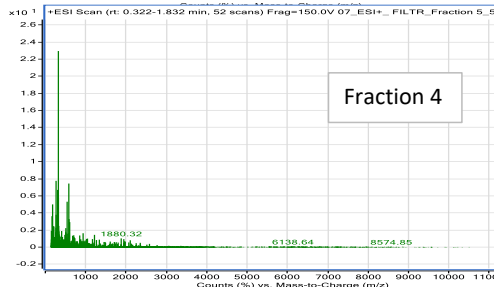
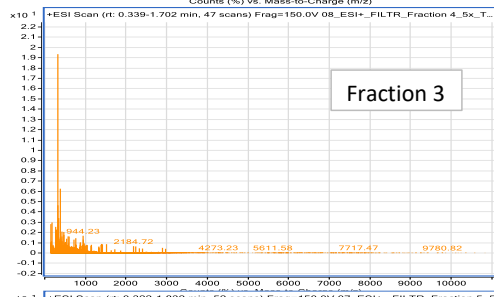
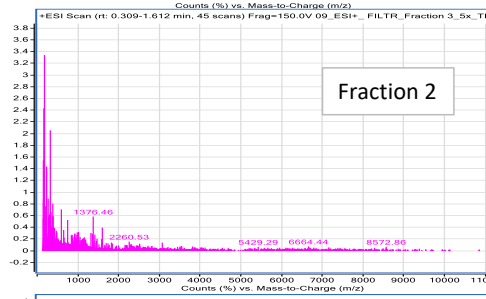
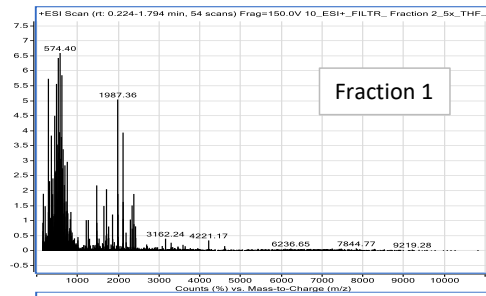
III.1.2.3. Mean molecular weights of the fractions obtained

As expected, number-average and weight-average molecular weights (M_n and M_w) determined by SEC calibration for each fraction showed sequentially smaller values as the fractions proceeded from 1 to 5, while unfractionated lignin showed M_n and M_w in the mid-range of the fractions' values. The lignin PDI followed a similar pattern.

ESI-TOFMS analysis of Fractions 1 - 5 shown in Figure 48 also reflected this expected trend through the sequence of chromatograms; Fraction 1 clearly showed an abundance of mid- and high-MW values for compounds, while Fractions 2 – 4 showed steadily fewer high-MW compounds, then fewer mid-MW species, and finally, by Fraction 5, only low-MW compounds were in evidence.

Using the MS data, the mean MW values were determined, which are listed in Table 31 for all fractions. Figure 48 compares M_n and M_w values determined by ESI-TOFMS vs SEC. Even

though these two methods yielded somewhat different MW values, the difference was significant only for Fractions 1 and, to some extent, 5 – as expected, given the observed carryover and the limitation of MW determination by MS, as large MW species may not volatilize as much as those of lower MW.



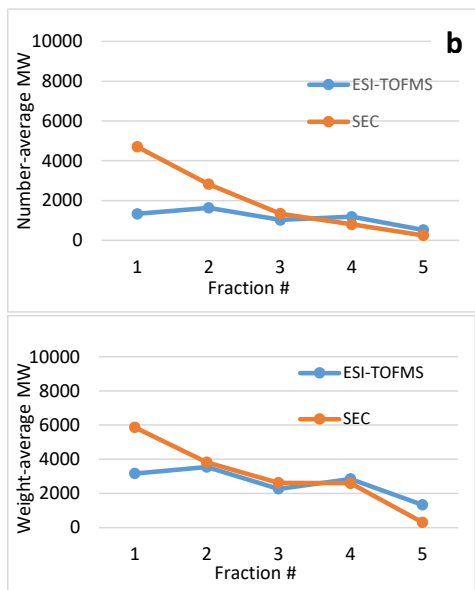


Figure 48. (a) ESI-TOFMS spectra of molecular counts vs m/z based on deconvoluted data for lignin fractions 1 – 5. Spectra are scaled to a maximum of 10,000 m/z , with the exception of fraction 5 which has a maximum of 9000 m/z . (b) Comparison of SEC vs ESI-TOFMS number-average and weight-average molecular weights for all lignin fractions.

Table 31. ESI-TOFMS and SEC calibration number-average (M_n) and weight-average (M_w) values for five fractions of lignin and unfractionated lignin.

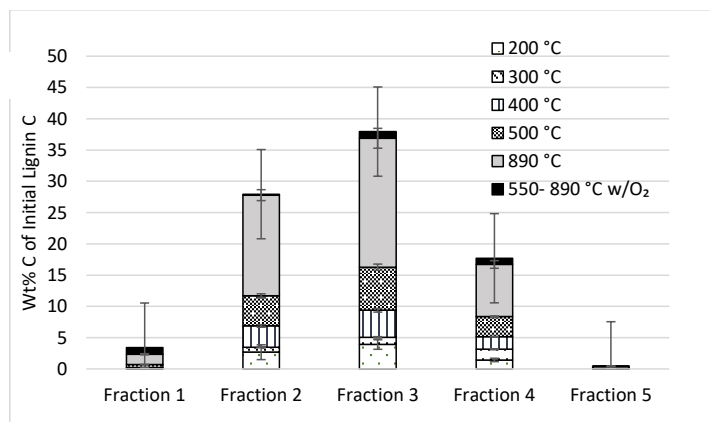
Fraction	1	2	3	4	5	Alkali Lignin
ESI-TOFMS						
M_n	1330	1634	1028	1188	522	869
M_w	3160	3547	2266	2853	1335	1881
PDI	2.38	2.17	2.20	2.40	2.56	2.16
SEC						
M_n	4698	2824	1342	802	248	1631
M_w	5862	3823	2626	2595	313	2740
PDI	1.25	1.35	1.96	3.24	1.26	1.68

III.1.2.4. Thermal carbon analysis of fractions

The fractions produced from preparative SEC were subjected to thermal carbon analysis. This method, in addition to determining the total carbon amount in each fraction (Table 29), provided distribution of the evolved carbon among temperature fractions.

TCA is a relatively novel method of accounting for all the carbon mass in an organic sample, with the added benefit that the temperature programs provide the fractionation by volatility, i.e., higher molecular weight compounds evolve at higher temperatures. Further, the evolved fractions are separated into two kinds: 1) those due to thermal physical desorption, ambient temperature to 300 °C, and 2) pyrolytic products evolving at higher temperature, reflecting those lignin components that cannot volatilize without chemical decomposition – presumably, higher-MW compounds. Char or coked fraction was the material that was not volatilized pyrolytically at 890 °C, being subsequently combusted post pyrolysis for quantification.

The obtained profiles (Figure 49) showed significant differences between Fractions 1-5 and the original lignin.



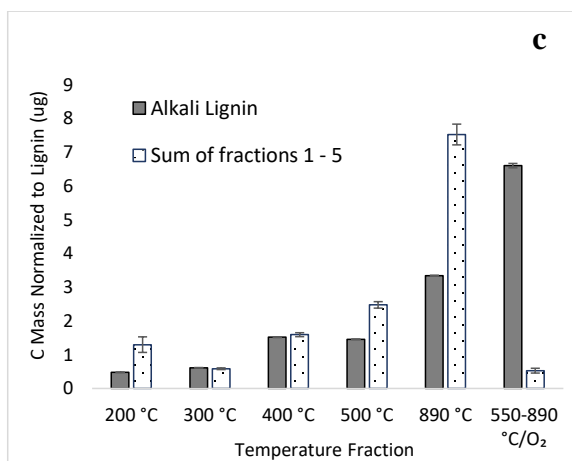
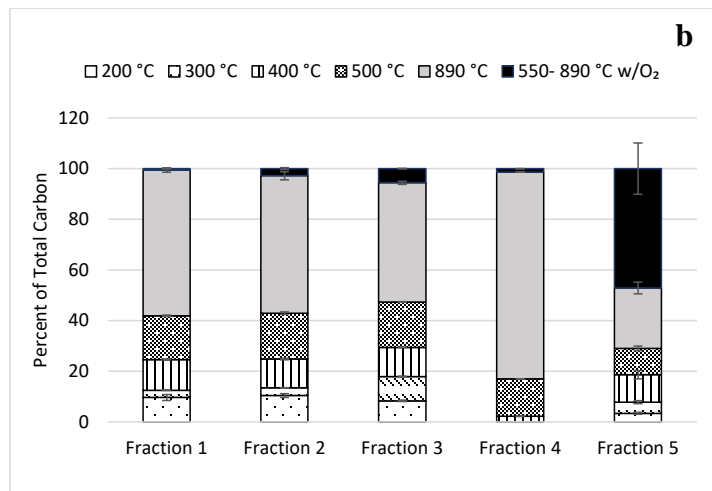


Figure 49. (a) Carbon mass distribution by TCA temperature fraction for each lignin fraction as stacked columns, (b) Normalized carbon mass distribution for each individual lignin fraction (and unfractionated lignin) by TCA temperature fraction, (c) Carbon mass sums for all SEC fractions at each temperature step of TCA compared to alkali lignin carbon masses (normalized) generated at the same temperature fractions.

To enable an accurate comparison regardless of the fraction size, the normalized TCA data of the combined fractions 1-5 and unfractionated lignin are shown in Figure 49b. Fractions 1-3 showed low amounts of char and sequentially decreasing volatilization at 890 °C, with increased representation of lower molecular weight compounds volatilized at lower temperatures (Figure 49b). Less expected was the occurrence of sizable TD portions in the TCA profiles of Fractions 1-3. This deviation from the expected pattern can be explained from the standpoint of Figure 47a and Table 29, which show a significant adsorption of high- and low-MW compounds in Fractions 1-3. TCA thus confirms that Fractions 1-3 contain some low-MW compounds volatilizing at TD temperatures.

The TCA profiles of Fractions 4 and 5 (Figure 49b) were inconsistent with their low MW. Contrary to the expectations of volatilization at TD temperatures, their TCA profiles actually showed rather large portions volatilizing at 890 °C or even as char (Fraction 5). However, this deviation may also be explained by the carryover of high-MW lignin components in these fractions. The presence of high-MW compounds appears to enhance polymerization upon heating during the TCA analysis, just like in the original lignin, presumably resulting in the formation of cross-linked polymers, potential char precursors. This phenomenon of re-polymerization during lignin thermal treatment is well known.^{174,175,177,180,185} Nonetheless, polymerization of any fraction (1-5) within the TCA apparatus does not appear to produce cross-linking or char precursors nearly as much as in the unfractionated lignin. Namely, unfractionated lignin upon TCA yielded about 47% char while 24% carbon volatilized at 890 °C.

The information presented, once again, the latter showed a much smaller char fraction; by contrast, the fraction evolving at 890 °C without oxygen increased proportionally. Apparently, charring is enhanced when polymers strongly interact with small-MW fragments, as in the

unfractionated lignin, resulting in cross-linking polymerization upon heating. Even though such interactions still skewed the expected TCA pattern in Fractions 4 and 5, the extent of their charring was nowhere near that in the original lignin.

Normalized organics for each fraction are shown in Figure 50.

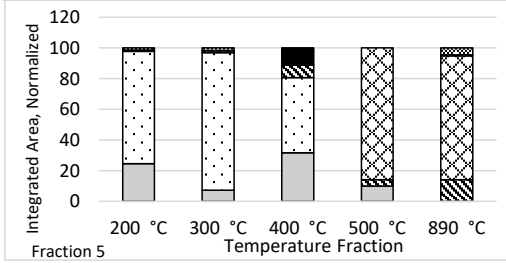
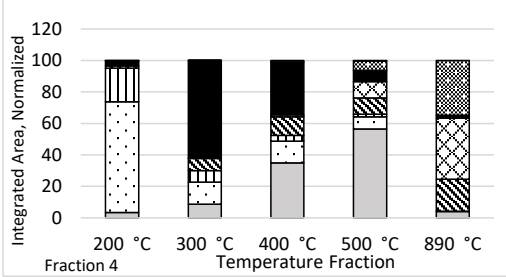
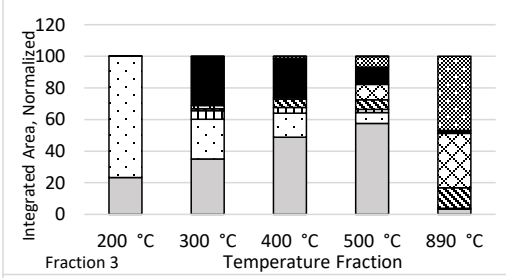
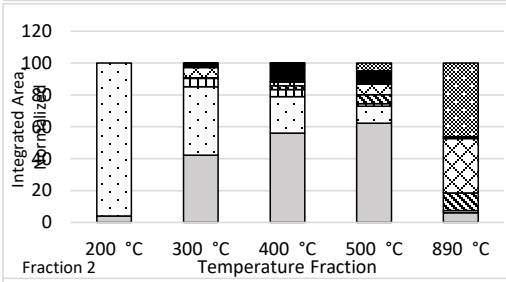
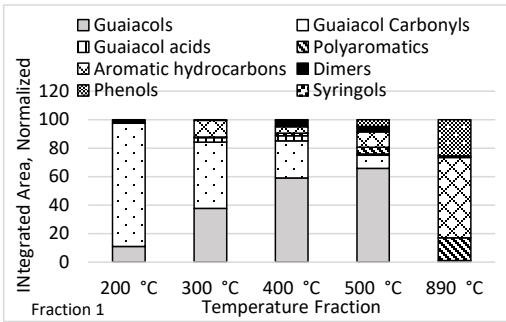
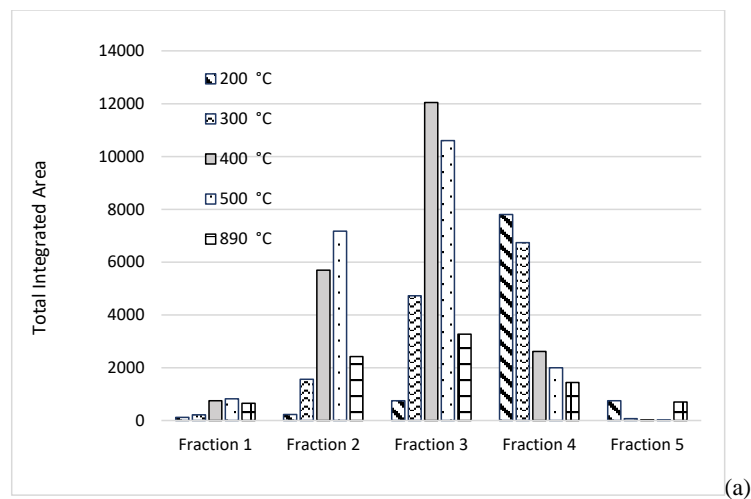


Figure 50. Organic species by temperature fraction normalized for each sample as SEC Fractions 1 – 5.

There was also a question of what type and size of compounds would evolve at each temperature step and how this was related to the expected MWs in each fraction. This particular relationship was investigated by comparing TD-Py-GC-MS data to TCA and SEC data.

III.1.2.5. Identification of species in fractionated lignin

The five fractions of lignin were analyzed via TD-Py-GC-MS to identify various compounds volatilizing during the same temperature fractionation program as for TCA, i.e., analysis at 200, 300, 400, 500, and 890 °C. The most common evolving constituents were evaluated in the normalized form, as shown in Figure 50. Then, the data were normalized to 100% within each fraction for their comparison in terms of temperature patterns, regardless of the fraction size, as shown in Figure 51.



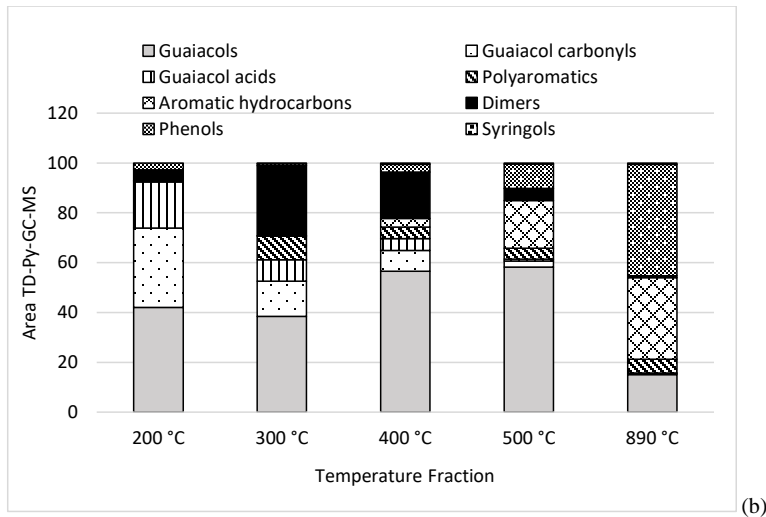


Figure 51. (a) TD-Py-GC-MS analysis of evolution of species by temperature fraction by area (mass) for lignin fractions 1 – 5. (b) % mass (by area) evolved for fractions 1-5 normalized to lignin area.

The identified compounds in the fractionated lignin consisted mainly of monomeric phenolics thermally desorbed (TD) up to about 300 °C, and then pyrolyzed (Py) evolving as pyrolytic products from temperature 300 °C and above. The major TD components across all fractions were guaiacol carbonyls (mostly vanillin), although Fraction 4 also featured significant amounts of guaiacyl acids and Fraction 5 – guaiacols (Figure 50). As expected, the TD fractions were small for higher-MW fractions (Figure 51). This information is corroborated by a similar TCA pattern (Figure 48).

By contrast and as expected, the Py components were abundant for higher-MW fractions and less – for Fractions 4 and 5. The large 890 °C portion of Fraction 5 was an exception – also as expected, as it appears to adsorb large amounts of high-MW lignin. This information is also corroborated by a similar TCA pattern.

Guaiacol carbonyls continued to be among the main products of the evolving Py products until 890 °C, this temperature presumably being too high for their occurrence. With temperature, they gradually become replaced with guaiacols and other pyrolytic products: phenols, aromatic hydrocarbons and, ultimately, PAHs, char precursors that become most abundant in the final, 890 °C temperature fraction. Toward this temperature, aromatic and polycyclic aromatic compounds become dominant in highest-MW Fraction 1 and also Fraction 5, presumably as a result of their components' interactions discussed earlier.

Notably, dimers evolving as pyrolytic products up to 500 °C were more prominent in lower-MW fractions. The lowest-MW Fraction 5 evolved them at 300 °C, presumably as TD components. These trends are consistent with the MW fractionation, as Fraction 5 should contain those dimers before any pyrolysis. Less expected is the observation that dimers form more abundantly upon pyrolysis of lower-MW lignin components. This appears to be a consequence of greater recalcitrance of higher-MW fractions, along with their propensity to form aromatic hydrocarbons upon “hard” pyrolysis, at 890 °C. Apparently, they release only monomers and other small molecules at low pyrolytic temperatures while gradually becoming more charred (less oxygenated), releasing hydrocarbons at higher Py temperatures.

When the fractions' temperature evolution patterns are compared with that of lignin (Figure 50), one significant difference becomes apparent. Namely, lignin does not produce a significant 890 °C (char precursors) fraction – instead, as was shown by TCA, it produces abundant char.

III.1.2.6. Hydroxyl group quantitation by ³¹P NMR spectroscopy

The ³¹P NMR spectra of SEC weight fractionated lignin samples are shown in Figure 52. The number of hydroxyl groups present in each sample was calculated through integration relative

to the cyclohexanol peak found at 145.2 ppm with a known concentration. The following regions were used for the classification of hydroxyl groups found in the weight fractionated samples: 143–150 ppm for alcohols, 138–143 ppm for phenols, and 135–138 ppm for carboxylic acids.⁹⁸ The number of mmoles found in each sample are summarized in Table 32 for the non-fractionated lignin and Table 33 for MW-based fractions. It is noteworthy that the spectra of all fractions contained a cluster of unidentified signals centered around 150.6 ppm. These signals have not been reported in other studies of phosphitylated lignin-based samples, nor were they observed in the spectra of other lignin and lignin-derived samples investigated by our group. It is possible that TMDP is reacting with some other highly electronegative species such as sulfur, which is present in alkali lignin.

Table 32. Comparison of the number of mmoles of hydroxyl groups present per g of unfractionated alkali lignin found by Meadwestvaco Corp. vs the results obtained in the present study using ³¹P NMR spectroscopy.

	Meadwest Vaco data	³¹ P NMR data	
		Alkali	Indulin
Phenolic OH	3.6	2.85 ± 0.04	2.4 ± 0.3
Benzylic OH	0.06		2.4 ± 0.3
	2.9	2.7 ± 0.2	
Aliphatic OH			
Carboxylic Acid OH	Not Reported	0.78 ± 0.01	0.7 ± 0.1
Total	6.5	6.3 ± 0.2	5.5 ± 0.6

Then, the number of moles of hydroxyl groups post SEC was determined in all five fractions – and their sum turned out to be significantly larger (>3.5 times) than the number determined in alkali lignin before the fractionation, as presented in Table 33.

Table 33. Number of mmoles determined in NMR samples in the SEC weight fractions per g of alkali lignin.

Sample	Unidentified	Mmoles			Total
		Alcohols	Phenols	Acids	
Fraction 1	0.49	1.61	0.40	0.00	2.50
Fraction 2	0.71	3.10	1.78	0.15	5.74
Fraction 3	0.57	3.79	2.08	1.82	6.68
Fraction 4	0.78	2.48	1.82	0.37	5.45
Fraction 5	0.46	1.30	0.13	0.08	1.96
Total	3.01	12.19	6.21	2.42	22.35

the *Meadwestvaco Corp.* and our data for the total amount of OH-containing groups was negligible when the acids were added.

Two possible explanations were considered to explain the observed difference. THF used in the SEC method could be a source of some additional OH groups determined in our experiments. For example, THF could react with lignin under the conditions used during the SEC resulting in the cleavage of the THF ring to allow for the formation of a new hydroxyl group. THF peroxide formation is also a possibility, and the compound has a new OH group and, therefore, will readily react with TMDP. Finally, the ether bond cleavage in THF could be occurring either before or during the SEC method. However, these qualitative considerations did not pass the quantitative test. Namely, the ^{31}P NMR spectrum of the phosphitylated concentrated THF contained two phospholane signals. The first is a signal in the aliphatic hydroxyl group region at 147.4 ppm, while the other is in the phenolic region at 142.0 ppm. While this does add to the μmolar total, both have relatively small integrations and an insignificant impact on the final total.

The most plausible explanation is thus that the hydroxyl groups in lignin before SEC are inaccessible for phosphitylation due to steric hindrance to undergo phosphitylation. The fractionation process is possibly causing modifications of the complex three-dimensional structure of lignin in such a way as to allow more hydroxyl groups to undergo phosphitylation. This explanation is consistent with the observed strong interactions between low- and high-MW lignin fractions that may be responsible for lignin association to make the internal hydroxyl groups inaccessible.

Detailed fraction analysis confirms this explanation. Based on Table 33 (the rightmost column), Fractions 1 and 5 contain some sizable percentages of hydroxyl groups, 11.2% and 8.8%, respectively. However, according to Table 29, these two fractions account for only 3.9 and 0.7%

of the total carbon (determined by TCA), respectively. Thus, these two fractions, particularly, the lowest-MW Fraction 5, contain disproportionately large hydroxyl group contents (mostly, at the expense of the most abundant Fraction 3). This finding may explain the observed strong interactions between low- and high-MW lignin components resulting in significant fronting and tailing of the SEC peaks (Figure 47b). These interactions may be enabled by strong hydrogen bonding, which would reduce the effective charges. In turn, in non-fractionated lignin dissolved in a polar solvent, this may cause the movement of such interacting hydroxyl groups into the internal domains of lignin particles, making them less accessible and less amenable to analysis.

Fractions 1 and, particularly, 5 show some enrichment in aliphatic hydroxyl groups at the expense of phenolic. This difference may also be significant for the strongest interactions between the highest- and lowest-MW lignin components.

III.1.3. Conclusions

Lignin fractionation by MW using SEC caused several significant and unexpected changes not only in lignin component structure, e.g., uneven distribution of phenolic and aliphatic hydroxyl groups, but also for the whole sample. Namely, the number of accessible hydroxyl groups, e.g., those amenable to ^{31}P -NMR analysis, increased more than 3-fold and the stepwise thermal treatment of fractionated lignin yielded significantly less char compared to the untreated lignin. Both of these phenomena can be explained by association between high- and low-MW lignin components, presumably via hydrogen bonding. Such interactions were indeed observed upon the re-run of separated MW fractions through the same S column, resulting in significant peak fronting and tailing.

III.2. Oxidation of Lignin by Hydrogen Peroxide with and without alcohol solvents

Characterization studies of lignin subjected to oxidative depolymerization entail the addition of hydrogen peroxide and methanol in this project- determining the percentage of original lignin which has degraded and goes into solution as oligomers was an important goal, as well as characterization of the products of hydrogen peroxide attack on lignin in terms of MW distribution.

III.2.1. Experimental

III.2.1.1. Materials

Methanol ($\geq 99.8\%$), ethanol ($\geq 99.5\%$), isopropanol ($\geq 99.5\%$) and hydrogen peroxide (30%) reagents were ACS grade or higher, as were NaOH (97%) and HCl (37%, < 5 ppm ign residue) used to adjust pH. Calibration standards for SEC as polystyrene and poly methyl methacrylate standards were obtained from Agilent. Deionized water was supplied through a Millipore Direct Q-3 water purification system (Millipore-Sigma, Burlington, MA), with resistivity < 18.2 M Ω •cm. High pressure glass reaction vessels (25 or 50 mL) by Ace Glass (Vineland, NJ), with PTFE screw-on caps with o-rings, were used for autoclave processing of lignin samples, rated for 150 psig of pressure.

III.2.1.2. Lignin degradation procedure

The lignin degradation experiments were carried out by preparing solutions of varying pH, followed by the addition of lignin, then subsequently by addition of MeOH/H₂O₂, whereby the oxidation process of the hydrogen peroxide. The prepared solutions were heated in an autoclave (additional thermal breakdown) to further enhance lignin degradation, measurable as

molecules small enough to become solubilized in solution, which would be separated from lignin solid residue too large to solubilize.

To this end, aqueous solutions of pH 0.5, 3, 7, 11 and 13 were prepared for lignin addition in 50-mL high-pressure glass reaction tubes using appropriate concentration of HCl and NaOH. For preparation of aqueous alkaline solutions, NaOH (1 M) was used to adjust separate solutions to pH 11 and 13, which were then divided into 25 mL tubes for a total of nine samples (differing H₂O₂ and MeOH combinations) for each pH. The pH for preparation of aqueous acidic solutions was adjusted to pH 0.5 and 3 with HCl (1 M), for nine samples each. A third set of nine samples of aqueous solution was left unadjusted (“neutral” pH). Kraft alkali lignin (1.00 g) was added to each of these solutions, which were brought to a total volume of 25 mL after the addition of first methanol (0 – 6.25 mL), and then 30% w/w hydrogen peroxide of (0 – 2.5 mL) to achieve the desired concentration listed in Table 34, and then quickly capped to avoid losing gases which were generated.

A schematic setup of the nine lignin samples (for each of five different initial pH values) with H₂O₂ and methanol percentages is shown in Table 34.

Table 34. Experimental set-up for lignin oxidation by H₂O₂; percentages of hydrogen peroxide, methanol and water were on a (v/v) basis; pH was ensured by using appropriate HCl and NaOH concentration prior to lignin, peroxide and methanol addition.

Sample designation based on H₂O₂-MeOH volume % (below) for each pH level	% H₂O₂ (v/v)	% MeOH (v/v)	% Water (v/v)
(0-0)	0	0	100
(0-10)	0	10	90
(0-25)	0	25	75
(3-0)	3	0	97
(3-10)	3	10	87
(3-25)	3	25	72
(10-0)	10	0	90
(10-10)	10	10	80
(10-25)	10	25	65

A second experimental setup performed at neutral pH investigated the impact of varying concentration of hydrogen peroxide (0, 5, 10%) and MeOH (0, 10, 25%), respectively. Table 35 shows percentages of H₂O₂ and methanol additions (v/v) that were made to the aqueous solutions containing only lignin initially. The initial pH values of neutral samples in Table 35 were measured after addition of lignin, and ranged from 6.3 to 7.1.

Table 35. Experimental set-up for lignin oxidation by H₂O₂; percentages of hydrogen peroxide, methanol and water were on a (v/v) basis, out of a total solution volume of 25 mL.

Neutral pH samples Sample designation	% H₂O₂ (v/v)	% MeOH (v/v)	% Water (v/v)
(0-0)	0	0	100
(0-10)	0	10	90
(0-25)	0	25	75
(5-0)	5	0	95
(5-10)	5	10	85
(5-25)	5	25	70
(10-0)	10	0	90
(10-10)	10	10	80
(10-25)	10	25	65

Samples for both experimental setup (Tables 1 and 2) were autoclaved in the same manner, at 120 °C at 17 psig for 30 minutes in a Tuttnauer EZ10 autoclave steam sterilizer (Hauppauge, NY). Samples were then cooled to room temperature by air, and the liquid fraction, with the solubilized portion of lignin products, was separated from solid residue by filtration through pre-weighed coarse filtration paper (20- μ m pore size average) and vacuum pressure. Then 10 μ L aliquots of the filtrate were further filtered through syringe filters (0.20 μ m pore size) to obtain 5 μ L of the liquid fraction for TCA analysis as syringe-filtered samples (as compared to 5 μ L samples which were not syringe filtered and labeled as vacuum-filtered).

Typically three replicates for each H₂O₂/MeOH combination were evaluated. Solid residues on filter papers were dried in a 75 °C oven for 24 hours until a constant weight was attained.

III. 2.1.3. Chemical characterization of peroxide-treated lignin samples

Both gravimetry and TCA were utilized to determine the wt% carbon of the initial lignin (1 g or 0.64 g C) in the liquid and solid fractions obtained for each sample using equations below. For characterization of liquid fraction the total solution of the liquid filtrate was considered as initial 25 mL, and for the TCA sample solution volume was 5 μ L filtered as described above. In order to convert mass of lignin to carbon mass, final masses of lignin occurring in the liquid fraction or remaining in the solid fraction were multiplied by 64% as carbon content of untreated lignin, as determined by elemental analysis (Atlantic Microlabs, Inc., Norcross, GA). Wt% carbon in samples was calculated in several different ways:

Wt% C in solid fraction by gravimetry (indirect mass):
(Mass dried solids/ initial mass of lignin sample) x 0.64 [1]

Wt% C in liquids by gravimetry: 100- wt% solids [2]

Wt% C in liquids for entire sample by TCA:
((Mass of TCA sample x (total solution volume/TCA sample volume))/initial mass of lignin x100)/ 0.64
determined for both vacuum filtered and syringe-filtered TCA [3]

Additionally, the pH of all samples was measured prior to and 48 hours after the autoclaving step.

Thermal carbon analysis (TCA) of samples was performed using the thermal optical analyzer from Sunset, Inc. (Tigard, OR) as reported previously.¹⁹⁴ TCA is a process similar to thermal gravimetry analysis; in this case a sample was heated through a programmed series of temperatures (ambient, 200, 300, 400, 500 and 890 °C), with each step lasting six minutes. Samples were first heated in a pure He atmosphere up to 890 °C, and then in an He atmosphere

with 2% O₂ for five minutes (temperature was dropped to 550 °C and then increased again to 890 °C), to allow combustion of char (coked) material.

The organic compounds in the sample underwent thermal desorption in the 200 – 300 °C range, in which low-molecular weight compounds evolved as gases from the mixture; condensable gases became bio-oil. At temperatures above 400 °C, the process is considered as pyrolytic, where breakdown products were volatilized from bulk heteropolymeric lignin at an increased thermal energy level. Additional bio-oil and gases such as H₂, methane, carbon monoxide and carbon dioxide were released in this part of the process. The designation of “char” represented condensed, deoxygenated materials left unvolatilized after the peak temperature of 890 °C.

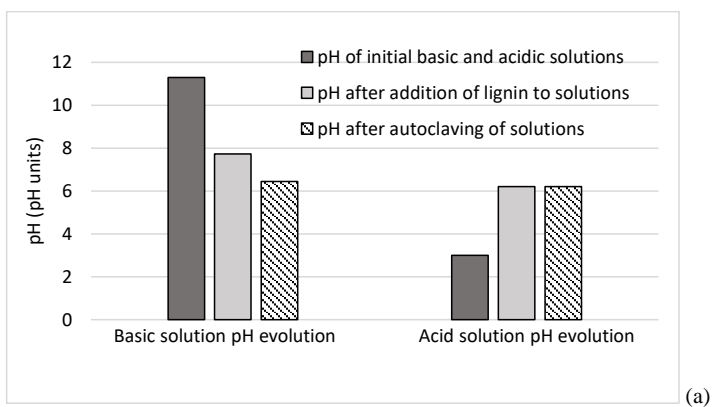
Products of the autoclaved lignin samples were analyzed as 5 µL liquid aliquots and 20 – 50 µg solid samples from residues. All samples were dried at 45 °C for five minutes on a hot plate to eliminate any traces of methanol which would appear as carbon signal in TCA. Calibration was performed with sucrose standards as recommended by the manufacturer of the thermal optical analyzer.

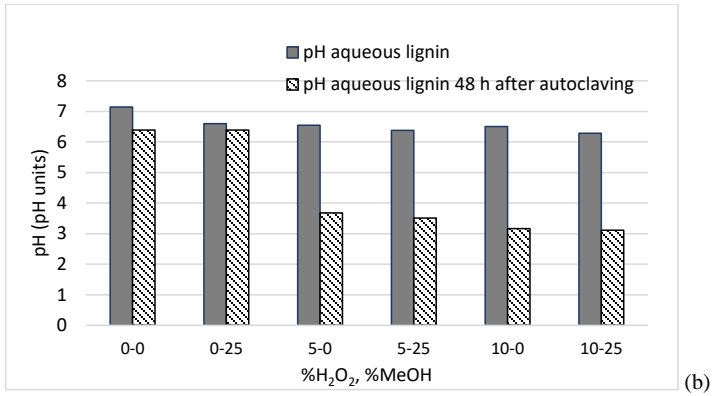
Gel permeation chromatography (GPC) was performed using a high performance liquid chromatograph (Agilent model 1100 System) via a PLgel column with polystyrene divinylbenzene (PSDVB) stationary phase, 1000 Å pore size, 5 µm particle size, 7.5 x 300 mm (Agilent). Samples were solubilized in THF:water (9:1) and injected into the unstabilized tetrahydrofuran (THF) mobile phase, with a flow rate of 1 mL/min and underwent detection by diode array detector (DAD) at 212-750 nm. Column calibration was performed with PMMA (poly-methyl methacrylate) and PS (polystyrene) particles (500 to 30,000 Da available commercially).

III.2.2. Results

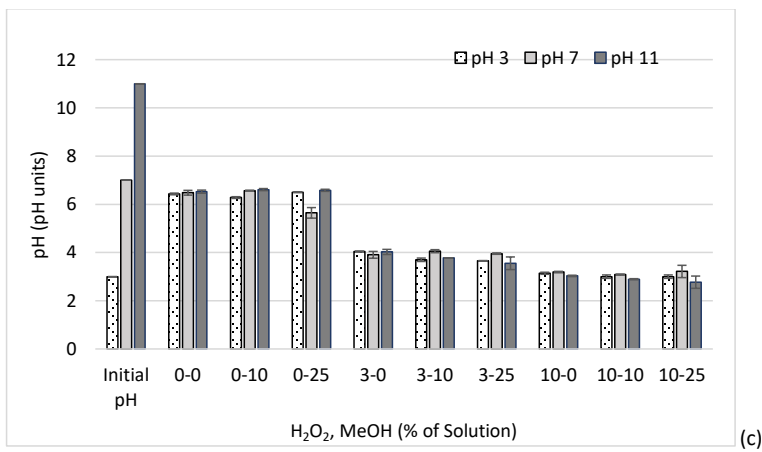
III.2.2.1. Lignin buffering capacity

Initial pH values of the aqueous solutions were compared to the pH values of the treated lignin solutions 48 hours after autoclave processing; this time span allowed the solutions to equilibrate at a final pH. Furthermore, pH had also been monitored after lignin was added to the basic and acidic solutions before treatment with H₂O₂/MeOH. Figure 53a shows the pH for nontreated lignin samples before and after lignin addition to acidic and basic solutions, with the most pronounced change in pH after addition of lignin; this showed little difference in pH after autoclaving in acid addition, and a small pH difference for base addition. The charts in Figure 53b, c, and d show the apparent buffering capacity of lignin except in the case of extreme acidity or basicity (Figure 53b).





(b)



(c)

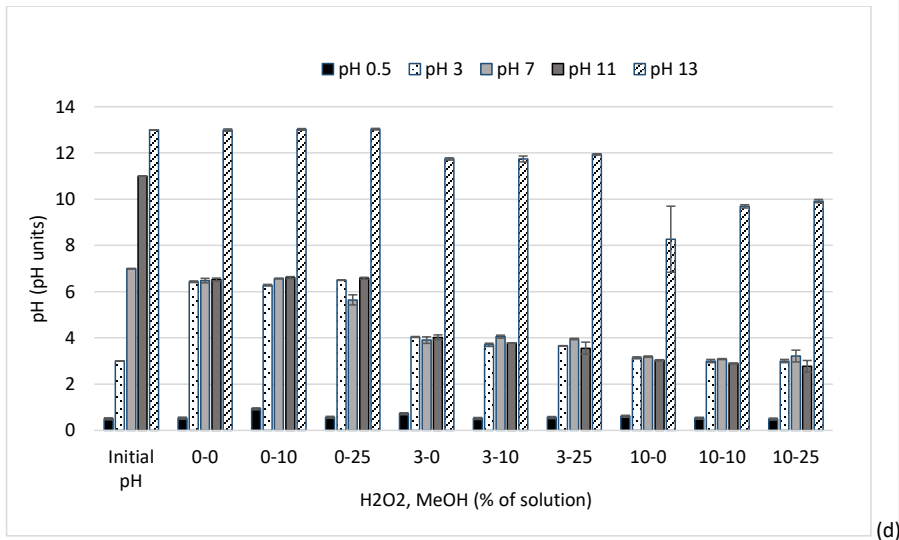


Figure 53. (a) The initial pH values for basic and acidic solutions at pH 11 and 3 respectively, and change of pH of the solutions after addition of lignin, and the subsequent change in pH after autoclaving of the lignin solution (0% H₂O₂, 0% MeOH); Comparison of initial pH with pH after treatment with H₂O₂/MeOH and autoclaving, for (b) a second set of neutral pH samples, (c) samples with initial pH values of 3, 7 and 11; (d) samples with initial pH values of 0.5, 3, 7, 11, 13, in order to assess extreme pH impact.

For the solutions with pH of initial base and acid water solutions (11 and 3 respectively) the impact of autoclaving at 120 °C was thought to be less important than lignin addition when were compared to pH taken upon addition of lignin and then further compared to pH of the solution after autoclaving at 120 °C for 30 min, as in Figure 53a.

The addition of lignin to each solution clearly counteracted acidity and alkalinity in the samples with no H₂O₂ or methanol (0-0), with initial pH values of 3 and 11 in Figure 53b and 53c; lignin buffering capacity was able to neutralize acid and base additions to a pH close to 6.5, at which point these samples then changed almost identically to neutral samples upon H₂O₂ and MeOH treatment.

Acidic groups able to release proton to neutralize hydroxyl ion include any carboxylic acid groups (pKa 3 - 5), a number of which might be associated with polysaccharide complexes left as impurities, or which occur naturally. Phenolic OH groups are also available on a much larger scale, with pKa values of 9.5 – 10.5., or lower if the ring is attached to an alkoxy group (pKa 7 -8). Alcohol and thiol groups are possibilities, but have low acidity (pKa 13.5 – 17).²⁰⁵

In the case of acid addition, lignin contains a substantial number of functional groups such as hydroxyl and ethers, which may serve as weak bases, becoming protonated in acidic solutions. Thiols may serve the same purpose, but are less numerous. There are also phenolate sites which can be protonated to produce neutral phenol hydroxyls.

There is also the possibility that cleavage of ether bonds has consumed acid or base, but cleavage of ethers in general is usually accomplished only by acid, as HBr and HI, and typically at 130 – 140 °C,²⁰⁶ although a study by Melro et al. has shown some alkaline breakdown of lignin at room temperature (4.3 wt% for 0.1 M NaOH).⁹⁰ Structural change under either treatment is apparently minimal at ambient temperature and changes in lignin placed into an acid or base solution would be more related to surface charge and thus solubility than to depolymerization at a stage prior to autoclaving.

The second set of neutral samples in Figure 53d were evaluated in nearly the same manner as the first set of neutral samples, except that initial pH was measured (pH 6.3 – 7.1) and the additions of H₂O₂ were changed from 0, 3, 10% to 0, 5, 10%. The pH of each sample before autoclaving was measured since actual neutrality was not expected; kraft lignin is generally near 6.5 in aqueous solution at 10% concentration in aqueous solution.³⁰

Aside from early buffering of acid and base in pH 3 and pH 11 samples, it was clear that hydrogen peroxide had an acidic effect on the final pH of all samples other than extreme cases (pH 0.5 and 13). Of note, 3 and 5% H₂O₂ made little difference in results, and even pH change between 5 and 10% H₂O₂ was not substantial (one pH unit). However, the drop in pH was indicative of a large amount of acidic material being produced upon mixing/heating with hydrogen peroxide. The presence of MeOH reduced pH by a very small amount.

Ring-opening by hydrogen peroxide was considered to be a reaction of some importance in both base- and acid-catalyzed depolymerization strategies of lignin.^{153,154,157,158,160} Attack by the OH⁺ ion in acidic solution mediated the ring opening^{153,160} while Asha et al. suggested that superoxide radical in alkaline solutions might lead to ring opening and Xiang et al. considered the perhydroxyl anion as the main oxidative species, leading to not only aryl-ether cleavage but ring-opening of aromatic rings.^{157,159}

A substantial increase in carboxylic acid groups was recorded by studies of both base- and acid-catalyzed depolymerization studies utilizing hydrogen peroxide,^{153,156-158,162,207} and Xiang et al. found that 51 wt% acids (of original lignin) and 34% acids resulted for basic and acidic solutions of acid hydrolysis lignin treated with 1.5 M H₂O₂ at 120 and 160 °C respectively. The acid was primarily formic acid, with a lesser amount of acetic acid.¹⁵⁷ Hasegawa et al. maximized carboxylic acid production in a flow reactor with a pH-neutral solution with 0.1% H₂O₂ at 200 °C for 2 min, which produced 0.45 g acid/g alkali lignin, as mainly formic acid, followed by acetic acid.²⁰⁷ Evstigneev reported acid solution H₂O₂ oxidation of hydrolysis lignin to double carboxyl groups from 34 per 100 phenylpropanoid units to 68.¹⁵⁸

The results of our study substantiated the reports of high amounts of acid present after H₂O₂ treatment,^{157,158,207} which seemed to occur for a variety of oxidative parameters and lignin types. The

high carboxylic acid content, linked to ring-opening in several proposed mechanisms was believed to be responsible for the proliferation of simple acids.^{153,154,158-160} However, pH monitoring results in our study implied that acid or base catalyzation for this type of reaction did not appear to be necessary, i.e., the acid and base solutions in our study were reduced to neutral solutions before hydrogen peroxide was added. The same amount of acid was produced for the neutral solution in comparison to the pH 3 and pH 11 solutions. Of note, extreme acid or alkaline conditions (pH 0.5, 13) reduced the buffering effect, but did not show any particular ability to produce acid from ring-opening or any other reaction.

III.2.2.2. Depolymerization and mass balance

The presence of monomers and oligomers in the liquid fraction of samples after hydrogen peroxide treatment and autoclaving, in comparison to untreated lignin (also autoclaved), generally indicated the depolymerization effectiveness of the H₂O₂/MeOH method; the quantification of low-MW lignin compounds was accomplished by gravimetry for all pH's and by TCA for neutral pH samples. Lignin mass present in the liquid fraction for the various H₂O₂/MeOH treatments for lignin at three initial pH levels (3, 7 and 11) are shown in Figure 54. Noticeably, the neutral and base-added samples, with no H₂O₂ reagent, had higher levels of the original lignin mass in the liquid fraction (up to 37 wt% of the original lignin) compared to neutral and alkaline samples that were treated with H₂O₂, contrary to expectations. It was also noted that acid-added samples evolved far less mass in the liquid fraction (a maximum of 15 wt%) than basic or neutral solutions, although this percentage increased in the liquid fraction with increasing H₂O₂.

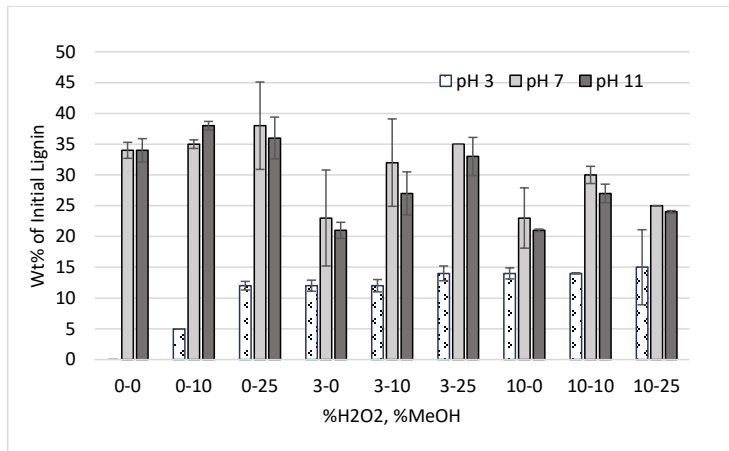


Figure 54. Percent of original lignin mass present in the liquid fractions of autoclaved samples which had been treated (H₂O₂ and MeOH) or left untreated; mass was determined by gravimetry. Initial pH values were 3, 7 and 11.

Kraft lignin in general is more soluble in alkaline solution than in acid solution (acidification is used to precipitate it from “black liquor” waste in paper mills); however, the pH of solutions after lignin addition showed a similar pH of about 6.5, even for previously acid solutions. From the results in Figure 54, it appears that alkaline and neutral solutions, both at pH 6.5 after buffering, were amenable to solubilization and depolymerization due to thermal reaction at 120 °C, since lignin is generally considered to be insoluble in aqueous solution at a pH of 6.5.,⁹⁰ while acid-treated samples were not.

Of interest, breakdown products for alkaline and neutral solutions were high for (0-0) samples (close to 35 wt%) so that thermal treatment rather than chemical treatment (NaOH or H₂O₂) was probably responsible for the degradation which occurred. The notable trend in the chart is the reduction of solubility in samples with added H₂O₂/ no MeOH in relation to untreated lignin. This tendency occurred for both base- and acid-treated samples, although the trend is not nearly as emphasized for acid-treated lignin.

The lack of solubility of lignin reaction products for alkaline and neutral samples with added H₂O₂ may seem unusual, but a study by Kadla et al. of H₂O₂ oxidation of lignin in an alkaline solution noted that MW of lignin increased after oxidation; they attributed this to condensation or rapid depolymerization followed by repolymerization.¹⁵⁶ The same effect was noted in an acid solution with H₂O₂.¹⁶² Of note, the presence of MeOH appeared to allow increased solubility, possibly by acting as a capping agent and preventing further condensation or repolymerization.

The presence of lignin in acid solutions is limited, which is reflected in (0-0) samples, even after thermal treatment; solubility of acid-treated samples is the primary cause for concern. Lignin in alkaline solution and neutral lignin may have retained enough negatively charged phenolate sites to be soluble in water at 120 °C and 17 psig (0.22 MPa), wherein water becomes a better solvent for nonpolar or partially polar analytes at lower temperature through reduction of dielectric constant and changes in other parameters.²⁰⁸ Subcritical water treatment studies show that lignin at neutral pH becomes at least partially soluble with thermal treatment; 23% solubilization of cellulolytic enzyme lignin at 180 C for 12 min was reported by Trajano for a batch reactor.¹⁸³ Zhou et al. showed a conversion of kraft lignin of 13.5 wt% at 130 °C for 15 min in a batch reactor.¹⁸²

However, lignin in acid solutions apparently had a different fate. Many of the available negatively charged sites, which can exist even to pH 2,²⁰⁹ were probably protonated and then limited the solubility of these samples, even at temperatures of 120 °C.

Of interest, MeOH in the absence of H₂O₂ improved solubility of acid-treated samples to the point where product levels were as high as those for treated samples. MeOH also improved the solubility of base-treated and neutral samples, but to a lesser extent. The ability of MeOH to enhance solubility is most likely related to electrostatic, or charge, effects. To add to the complexity, the addition of H₂O₂ appeared to produce some depolymerization for acid-treated samples, even in the

absence of MeOH. However, the ubiquitous nature of H₂O₂ attack on aromatic rings, with the production of simple acids, is apparent for both base and acid-treated samples.^{153, 158}

III.2.2.3. Carbon mass balance closure

Total solubilities for pH 7 samples for each combination of H₂O₂ and MeOH by TCA analysis were calculated as wt% carbon of initial lignin carbon; two filtration methods were utilized (syringe- and vacuum-filtered) and values are given for both, along with comparison to wt% carbon by indirect mass (also by vacuum filtration) measurement in Figure 55. In determining method development of carbon mass balance, there was some question as to whether vacuum-filtered solids (as the entire 25 mL sample), or the same samples subjected to syringe-filtration, would be better for TCA analysis. The concern was that filtration through paper with an average pore size of 20 μm, which was necessary in light of the cohesive nature of the solids, would reflect an overabundance of high-MW particles, producing TCA profiles which would be difficult to compare to studies normally working with lower pore size filters.

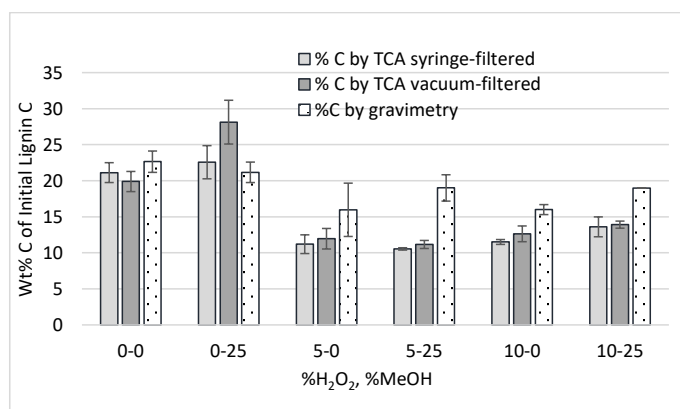


Figure 55. Comprehensive total carbon analysis of neutral (pH 7) liquid fractions for varying H₂O₂/MeOH treatments and autoclaving, and then subjected to vacuum- and syringe-filtered (20 and 0.2 μm, respectively) filtration, compared to wt% carbon by gravimetry (and vacuum filtration).

It was noteworthy that there was similar wt% carbon in the liquid fraction for both syringe-filtered and vacuum-filtered samples analyzed by TCA. Solid residue filtered from all liquid fractions appears to consist of oligomer dimensions which exceeded a 20-μm pore in size in order for solubilized material to be similar in amount as filtrate passing through both 20-μm (average) vacuum filters and 0.20-μm syringe filters.

Thermal carbon analysis of neutral pH samples which underwent H₂O₂/MeOH treatment and autoclaving showed similar results for depolymerized lignin mass in comparison to mass determined by gravimetry. For the pH neutral samples from this study it was apparent that overall solubility for reaction products was decreased for samples with H₂O₂ addition. Results from thermal carbon analyses which show this trend are shown in Figure 56 for vacuum-filtered TCA samples.

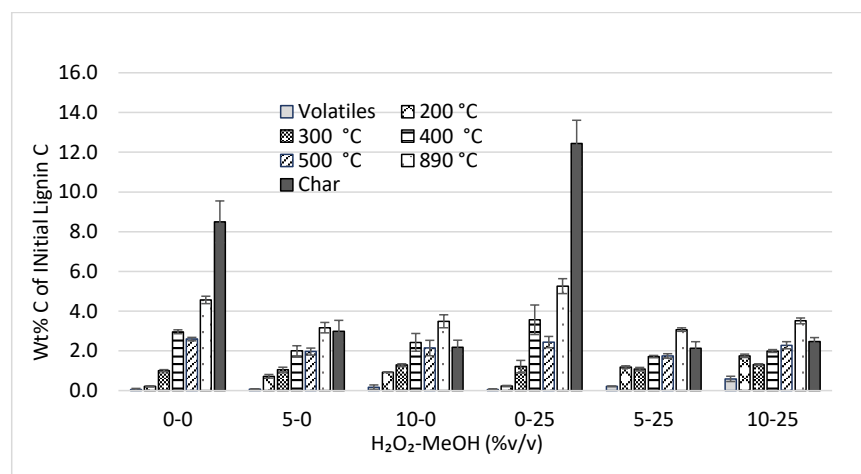


Figure 56. Distribution of carbon by the TCA temperature fraction for the liquid fraction of neutral pH samples subjected to varying H₂O₂/MeOH treatment and autoclaving, followed by vacuum filtration.

In viewing the results of the thermal carbon analysis of pH neutral lignin samples, which had been reacted with H₂O₂ and methanol in various combinations and then autoclaved, it was apparent that carbon mass was concentrated at higher temperatures, indicating larger oligomers as the predominant species in all liquid fraction samples. As noted earlier, more solubilized material occurred in the 0% H₂O₂ samples than in samples with H₂O₂, but the majority of it occurred in 890 °C and char fractions. The absence of this size of oligomer in the H₂O₂ treated samples may have resulted from condensation due to pyrolysis or due to an increase in low-mass oligomers in neutral/alkaline solutions which resulted in mass repolymerization; overall mass loss was thus due to aggregation prior to filtering. The addition of MeOH appeared to increase solubility somewhat, as noted previously.

Total solubilities for pH 7 samples for each combination of H₂O₂ and MeOH by TCA analysis were calculated as wt% carbon of initial lignin carbon; two filtration methods were utilized (syringe- and vacuum-filtered) and values are given for both, along with comparison to wt% carbon by indirect mass (also by vacuum filtration) measurement..

III.2.2.4. Solvent effect

Ethanol and isopropanol were also added as solvents in the place of methanol for a series of runs with either 0% H₂O₂ or 10% H₂O₂. The charted results are shown in Figure 57.

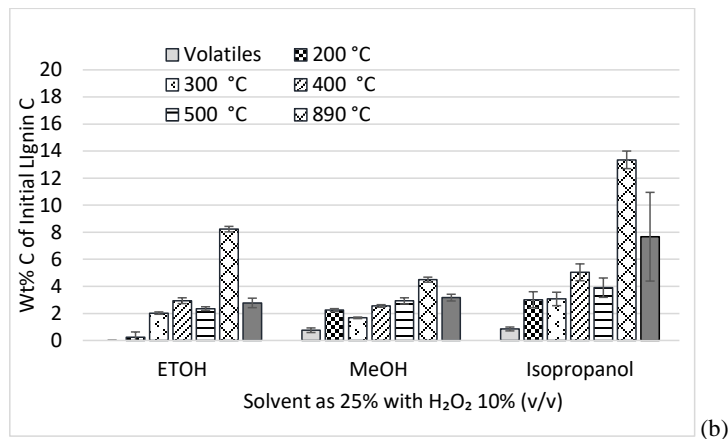
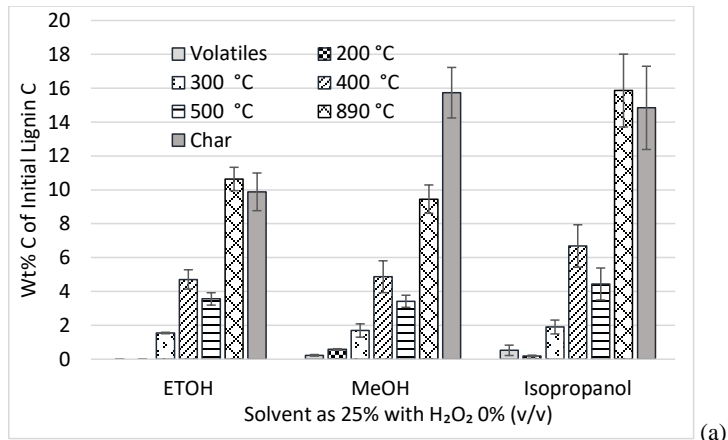


Figure 57. Comparison of wt% carbon in liquid fractions of lignin, post autoclaving, in aqueous solutions with methanol, ethanol and isopropanol (a) at 0 and 25% v/v (no hydrogen peroxide), and (b) at 0 and 25% v/v in 10% H₂O₂ solutions

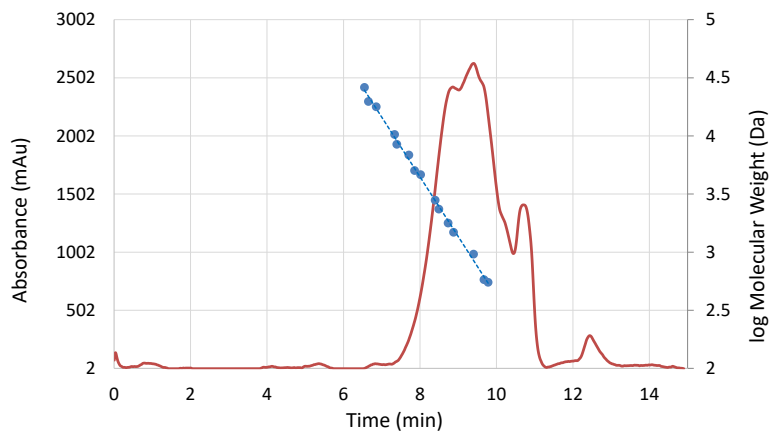
Methanol, as a solvent in previous experiments, appeared to promote depolymerization best in conditions with no H₂O₂ present, and this trend held true for ethanol and isopropanol as well; the latter solvents even improved yield. The thermal treatment alone may have promoted degradation of the lignin, and the presence of alcohols may have worked in a capping or barrier

capacity, keeping lignin molecules solubilized without condensing or repolymerizing. The increased size of the alcohols may have increased isolation efficiency. As in previous experiments, however, the presence of hydrogen peroxide may have resulted in very small molecules, ostensibly due to ring-opening, which apparently reassembled as condensed molecules more rapidly than alcohol scrounging could occur, although the increased alcohol concentration appeared to slow repolymerization tendencies.

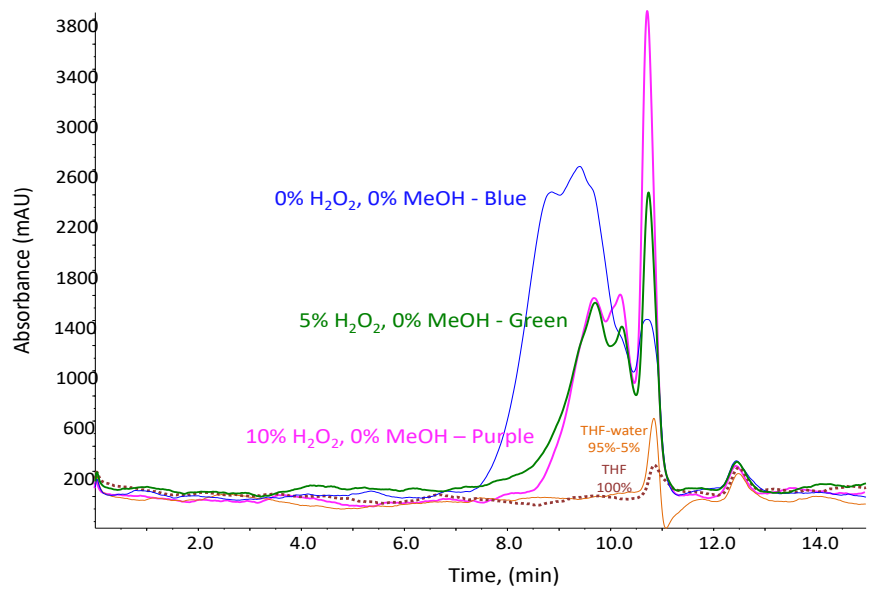
III.2.2.5. Size exclusion chromatography

Gel permeation chromatographic data substantiated TCA evidence, showing lower abundance of oligomeric species in solution with increased hydrogen peroxide addition and also illustrated the tendency for methanol addition to increase the concentration of solubilized species in samples evaluated via TCA (Figure 57). In GPC charts the larger molecular weight species elute first, with the shortest retention time, and the smallest size fraction appears at the latest retention time. Height of the vertical axis shows relative intensity of the size fraction; values of the molecular weights are calculated through a calibration curve of commercially available polystyrene/poly-methyl methacrylate spheres of known M_p (peak MW) with narrow dispersity.

A chromatograph of untreated lignin and the calibration standards curve is shown in Figure 58a. GPC chromatograms were overlaid for 0, 5 and 10% H_2O_2 treated lignins with 0% MeOH (Figure 58b) and also for 0% and 10% H_2O_2 treated lignins with 0 and 25% MeOH (Figure 58c) in order to assess the extent of depolymerization for H_2O_2 and MeOH trends.



(a)



(b)

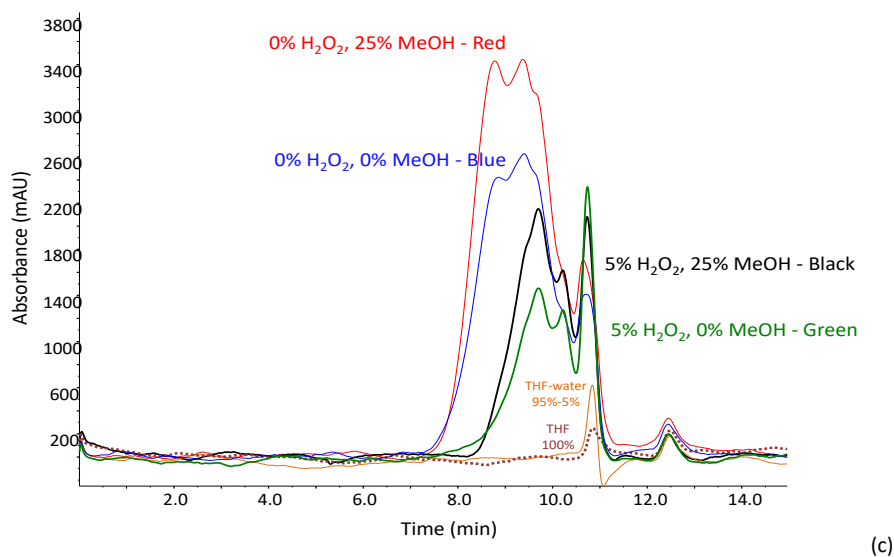


Figure 58. Gel permeation chromatograms showing (a) the calibration standards curve (PS and PMMA) for an untreated lignin profile (b) decrease in average molecular weight with increased H_2O_2 addition, without methanol and (c) increased signal (higher concentration) of solution species with increased methanol (for the same percentage of H_2O_2).

In Figure 53a, GPC results clearly delineated the tendency for H_2O_2 addition to result in less high-MW oligomers in solution, and a decreased overall abundance of material as indicated by the lower intensities for 5 and 10% H_2O_2 profiles. In Figure 53b, the tendency for MeOH to increase abundance of solubilized material for each percentage of H_2O_2 was evident. MW as number-average M_n , weight-average M_w and z-average M_z are presented in Table 36 for each combination of H_2O_2 and MeOH.

Table 36. Molecular weight as number-average M_n , weight-average M_w , and z-average M_z of liquid fractions of treated lignin by various combinations of hydrogen peroxide and methanol (% v/v).

Sample	M_n	M_w	M_z
0% H ₂ O ₂ , 0% MeOH	1296	2465	3822
0% H ₂ O ₂ , 25% MeOH	1315	2355	3454
5% H ₂ O ₂ , 0% MeOH	960	4443	10186
5% H ₂ O ₂ , 25% MeOH	597	927	1277
10% H ₂ O ₂ , 0% MeOH	471	785	1131
10% H ₂ O ₂ , 25% MeOH	577	921	1271

III.2.3. Conclusions

- The buffering capacity of lignin (alkali kraft) was extensive. Alkaline and acidic solutions (pH 11 and 3 respectively) were returned to mid pH levels rapidly upon addition of lignin, with and without autoclaving. Upon treatment of these solutions with H₂O₂ and MeOH, they behaved almost identically to neutral pH samples. Solutions which were extremely alkaline and acidic (pH 13 and 0.5 respectively) neutralized buffering capacity, but also prevented extensive change upon addition of H₂O₂ and MeOH.
- Low pH levels for lignin solutions after treatment with H₂O₂ and MeOH indicated a significant release of acids- these were probably due to ring-opening processes mediated by hydrogen peroxide.
- The major trend uncovered by total carbon analysis was the effect of H₂O₂ on autoclaved lignin solution, which was the decreased abundance of solubilized species due to decreased hi-MW oligomer fraction compared to lignin untreated by H₂O₂. This was probably due to repolymerization or condensation of simple molecules released during rapid depolymerization, including ring-opening processes.

- GPC, in particular, showed that methanol increased solubilization of lignin through preservation of lower-MW oligomers in solution, perhaps as a capping agent, thus preventing repolymerization or condensation.

III.3. Subcritical Water Treatment of Alkali Lignin

III.3.1. Experimental

III.3.1.1. Materials and methods

This study used alkali (i.e., kraft) lignin purchased from Sigma Aldrich (St. Louis, MO, USA). The elemental composition of alkali lignin was 64.14% C, 5.79% H, 1.39% S and 0.46% N, conducted by Atlantic Microlab, Inc. (Norcross, GA). The solvents used included dichloromethane (DCM), methanol (MeOH), tetrahydrofuran (THF) (VWR, Arlington Heights, IL, USA), which were GC and HPLC grade; as well as deionized water obtained from a Direct-Q3 UV system purifier (Millipore, Billerica, MA, USA) with the total organic carbon content below 5 ppb (manufacturer specification). ACS grade sucrose for calibration of the thermal carbon analyzer instrument was obtained from Alfa Aesar (Ward Hill, MA, USA). The internal standard and recovery standard for GC-MS, *o*-terphenyl (99%) and 4'-chloroacetophenone (97%), respectively, were purchased from Sigma-Aldrich (St. Louis, MO, USA). N,O-Bis(trimethylsilyl)trifluoroacetamide, a derivatization agent for GC-MS analysis of acids and alcohols, was also obtained from Sigma-Aldrich.

GPC calibration standards included poly(methyl methacrylate) (PMMA) narrow standards (M_p 550-26080 Da) purchased from Agilent Technologies (Santa Clara, CA, USA) and

polystyrene (PS) narrow standards (M_p 580-19760 Da) purchased from Varian (Amherst, MA, USA).

III.3.1.2. Subcritical water treatment

The experimental steps are outlined in Table 2. An in-house fabricated laboratory-scale batch reactor allowed for conducting up to five simultaneously controlled SW reactions.¹⁹⁶ Reactions were carried out in stainless steel vessels with a volume of 4.7 mL when capped. The experiments were performed at four different reaction temperatures: 200, 250, 275, and 300 °C. For experiments conducted at 200 °C, 0.10 ± 0.01 g of lignin and water (3.2 mL) were mixed and the calculated internal pressure was 16 bar. For the reactions conducted at 250, 275 and 300 °C, 0.25 ± 0.01 g of lignin and water (2.9 mL) were used, and the internal pressures were 40, 59 and 86 bar, respectively.¹⁹⁷ Headspace for gas/liquid equilibrium was carefully monitored to ensure safe operation.

Vessels in the reactor were rotated at approximately 3 rpm while being heated for 6 - 10 min to 200 to 300 °C, respectively, then the reaction time was set to 30 min. After completion of the treatment, vessels were cooled under a stream of cold tap water, and solid and liquid fractions were collected. The liquid content was decanted from the solid residue, combined with several rinses of the reaction vessel, and adjusted to a final volume of 7 mL to be used for further quantitative analysis. The accurate gravimetric determination of solid residue was ensured by weighing the reaction vessel prior to and after the reaction, and again after removal of the liquid and after drying of the vessel.

III.3.1.3. Analysis of subcritical water reaction products

Chemical characterization of SW treated lignin involved the sequence of analytical steps shown in Table 37. The low-MW products (TD fraction) were analyzed directly by TD-Py-GC-MS and compared to a frequently used method, LLE, followed by GC-MS. The high-MW products are non-GC-elutable, so they could not be analyzed directly by GC-MS. Thus, analysis was conducted based on their pyrolytic markers evolving at temperatures 400 °C and higher in subsequent Py-GC-MS. The sum of TD and Py GC-MS was normalized with TCA to close carbon mass balance. Analytical methods are described below in detail.

Table 37. Experimental steps and methods of this study

Work step analysis	1. Subcritical water treatment	2. Phase separation	3. Product
Method(s)	30 min at 200, 250, 275, 300 C (16, 40, 50 and 86 bar resp.)	Decantation (Figure 1 only) or filtration to yield: A. Liquid fraction, ¹ B. Solid fraction/residue C. Untreated lignin	GPC, TCA ^{2,3} (all MW) TD-GC-MS (low-MW) Py-GC-MS (high-MW) ³ (with gas quantification) Elemental analysis

¹ For low-MW products in the liquid fraction LLE-GC-MS (with DCM) was used to verify TD-GC-MS results

² Novel methods

³ Conducted stepwise at temperatures matching those for TCA and TD-Py-GC-MS: 200, 300 (TD), 400, 500 and 850 (Py) °C.

III.3.1.4. Thermal Carbon Analysis

TCA of lignin SW treatment products was carried out on a Sunset (Tigard, OR, USA) thermal optical analyzer, based on a previously developed protocol.¹⁹⁴ Briefly, a sample, either solid (30–60 µg) or liquid suspension (5–10 µL either directly or after filtration via 0.45 µm filter), corresponding to typically up to 40 µg carbon, was submitted to TCA analysis conducted as described previously.¹⁹⁴ Compounds were thermally desorbed in a helium atmosphere at ambient

temperature, 200, and 300 °C, then pyrolyzed products were evolved at 400, 500 and 890 °C. Each temperature step from ambient through 500 °C was 6.00 min in duration, while the 890 °C step lasted 12.75 min. Then the oven was cooled to 550 °C and the flow stream switched to an oxidizing He/O₂ (10% O₂) carrier gas mixture followed by a second temperature ramp (550 to 890 °C). During the second heating step, char products were oxidized and detected. All species were quantitatively converted to CH₄ and measured by a flame ionization detector (FID).

III.3.1.5. Gel Permeation Chromatography

GPC was carried out on an Agilent 1100 Series HPLC with a diode array detector (DAD), monitoring wavelengths from 212 to 750 nm, using the method developed previously¹⁹⁸. Separation was accomplished using an Agilent PLgel 1000 Å column with a stationary phase consisting of a cross-linked porous polystyrene/divinylbenzene matrix (PSDVB). Unstabilized THF with water (9:1 ratio) was utilized as the mobile phase, with a flow rate of 1.0 mL/min, and an injection volume of 100 µL.

III.3.1.6. Gas Chromatography-Mass Spectrometry analysis

For direct LLE GC-MS analysis, an aliquot (1 mL) of SW samples (liquid phase) was spiked with a recovery standard (4-chloroacetophenone), acidified to pH 4 with glacial acetic acid and then extracted with three 1-mL aliquots of DCM. DCM extracts were analyzed directly or after derivatization with BSTFA, with further addition of an internal standard (*o*-terphenyl). For derivatization, a DCM extract of lignin reaction products (100 µL) was mixed with the BSTFA derivatization reagent in 1:1 (v/v) ratio and heated at 70 °C overnight (12 h).

GC-MS analyses were conducted on an Agilent (Santa Clara, CA, USA) GC7890 system with an MS 5975C detector, equipped with an HP-5MS capillary column (45 m length, 0.25 mm internal diameter and 0.25 μm film thickness). Injection was done in a splitless mode (0.2 min and 0.2 μL injection volume) and the injector temperature was set at 300 $^{\circ}\text{C}$. The column flow rate, with helium as a carrier gas, was 1.5 mL/min. The temperature program started at 50 $^{\circ}\text{C}$, was held for 1 min, and proceeded with a 40 $^{\circ}\text{C}/\text{min}$ gradient up to 80 $^{\circ}\text{C}$, followed by a second gradient of 25 $^{\circ}\text{C}/\text{min}$ up to 320 $^{\circ}\text{C}$, which was held for 7 min. The MS analysis included a solvent delay of 4 min and a scan mass range of 10–550 m/z using an electron ionization (EI) source at 70 eV.

III.3.1.7. Thermal Desorption-Pyrolysis-Gas Chromatography-Mass Spectrometry analysis

The TD-Py-GC-MS analyses were performed using a 5200 Series Pyroprobe (CDS Analytical, Inc., Oxford, PA, USA) with the GC-MS system described above. The TD-Py program consisted of sequential thermal treatment of liquid samples (5 μL) for 30 s at 110, 200, 300, 400, 500, and 10 s at 890 $^{\circ}\text{C}$, matching the temperature sequence used for TCA, with the exception of an early temperature fraction at 110 $^{\circ}\text{C}$ used to evolve water for SW treated samples. Solid samples were weighed to 30–60 μg on a microscale (Mettler Toledo, Columbus, OH, USA) and subjected to the same TD-Pyr temperature program, only without the 110 $^{\circ}\text{C}$ step. After each temperature step, the pyroprobe-GC-MS interface was opened for 2.5 min to allow full transfer of the analytes to the GC with a transfer line maintained at 300 $^{\circ}\text{C}$. Analytes were delivered to the GC-MS injection port operated in a split mode with a split ratio of 10:1. The MS mass range was lowered to 10 m/z in order to analyze air gases (H_2O , N_2 , O_2 , CO_2) and monitored up to 550 m/z as described in the data processing section. A solvent delay of 4.25 min was used only for the 110 $^{\circ}\text{C}$ step.

III.3.1.8. Elemental analyses

The elemental analysis of both non-treated lignin and SW-treated solid phase product (obtained at 300 °C) were conducted at Atlantic Microlab, Norcross, GA, USA).

III.3.2. Data Processing

GPC determination of MW as M_n (number-average MW), and M_w (mass-average MW) and M_z (z-number MW) values were based on standard GPC equations.⁷⁵ Data acquisition and chromatographic processing of LLE GC-MS and TD-Py-GC-MS data was accomplished via ChemStation software (Agilent, Santa Clara, CA, USA), with identification of analytes based on retention times and matching of mass spectra with EI library spectra (National Institute of Standards and Technology).²¹⁰ Quantification of LLE GC-MS species was accomplished through external standards as reported previously²⁰¹. Semi-quantitative profiles for TD-Py-GC-MS results were based on mean values of duplicate analyses, after subtraction of blanks (distilled water only), using extracted ion chromatograms characteristic for specific compounds.

To investigate the relationship between TCA and TD-Py-GC-MS results, the integrated chromatographic peak areas of TD-Py-GC-MS species (adjusted for carbon percentage) were normalized to the profiles of the corresponding TCA temperature fractions as wt.% carbon of the thermally desorbed fraction (obtained at 200 and 300 °C).

The approach to identification of gas species within TD-Py-GC-MS entailed the identification of a quantification ion and confirmation ions. The ions indicative of individual noncondensable gases were based on NIST EI mass spectra.²¹⁰

The CO₂ quantification was based on the base peak and molecular ion of 44 m/z , while ions 28, 16 and 12 m/z and their ratios were used for confirmation. The CO quantification was based primarily on 28 m/z , although this ion can also occur as the molecular ion of N₂ and a fragment for

CO₂. However, N₂ was observed only within the first minute of column elution together with O₂ with *m/z* of 32 as result of valve switching during sample introduction.

To prevent the overestimation of CO, the peak area of 28 *m/z* was adjusted (reduced) taking into account that this ion constitutes 10% of the 44 *m/z* peak for CO₂. CH₄ quantification was not based on the molecular ion of 16 *m/z* due to the common occurrence of this ion within the CO₂ mass spectrum; instead, 15 *m/z* (90% of 16 *m/z*) was used for this purpose as it appeared to be unique with regard to the other gases present in this mixture. Namely, although ion 15 *m/z* accounts for 12% and 8%, respectively, of the methanol and ethanol MS responses, the amounts of these compounds appeared to be negligible (less than 1% of CO₂). As ion 15 *m/z* was 90% of the CH₄ molecular peak (16 *m/z*), it was multiplied by 1.10 for quantification of CH₄. Confirmation ions 16, 14, and 12 *m/z* were also present.

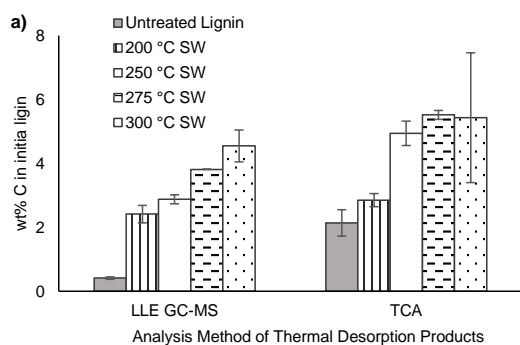
The occurrence of C₂H₄ in trace amounts was supported by the presence of characteristic ions 28, 27, 26, 25, 24 and 29 *m/z*. Ethane and propane were also possibly present in trace amounts, i.e., less than 1% of CO₂, but their characteristic ions shared with many gases made identification difficult; thus, the integrated areas were attributed to vastly more abundant gases such as CO₂, CO or CH₄.

The unidentified and unresolved peak areas were determined as integration total ion current after the subtraction of the identified species and baseline (obtained by running a blank sample). The C/H and C/O molar ratios were calculated based on TD-Py-GC-MS data. The relative atomic abundances were determined for each compound by multiplying the extracted ion ratio of the molar weight of the target atom (C, H or O) carbon atoms vs molar weight of the compound. The summed abundances for each element were used to determine the overall ratios in the sample for each temperature fraction.

III.3.3. Results and Discussion

III.3.3.1. Mass balance closure of subcritical water-treated lignin products

TCA enabled the mass balance closure and in-depth study of the thermal carbon fractionation of SW lignin treatment products in the liquid fraction (Figure 59). A nearly complete mass balance closure (~100 wt.%) was obtained based on the TCA quantification of carbon in the liquid fraction (unfiltered) and solid residues by gravimetry. The results of TCA analysis clearly demonstrated that the semivolatile (i.e., monomeric) fraction evolving by thermal desorption at 200 °C (including the products evolving at lower temperatures) and 300 °C represented only a small portion of the liquid product, which increased with higher temperatures of SW treatment. That is, while for the 200 °C SW treatment the TD fraction represented 2.9 wt.% (of the initial lignin), at 300 °C SW treatment the TD fraction increased to 5.4 wt.%, doubling the amount. A similar increase in the yield of monomer-like species with increasing SW temperature was observed earlier for individual compounds.¹⁸⁵



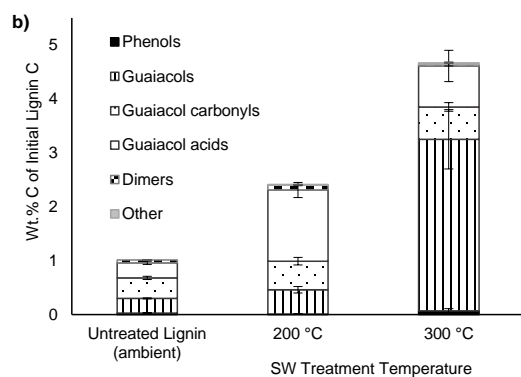


Figure 59. LLE-GC-MS characterization (a) compared of yields to TCA analyses of TD fractions (200 and 300 °C) of SW treated lignin samples; (b) distribution of classes of organic compounds in LLE extracts in untreated lignin, 200 °C SW treated lignin and 300 °C SW treated lignin. Data are presented as mean values and one standard deviation for three replicates.

Overall, the ratio of semivolatile products evolving during analysis at TD temperatures (200-300 °C, Figure 59a) to high MW products (recovered by the subsequent pyrolysis at temperatures above 400 °C to yield their pyrolytic markers, Figure 59a) increased with the temperature of SW treatment, thus indicating the occurrence of lignin depolymerization. By striking contrast to the study conducted under the conditions of enzyme catalyzed lignin cross-linking polymerization,²¹¹ the char fraction (denoted in charts as ‘550 – 890 °C with O₂’) obtained for liquid fraction samples *decreased* rather than increased after the SW treatment. This observation indicates a reduced impact of cross-linking/repolymerization for the SW treatment at temperatures below 350 °C.

Reduction of the char fraction was also particularly notable after liquid-phase sample filtering (demonstrated for the 300 °C SW treatment, Figure 59a). This unexpected effect becomes particularly pronounced when considering the normalized distribution over the temperature fractions (Figure 59b).

The use of unfiltered samples in this experiment was essential for accurate mass balance closure within each sample. The higher abundance of char observed in all unfiltered liquid samples after SW treatment (Figure 59a) was attributed to colloidal particles, i.e., resuspension of the solid phase products. Once filtered, the char fraction (i.e., that evolving only with oxygen, i.e., as a result of combustion) was virtually eliminated in the 300 °C SW treated sample (Figure 59b, the filtered sample), providing evidence that the liquid fraction contained little, if any, crosslinked repolymerization product up to 300 °C. However, in this sample the contribution of non-charred high-MW products (evolving at higher temperatures as pyrolytic markers) was found to be high, when normalized to the total product, as well as in the rest of the samples (Figure 59b), thus calling for a MW analysis to assess the balance of depolymerization/repolymerization trends.

III.3.3.2 Molecular weight distribution of lignin treatment products

A validated GPC analysis, with two sets of standards⁸¹ yielded information on average MW and molecular weight distribution of species in the liquid fractions of untreated alkaline lignin samples, SW treated filtered and unfiltered (300 °C) samples, as well as the solid fraction (residue) taken from the unfiltered and filtered SW treated samples (Figure 60). The M_n , M_w , and M_z values obtained from these samples are shown in Table 38.

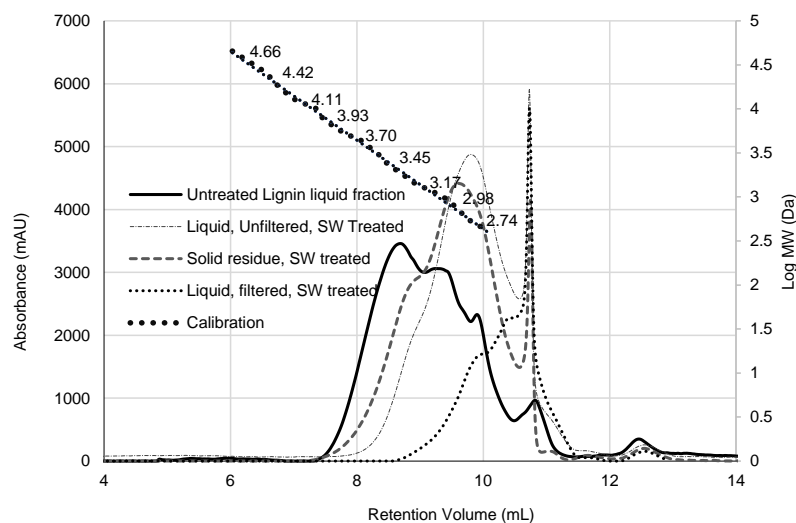


Figure 60. GPC analysis of thermally untreated lignin and SW treated (300 °C) lignin (filtered and unfiltered liquid fractions and solids residue) including PMMA and PS calibration on logarithmic scale.

Table 38. MW values calculated for liquid and solid fractions of alkali lignin degradation products (300 °C SW treated) and untreated alkali lignin, determined by GPC.

Treatment Type	M_n (Da)	M_w (Da)	M_z (Da)	Dispersity Index
300 °C SW treated, filtered liquid	460	615	823	1.34
300 °C SW treated, unfiltered liquid	812	1328	2086	1.64
300 °C SW treated, solid residue	1130	2039	3287	1.80
Untreated lignin	1631	2741	3723	1.68

The GPC data for the liquid phase products are consistent with the TCA analysis, showing lower MW organics in the filtered SW treated samples, although an M_z value of 823 suggested the

occurrence of oligomers (Table 38). The higher mass range for unfiltered liquid sample supported the occurrence of solid particles in suspension, which were subsequently completely dissolved in THF/water for GPC analysis. It is of note that all samples including the solid residue after the SW treatments dissolved in THF completely.

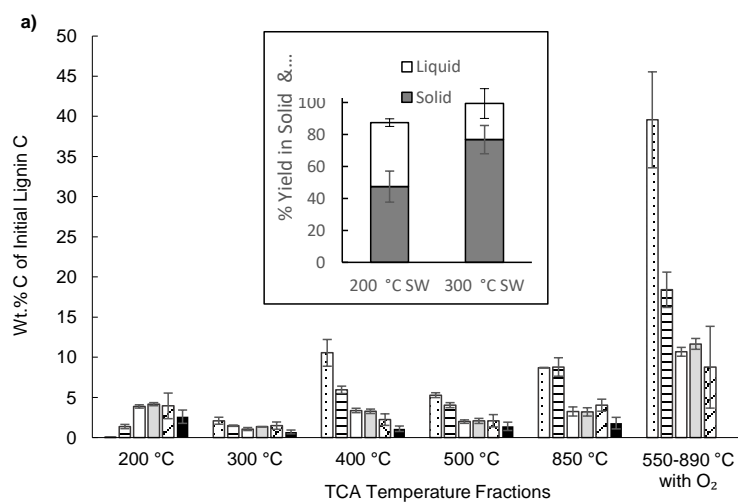
Both the average MW values (Table 38) and MW distribution (Figure 60) showed a significant lignin depolymerization compared to untreated lignin. It is of note that even the solid residue showed some reduction in molecular mass compared to lignin, corresponding to effective thermal breakdown. This finding is unexpected and counterintuitive, as the solid fraction may be viewed as a direct char precursor, i.e., a product of cross-linking/repolymerization. Yet, both TCA and GPC showed the reduction of cross-linked char and average MW, respectively, in the solid fraction compared to untreated lignin, thus indicating negligible repolymerization at the selected SW treatment temperatures.

As seen in Figure 60 and Table 38, the M_w of unfiltered lignin products was between that of soluble products and the solid residue, lending support to the idea that solids formed a suspension in water.

Once the evaluation of MW distribution was conducted, the next logical step in sample characterization was the assessment of chemical speciation, looking for insights into chemical composition, while using TCA as a “measuring stick,” i.e., carbon mass balance closure. The obtained information is analyzed in the following sections, separating low-MW and high-MW products.

III.3.3.3. Contribution of low molecular weight (TD) products

The comparison of thermally desorbed species in the combined TCA fractions at 200 and 300 °C to the total of quantified compounds using LLE GC-MS analysis results showed a good match for all SW treatments (Figure 61a). Thus, thermal and solvent extractions generally yielded similar efficiencies, as reported in previous studies as well.¹⁹⁴



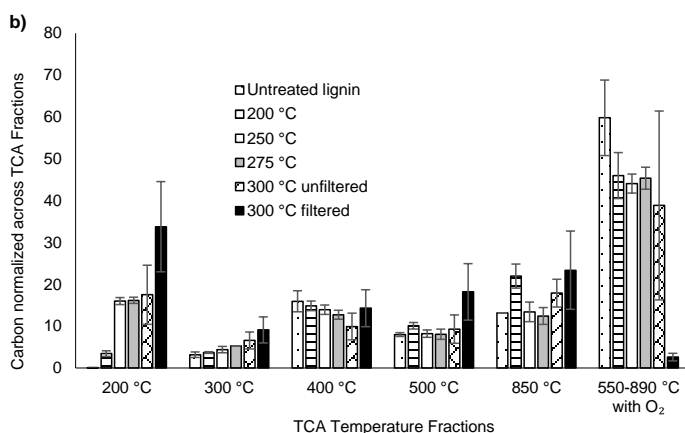


Figure 61. TCA characterization of liquid product SW treated lignin samples and comparison to untreated lignin: (a) wt.% C of initial lignin C. The insert shows gravimetric yield for solid and liquid fractions; (b) normalized to total carbon content.

A closer look at these data shows that the TCA based wt% of carbon for each temperature fraction was slightly higher than the total carbon of the GC-quantified compounds, possibly due to an incomplete quantification of LLE GC-MS data, as not all compounds may be GC-elutable. Furthermore, the lack of standards for some GC-elutable products, notably phenolic dimers, may lead to their underestimation as shown in our previous work.¹⁹⁶ Nevertheless, the similar data obtained by both methods support the suitability of a more rapid TCA as a tool for initial screening of lignin decomposition products as opposed to the LLE GC-MS extraction/analysis methodology since the TCA comparison provides a more comprehensive sum of carbon wt%.

While TCA provides a quantitative report of all (both low and high MW) organics over a broad range of TD-Py temperature fractions, LLE GC-MS shows the detailed speciation of low MW species (Figure 61b). Similar to Zhao et al., we observed by LLE GC-MS a significant increase in yields of guaiacol derivatives following the SW treatment at 300 °C in comparison to

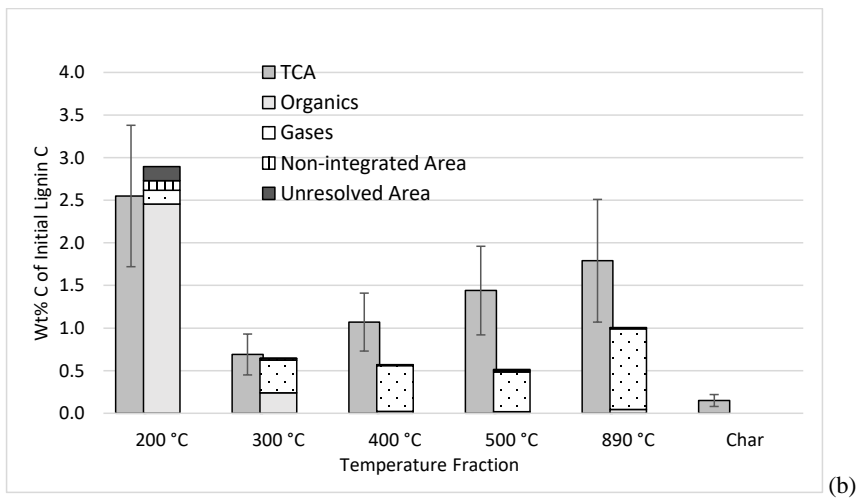
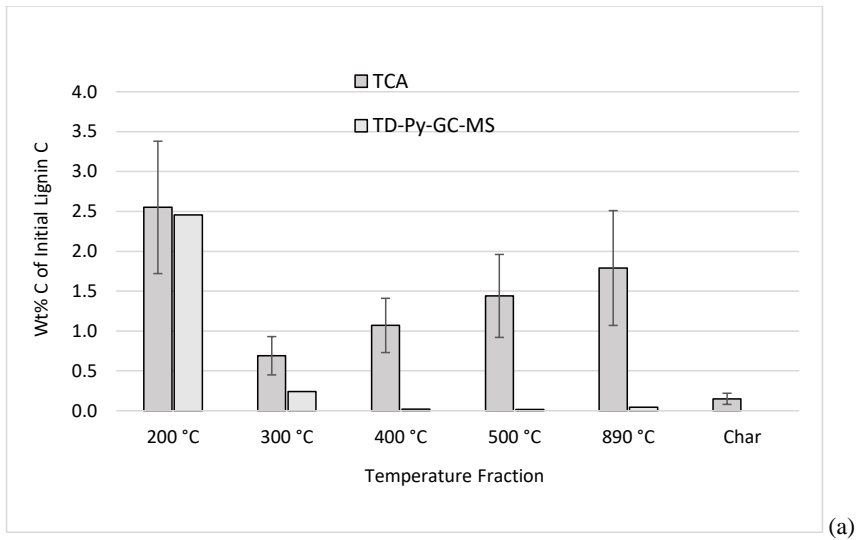
that at 200 °C, from approximately 20% (200 °C) to 60% (300 °C) of the LLE extractable species by mass (Figure 61b).¹⁹⁷ Yet, also just as in that study, the total yields of LLE extractable species in our study accounted only for a small fraction of initial lignin (~5%).

III.3.3.4. Comprehensive characterization of SW lignin degradation products obtained at 300 °C

Further analysis focused on products formed at 300 °C via SW treatment, as these showed the prevalence of low-MW products (Figure 61), along with the lowest char fraction (Figure 59). We evaluated the SW products based on TD-Pyr-GC-MS investigation of pyrolytic markers evolving as non-condensable gases, semi-quantification of unresolved and unidentified species-enabling improved quantification, distribution profiles of monomeric and dimeric species, and C/H and C/O ratios reported in the next two sections (3.3.5 and 3.3.6).

III.3.3.5. Gas phase and unresolved pyrolytic analysis markers

A significantly higher total carbon abundance was observed in the TCA pyrolytic (>300 °C) fractions compared to Py-GC-MS when the sum of compounds identified by Py-GC-MS was matched to the corresponding carbon data obtained from TCA (Figure 62a). This discrepancy appears to be too large to be fully explained by semi-quantitative GC-MS analysis using specific ions of varied ionization efficiency, especially as TD yields for LLE GC-MS and TCA SW treated samples were fairly closely aligned (Figure 62a, the leftmost set of bars).



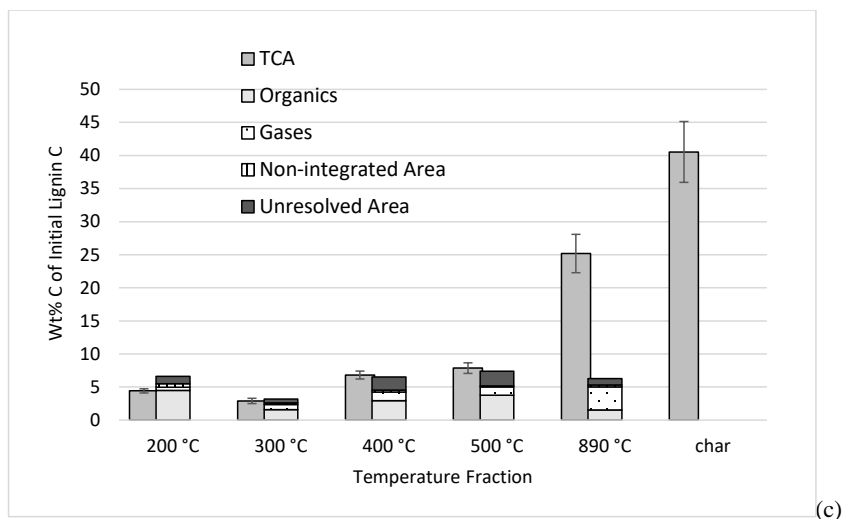


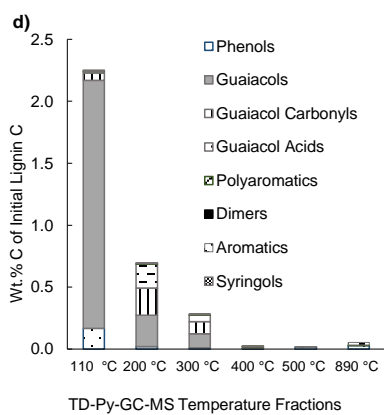
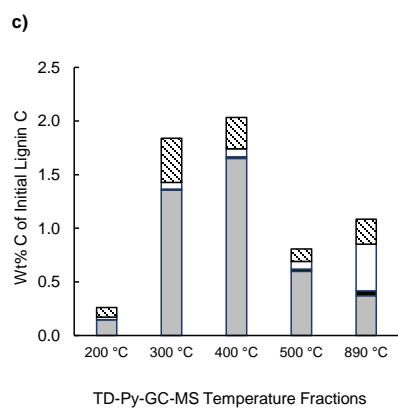
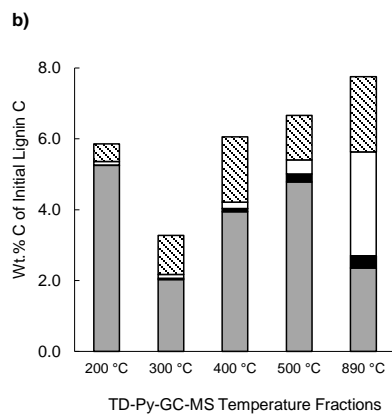
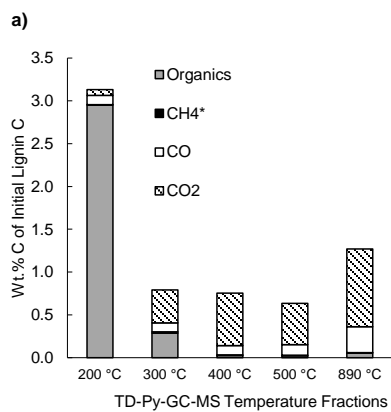
Figure 62. Comparison of TD-Py-GC-MS and TCA analyses of organic products from 300 °C SW treated lignin as (a) liquid filtered fraction without gas determination, (b) liquid filtered fraction including gases, nonintegrated area, and unresolved area (c) solid residue including including gases, nonintegrated area, and unresolved area.

So, a question was raised whether anything was missing in the obtained chromatograms. The missing information could be due to either unidentified or unresolved compounds (the latter comprising the chromatographic “hump”) often reported in complex matrices. Thus, the areas in chromatograms that are due to the unidentified and unresolved compounds were tentatively quantified and this information has been added to Figure 62.

As one can see, this addition did not make a significant contribution, particularly for the liquid product fraction, which showed only few unidentified and unresolved area, i.e., no chromatographic “hump.” This observation indicates that the products in the liquid fraction tend to pyrolyze into identifiable products, i.e., along well-defined patterns. The content of unresolved material in the chromatograms was higher in the SW treated solid residue but appeared most significantly in untreated lignin samples (being >30% in all Py fractions). This difference indicates

a greater recalcitrance of the solid residue toward random bond-breaking pyrolysis compared to untreated lignin.

A more plausible explanation for the discrepancy in results between the methods is a formation of low-molecular weight gases ($< 30 m/z$). Indeed, the MS analysis showed the production of significant amounts of gases during Py-GC. To adjust for the observed difference between the TCA and Py-GC-MS data, we have included gas species' semi-quantification (e.g., that of methane, CO/ ethene, and CO₂); the results of detailed gas analysis are provided in Figure 63a-c. This treatment led to a good match between the TCA and Py-GC data (Figure 62, panel b), except for the “hard” pyrolysis occurring at 890 °C, which may result from the formation of such reactive species, e.g., free radicals, that do not reach the GC detector being instead adsorbed on the column material.



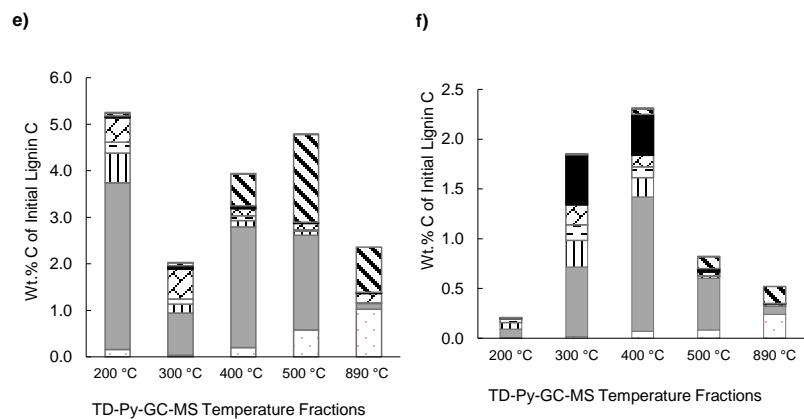


Figure 63. TD-Py-GC-MS semiquantitative gases (a-c) & organics (d-f) profiles for (a, d) SW treated (300 °C) liquid fraction, (b, e) SW treated (300 °C) solid fraction and (c, f) thermally untreated lignin samples. For SW treated liquid fraction the pyroprobe program was started at 110 °C to eliminate impact of water on consecutive fractions. Thus, a total of 110 and 200 °C should be compared to 200 °C for untreated lignin.

The predominant pyrolytic marker was CO₂, evolving along with water for temperatures at 300–500 °C (Figure 63a-c). While the CO₂ occurrence at lower temperature can be ascribed to decarboxylation, its high abundance at higher pyrolytic temperature suggests decomposition in a combustion-like process. Other pyrolytic markers including methane, ethene and CO were observed, significantly increasing in abundance toward 890 °C.

Although conversion to noncondensable gases is known to occur during pyrolytic processes,^{212,213} the amounts of gases observed in our study were rather extensive for pyrolytic events of 30 s duration, particularly at high temperatures. A plausible explanation may be the full decomposition of some organics at pyrolytic temperatures to CO₂ and other low MW gases, which was reported for matrices with a sufficient content of oxygen,^{212,213} e.g., lignin.

It is of note that the untreated lignin forms less gases upon pyrolysis whereas the solid residue of SW treatment products forms the most of them (Figures 63c and d, respectively –

compare the y-axis scales). This difference, along with the observed reduction in MW and a lower propensity to form char upon pyrolysis (shown in the earlier sections) indicate that the oligomeric products of lignin breakdown appear to be significantly altered compared to the original lignin. This assumption is evaluated in the next section based on characteristic speciation markers in the pyrolytic fractions.

III.3.3.6. Comparison of oligomer/polymer distribution

The distribution of organic compound classes within the temperature fractions of TD-Py-GC-MS analysis was compared for both SW treated (300 °C) filtered liquid and solid fractions as well as untreated lignin (Figure 63d-f, respectively). The products of SW treatment showed abundant GC-elutable compounds evolving at low TD temperatures (Figure 63d,e), thus confirming significant lignin depolymerization. The majority of volatile TD species following the SW treatment was represented by guaiacol derivatives (90%); this was in contrast to the untreated lignin, for which these species represented only about 50% while most of the peaks evolved at higher temperatures.

The Py profiles of the solid residue and untreated lignin (Figure 63b and c, respectively) also exhibited two notable exceptions. First, the solid residue from SW treated lignin showed few dimers or guaiacol carbonyl compounds, unlike lignin for which these pyrolytic markers were abundant. The absence of dimers and retene derivatives in either liquid or solid fractions evolving as pyrolytic markers following the SW treatment suggests a breakdown to simpler compounds or increased conversion to more recalcitrant solids occurring during the SW treatment. By contrast, guaiacols, phenol and methylphenols evolved at low TD temperatures from the solid residues of SW treated samples as well as from the liquid fraction- in contrast to untreated lignin, which

evolved these compounds only as pyrolytic markers at higher TD-Py temperatures. Their occurrence in the TD fraction suggests that they were unaltered products of SW treatment rather than the species formed during the GC-Py analysis. Furthermore, these observations indicate that the solid residue after the treatment is more recalcitrant toward pyrolysis than the original lignin.

Second, aromatic hydrocarbons were more abundant evolving during the pyrolytic steps of analysis for SW treated solid residue compared to the untreated lignin, indicating that the evolving species contain less oxygen. Note that the peak areas of phenols and aromatic hydrocarbons were small in the solids' TD fractions, below 300 °C (10% of all phenol and 3% of all aromatic hydrocarbons); they occurred mainly in high temperature (pyrolytic) fractions. Deoxygenation of the solid residue appears to explain that, despite a lower MW than that of the original lignin (as shown by GPC), the solid residue becomes more recalcitrant toward further depolymerization compared to the untreated lignin.

III.3.3.7. Elemental analysis and C/H and C/O ratios

This conclusion was directly supported by elemental analysis of both the solid residue obtained at 300 °C and untreated lignin (Table 39). Unlike the element ratios reported in Table 39, elemental analysis provides the comprehensive, overall sample characterization including the char. The results showed that the percentage of oxygen in solid residue became significantly reduced compared to lignin, while the carbon content increased.

Table 39. Elemental analysis and C/H and C/O ratios calculated for SW treated samples (filtered liquid and residue solids) and for untreated lignin samples. The ratios are based on C, H, and O content of identified species present in samples from TD-Py-GC-MS analysis. Ratios were calculated without noncondensable gases generated during analysis, and also with the gases (CO₂, CO and CH₄).

Elemental analysis										
	% Carbon		% Hydrogen		% Nitrogen		% Sulfur		% Oxygen	
	mean	SD	mean	SD	mean	SD	mean	SD	mean	SD
SW treated solids	69.76	0.23	5.48	0.05	0.60	0.08	0.67	0.06	23.48	0.33
Untreated lignin	63.11	0.88	5.71	0.21	0.53	0.10	1.25	0.03	29.35	0.70

C/H & C/O ratios at TD-Py temperature fractions									
	110 °C	200 °C	300 °C	400 °C	500 °C	890 °C	TD fraction	Pyr fraction	Total sample
C/H w/o gases									
SW filtered liquid	0.84	0.84	0.86	0.90	0.90	0.94	0.84	0.92	0.84
SW treated solids		0.80	0.79	0.85	0.84	0.92	0.80	0.86	0.83
Untreated lignin		0.90	0.87	0.84	0.83	0.88	0.87	0.84	0.85
C/H gases included									
SW filtered liquid	0.84	0.86	1.02	3.61	3.83	3.70	0.86	3.71	0.94
SW treated solids		0.81	0.83	0.90	0.87	1.12	0.81	0.93	0.87
Untreated lignin		0.99	0.90	0.86	0.85	0.99	0.91	0.87	0.89
C/O w/o gases									
SW filtered liquid	3.82	3.14	3.23	4.51	10.93	13.57	3.57	8.50	3.63
SW treated solids		4.29	5.58	4.16	4.58	10.23	4.64	4.94	4.80
Untreated lignin		3.06	4.12	4.05	4.34	6.95	4.02	4.31	4.19
C/O gases included									
SW filtered liquid	3.82	2.88	1.82	0.68	0.71	0.75	3.17	0.72	2.29
SW treated solids		3.97	3.82	2.96	3.55	2.59	3.92	3.07	3.39
Untreated lignin		2.12	3.34	3.51	3.53	2.68	3.20	3.37	3.30

To compare the level of deoxygenation among the fractions (liquid vs. solid), we determined the C/H and C/O molar ratios from the Td-Pyr-GC-MS analyses (Table 39) with and without taking into account the gases produced during the TD-Py-GC analysis. The further discussion will focus on the totals for TD and Py fractions, which are boldfaced in the table for reader's convenience.

Comparison of treated and untreated lignin showed that the TD fraction ratios were not significantly altered by the gas phase species addition into calculations – as expected, because very little CO₂, if any, was released during TD-Py-GC-MS analysis at 200 °C while the amount of gases released at 300 °C was still low. By contrast, some C/H values significantly increased and C/O values significantly decreased for Py temperatures when gases (mainly CO₂) were added into calculations. This observation is consistent with the high CO₂ amounts evolving at these temperatures (Figure 63a-c).

However, this effect was not uniform, being the least significant for untreated lignin (Table 39). The effect was more significant for the solid residue and became particularly conspicuous for the liquid product fraction. Thus, the high-MW products (i.e., those evolving at pyrolytic temperatures) in the liquid fraction were significantly oxygenated, much more than their Py-GC chromatograms showed, because the main path of their pyrolysis was decarboxylation releasing large amounts of CO₂.

The solid residue did not release as much of CO₂ upon pyrolysis as the liquid product fraction. Nonetheless, the C/O ratio significantly increased for the solid residue compared to the liquid product fraction, thus pointing at the solid phase products' significant deoxygenation. This calculation confirms quantitatively a similar qualitative observation obtained from the analysis of Py chromatograms.

III.3.3.8. Repolymerization vs. deoxygenation: considerations and insights

The observation of significant solid residue deoxygenation may explain the notoriously low efficiency of lignin depolymerization to phenolic monomers observed in literature, even under the conditions when the competing repolymerization is hindered, as in this study. If most of oxygen is removed, an SW treatment *per se* is unlikely to break the remaining C-C bonds. This hypothesis is corroborated by recent studies which have demonstrated that technical lignins, i.e., those isolated from plants by harsh treatments, such as the kraft process, feature a rather low content of the original ether bonds characteristic of native plant lignin, being replaced with C-C bonds.^{50,214,215} When lignin was isolated in the presence of formaldehyde, protecting the ether bonds from cleavage, the resulting near-native lignin yielded 47–78 mol% of phenolic monomers upon hydrogenolysis, 3–7 times greater than without the formaldehyde pretreatment.²¹⁶ Thus, deoxygenation of lignin results in its greater recalcitrance.

Corroborating our observations, several authors pointed out increased C/O and C/H ratios with higher temperature SW treatments.^{173,186} It was suggested that insoluble fractions may consist of undissolved modified lignin, whose amount increases with higher temperatures due to cross-linking reactions.¹⁶⁹ Given that the study of Pinkowska was conducted at higher temperatures, our study did not show any significant cross-linking for SW treatment at 300 °C: In addition to decreased MW (Figure 60), the recovered solid residue featured a similar hydrogen content to the original lignin (Table 39), which would be inconsistent with crosslinking occurring via condensation reactions. It is assumed that repolymerization rates increase with temperature as a result of increased degradation, but requires longer residence times to occur.^{174,178} Our observations are consistent with these conclusions, adding deoxygenation as a specific process

occurring at relatively low treatment temperatures instead of repolymerization, although it may be ‘disguised’ as repolymerization based on the solid residue’s recalcitrance.

The study by Zhao et al. found that repolymerization rates became significant only at temperatures above 325 °C.¹⁸⁵ Thus, deoxygenation appears to be the main process route within a narrow temperature range not significantly exceeding 300 °C. It may still be significant at higher temperatures being combined with repolymerization.

By contrast, several studies conducted as lignin solvent-free fast pyrolysis (as opposed to SW treatment) claimed repolymerization as the main reaction path, even at relatively low temperatures. Namely, for pyrolysis of the THF-soluble (i.e., low-MW) lignin fraction repolymerization became significant even at 175 °C, as the product became mostly THF-insoluble.²¹⁷ A 100-fold increase in free radical concentration was observed upon lignin fast pyrolysis when temperature increased from 100 to 300 °C.²¹⁸ In contrast to our study, a rather high C/H ratio (near 1.25) was observed by elemental analysis in the solid-phase product of lignin pyrolysis at 200 °C.²¹⁹ Thus, the different process path observed in this study for SW treatment points at the significant solvent effect that appears to reduce the interactions between the reactive intermediates.

III.3.4. Conclusions

The current study complements the earlier investigations of polymeric products after SW treatment at intermediate temperatures, 250-300 °C, by reporting significant solid product deoxygenation rather than cross-linking repolymerization as the main reaction path. The bottleneck in increasing the lignin depolymerization efficiency thus becomes the treatment of deoxygenated, i.e., more resilient, solid residue. This feature may explain, either by itself or

combined with repolymerization, the well-known recalcitrance of solid products of lignin treatment, i.e., they cannot be efficiently re-treated or recycled. Perhaps a separate subsequent oxidative treatment of this residue may increase the yield of useful low-MW phenolic products.

IV. References

1. McCarthy, J., Islam, A. Lignin chemistry, technology and utilization- a brief history In *Lignin: Historical, Biological and Materials Perspectives*. Glasser, W., Northey, R., Schultz, T., Ed. American Chemical Society: 2000; pp 2 – 99.
2. Hon, D., and Shiraishi, N. *Wood and Cellulosic Chemistry*. 2nd ed.; CRC Press: 2000.
3. Welker, C., Balasubramanian, V., Petti, C., Rai, K., DeBolt, S., Mendu, V. Engineering Plant Biomass Lignin Content and Composition for Biofuels and Bioproducts. *Energies*. **2015**, *8*, 7654–7676.
4. De Jong, E., Gosselink, R. Lignocellulose-Based Chemical Products In *Bioenergy Research, Advances and Applications*. Gupta, V., Kubicek, C., Saddler, J., Xu, F., Tuohy, M., Ed. Elsevier: 2013; pp 277 – 309.
5. Hatakeyama, T., Hatakeyama, H., Lignin. In *Thermal Properties of Green Polymers and Biocomposites*. Kluwer Academic Publishers: 2006; pp 171 – 215.
6. Gellerstedt, G., Tomani, P., Axegard, P., Backlund, B. Lignin Recovery and Lignin-Based Products. In *Integrated Forest Biorefineries: Challenges and Opportunities*. Christopher, L., Clark, J., Kraus, G., Ed. Royal Society of Chemistry: 2012; pp 180 – 210.
7. Pure Lignin. Lignin. <http://purelignin.com/lignin/> (accessed Jan. 2017).
8. Electronic Take Back Coalition. Facts and Figures on E-Waste and Recycling. http://www.electronicstakeback.com/wp-content/uploads/Facts_and_Figures_on_EWaste_and_Recycling.pdf (accessed Jan. 2017).
9. Eco360 Trust. Plastic Garbage. <http://www.sustainablecommunication.org/eco360/what-is-eco360s-causes/plastic-garbage> (accessed Jan. 2017).
10. U.S. Environmental Protection Agency. Municipal Solid Waste Generation, Recycling, and Disposal in the United States: Facts and Figures for 2012. <https://www.epa.gov/facts-and-figures-about-materials-waste-and-recycling/advancing-sustainable-materials-management> (accessed April 2018)
11. Bajpai, P. Biopulping. In *Biotechnology for Pulp and Paper Processing*, 2nd ed.; Springer: 2018; pp 113 – 147.
12. Gargulak, J., Lebo, S. Commercial Use of Lignin-Based Materials In *Lignin: Historical, Biological, and Materials Perspectives*. Glasser, W., Northey, R., Schultz, T., Ed. ACS Publications: 1999; pp 304 – 320.
13. Upton, B., Kasko, A. Strategies for the Conversion of Lignin to High-Value Polymeric Materials: Review and Perspective. *Chem. Rev.* **2015**, *116* (4), 2275 – 2306.

14. Fakhrai, R. Black Liquor Combustion in Kraft Recovery Boilers- Numerical Modelling. Dissertation, Kungl Tekniska Hogskolan, Stockholm, Sweden, 2002.
15. Doherty, W., Mousavioun, P., Fellows, C. Value-Adding to Cellulosic Ethanol: Lignin Polymers. *Ind. Crop. Prod.* **2011**, 33 (2), 259 – 276.
16. International Lignin Institute. About Lignin. Accessed May 2018 at <http://www.ili-lignin.com/aboutlignin.php>
17. Garcia, J., Diez, A. Use of Kraft Pine Lignin in Controlled Release Fertilizer Formulations. *Chem. Res.* **1996**, 35, 245 – 249.
18. Sipponen, M., Rojas, O. Calcium Chelation of Lignin from Pulping Spent Liquor for Water-Resistant Slow-Release Urea Fertilizer Systems. *ACS Sustain. Chem. Eng.* **2017**, 5 (1), 1054 – 1061.
19. Calvo-Flores, F., Dobado, J., Isac-Garcia, J., Martin-Martinez, F. Applications of modified and unmodified lignins. In *Lignins and Lignans as Renewable Raw Materials: Chemistry, Technology and Applications*. John Wiley and Sons: **2015**; pp 269 – 313.
20. Meier, D., Zuniga-Partida, V. Conversion of technical lignins into slow-release nitrogenous fertilizers by ammoxidation in liquid phase. *Bioresour. Technol.* **1994**, 49 (2), 121 – 128.
21. Obst, J., Kirk, K. Isolation of Lignin. In *Methods in Enzymology- Biomass, part b. Lignin, pectin and chitin*. Wood, W., Kellogg, S. , Ed. Academic Press: **1988**; Vol. 161, pp 3 –12.
22. Espinoza-Acosta, J., Torres-Chavez, P., Ramirez-Wong, B., Lopez-Saiz, C., Montano-Leyva, B. Antioxidant, Antimicrobial, and Antimutagenic Properties of Technical Lignins and Their Applications. *Bioresources* **2016**, 11 (2), 5452 – 5481.
23. Chundawat, S., Sousa, L., Dale, B. , Thermochemical pretreatment of lignocellulosic biomass. In *Bioalcohol Production*, Waldron, K., Ed. Woodhead Pub., **2010**, 24 –72.
24. Bruijninx, P., Gruter, G. The Importance of a Full Value Chain Approach. [www.dutchbiorefinerycluster.nl/download/413/documenten/Lignin_valorisation - APC June 2016](http://www.dutchbiorefinerycluster.nl/download/413/documenten/Lignin_valorisation_-_APC_June_2016) (accessed April 2019).
25. Nasrullah, A., Bhat, A., Khan, A., Ajab, H. , Comprehensive approach on the structure, production, processing and application of lignin. In *Lignocellulosic Fibre and Biomass-Based Composite Materials Processing, Properties and Applications*, Woodhead Publishing: 2017; pp 165 – 178.
26. Ashter, S., Derivation of monomers from biomass In *Technology and Applications of Polymers Derived from Biomass*, Elsevier: 2018; pp 137 – 147.
27. Sahoo, S., Seydibeyoglu, M., Mohanty, A., Misra, A. Characterization of industrial lignins for their utilization in future value added applications. *Biomass Bioenergy.* **2011**, 35 (110), 4230 – 4237.

28. Agrobiobase. Protobind (GreenValue Enterprises LLC). <http://www.agrobiobase.com/en/database/bioproducts/plastics-composites-rubber/protobind> (accessed April 2021).
29. TCI (Tokyo Chemical Industry Co. LTD). Lignin Products. <https://www.tcichemicals.com/JP/en/search/?text=lignin> (accessed April 2021).
30. Millipore-Sigma Inc. Lignin Products. <https://www.sigmaaldrich.com/US/en/search/lignin?focus=products&page=1&perPage=30&sort=relevance&term=lignin&type=product> (accessed April 2021).
31. Ingevity, Inc. Indulin AT. <https://www.ingevity.com/products/indulin-at-batteries/> (accessed April 2021).
32. Beis, S., Mukkamala, S., Hill, N., Joseph, J., Baker, C., Jenson, B., Stemmler, E., Wheeler, C., Frederick, B., Van Heiningen, A., Berg, A., DeSisto, J. Fast pyrolysis of lignin. *Bioresources*. **2010**, 5 (3), 1408 – 1424.
33. Aro, T., Fatehi, P. Production and Application of Lignosulfonates and Sulfonated Lignin. *ChemSusChem*. **2017**, 10 (9), 1861 – 1877.
34. Green AgroChem Co. Sodium Lignosulfonate Products. <https://www.greenagrochem.com/products/sodium-lignosulfonate/> (accessed April 2021).
35. Klason, P. *Svensk Kem. Tidskr.* **1897**, 9, 133.
36. Erdtman, H. Dehydrierungen in der coniferylreihe (1) Dehydrodieugenol und dehydrodiisoeugenol. *Biochem Z.* **1933**, 258, 172 – 180.
37. Lange, P. On the nature of the lignin and its distribution in spruce wood. *Svensk. Papperstidn.* **1944**, 47, 262 – 265.
38. Freudenberg, K. Lignin: Its Constitution and Formation from p-Hydroxycinnamyl Alcohols. *Science*. **1965**, 148 (3670), 595 – 600.
39. Adler, E. Lignin Chemistry- Past, Present and Future. *Wood Sci. Technol.* **1977**, 11, 169 – 218.
40. Goldschmid, O. Determination of Phenolic Hydroxyl Content of Lignin Preparations by Ultraviolet Spectrophotometry. *Anal. Chem.* **1954**, 26 (9), 1421 – 1423.
41. Hergert, H., Infrared Spectra. In *Lignins: Occurrence, Formation, Structure and Reactions*, Sarkanen, K., Ludwig, C., Ed. Wiley Interscience: **1971**; pp 267-293.
42. Lundquist, K. ¹H-NMR Spectral Studies of Lignins: Quantitative Estimates of Some Types of Structural Elements. *Nord.Pulp Paper Res. J.* **1991**, 6 (3), 140 – 146.

43. Gellerstedt, G. Gel Permeation Chromatography. In *Methods in Lignin Chemistry* Lin, Y., Dence, C., Ed. Springer-Verlag: **1992**; pp 487– 497.
44. Lancefield, C., Constant, S., de Peinder, P., Bruijninx, P. Linkage Abundance and Molecular Weight Characteristics of Technical Lignins by Attenuated Total Reflection-FTIR Spectroscopy Combined with Multivariate Analysis. *ChemSusChem*. **2019**, *12* (6), 1139 –1146.
45. Moon, D., Shin, S., Choi, J., Park, J., Kim, W., Kwon, M. Chemical modification of secondary xylem under tensile stress in the stem of *Liriodendron tulipifera*. *Forest Sci. Technol.* **2011**, *7*, 53 – 59.
46. Tarasov, D., Leitch, M., Fatehi, P. Lignin-carbohydrate complexes: properties, applications, analyses, and methods of extraction: a review. *Biotechnol. Biofuels*. **2018**, *11*, 269.
47. Liu, X., Bouxin, F., Fan, J., Budarin, V., Hu, C., Clark, J. Recent Advances in the Catalytic Depolymerization of Lignin towards Phenolic Chemicals: A Review. *ChemSusChem*. **2020**, *13* (13), 4296 – 4317
48. Farmers Weekly. 9 reasons to plant trees on your land. <https://www.fwi.co.uk/news/9-reasons-plant-trees-land> (accessed April 2021).
49. Rinaldi, R., Jastrzebski, R., Clough, M., Ralph, J., Kennema, M., Bruijninx, P., Weckhuysen, B. Paving the Way for Lignin Valorisation: Recent Advances in BioEngineering, Biorefining and Catalysis. *Angew. Chem. Int. Ed.* **2016**, *55*, 8164 – 8215.
50. Constant, S., Wienk, H., Frissen, A., de Peinder, P., Boelens, R., Van Es, D., Grisel, R., Weckhuysen, B., Huijgen, W., Gosselink, R., Bruijninx, P. New insights into the structure and composition of technical lignins: a comparative characterization study. *Green Chem.* **2016**, *18*, 2651– 2665.
51. Parthasarathi, R., Romero, R., Redondo, A., Gnanakaran, S. Theoretical Study of the Remarkably Diverse Linkages in Lignin. *J. Phys. Chem. Lett.* **2011**, *2* (20), 2660– 2666.
52. Huang, J., Wu, S., Cheng, H., Lei, M., Liang, J., Tong, H. Theoretical study of bond dissociation energies for lignin model compounds. *J. Fuel Chem. Technol.* **2015**, *43* (4), 429 – 436.
53. Vanholme, R., Demedts, B., Morreel, K., Ralph, J., Boerjan, W. Lignin Biosynthesis and Structure. *Plant Physiol.* **2010**, *153*, 895 – 905.
54. La Flouche, A., Jourdes, M. Polysaccharides and lignin from oak wood used in cooperage: Composition, interest, assays: A review. *Carbohyd. Res.* **2015**, *417*, 94 – 102.
55. Marton, J. Reactions in alkaine pulping. In *Lignins: Occurrence, Formation, Structure and Reactions*, Sarkanen, K., Ed. John Wiley & Sons: 1971; pp 639 – 694.

56. Gierer, J. Chemistry of delignification, Part 1: General concept and reactions during pulping. *Wood Sci. Technol.* **1985**, *19*, 289 – 312.
57. Sjöström, E. *Wood Chemistry, Fundamentals and Applications*. Academic Press: 1993.
58. Rak, M., Tomislav, F. Mechanochemical synthesis of Au, Pd, Ru and Re nanoparticles with lignin as a bio-based reducing agent and stabilizing matrix. *Faraday Disc.* **2014**, *170*, 155 –167.
59. Zakzeski, J., Bruijninx, P., Jongerius, A., Weckhuysen, B. The Catalytic Valorization of Lignin for the Production of Renewable Chemicals. *Chem. Rev.* **2010**, *110*, 3552 – 3599.
60. Xue, Y., Li, Y., Liu, Z., Hou, Y. Structural Changes of Lignin in Soda Delignification Process and Associations with Pollution Load. *Bioresources* **2019**, *14* (4), 7869 –7885.
61. Svensson, S. Minimizing of the sulphur content in Kraft lignin. Thesis, Mälardalen University, Vasteras, Sweden, 2008.
62. Oberlerchner, J., Rosenau, T., Potthast, A. Overview of Methods for the Direct Molar Mass Determination of Cellulose. *Molecules* **2015**, *20* (6), 10313 – 10341.
63. Malvern Instruments. White paper: Static Light Scattering Technologies for GPC-SEC Explained. <https://www.chem.uci.edu/~dmitryf/manuals/Fundamentals/SLS%20Technologies%20GPC-SEC%20Explained.pdf> (accessed April 2020).
64. Lange, H., Rulli, F., Crestini, C. Gel Permeation Chromatography in Determining Molecular Weights of Lignins: Critical Aspects Revisited for Improved Utility in the Development of Novel Materials. *ACS Sustain. Chem. Eng.* **2016**, *4* (10), 5167 – 5180.
65. Glasser, W., Frazier, C., Dave, V. Molecular Weight Distribution of (Semi-) Commercial Lignin Derivatives. *J. of Wood Chem. & Tech.* **1993**, *13* (4), 545 –559.
66. Tolbert, A., Akinosho, H., Khunsupat, R., Naskar, A., Raugauskas, A. Characterization and analysis of the molecular weight of lignin for biorefining studies. *Biofuels.* **2014**, *8*(6), 836 –56.
67. Agilent Technologies. An Introduction to Gel Permeation Chromatography and Size Exclusion Chromatography. <https://www.agilent.com/cs/library/primers/Public/5990-6969EN%20GPC%20SEC%20Chrom%20Guide.pdf> (accessed April 2020).
68. Held, D. (Chromatography Online) What are the differences between GPC, SEC and GFC, and how do you get started with the technique? <http://www.chromatographyonline.com/tips-tricks-gpc-sec-what-are-differences-between-gpc-sec-and-gfc-and-how-do-you-get-started-technique> (accessed April 2020).
69. Gellerstedt, G. Gel Permeation Chromatography, in *Methods in Lignin Chemistry*, Chap. 8. Eds. Lin, Y., Dence, C., Springer Series in Wood Chemistry; Springer-Verlag, New York, N.Y. 1992, 487 – 497.

70. Byrne, F., Jin, S., Paggiola, G., Petchey, T., Clark, J., Farmer, T., Hunt, A., McElroy, C., Sherwood, J. Tools and techniques for solvent selection: green solvent selection guides. *Sust. Chem. Proc.* **2016**, *4*, 7.
71. Rudatin, S., Sen, Y. L., and Woerner, D. L. Association of kraft lignin in aqueous solution. In *Lignin: Properties and Materials*, W. G. Glasser, Ed. American Chemical Society: 1989; pp 144 – 154.
72. Vermaas, J., Crowley, M., Beckham, G. Molecular Lignin Solubility and Structure in Organic Solvents. *ACS Sust.Chem. Eng.* **2020**, *8*, 17839 – 850.
73. Jackson, C., Barth, H. Molecular Weight-Sensitive Detectors for Size Exclusion Chromatography In *Handbook of Size Exclusion Chromatography and Related Techniques*, 2nd ed.; Wu, C., Ed. Marcel Dekker: 2004; pp 99 –139.
74. Brewer, A. GPC Column Materials. In *Encyclopedia of Polymeric Nanomaterials*, Kobayashi, S., Mullen, K., Ed. Springer: 2015.
75. Agilent. Technical Overview: Polymer Molecular Weight Distribution and Definitions of MW Averages. <https://www.agilent.com/cs/library/technicaloverviews/public/5990-7890EN.pdf> (accessed April 2020).
76. Brodin, I. Chemical properties and thermal behaviour of kraft lignins. Thesis, KTH Royal Institute of Technology, Stockholm, Sweden, 2009.
77. Delgado, N., Chavez, G., Ysambertt, F., Bravo, B. Valorization of Kraft Lignin of Different Molecular Weight as Surfactant Agent for the Oil Industry. *Waste Biomass Valori.* **2019**, *10*, 3383 – 3395.
78. Asikkala, J., Tamminen, T., Argyropoulos, D. Accurate and reproducible determination of lignin molar mass by acetobromination. *J. Agric. Food Chem.* **2012**, *60*, 8968 – 8973.
79. Chen, F., Li, J. Aqueous gel permeation chromatographic methods for technical lignins. *J. Wood Chem. Technol.* **2000**, *20*, 265 – 276.
80. Schmidl, G. Molecular Weight Characterization and Rheology of Lignins for Carbon Fibers. Dissertation, University of Florida, Gainesville, FL, 1992.
81. Andrianova, A., Yeudakimenka, N., Lilak, S., Kozliak, E., Ugrinov, A., Sibi, M., Kubátová, A. Size exclusion chromatography of lignin: The mechanistic aspects and elimination of undesired secondary interactions *J. Chromatogr. A* **2018**, *1534*, 101 – 110.
82. Waters Corp. What can polymer scientists do when using GPC/SEC? https://www.waters.com/waters/en_US/GPC-%26-SEC-Columns/nav.htm?cid=513226 (accessed April 2020).

83. Sameni, J., Krigstin, S., and Sain, M. Characterization of lignins isolated from industrial residues and their beneficial uses. *Bioresources*. **2016**, *11*(4), 8435 – 8456.
84. Fredheim, G., Braaten, S., Christensen, B. Molecular weight determination of lignosulfonates by size-exclusion chromatography and multi-angle laser light scattering. *J. Chromatogr. A*. **2002**, *942*, 191 – 199.
85. Yuan, T., You, T., Wang, W., Xu, F., Sun, R. Synergistic benefits of ionic liquid and alkaline pretreatments of poplar wood. Part 2: Characterization of lignin and hemicelluloses. *Bioresour. Technol.* **2013**, *136*, 345 – 350.
86. Wörmeyer, K., Ingram, T., Saake, B., Brunner, G., Smirnova, I. Comparison of different pretreatment methods for lignocellulosic materials. Part II: Influence of pretreatment on the properties of rye straw lignin. *Bioresour. Technol.* **2011**, *102*, 4157 – 4164.
87. Sadeghifar, H., Wells, T., Le, R., Sadeghifar, F., Yuan, J., Ragauskas, A. Fractionation of Organosolv Lignin Using Acetone:Water and Properties of the Obtained Fractions. *ACS Sustain. Chem. Eng.* **2017**, *5* (1), 580 – 587.
88. Allegretti, C., Fontanay, S., Rischka, K., Strini, A., Troquet, J., Turri, S., Griffini, G., D'Arrigo, P. Two-Step Fractionation of a Model Technical Lignin by Combined Organic Solvent Extraction and Membrane Ultrafiltration. *ACS Omega* **2019**, *4* (3), 4615 – 4626.
89. Ang, A., Ashaari, Z., Bakar, E., Ibrahim, N. Characterisation of Sequential Solvent Fractionation and Base-catalysed Depolymerisation of Treated Alkali Lignin. *Bioresources*. **2015**, *10* (3), 4137 – 4151.
90. Melro, E., Filipe, A., Sousa, D., Valente, A., Romano, A., Antunes, F., Medronho, B. Dissolution of kraft lignin in alkaline solutions. *Intl. J. Biol. Macromol.* **2020**, *148*, 688 – 695.
91. Liu, C., Sia, C., Wang, G., Jia, H., Ma, L. A novel and efficient process for lignin fractionation in biomass-derived glycerol-ethanol solvent system. *Ind. Crop. Prod.* **2018**, *111*, 201 – 211.
92. Klett, A. Purification, Fractionation, and Characterization of Lignin from Kraft Black Liquor for Use as a Renewable Biomaterial. Dissertation, Clemson University, Clemson, S.C., 2017.
93. Schumaker, J. Quantification of Lignin Hydroxyl Containing Functional Groups via $^{31}\text{P}\{^1\text{H}\}$ NMR Spectroscopy and Synthesis of Degradation Standards. Thesis, University of North Dakota, Grand Forks, ND, 2017.
94. Bancuta, O., Chilian, A., Bancuta, R., Ion, R., Setnescu, R., Setnescu, T., Gheboianu, A. Improvement of Spectrophotometric Method for Determination of Phenolic Compounds by Statistical Investigations. *Rom. J. Phys.* **2016**, *61* (1 – 2), 1255.

95. Blainski, A., Lopes, G., de Mello, J. Application and Analysis of the Folin Ciocalteu Method for the Determination of the Total Phenolic Content from *Limonium Brasiliense* L. *Molecules*. **2013**, *18*, 6852 – 6865.
96. Everette, J., Bryant, Q., Green, A., Abbey, Y., Wangila, G., Walker, R. A thorough study of reactivity of various compound classes towards the Folin-Ciocalteu reagent. *J. Agr. Food Chem.* **2010**, *58* (14), 8139 – 8144.
97. Folin, O., Denis, W. On Phosphotungstic-Phosphomolybdic Compounds as Color Reagents. *J. Biol. Chem.* **1912**.
98. Rangel, J., Lozano, J., Heredia, J., Zevallos, L. The Folin-Ciocalteu assay revisited: Improvement of its specificity for total phenolic content determination. *Anal. Methods-UK*. **2013**, *5* (2), 5990 – 5999.
99. ChemgaPedia Oxidation of Phenols to Benzoquinones
http://www.chemgapedia.de/vsengine/vlu/vsc/en/ch/2/vlu/oxidation_reduktion/oxi_phenol.vlu/P age/vsc/en/ch/2/oc/reaktionen/formale_systematik/oxidation_reduktion/oxidation/entfernen_was_serstoff/oxidation_phenole/mechanismus.vscml.html (accessed April 2019).
100. Rover, M., Brown, R. Quantification of total phenols in bio-oil using the Folin-Ciocalteu method. *J. Anal. Appl. Pyrol.* **2013**, *104*, 366 – 371.
101. Stratil, P., Klejdus, B., Kuban, V. Determination of Total Content of Phenolic Compounds and Their Antioxidant Activity in Vegetables- Evaluation of Spectrophotometric Methods. *J. Agr. Food Chem.* **2006**, *54*, 607 – 616.
102. Kang, S., Chang, J., Fan, J. Phenolic Antioxidant Production by Hydrothermal Liquefaction of Lignin. *Energ. Source Part A*. **2015**, *37* (5), 494 – 500.
103. Napoly, F., Kardos, N., Jean-Gerard, L., Goux-Henry, C., Andrioletti, B., Draye, M. H₂O₂-mediated kraft lignin oxidation with readily available metal salts: What about the effect of ultrasound? *Ind. Eng. Chem. Res.* **2015**, *54*, 6046 – 6051.
104. Gu, X. H., M., Shi, Y., Li, Z. La-containing SBA-1/H₂O₂ systems for the microwave assisted oxidation of a lignin model phenolic monomer. *Maderas. Cienc. Technol.* **2010**, *12* (3), 181 – 188.
105. Wang, Y., Yang, F., Liu, Z., Yuan, L., Li, G. Electrocatalytic degradation of aspen lignin over Pb/PbO₂ electrode in alkali solution. *Catal. Commun.* **2015**, *67*, 49 –53.
106. Deng, H., Lin, L., Sun, Y., Pang, C., Zhuang, J., Ouyang, P., Li, J., Liu, S. , Activity and stability of perovskite-type oxide LaCoO₃ catalyst in lignin catalytic wet oxidation to aromatic aldehyde. *Process. Energy Fuels*. **2009**, *23* (1), 19 – 24.

107. Wang, W., Ren, X., Chang, J. Characterization of bio-oils and bio-chars obtained from the catalytic pyrolysis of alkali lignin with metal chlorides. *Fuel Process. Technol.* **2015**, *138*, 605 – 611.
108. Jääskeläinen, A., Liitiä, T., Mikkelsen, A., Tamminen, T. Aqueous organic solvent fractionation as means to improve lignin homogeneity and purity. *Ind. Crop. Prod.* **2017**, *103*, 51 – 58.
109. Werhan, H., Farshori, A., von Rohr, P. Separation of lignin oxidation products by organic solvent nanofiltration. *J. Memb. Sci.* **2012**, *423 – 424*, 40 – 412.
110. Wenten, I. Ultrafiltration in Water Treatment and its Evaluation as Pre-treatment for Reverse Osmosis Systems. https://www.researchgate.net/publication/228912158_Ultrafiltration_in_Water_Treatment_and_Its_Evaluation_as_Pretreatment_for_Reverse_Osmosis_System (accessed April 2020).
111. Humpert, D., Ebrahimi, M., Czermak, P. Membrane Technology for the Recovery of Lignin: A Review. *Membranes.* **2016**, *6* (3), 42.
112. Toledano, A., Garcia, A., Mondragon, I., Labidi, J. Lignin separation and fractionation by ultrafiltration. *Sep. Purif. Technol.* **2010**, *71*, 38 – 43.
113. Zinovyev, G., Sumerskii, I., Korntner, P.; Sulaeva, I., Rosenau, T., Potthast, A. Molar mass-dependent profiles of functional groups and carbohydrates in kraft lignin. *J. Wood Chem. Technol.* **2016**, *37* (3), 171 – 183.
114. Norgren, M., Lindström, B. Physico-chemical characterization of a fractionated kraft lignin. *Holzforschung.* **2000**, *54* (5), 528 – 534.
115. Sevastyanova, O., Helander, M., Chowdhury, S., Lange, H., Wedin, H., Zhang, L., Ek, M., Kadla, J. F., Crestini, C., Lindström, M. E. Tailoring the molecular and thermo-mechanical properties of kraft lignin by ultrafiltration. *Sep. Purif. Technol.* **2014**, *71* (1), 38 – 43.
116. Busse, N., Fuchs, F., Kraume, M., Czermak, P. Treatment of enzyme-initiated delignification reaction mixtures with ceramic ultrafiltration membranes: Experimental investigations and modeling approach. *Sep. Sci. Technol.* **2016**, 1 – 20.
117. Wallberg, O., Jönsson, A.-S., Wimmerstedt, R. Ultrafiltration of kraft black liquor with a ceramic membrane. *Desalination.* **2003**, *156* (1), 145 – 153.
118. Guo, G., Li, S., Wang, L., Ren, S., Fang, G. Separation and characterization of lignin from bio-ethanol production residue. *Bioresour. Technol.* **2013**, *135*, 738 – 741.
119. Toledano, A., Serrano, L., Garcia, A., Mondragon, I., Labidi, J. , Comparative study of lignin fractionation by ultrafiltration and selective precipitation. *Chem. Eng. J.* **2010**, *157* (1), 93 – 99.

120. Helander, M., Theliander, H., Lawoko, M., Henriksson, G., Zhang, L., Lindström, M. E. Fractionation of technical lignin: Molecular mass and pH effects. *Bioresources*. **2013**, *8* (2), 2270 – 2282.
121. Brodin, I., Sjöholm, E., Gellerstedt, G. Kraft lignin as feedstock for chemical products: The effects of membrane filtration. *Holzforschung*. **2009**, *63* (3), 290 – 297.
122. Šurina, I., Jablonský, M., Ház, A., Sladková, A., Briškárová, A., Kačík, F., Šima, J. Characterization of non-wood lignin precipitated with sulphuric acid of various concentrations. *Bioresources*. **2015**, *10* (1), 1408 – 1423.
123. Sun, R., Tomkinson, J. Fractional separation and physico-chemical analysis of lignins from the black liquor of oil palm trunk fibre pulping. *Sep. Purif. Technol.* **2001**, *24* (3), 529 – 539.
124. Lourençon, T., Hansel, F., da Silva, T., Ramos, L., de Muniz, G., Magalhães, W. Hardwood and softwood kraft lignins fractionation by simple sequential acid precipitation. *Sep. Purif. Technol.* **2015**, *154*, 82 – 88.
125. Wang, G., Chen, H. Fractionation of alkali-extracted lignin from steam-exploded stalk by gradient acid precipitation. *Sep. Purif. Technol.* **2013**, *105*, 98 – 105.
126. Wang, S., Wang, Y., Cai, Q., Wang, X., Jin, H., Luo, Z. Multi-step separation of monophenols and pyrolytic lignins from the water-insoluble phase of bio-oil. *Sep. Purif. Technol.* **2014**, *122*, 248 – 255.
127. Li, X.-H., Wu, S.-B. Chemical structure and pyrolysis characteristics of the soda-alkali lignin fractions. *Bioresources*. **2014**, *9* (4), 6277 – 6289.
128. Dodd, A., Kadla, J., Straus, S. Characterization of fractions obtained from two industrial softwood kraft lignins. *ACS Sustain. Chem. Eng.* **2015**, *3* (1), 103 – 110.
129. Boeriu, C., Fițigău, F., Gosselink, R., Frissen, A., Stoutjesdijk, J., Peter, F. Fractionation of five technical lignins by selective extraction in green solvents and characterisation of isolated fractions. *Ind. Crop. Prod.* **2014**, *62*, 481 – 490.
130. Li, M.-F., Sun, S.-N., Xu, F., Sun, R.-C. Sequential solvent fractionation of heterogeneous bamboo organosolv lignin for value-added application. *Sep. Purif. Technol.* **2012**, *101*, 18 – 25.
131. Jiang, X., Savithri, D., Du, X., Pawar, S., Jameel, H., Chang, H.-M., Zhou, X. Fractionation and characterization of kraft lignin by sequential precipitation with various organic solvents. *ACS Sustain. Chem. Eng.* **2017**, *5* (1), 835 – 842.
132. Lange, H., Schiffels, P., Sette, M., Sevastyanova, O., Crestini, C. Fractional precipitation of wheat straw organosolv lignin: Macroscopic properties and structural insights. *ACS Sustain. Chem. Eng.* **2016**, *4* (10), 5136 – 5151.

133. Cui, C., Sun, R., Argyropoulos, D. S. Fractional precipitation of softwood kraft lignin: Isolation of narrow fractions common to a variety of lignins. *ACS Sustain. Chem. Eng.* **2014**, *2* (4), 959 – 968.
134. Duval, A., Vilaplana, F., Crestini, C., Lawoko, M. Solvent screening for the fractionation of industrial kraft lignin. *Holzforschung.* **2016**, *70* (1), 11 – 20.
135. Liang, X., Liu, J., Fu, Y., Chang, J. Influence of anti-solvents on lignin fractionation of eucalyptus globulus via green solvent system pretreatment. *Sep. Purif. Technol.* **2016**, *163*, 258 – 266.
136. Yuan, T.-Q., He, J., Xu, F., Sun, R.-C. Fractionation and physico-chemical analysis of degraded lignins from the black liquor of Eucalyptus pellita KP-AQ pulping. *Polym. Degrad. Stab.* **2009**, *94* (7), 1142 – 1150.
137. Miller-Chou, B., Koenig, J. A review of polymer dissolution. *Prog. Polym. Sci.* **2003**, *28* (8), 1223 – 1270.
138. Ouano, A., Carothers, J. Dissolution dynamics of some polymers: Solvent-polymer boundaries. *Polym. Eng. Sci.* **1980**, *20*(2), 160 – 166.
139. Kirk, T., Brown, W., Cowling, E. Preparative fractionation of lignin by gel-permeation chromatography. *Biopolymers.* **1969**, *7* (2), 135 – 153.
140. Xiao, L., Xu, F., Sun, R.-C. Chemical and structural characterization of lignins isolated from *Caragana sinica*. *Fibers Polym.* **2011**, *12* (3), 316 – 323.
141. Wang, G., Chen, H. Fractionation and characterization of lignin from steam-exploded corn stalk by sequential dissolution in ethanol–water solvent. *Sep. Purif. Technol.* **2013**, *120*, 402 – 409.
142. Ropponen, J., Räsänen, L., Rovio, S., Ohra-aho, T., Liitiä, T., Mikkonen, H., van de Pas, D., Tamminen, T. Solvent extraction as a means of preparing homogeneous lignin fractions. *Holzforschung.* **2011**, *65* (4), 543 – 549.
143. Li, Z., Gu, Y., Gu, T. Mathematical modeling and scale-up of size-exclusion chromatography. *Biochem. Eng. J.* **1998**, *2*(2), 145 – 155.
144. Janson, J.-C., *Process Scale Liquid Chromatography*. Wiley-VCH Verlag GmbH: 2007.
145. Botaro, V., Curvelo, A. Monodisperse lignin fractions as standards in size-exclusion analysis: comparison with polystyrene standards. *J. Chromatogr. A.* **2009**, *1216*(18), 3802 – 3806.
146. Hortling, B., Turunen, E., Kokkonen, P. Molar mass and size distribution of lignins In *Handbook of Size Exclusion Chromatography and Related Techniques*, 2nd ed.; Wu, C. S., Ed. Marcel Dekker: 2004; pp 359 – 386.

147. Banoub, J., Delmas, G. H., Jr., Joly, N., Mackenzie, G., Cachet, N., Benjelloun-Mlayah, B., Delmas, M. A. Critique on the structural analysis of lignins and application of novel tandem mass spectrometric strategies to determine lignin sequencing. *J. Mass Spectrom.* **2015**, *50*(1), 5 – 48.
148. Uliyanchenko, E., van der Wal, S., Schoenmakers, P. Challenges in polymer analysis by liquid chromatography. *Polym. Chem.* **2012**, *3*(9), 2313 – 2335.
149. Agnemo, R., Gellerstadt, G. The Reactions of Lignin with Alkaline Hydrogen Peroxide. Part II. Factors Influencing the Decomposition of Phenolic Structures. *Acta Chem. Scand.* **1979**, *33*(5), 337 – 42.
150. Gu, X., Cheng, K., He, M., Shi, Y., Li, Z. La-Modified SBA-15/H₂O₂ Systems for the Microwave Assisted Oxidation of Organosolv Beech Wood Lignin. *Maderas- Cienc. Tecnol.* **2012**, *14*(1), 31 – 42.
151. Crestini, C., Caponi, M., Argyropoulos, D., Saladino, R. Immobilized methyltrioxorhenium (MTO)/ H₂O₂ systems for the oxidation of lignin and lignin model compounds. *Bioorg. Med. Chem.* **2006**, *14*, 5292 – 5302.
152. Cheng, Y., Zhao, P., Alma, M., Sun, D., Li, R., Jiang, J. Improvement of direct liquefaction of technical alkaline lignin pretreated by alkaline hydrogen peroxide. *J. Anal. Appl. Pyrol.* **2016**, *122*, 277 – 281.
153. Ahmad, A., Al Dajani, W., Paleologou, M., Xu, C. Sustainable Process for the Depolymerization/Oxidation of Softwood and Hardwood Kraft Lignins using Hydrogen Peroxide under Ambient Conditions. *Molecules.* **2020**, *25*, 2329.
154. He, W., Gao, W., Fatehi, P. Oxidation of Kraft Lignin with Hydrogen Peroxide and its Application as a Dispersant for Kaolin Suspensions. *ACS Sustain. Chem. Eng.* **2017**, *5*, 10597 – 10605.
155. Junghans, U., Bernhardt, J., Wollnik, R., Triebert, D., Unkelbach, G., Pufky-Heinrich, D. Valorization of Lignin via Oxidative Depolymerization with Hydrogen Peroxide: Towards Carboxyl-Rich Oligomeric Lignin Fragments. *Molecules.* **2020**, *25*, 2717.
156. Kadla, J., Chang, H., Jameel, H. The Reactions of Lignins with Hydrogen Peroxide at High Temperature. *Holzforschung.* **1997**, *51*, 428 – 34.
157. Xiang, Q., Lee, Y. Oxidative Cracking of Precipitated Hardwood Lignin by Hydrogen Peroxide. *Appl. Biochem. Biotechnol.* **2000**, *84*, 153 – 162.
158. Evstigneev, E. Oxidation of Hydrolysis Lignin with Hydrogen Peroxide in Acid Solutions. *Russ. J. Appl. Chem.* **2013**, *86*(2), 278 – 285.
159. Asha, K., Badamali, S. Highly efficient photocatalytic degradation of lignin by hydrogen peroxide under visible light. *Mol. Catal.* **2020**, *497*, 111236.

160. Gierer, J. Chemistry of delignification, Part 2: Reactions of Lignin during bleaching. *Wood Sci. Technol.* **1986**, *20* (1 – 33).
161. Kishimoto, T., Kadla, J., Chang, H., Jameel, H. The Reactions of Lignin Model Compounds with Hydrogen Peroxide at Low pH. *Holzforschung.* **2003**, *57*, 52 – 58.
162. Mancera, A., Fierro, V., Pizzi, A., Dumarcay, S., Gerardin, P., Velasquez, J., Quintana, G., Celzard, A. Physicochemical characterization of sugar cane bagasse lignin oxidized by hydrogen peroxide. *Polym. Degrad. Stab.* **2010**, *95*, 470 – 476.
163. Izumrudova, T., Derevenchuk, L., and Shorygina, N. Modification of hydrolysis lignin by oxidation with hydrogen peroxide. *Zh. Prikl. Khim.* **1964**, *37*(7), 1638 – 1640.
164. Kumar, A., Biswas, B., Saini, K., Kumar, A., Kumar, J., Krishna, B., Bhaskar, T. Effect of hydrogen peroxide on the depolymerization of prot lignin. *Ind. Crop. Prod.* **2020**, *150*, 112355.
165. Hawthorne, S., Kubátová, A. Hot (subcritical) water extraction In *Comprehensive Analytical Chemistry*, 1st ed.; **2002**; Vol. 37, pp 587 – 608.
166. Abad-Fernandez, N., Perez, E., Cocero, M. Aromatics from lignin through ultrafast reactions in water. *Green Chem.* **2019**, *21*(6), 1351 – 1360.
167. Bembenic, M., Clifford, C. Subcritical Water Reactions of a Hardwood Derived Organosolv Lignin with Nitrogen, Hydrogen, Carbon Monoxide and Carbon Dioxide Gases. *Energ. Fuel.* **2012**, *26*(7), 4540 – 4549.
168. Wahyudiono, Sasaki, M., Goto, M. Recovery of phenolic compounds through the decomposition of lignin in near and supercritical water. *Chem. Eng. Process.* **2008**, *47*(9 – 10), 1609 – 1619.
169. Pinkowska, H., Wolak, P., Zlocinska, A. Hydrothermal decomposition of alkali lignin in sub- and supercritical water. *Chem. Eng. J.* **2012**, *187*, 410 – 414.
170. Dell’Orco, S., Miliotti, E., Lotti, G., Rizzo, A., Rosi, L., Chiamonti, D. Hydrothermal Depolymerization of Biorefinery Lignin-Rich Streams: Influence of Reaction Conditions and Catalytic Additives on the Organic Monomers Yields in Biocrude and Aqueous Phase. *Energies* **2020**, *13*, 1241.
171. Miliotti, E., Dell’Orco, S., Lotti, G., Rizzo, A., Rosi, L., Chiamonti, D., Lignocellulosic ethanol biorefinery: valorization of lignin-rich stream through hydrothermal liquefaction. *Energies.* **2019**, *12*(4), 723.
172. Jiang, W., Lyu, G., Wang, C., Lucia, L. Quantitative Analyses of Lignin Hydrothermolysates from Subcritical Water and Water-Ethanol Systems. *Ind. Eng. Chem. Res.* **2014**, *53*, 10328 – 10334.

173. Barbier, J., Charon, N., Dupassieux, N., Loppinet-Serani, A., Mahe, L., Ponthus, J., Courtiade, M., Ducrozet, A., Quoineaud, A., Cansell, F. Hydrothermal conversion of lignin compounds. A detailed study of fragmentation and condensation reaction pathways. *Biomass Bioenergy*. **2012**, *46*, 479 – 491.
174. Yong, T., Matsumura, Y. Kinetic analysis of lignin hydrothermal conversion in sub- and supercritical water. *Ind. Eng. Chem. Res.* **2013**, *52*, 5626 – 5639.
175. Zhang, B., Huang, H., Ramaswamy, S. Reaction kinetics of the Hydrothermal Treatment of Lignin. *Appl. Biochem. Biotechnol.* **2008**, *147*, 119 – 131.
176. Forchheim, D., Hornung, U., Kruse, A., Sutter, T. Kinetic Modelling of Hydrothermal Lignin Depolymerisation. *Waste Biomass Valori.* **2014**, *5*, 985 – 994.
177. Hu, J., Shen, D., Wu, S., Zhang, H., Xiao, R. Effect of temperature on structure evolution in char from hydrothermal degradation of lignin. *J. Anal. Appl. Pyrol.* **2014**, *106*, 118 – 124.
178. Hashmi, F., Merio-Talvio, H., Hakonen, K., Ruuttunen, K., Sixta H. Hydrothermolysis of organosolv lignin for the production of bio-oil rich in monoaromatic phenolic compounds. *Fuel Process. Technol.* **2017**, *168*, 74 – 83.
179. Islam, M., Taki, G., Rana, M., Park, J. Yield of Phenolic Monomers from Lignin Hydrothermolysis in Subcritical Water System. *Ind. Eng. Chem. Res.* **2018**, *57*, 4779 – 4784.
180. Yang, S., Yuan, T., Li, M., Sun, R. Hydrothermal degradation of lignin: Products analysis for phenol formaldehyde adhesive synthesis. *Int. J. Biol. Macromol.* **2015**, *72*, 54 – 62.
181. Kang, S., Chang, J., Fan, J. Phenolic Antioxidant Production by Hydrothermal Liquefaction of Lignin. *Energ. Sources Part A.* **2015**, *37*, 494 – 500.
182. Zhou, X. Conversion of kraft lignin under hydrothermal conditions. *Bioresour. Technol.* **2014**, *170*, 583 – 586.
183. Trajano, H., Wyman, C., Engle, N., Foston, M., Ragauskas, A., Tschaplinski, T. The fate of lignin during hydrothermal pretreatment. *Biotechnol. Biofuels.* **2013**, *6*(1), 110.
184. Long, J., Xu, Y., Wang, T., Shu, R., Zhang, Q., Zhang, X., Fu, J., Ma, L. Hydrothermal depolymerization of Lignin: Understanding the Structural Evolution. *BioResource.s* **2014**, *9*(4), 7162 – 7175.
185. Zhao, Y., Li, X., Wu, S., Li, Y. Temperature Impact on the Hydrothermal Depolymerization of *Cunninghamia lanceolata* Enzymatic/Mild Acidolysis Lignin in Subcritical Water. *Bioresources.* **2016**, *11*(1), 21 – 32.

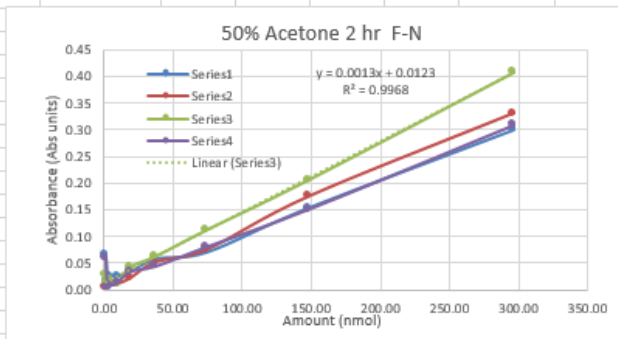
186. Kang, S., Li, X., Fan, J., Chang, J. Characterization of Hydrochars Produced by Hydrothermal Carbonization of Lignin, Cellulose D-Xylose, and Wood Meal. *Ind. Eng. Chem. Res.* **2012**, *51*, 9023 – 9031.
187. Yang, J., He, Q., Niu, H., Dalai, A., Corscadden, K., Zhou, N. Microwave-assisted hydrothermal liquefaction of biomass model components and comparison with conventional heating. *Fuel*. **2020**, *277*, 118202.
188. Tang, K., Zhou, X. The degradation of kraft lignin during hydrothermal treatment for phenolics. *Pol. J. Chem. Technol.* **2015**, *17*(3), 24 – 28.
189. Kozliak, E., Kubátová, A., Artemyeva, A., Nagel, E., Zhang, C., Rajappagowda, R., Smirnova, A. Thermal Liquefaction of Lignin to Aromatics: Efficiency, Selectivity, and Product Analysis. *ACS Sustain. Chem. Eng.* **2016**, *4*, 5106 – 5122.
190. Kim, J.-S. Production, separation and applications of phenolic-rich bio-oil--a review. *Bioresour. Technol.* **2014**, *178*, 90 – 98.
191. Xu, C., Ferdosian, F. *Conversion of Lignin into Bio-Based Chemicals and Materials*, 1st ed.; Springer-Verlag: 2017.
192. Fan, L., Zhang, Y., Liu, S., Zhou, N., Chen, P., Cheng, Y., Addy, M., Lu, Q., Omar, M., Liu, Y., Wang, Y., Dai, L., Anderson, E., Peng, P., Lei, H., Ruan, R. Bio-Oil from Fast Pyrolysis of Lignin: Effects of Process and Upgrading Parameters. *Bioresour. Technol.* **2017**, *241*, 1118 – 1126.
193. Voeller, K., Bilek, H., Kozliak, E., Kubátová, A. Characterization of alkaline lignin and its degradation products using thermal desorption and pyrolysis methods. *ACS Sustain. Chem. Eng.* **2017**, *5*(11), 10334 – 10341
194. Voeller, K., Bilek, H., Kreft, J., Dostalkova, A., Kozliak, E., Kubátová, A. Thermal Carbon Analysis Enabling Comprehensive Characterization of Lignin and Its Degradation Products. *ACS Sustain. Chem. Eng.* **2017**, *5*(11), 10334 – 10341.
195. Wells, T. and Ragauskas, A. On the Future of Lignin-Derived Materials, Chemicals and Energy. *Innov. Energy. Res.* **2016**, Vol 5(2): e117.
196. Deepa, A., Dhepe, P. Lignin depolymerization into aromatic monomers over solid acid catalysts. *ACS Catal.* **2015**, *5*(1), 36 – 379.
197. Ariton, A., Creanga, S., Trinca, L., Silviu, I. Valorization of lignin modified by hydroxymethylation to ensure birch veneer bioprotection. *Cellulose Chem. Technol.* **2015**, *49*(9-10), 765 – 774.

198. Microsoft, Inc. Test hypothesis using t-test. Microsoft docs/Machine Learning Studio. <https://docs.microsoft.com/en-us/azure/machine-learning/studio-module-reference/test-hypothesis-using-t-test> (accessed April 2018).
199. Solvents for UV Spectrophotometry, from *CRC Handbook of Chemistry and Physics*, 91st ed.; Ed.: Haynes, W.M; CRC Press (Taylor and Francis Group): Boca Raton, FL, **2010**.
200. Zhor, J. and Bremner, T.W. Role of Lignosulfonates in High Performance Concrete and the Role of 814 Admixtures in High Performance Concrete. *Proceedings of the International RILEM Conference*, **1999**, Edited by Cabrera, J. and Rivera-Villareal, R., p. 143-146.
201. Vishtal, A., Kraslawski, A. Challenges in industrial applications of technical lignins. *Bioresources*. **2011**, 6(3), 3547 – 3568.
202. Moerk, R., Yoshida, H., Kringstad, K., Hatakeyama, H. Fractionation of kraft lignin by successive extraction with organic solvents. 1. Functional groups (13)C-NMR-spectra and molecular weight distributions. *Holzforschung*. **1986**, 40, 51 – 60.
203. Voeller, K. M. Characterization of Kraft alkali lignin and products of its thermal degradation by fractional pyrolysis method. A thesis submitted to the graduate faculty of the University of North Dakota in partial fulfillment of the requirements for Master's degree, University of North Dakota, 2016.
204. Andrianova, A., DiProspero, T., Geib, C., Smoliakova, I., Kozliak, E. & Kubátová, A. Electrospray Ionization with High-Resolution Mass Spectrometry as a Tool for Lignomics: Lignin Mass Spectrum Deconvolution, *J. Am. Soc. Mass Spect.* **2019**, 1044 – 59.
205. Hubbe, M., Alen, R., Paleologou, M., Kannangara, M., Kihlman, J. Lignin Recovery from Spent Alkaline Pulping Liquors Using Acidification, Membrane Separation, and Related Processing Steps: A Review. *Bioresources*. **2019**, 14(1), 2300 – 51.
206. Ashenhurst, J. Alcohols to Ethers via Acid Catalysis. <https://www.masterorganicchemistry.com/2014/11/14/ether-synthesis-via-alcohols-and-acid/> (accessed April 2021)
207. Hasegawa, I., Inoue, Y., Muranaka, Y., Yasukawa, T., Mae, K. Selective Production of Organic Acids and Depolymerization of Lignin by Hydrothermal Oxidation with Diluted Hydrogen Peroxide. *Energy Fuels*. **2011**, 25, 791 – 796.
208. Galamba, N., Paiva, A., Barreiros, S., Simoes, P. Solubility of Polar and Nonpolar Aromatic Molecules in Subcritical Water: The Role of the Dielectric Constant. *J. Chem. Theory Comput.* **2019**, 15, 6277 – 93.
209. Kwak, H., Lee, H., Lee, K. Surface-modified spherical lignin particles with superior Cr(VI) removal efficiency. *Chemosphere*. **2020**, 239, 124733.

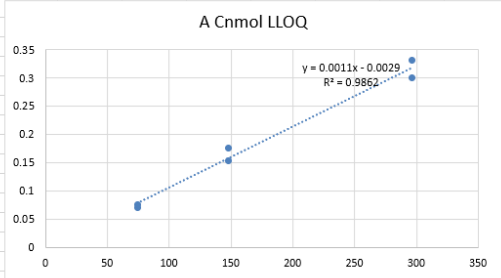
210. NIST Mass Spectrometry Data Center (Mass Spectra-electron ionization), NIST Chemistry WebBook, NIST Standard Reference Database Number 69. <https://doi.org/10.18434/T4D303> (accessed 2018 – 2019).
211. Brzonova, I., Kozliak, E., Andrianova, A., LaVallie, A., Kubatova, A., Ji, Y., Production of Lignin Based Insoluble Polymers (Anionic Hydrogels) by *C. versicolor*. *Sci. Rep.* **2017**, 7 (1).
212. Brebu, M.; Cazacu, G.; Chirila, O. Pyrolysis of Lignin- a Potential Method for Obtaining Chemicals and/or Fuels. *Cellul Chem Technol* **2011**, 45(1), 43 – 50.
213. Simmons, G.; Gentry, M. Kinetic Formation of CO, CO₂, H₂ and Light Hydrocarbons from Cellulose Pyrolysis. *J. Anal. Appl. Pyrol.* **1986**, 10 (2), 129 – 138.
214. Crestini, C., Lange, H., Sette, M., Argyropoulos, D. On the structure of softwood kraft lignin. *Green Chem.* **2017**, 19(17), 4104 – 4121.
215. Deuss, P., Lancefield, C., Narani, A., De Vries, J., Westwood, N., Barta, K. Phenolic acetals from lignins of varying compositions via iron (III) triflate catalysed depolymerisation. *Green Chem.* **2017**, 19(12), 2774 – 2782.
216. Li, S., Talebi, A., Questell-Santiago, Y., Florent, H., Luterbacher, J., Yanding, L., Hoon, K., John, R. Formaldehyde stabilization facilitates lignin monomer production during biomass depolymerization. *Science.* **2016**, 354 (6310), 329 – 333.
217. Chua, Y., Yu, Y., Wu, H. Structural changes of chars produced from fast pyrolysis of lignin at 100 – 300 °C. *Fuel*, **2019**, 255, 115754.
218. Zhu, J., Yang, H., Hu, H., Zhou, Y., Li, J., Jin, L. Novel insight into pyrolysis behaviors of lignin using in-situ pyrolysis-double ionization time-of-flight mass spectrometry combined with electron paramagnetic resonance spectroscopy. *Bioresour. Technol.*, **2020**, 312, 123555.
219. Zhang, C., Shao, Y., Zhang, L., Zhang, S. Westerhof, R., Liu, Q., Jia, P., Li, Q., Wang, Y., Hu, X. Impacts of temperature on evolution of char structure during pyrolysis of lignin. *Sci.Total Environ.* **2020**, 699, 134381.

Appendix 1: UV-Vis absorbances for lignin samples for F-C project. Two replicate slopes were used to calculate an average slope with LOD.

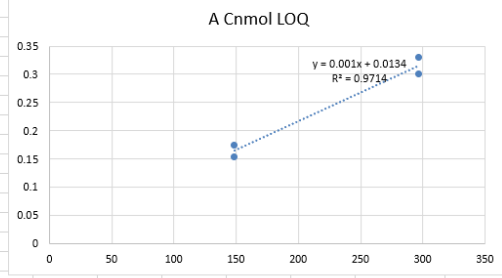
50% Acetone	nmoles	blank	0.58	1.16	2.32	4.63	9.27	18.53	37.07	74.13	148.27	296.53			
			guaiacol stand.												
		1	2	3	4	5	6	7	8	9	10	11	12		
50% Acetone	A1	0.067215003	1.413012981	0.068865	0.13034	0.14728	0.19014	0.090907	0.09793	0.18301	0.13562	0.21967	0.266769	50% ace A	20-02-14
	A2	0.064193003	1.398277998	0.06405	0.06899	0.07168	0.07451	0.076995	0.08763	0.11788	0.14128	0.24114	0.396587	50% ace A	20-02-14
			1.40564549												
	B1	0.062802002	1.654608965	0.06342	0.08974	0.0731	0.07859	0.172515	0.10206	0.12234	0.17208	0.26694	0.469261	50% ace A	20-02-17
	B2	0.05906	1.503775954	0.07011	0.11964	0.06498	0.06952	0.11348	0.09493	0.10492	0.1413	0.21214	0.369699	50% ace A	20-02-17
50% Acetone	outlier		1.57919246												
		0.0657	1.3473	0.0029	0.0646	0.0160	0.0244	0.0252	0.0322	0.0573	0.0699	0.1540	0.3011	50 µL FC	20-02-14
			1.3326	-0.0017	0.0033	0.0060	0.0088	0.0113	0.0219	0.0522	0.0756	0.1754	0.3309	50 µL FC	20-02-14
		0.0609	1.5937	0.0025	0.0288	0.0122	0.0177	0.0112	0.0411	0.0614	0.1112	0.2060	0.4083	50 µL FC	20-02-17
			1.4428	0.0092	0.0587	0.0040	0.0086	0.0125	0.0340	0.0440	0.0804	0.1512	0.3088	50 µL FC	20-02-17



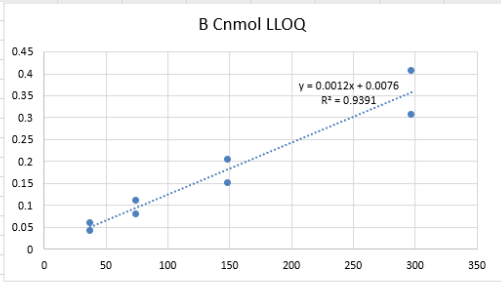
LOD, LOQ of Absorbance vs nmol C for 50% acetone sample



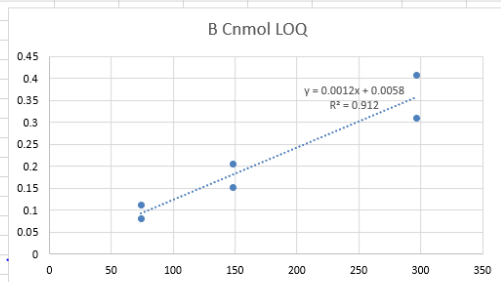
0.001083	-0.002898
6.41E-05	0.012564
0.986205	0.014508
285.9599	4
0.060189	0.000842



0.00102	0.013409481
0.000124	0.029024341
0.971399	0.018356605
67.92686	2
0.022889	0.00067393



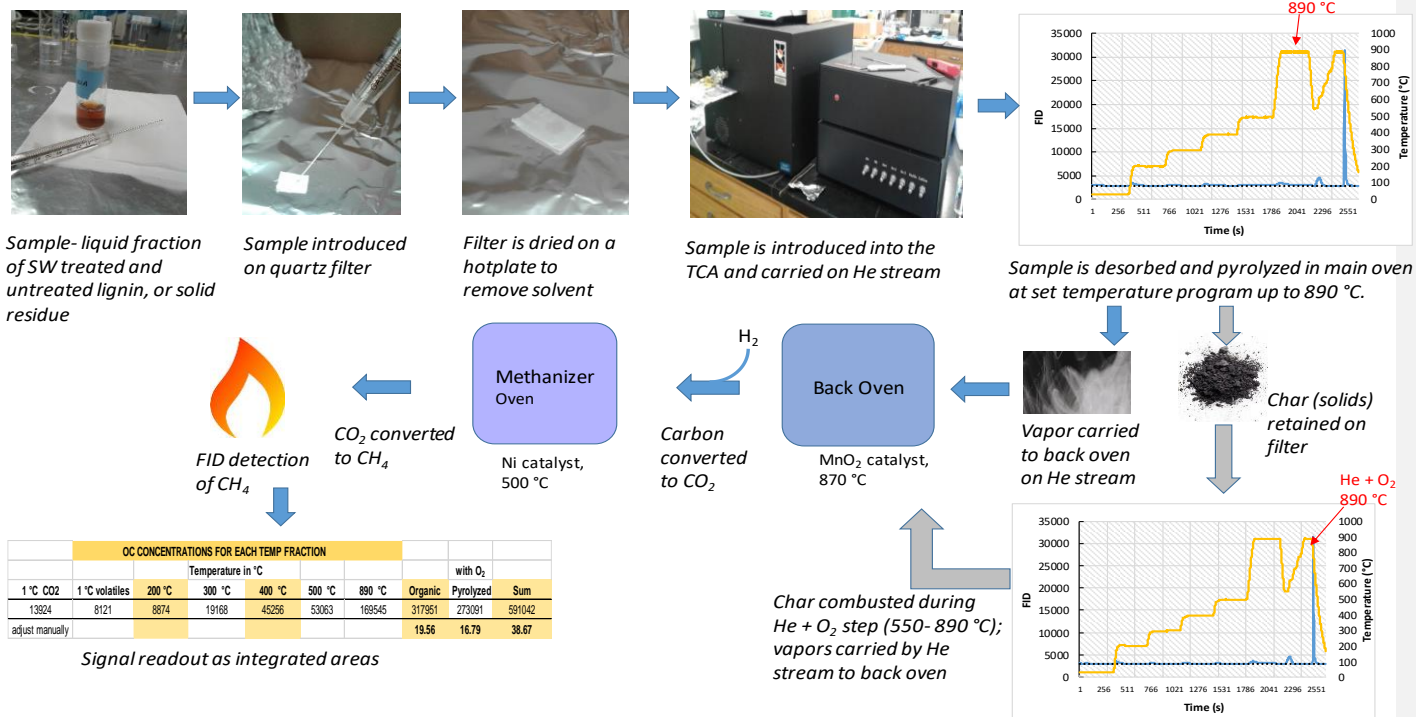
0.001179	0.007579
0.000123	0.020943
0.939066	0.03445
92.46689	6
0.109739	0.007121



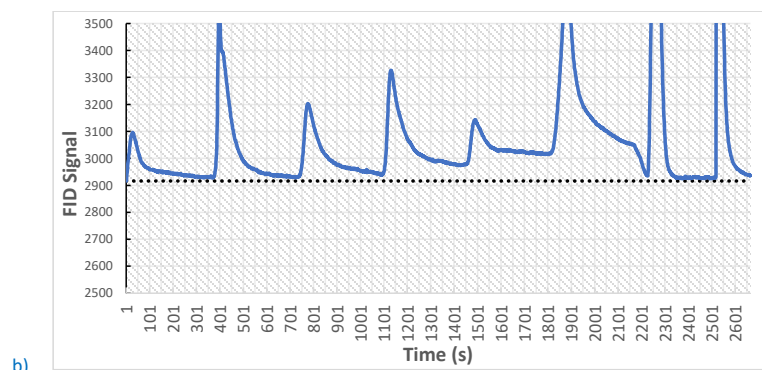
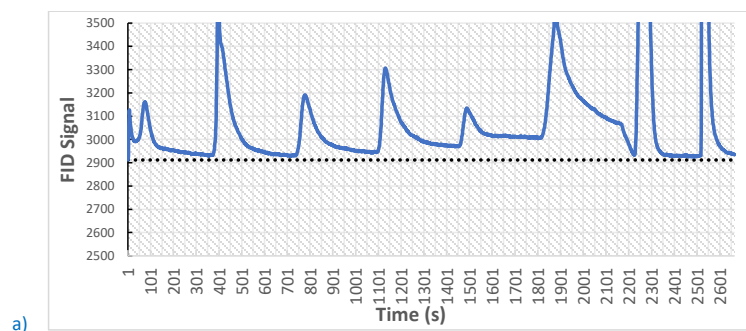
0.001186186	0.00579
0.000184189	0.036126
0.912037883	0.041715
41.47412162	4
0.072171238	0.006961

Analytical Methodology

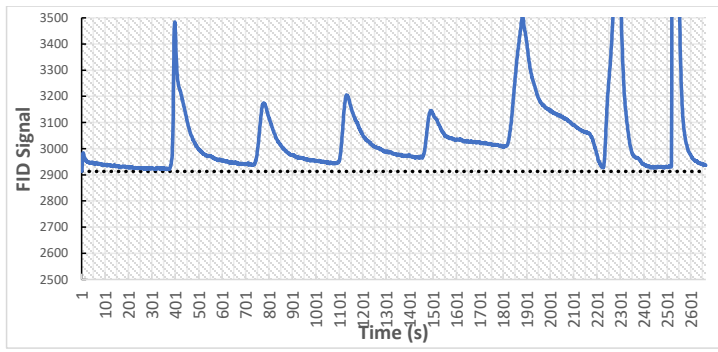
TCA



Appendix 3: Thermograms of the 10% H₂O₂, 25% methanol sample with an increased ambient temperature section of the TCA program, but with varied drying times: a) 4.5 minutes, b) 5 minutes, and c) 7 minutes.



c)



Appendix 4: Minitab data

Table S1. Minitab data entry for 2^4 factorial evaluation (with four replicates), before factorial design selection

Worksh								
↓	C1	C2	C3	C4	C5	C6	C7	C8
	time-hr	Na2CO3 conc.	FC amount	conc. ACN	rep 1	rep 2	rep 3	rep 4
1	1	0.4	100	8	1.08416	1.00921	1.10194	1.14221
2	1	0.4	100	16	0.16056	0.14646	0.15711	0.20133
3	1	0.4	50	8	0.78884	0.84474	0.74939	0.80536
4	1	0.4	50	16	0.47260	0.47151	0.44601	0.52434
5	1	0.2	100	8	1.10267	0.84051	1.23894	1.16396
6	1	0.2	100	16	0.11327	0.11874	0.11497	0.11492
7	1	0.2	50	8	0.58720	0.80005	0.82063	0.76514
8	1	0.2	50	16	0.16526	0.17006	0.16935	0.18344
9	2	0.4	100	8	1.28946	1.18877	1.29725	1.32434
10	2	0.4	100	16	0.23124	0.21450	0.22522	0.28120
11	2	0.4	50	8	0.91313	1.00385	0.94514	1.01489
12	2	0.4	50	16	0.50531	0.53355	0.48125	0.56544
13	2	0.2	100	8	1.23236	0.97489	1.42253	1.38044
14	2	0.2	100	16	0.14923	0.15304	0.14567	0.16184
15	2	0.2	50	8	0.83666	1.12856	1.17074	1.09493
16	2	0.2	50	16	0.21703	0.21929	0.23047	0.26530
17								

Table S2. Minitab data entry for 2^{4-1} factorial evaluation (with four replicates), after design selection.

↓	C1	C2	C3	C4	C5	C6	C7	C8	C9	pr
	StdOrder	RunOrder	CenterPt	Blocks	time	Na2CO3 conc.	FC amt.	ACN %	absorb.	
1	1	1	1	1	-1	-1	-1	-1	0.58720	
2	2	2	1	1	1	-1	-1	1	0.23047	
3	3	3	1	1	-1	1	-1	1	0.47260	
4	4	4	1	1	1	1	-1	-1	0.94514	
5	5	5	1	1	-1	-1	1	1	0.11327	
6	6	6	1	1	1	-1	1	-1	1.23236	
7	7	7	1	1	-1	1	1	-1	1.08416	
8	8	8	1	1	1	1	1	1	0.21450	
9	9	9	1	1	-1	-1	-1	-1	0.80005	
10	10	10	1	1	1	-1	-1	1	0.21703	
11	11	11	1	1	-1	1	-1	1	0.47151	
12	12	12	1	1	1	1	-1	-1	1.00385	
13	13	13	1	1	-1	-1	1	1	0.11874	
14	14	14	1	1	1	-1	1	-1	0.97489	
15	15	15	1	1	-1	1	1	-1	1.00921	
16	16	16	1	1	1	1	1	1	0.23124	
17	17	17	1	1	-1	-1	-1	-1	0.82063	
18	18	18	1	1	1	-1	-1	1	0.21929	
19	19	19	1	1	-1	1	-1	1	0.44601	
20	20	20	1	1	1	1	-1	-1	0.91313	
21	21	21	1	1	-1	-1	1	1	0.11492	
22	22	22	1	1	1	-1	1	-1	1.42253	
23	23	23	1	1	-1	1	1	-1	1.10194	
24	24	24	1	1	1	1	1	1	0.22522	
25	25	25	1	1	-1	-1	-1	-1	0.76514	
26	26	26	1	1	1	-1	-1	1	0.26530	
27	27	27	1	1	-1	1	-1	1	0.52434	
28	28	28	1	1	1	1	-1	-1	1.01489	
29	29	29	1	1	-1	-1	1	1	0.11497	
30	30	30	1	1	1	-1	1	-1	1.38044	
31	31	31	1	1	-1	1	1	-1	1.14221	
32	32	32	1	1	1	1	1	1	0.28120	

Table S3. Minitab data entry for 2⁴ factorial evaluation (with one replicate), before factorial design selection.

↓	C1	C2	C3	C4	C5	C6
	time-hr	Na2CO3 conc.	FC amount	conc. ACN	rep 1	
1	1	0.4	100	8	1.08416	
2	1	0.4	100	16	0.16056	
3	1	0.4	50	8	0.78884	
4	1	0.4	50	16	0.47260	
5	1	0.2	100	8	1.10267	
6	1	0.2	100	16	0.11327	
7	1	0.2	50	8	0.58720	
8	1	0.2	50	16	0.16526	
9	2	0.4	100	8	1.28946	
10	2	0.4	100	16	0.23124	
11	2	0.4	50	8	0.91313	
12	2	0.4	50	16	0.50531	
13	2	0.2	100	8	1.23236	
14	2	0.2	100	16	0.14923	
15	2	0.2	50	8	0.83666	
16	2	0.2	50	16	0.21703	

Table S4. Minitab data entry for 2^{4-1} factorial evaluation (with one replicate), after design selection.

↓	C2	C3	C4	C5	C6	C7	C8	C9	✓
	RunOrder	CenterPt	Blocks	time hr	Na2CO3 conc.	FC amt.	ACN %	absorb.	
1	1	1	1	-1	-1	-1	-1	0.58720	
2	2	1	1	1	-1	-1	1	0.21703	
3	3	1	1	-1	1	-1	1	0.47260	
4	4	1	1	1	1	-1	-1	0.91313	
5	5	1	1	-1	-1	1	1	0.11327	
6	6	1	1	1	-1	1	-1	1.23236	
7	7	1	1	-1	1	1	-1	1.08416	
8	8	1	1	1	1	1	1	0.23124	

LLE- GC-MS Method

1 mL aliquot of SW sample (RS chloroacetophenone added).

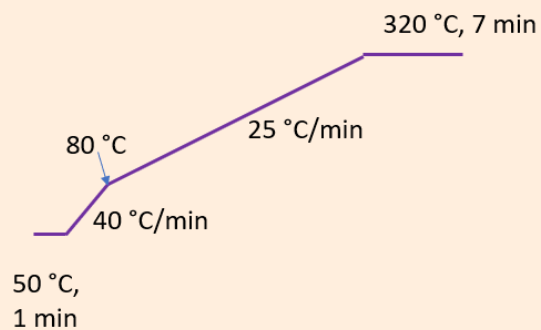
Acidified to pH 4 to keep phenol hydroxyls as OH for nonpolar DCM extraction (3 times with 1 mL DCM); IS o-terphenyl added.

The final GC-MS sample contained 400 μL of the solution and 10 μL of IS solution

GC: splitless with 0.2 min splitless time and 0.2 mL injection volume, He carrier, column flow 1.5 mL/min, septum purge 3 mL/min

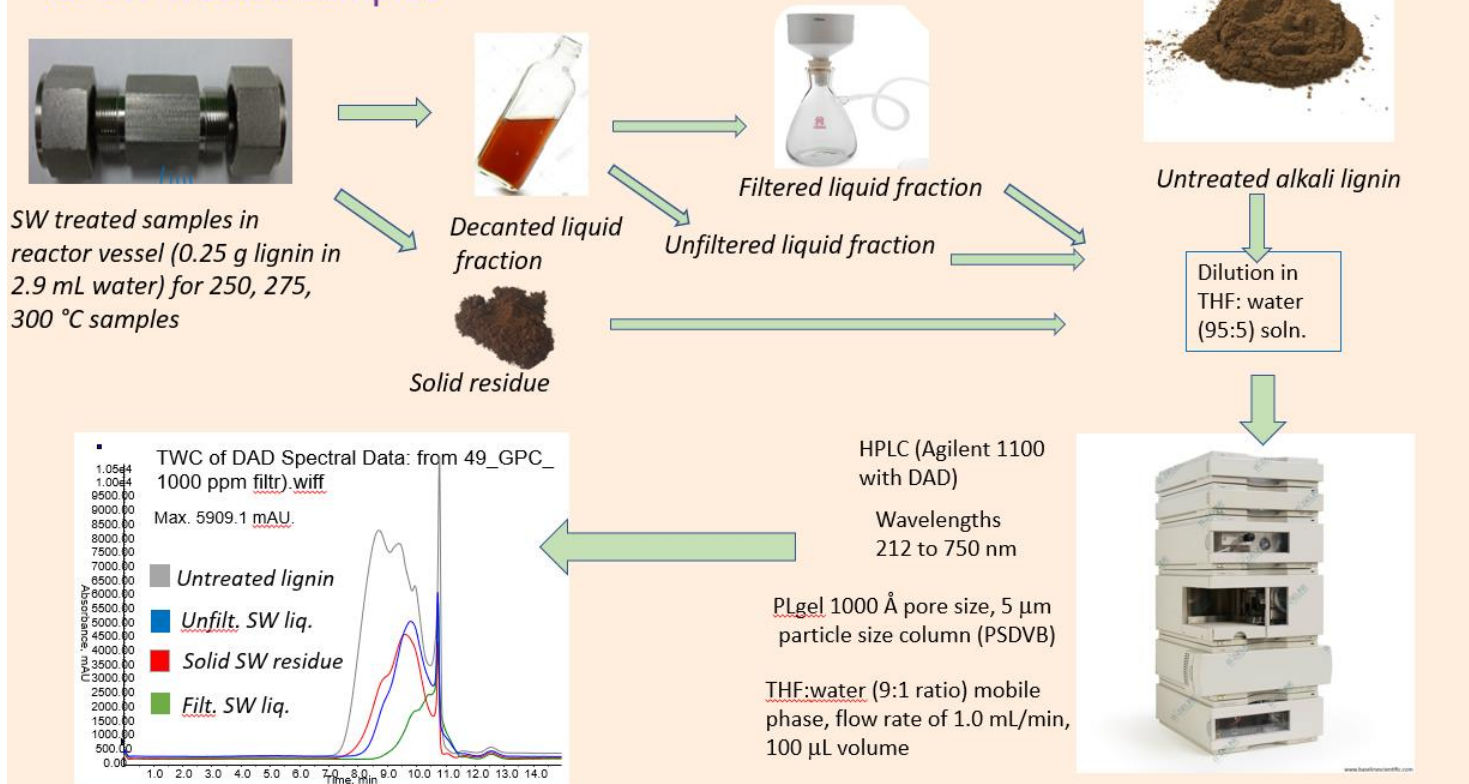
Injector temp 300 C, transfer line 280 C

The following temperature program was set:



The mass spectrometer parameters: solvent delay 4 min, mass range 33–500 amu, quadrupole temperature 150 °C and electron ionization (EI) source 230 °C.

Gel Permeation Chromatography (GPC) for SW Treated Samples



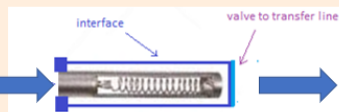
Appendix 7: TD-Py-GC-MS workflow

TD-Py-GC-MS

DCM samples dried at 50 °C for 30 s; MeOH and aqueous samples not dried, but 4.25 min solvent delay



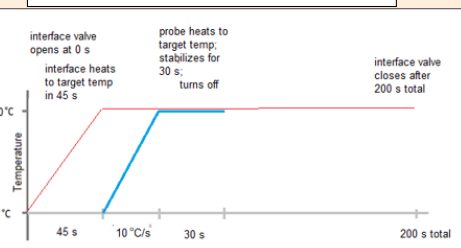
TD-Py-GC-MS consists of CDS Analytical 5200 Pyrolyzer connected by transfer line to GC inlet



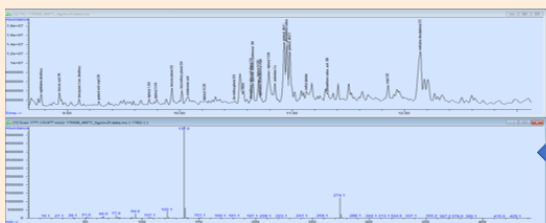
The **pyroprobe** wand tip is a platinum heating coil which surrounds a sample capped by quartz wool

Pyroprobe wand insertion

Pyroprobe Heating Program for One Temperature *



Valve oven temp 320 °C

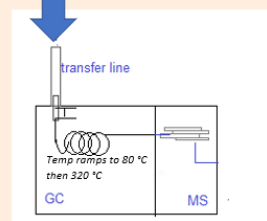


Chromatograms at each temperature fraction are evaluated for products by mass spectrograms of characteristic ions (NIST library)



Burnoff of char is external and products are not evaluated by GC-MS

Program repeated for 110, 200, 300, 400, 500 and 890 °C runs of 15 min.



HP-5MS column, nonpolar, 45 m, 0.25 ID and 0.25 μm thickness

GC-MS evaluation of thermally desorbed or pyrolyzed products in split mode (10:1), injector and transfer line at 300 °C. MS scanned 10-550 m/z using EI source at 70eV

*Note: Interface temp was the same as probe temp for 200 and 300 °C fractions, but was set at 350 °C for all others.